

# **DEVELOPMENT AND ASSESSMENT OF REGIONALISED APPROACHES TO DESIGN FLOOD ESTIMATION IN SOUTH AFRICA**

Report to the  
**WATER RESEARCH COMMISSION**

by

**JP CALITZ and JC SMITHERS**

Bioresources Engineering  
School of Engineering  
College of Agriculture, Engineering and Science  
University of KwaZulu-Natal

**WRC Report No. 2748/1/20**  
**ISBN 978-0-6392-0198-6**

**November 2020**



**Obtainable from**

Water Research Commission

Private Bag X03

GEZINA, 0031

[orders@wrc.org.za](mailto:orders@wrc.org.za) or download from [www.wrc.org.za](http://www.wrc.org.za)

**DISCLAIMER**

This report has been reviewed by the Water Research Commission (WRC) and approved for publication. Approval does not signify that the contents necessarily reflect the views and policies of the WRC nor does mention of trade names or commercial products constitute endorsement or recommendation for use.

## ABSTRACT

There is a need to update and modernise methods used for design flood estimation in South Africa as many of the methods were developed more than 40 years ago and hence there are longer hydrological records to use in the updating of the methods. The original aim of this study was to develop an improved and refined regionalised Probabilistic Rational Method (PRM) for South Africa, and this objective was expanded to include the development of a Regional Index Flood (RIF) method and a comparison of the performance of the two approaches was undertaken.

A critical aspect of regional flood frequency analysis is the identification of homogeneous flood producing regions. Both Region of Influence and Clustering approaches were investigated and forty-two relatively homogeneous flood producing regions were identified using clustering and manual adjustments. The mean annual flood (MAF) and 10% Annual Exceedance Probability C-value ( $C_{10}$ ) for the Rational Method coefficient were selected as scaling variables to produce growth curves for both methods and regionalised regressions were developed to estimate the scaling factors, and hence estimate flood quantiles, at ungauged sites in South Africa.

In order to estimate design peak discharges at gauged sites, a number of probability distributions were considered and the Generalised Pareto distribution was determined as the best distribution to estimate design peak discharges at a national scale.

The  $C_T$  and RIF were developed both at a National and homogeneous Cluster scale and were assessed using the ratio of modelled versus observed flows, Nash Sutcliffe model efficiency (NSE), slope of regression, bias and root mean squared error (RMSE). When considering the ratio, bias and RMSE the models perform similarly, however the cluster based RIF model performed best when reviewing the NSE and the regression slopes and is therefore recommended for application in South Africa.

In a pilot study, a structure for a website was developed to make available the data used in the project, the catchment attributes generated and the application of the methods developed in the study. News on advancements on the development of the tool will be available on the NFSP website (<https://www.nfsp.co.za>)

## EXECUTIVE SUMMARY

Engineers rely on design hydrological information for the design of hydraulic structures, such as dams, bridges and drainage culverts (Smithers and Schulze 2003). This information is often estimated at ungauged sites using models to estimate flood frequencies (Schulze *et al.* 2004, Smithers *et al.* 2015). No single Design Flood Estimation (DFE) method has been identified as the most appropriate method and, in many texts and manuals the use of a combination of these are recommended (e.g. Pilgrim and Cordery 1993, Alexander 2002, Chadwick *et al.* 2004, SANRAL 2013). In South Africa some of the recommended methods were developed outside of South Africa with little or no local assessment, and most of the recommended methods were developed prior to 1990. The development of new and updated methods can therefore benefit from the use of much longer observed data sets and new approaches used internationally.

Two DFE approaches widely used international are the Probabilistic Rational Method (PRM) and Regional Index Flood (RIF). The Standard Design Flood (SDF) method developed by Alexander (2002) is a locally developed PRM. However, the method has been recommended for review in a number of studies (Görgens 2002, Smithers and Schulze 2003, Van Bladeren 2005, Gericke 2010, Van Vuuren *et al.* 2013). Both Kjeldsen *et al.* (2002) and Haile (2011) applied the RIF approach in South Africa and showed the potential for implementation at a national scale. The RIF approach is also favoured over the PRM approach internationally as is evident from the recent exclusion of the PRM in the revised Australian Rainfall and Runoff guidelines (Rahman *et al.* 2015).

### **Aims and Objectives of Project**

The aim of this project was to develop and assess the PRM and RIF approaches for the estimation of design flood quantiles within South Africa utilising the most recently available data, which required the fulfilment of the following objectives:

- (a) Collation and quality control of selected gauged flow data in South Africa.
- (b) Produce at-site flood frequency curves for selected stations.
- (c) Compilation of catchment descriptors database.
- (d) Identify and verify homogeneous flood producing regions.
- (e) Calibration of the Rational Method within homogeneous regions.
- (f) Regional flood model development.

- (g) Assessment of the performance of the proposed methodology.
- (h) Develop a DFE utility for application of the newly proposed methodologies by design practitioners
- (i) Development of a RIF method for DFE and comparison of performance with the regionalised PRM developed.

### **Hydrological Descriptors and Streamflow Data**

DFE methods requires a range of catchment descriptors to be determined for use in models. Considering the requirement of ease of application by practitioners, the following descriptors that are readily available, or simple to estimate, were selected for inclusion in the study:

- (a) outlet location,
- (b) outlet elevation,
- (c) catchment area ( $A$ ),
- (d) catchment centroid,
- (e) catchment perimeter,
- (f) rainfall region,
- (g) rainfall seasonality ( $R_s$ ),
- (h) catchment runoff percentage ( $C_{ro}$ ),
- (i) SCS soil classifications (SCS),
- (j) distance from the coast ( $D_c$ ),
- (k) longest flow path ( $L$ ),
- (l) length to centroid ( $L_c$ ),
- (m) slope ( $S_{10-85}$ ,  $S_{ea}$ ,  $S_c$ ),
- (n) time of concentration ( $T_c$ ),
- (o) Areal Reduction Factor (ARF),
- (p) Mean Annual Precipitation ( $MAP$ ), and
- (q) Design rainfall depths ( $DR_{2-100yr}$ ).

The Department of Water and Sanitation (DWS) is the custodian of the flow monitoring network in South Africa and currently has 1 458 streamflow gauging stations within South Africa. The data was screened by considering a minimum record length of 20 years, after which a total of 383 stations remained and were utilised in the study. The stations are divided into 296 river gauges and 87 synthetic dam inflow records generated by the DWS flood studies group.

## **Identification of a Parent Distribution Suitable for Use in South African FFA**

SANRAL (2013) and Van der Spuy and Rademeyer (2018) provide methods to undertake FFA and provide the most commonly used Parent Distributions (PD) in South Africa. The PDs can, however, provide large variances in flood estimates and hence the selection of the most suitable PD for use in South Africa is required for FFA. Graphical, Goodness-of-fit (GOF), model fit criterion and model uncertainty were used for the selection of the most suitable PD out of the five PDs evaluated: (i) General Extreme Value (GEV), (ii) Generalised Pareto (GPA), (iii) 3-parameter Kappa (KAP3), (iv) Log Pearson Type III (LP3) and (v) Pearson Type III (PE3).

The graphical methods favoured the GPA, KAP3 and LP3 distributions equally, with the GOF methods ranking LP3 as the most suitable method. Conversely, the GPA was ranked highest for the model fit criterion and displayed the least model uncertainty. Given the overall ranking of the PDs, the GPA was selected to be the most suitable PD for use in South Africa.

## **Regionalisation**

Two approaches were considered to undertake the formation of the homogeneous regions: (i) Clustering, and (ii) Region of Influence (RoI). Using the RoI approach resulted in only 51% of the regions to be relatively homogeneous when considering a single parameter set, however, when combining two parameter sets, this increased to 71%. For the remaining 29% of sites, equivalent to 111 sites, homogeneous regions could not be formed using a RoI approach. Conversely, the Clustering approach was able to identify 42 relatively homogeneous clusters. Initial clustering was performed using the outlet location (Latitude and Longitude) and the distance from the coast ( $D_c$ ).

## **Model Development and Assessment**

A scaled growth curve approach (Dalrymple 1960) was used to develop both the  $C_T$ , a revised PRM, and RIF models. The Mean Annual Flood (MAF) and 10% Annual Exceedance Probability C-value ( $C_{10}$ ) were used as the Scaling Factors (SF) to develop the unitless regional FFA and C-value curves respectively. Regressions were developed, using Catchment Area, Mean Annual Precipitation and distance from the coast as predictor variables, to estimate the SFs on a national and cluster scale, with the cluster based estimates outperforming the national estimates.

To assess the quantile estimation performance of the developed models a Jack-knife resampling approach was adopted, which iteratively hides a site from the development of the regressions and unitless regional curves and compares the hidden estimates to observed values. The performance statistics included the ratio of modelled versus observed design values, Nash-Sutcliffe model efficiency (NSE), slope of regression, bias and root mean squared error (RMSE). When considering the ratio, bias and RMSE the models perform similarly, however, the RIF model performed best when including the NSE and the regression slopes and is therefore recommended for application in South Africa.

### **Development of a DFE Utility**

In a pilot study, a structure for a website was developed to make available the data used in the project, the catchment attributes generated and the application of the methods developed in the study. News on advancements on the development of the tool will be available on the NFSP website (<https://www.nfsp.co.za>)

## ACKNOWLEDGEMENTS

The project team would like to acknowledge the following individuals and organisations that provided valuable input:

The Water Research Commission for their support and funding of the entire project, and the Chair, Wandile Nomquphu for his continued guidance;

The Department of Water and Sanitation for providing the streamflow and synthetic reservoir streamflow data and their participation in the reference group;

The National Flood Studies Programme in collaboration with the Royal Academy of Engineers which hosted annual workshops as a platform for knowledge sharing and transfer. Special mention is to be made of Dr TR Kjeldsen who provided valuable input into the project.

The following reference group members whose time and input was greatly appreciated:

<b>Title</b>	<b>Initials</b>	<b>Surname</b>	<b>Affiliation</b>
Mr	M	Braune	BioEng
Mr	C	Brooker	Chris Brooker and Associates
Mr	D	Cameron-Ellis	ARQ Consulting Engineers
Prof	JA	du Plessis	Stellenbosch University
Mr	S	Dunsmore	Fourth Element Consulting
Dr	OJ	Gericke	Central University of Technology
Ms	KA	Johnson	University of KwaZulu-Natal
Dr	TR	Kjeldsen	University of Bath
Mr	E	Kruger	South African National Roads Agency SOC Ltd
Ms	I	Loots	University of Pretoria
Prof	SA	Lorentz	SRK Consulting
Prof	JG	Ndiritu	University of Witwatersrand
Mr	W	Nomquphu (Chair)	Water Research Commission
Mr	E	Oakes	Department of Water and Sanitation
Mr	M	Parak	South African National Roads Agency SOC Ltd
Mr	P	Rademeyer	Department of Water and Sanitation
Mr	TR	Rowe	JG Afrika
Prof	R	Schulze	University of KwaZulu-Natal
Mr	TA	Thobejane	Department of Water and Sanitation
Mr	D	van der Spuy	Department of Water and Sanitation
Mr	M	van Dijk	University of Pretoria

## TABLE OF CONTENTS

	Page
ABSTRACT.....	iii
EXECUTIVE SUMMARY.....	iv
ACKNOWLEDGEMENTS.....	viii
TABLE OF CONTENTS.....	ix
LIST OF FIGURES .....	xii
LIST OF TABLES .....	xv
1 INTRODUCTION.....	1
2 REVIEW OF REGIONALISATION METHODS FOR DESIGN FLOOD ESTIMATION.....	7
2.1 Formation of Regions.....	7
2.1.1 Index flood.....	10
2.1.2 Method of residuals .....	11
2.1.3 Canonical correlation analysis.....	12
2.1.4 Hierarchical.....	12
2.1.5 Region of influence.....	12
2.1.6 Cluster analysis.....	13
2.1.7 Geostatistical methods .....	15
2.1.8 Performance.....	15
2.2 Homogeneity Testing.....	16
2.3 Selection of an appropriate parent distribution.....	18
2.3.1 Parent distributions .....	19
2.3.2 Parameter estimation methods.....	21
2.3.3 Validation of selections .....	22
2.4 Information transfer .....	26
2.4.1 Response variable selection.....	28
2.4.2 Predictor variables .....	29
2.5 Performance Assessment .....	30
2.6 Conclusions.....	32
3 METHODOLOGY .....	33
3.1 Streamflow Data Assessment and Screening.....	33
3.2 Selection of an Appropriate Parent Distribution.....	36

3.3	Regionalisation.....	37
3.3.1	Clustering.....	39
3.3.2	Region of influence.....	40
3.4	Rational Method Calibration.....	42
3.5	Model Development and Performance Assessment.....	43
4	<b>HYDROLOGICAL PARAMETER DATABASE.....</b>	<b>44</b>
4.1	Base Data Collation .....	44
4.1.1	Digital elevation model.....	44
4.1.2	Rainfall .....	45
4.1.3	DWS data.....	45
4.2	Parameter Estimation .....	45
4.2.1	Catchment area .....	46
4.2.2	Longest flow path .....	47
4.2.3	Slope .....	47
4.2.4	Time of concentration.....	48
4.2.5	Areal reduction factor .....	49
4.2.6	Rainfall based parameters.....	49
4.2.7	Catchment runoff .....	51
5	<b>STREAMFLOW DATA .....</b>	<b>52</b>
5.1	Record Lengths .....	52
5.2	Station Information .....	53
6	<b>IDENTIFICATION OF A PARENT DISTRIBUTION SUITABLE FOR FLOOD FREQUENCY ANALYSIS IN SOUTH AFRICA .....</b>	<b>56</b>
6.1	National Kappa $h$ Value Estimation.....	56
6.2	Graphical Methods.....	56
6.3	Goodness-of-fit .....	59
6.4	Model Uncertainty .....	59
6.5	Model Selection Criterion.....	59
6.6	Distribution Ranking.....	60
6.7	Discussion and Conclusions.....	61
7	<b>REGIONALISATION.....</b>	<b>63</b>
7.1	Region of Influence.....	63
7.2	Clustering.....	63

7.3	Discussion and Conclusions.....	68
8	MODEL DEVELOPMENT AND ASSESSMENT .....	70
8.1	Regional Growth Curve Development.....	70
8.1.1	Quantile Growth Curves .....	71
8.1.2	RM Calibration .....	71
8.1.3	Scaling factor .....	75
8.1.4	Dimensionless growth curves .....	76
8.2	Model Development.....	79
8.3	Performance Assessment .....	88
8.4	Comparison to Standard Design Flood Method.....	94
9	DEVELOPMENT OF A DESIGN FLOOD ESTIMATION UTILITY .....	97
9.1	Technical specifications .....	97
9.2	User guide .....	98
10	DISCUSSION, CONCLUSIONS AND RECOMMENDATIONS .....	99
10.1	Data Collection and Screening.....	99
10.1.1	Catchment specific parameters .....	99
10.1.2	Development of a quality-controlled streamflow dataset.....	100
10.2	Selection of Parent Distribution.....	101
10.3	Regionalisation.....	102
10.3.1	Region of Influence .....	102
10.3.2	Clustering.....	102
10.4	RM Calibration .....	104
10.5	Model Development.....	104
10.6	Model Performance.....	104
10.7	Conclusions.....	105
10.8	Recommendation for Future Research.....	106
11	REFERENCES .....	107
	APPENDIX A: Dimensionless growth curves .....	117

## LIST OF FIGURES

	Page
Figure 1.1 Design flood estimation methods (after Smithers 2012) .....	2
Figure 2.1 RFFA methods used in the formation of regions (after Rahman <i>et al.</i> 2012) .....	9
Figure 3.1 Example of a rating curve exceedance and extension the adopted extension methodology.....	35
Figure 3.2 Example of a flow gauging weir on the Tongati River at Riet Kuil (DWS 2015) .....	35
Figure 3.3 Methodology flow diagram for the selection of a suitable parent distribution .....	38
Figure 3.4 Clustering methodology flow diagram .....	41
Figure 3.5 Region of Influence methodology flow diagram .....	42
Figure 4.1 Catchment area comparison .....	47
Figure 4.2 Average slope comparison .....	48
Figure 4.3 Normalised rainfall seasonality for station 0004816AW indicating the monthly (blue) and average (red) rainfall seasonality .....	50
Figure 4.4 National rainfall seasonality indicating the mean direction (radians) of each site investigated.....	50
Figure 5.1 Map indicating the DWS gauging stations (blue) and the synthetic dam stations (orange) selected for application.....	52
Figure 5.2 Number of gauging stations per DWS primary drainage region across South Africa .....	54
Figure 5.3 Histogram depicting the distribution of the station record lengths for the selected 383 gauging and synthetic dam stations.....	54
Figure 5.4 Catchment information for Gauging Station A2H061 .....	55
Figure 6.1 L-moment ratio diagram for all 383 selected sites using untransformed data indicating the KAPPA distribution $h$ value contours at 0.25 intervals and the record length weighted mean L-skew and L-kurtosis. ....	57
Figure 6.2 L-moment ratio diagram for all 383 selected sites using untransformed (left) and log transformed (right) data. The record length weighted mean (red cross) and moving average line are indicated (solid) in relation to the GEV, GPA, GNO, PE3, LNO and LP3 distributions. ....	57

Figure 6.3	L-moment ratio diagram indicating the position of the record length weighted mean L-skew and L-kurtosis per DWS drainage region, represented by the relevant alphabetic numeral, for natural (blue) and log transformed (black) data as well as the record length weighted means of the entire dataset .....	58
Figure 6.4	Variation of the 90% confidence bands presented as percentage variance of the balanced bootstrap confidence bands for the GPA, KAP3 ( $h = 0.77$ ), and LP3 distributions .....	61
Figure 7.1	Distribution of the 42 relatively homogeneous clusters identified .....	68
Figure 7.2	Delineation of national cluster association based on location and distance in relation to the DWS primary drainage regions (green) from the sea at a scale of 0.1 degrees .....	69
Figure 8.1	Dimensionless Peak flow (left) and Scaled $C_T$ growth curves (right) for Cluster 42 indicating the record length weighted average curves (red dash) in relation to the sites within the cluster (coloured lines) .....	76
Figure 8.2	Observed versus estimated $C_{10}$ for the national- (left) and cluster based (right) models .....	80
Figure 8.3	Observed versus estimated MAF for the national- (left) and cluster based (right) models .....	81
Figure 8.4	Estimated vs observed $Q_T$ using the $C_T$ National based approach for the 50, 20, 10, 5, 2, 1 and 0.5% annual exceedance probabilities .....	84
Figure 8.5	Estimated vs observed $Q_T$ using the $C_T$ Cluster based approach for the 50, 20, 10, 5, 2, 1 and 0.5% annual exceedance probabilities .....	85
Figure 8.6	Estimated vs observed $Q_T$ using the RIF National based approach for the 50, 20, 10, 5, 2, 1 and 0.5% annual exceedance probabilities .....	86
Figure 8.7	Estimated vs observed $Q_T$ using the RIF Cluster based approach for the 50, 20, 10, 5, 2, 1 and 0.5% annual exceedance probabilities .....	87
Figure 8.8	Percentage of $Q_T$ estimates within the desirable ratio defined by Rahman <i>et al.</i> (2012) using the <i>RIF</i> (top) and $C_T$ (bottom) approaches for both Cluster based and National based scaling factor estimation methods .....	89
Figure 8.9	Percentage of $Q_T$ estimates within the desirable ratio defined by Naidoo (In Preparation) using the <i>RIF</i> (top) and $C_T$ (bottom) approaches for both Cluster based and National based scaling factor estimation methods .....	90

Figure 8.10 Estimated vs observed  $Q_T$  using the  $C_{10}$  approach for the 50% AEP ..... 93

Figure 8.11 Comparison of the percentage of  $Q_T$  estimates within the desirable ratio defined by Rahman *et al.* (2012), between the RIF (top left),  $C_T$  (top right) and the SDF (bottom left) approaches ..... 95

Figure 8.12 Comparison of the percentage of  $Q_T$  estimates within the desirable ratio defined by Naidoo (In Preparation), between the RIF (top left),  $C_T$  (top right) and the SDF (bottom left) approaches ..... 96

Figure 9.1 Progressive web app..... 98

## LIST OF TABLES

	Page
Table 1.1 Social and monetary flood damages of recent flooding events in South Africa .....	1
Table 2.1 Categories of modelled vs at-site ratios Rahman <i>et al.</i> (2012) .....	30
Table 2.2 Revised categories of modelled vs at-site ratios .....	32
Table 3.1 Data errors and recommendations.....	34
Table 3.2 List of test categories and the selected methods for selection of an appropriate Parent Distribution.....	37
Table 5.1 Number of DWS flow-gauging stations and record lengths.....	53
Table 6.1 Rank of distributions based on the KP test in relation to the theoretical GEV, GPA, KAP3 ( $h = 0.77$ ), LP3, and PE3 distributions and the KP test .....	58
Table 6.2 Summary of the Anderson-Darling, Chi-squared, Cramer-von-Mises and Kolmogorof-Smirnov GoF test results for 383 sites in South Africa*. .....	59
Table 6.3 Summary of iterations of model criterion test selections for South Africa, the distribution with the highest selection rate for each iteration is indicated in bold .....	60
Table 6.4 Rank of distributions based on the uncertainty associated with the 1% AEP for 383 sites in South Africa .....	60
Table 6.5 Rank of distributions for the Goodness-of-fit, model fit criterion, graphical and uncertainty tests. The best performing distribution is highlighted in bold.....	61
Table 7.1 Homogeneity testing for national and drainage regions .....	65
Table 7.2 Initial clustering .....	66
Table 7.3 Accepted relatively homogeneous clusters .....	67
Table 8.1 Summary of calibrated $C_T$ values per AEP for the 42 homogeneous clusters .....	71
Table 8.2 Dimensionless $C_T$ curves for each relatively homogeneous cluster.....	77
Table 8.3 Dimensionless RIF growth curves for each relatively homogeneous cluster .....	78
Table 8.4 Scaling parameter model coefficients .....	82
Table 8.5 Performance statistics of $Q_T$ estimation using the RIF and $C_T$ approaches* for 10% and 1% AEP .....	91

Table 8.6	NSE and regression slope of observed and estimated $Q_T$ for the RIF and $C_T$ approaches at national and cluster scale. ....	93
-----------	---	----

# 1 INTRODUCTION

Engineers rely on design hydrological information for the design of hydraulic structures, such as dams, bridges and drainage culverts (Smithers and Schulze 2003). This information is often estimated at ungauged sites using models to estimate flood frequencies (Schulze *et al.* 2004, Smithers *et al.* 2015). The over- or under-estimation of design floods could lead to significant economic losses, loss of lives or under of over design of a structure, which results in loss of critical resources if under designed or a waste of capital resources if over designed. Local financial implications of flooding have been reported to be up to R1 billion in regions such as the Western Cape in 2008 by Holloway *et al.* (2010). Table 1.1 contains selected statistics of damage caused by recent flood events in South Africa.

Table 1.1 Social and monetary flood damages of recent flooding events in South Africa

<b>Year</b>	<b>Region</b>	<b>Estimated Damage</b>	<b>Reference</b>
2016	KwaZulu-Natal	7 Deaths	Davies (2017)
	Western Cape	10 000-15 000 people displaced	
2011	Northern Cape	R50 Million	Shiceka (2011)
	North West	R6 Million	
	KwaZulu-Natal	R300 Million	
2008	Western Cape	R1 Billion	Holloway <i>et al.</i> (2010)

Rahman *et al.* (2009) identified that in 1985 the estimated cost of projects involving the determination of design floods for small to medium sized rural catchments was approximately AU\$ 250 million per annum in Australia. This was estimated to be the equivalent of AU\$ 600 million (approximately R4 billion) in 2009 (Rahman *et al.* 2009). Stedinger and Griffis (2008) noted that the death toll caused by floods in the United States is approximately 140 per annum, with a financial cost of US\$ 6 billion annually, excluding recent events such as Hurricane Katrina.

Design Flood Estimation (DFE) techniques can be broadly categorised as analysis of streamflow data or rainfall based methods (Smithers and Schulze 2003), as indicated in Figure 1.1. Streamflow analysis uses statistics of observed floods to derive estimation techniques such

as flood envelopes or empirical formulae. Alternatively, Flood Frequency Analysis (FFA) can be performed to fit a parent distribution to the observed data. Rainfall based methods use design rainfall and rainfall-runoff models to estimate design floods, which range from event-based models, which utilise design rainfall as input, to the use of continuous simulation modelling.

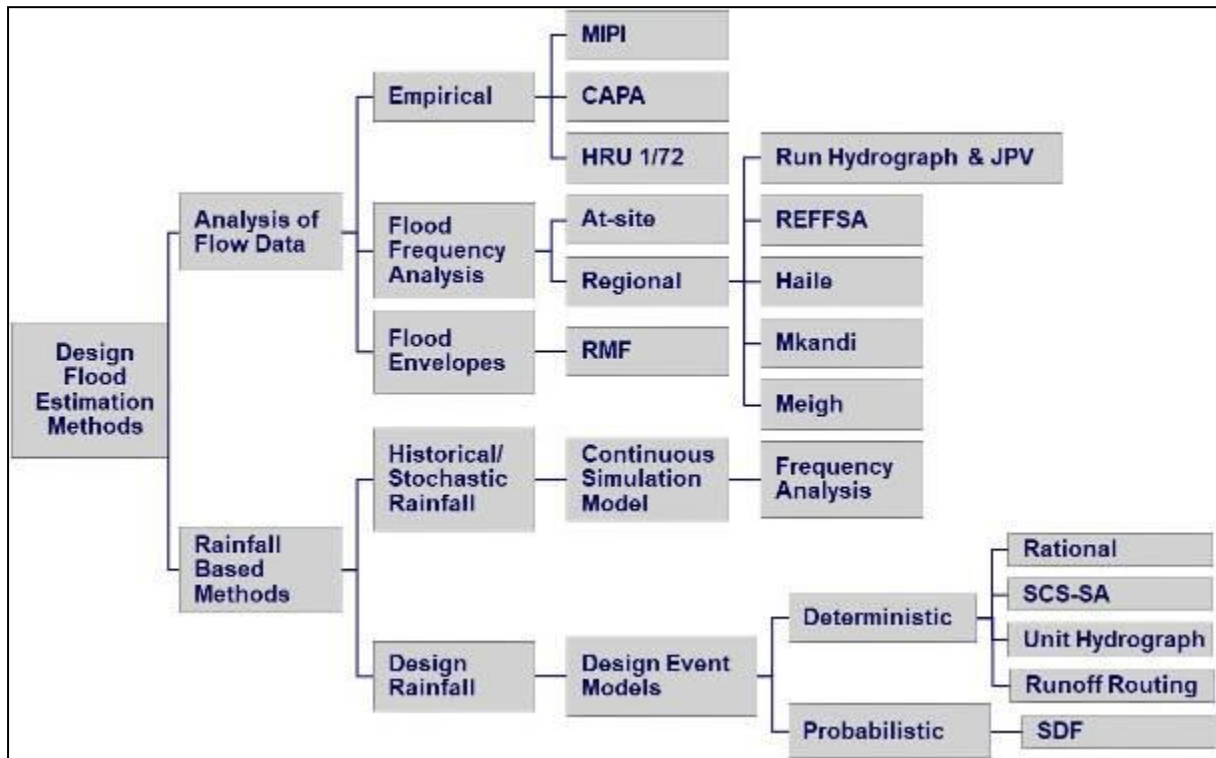


Figure 1.1 Design flood estimation methods (after Smithers 2012)

No single DFE method has been identified as the most appropriate method and, in many texts and manuals, the use of a combination of these are recommended (eg. Pilgrim and Cordery 1993, Alexander 2002, Chadwick *et al.* 2004, SANRAL 2013). When estimating design floods for a site, although several methods might be applicable, they may produce vastly different results, which poses the practitioners with the dilemma of which results to use. Pilgrim (1989) identified the following four requirements of a DFE method to ensure the selection of the best possible approach to DFE:

- (a) needs to be based on observed flood data,
- (b) needs to be simple, lack ambiguity and have familiarity in its application,
- (c) should be probabilistic rather than deterministic, and
- (d) should incorporate regional differences in hydrological responses.

Where adequate observed flood data are available FFA is the recommended approach and can be implemented locally or regionally. Even if flow data are available at the site of interest, the augmentation of at-site information can be achieved through applying Regional Flood Frequency Analysis (RFFA), which can substantially improve the accuracy of the frequency analysis (Kjeldsen *et al.* 2014, Rahman *et al.* 2019). In the UK and Europe, the use of regionalised approaches to flood frequency analysis is widely adopted (Castellarin *et al.* 2012). For ungauged sites, statistical approaches include regional methods (e.g. index flood method), direct regional regression of quantiles, and regional regression of distributional parameters (Aronica and Candela 2007)

For RFFA homogeneous regions need to be identified based on contiguous fixed regions, non-contiguous fixed regions, or on catchment and hydrologic similarity (Gado and Nguyen 2016). A region can have a fixed, common boundary for all sites within it, or the region can be flexible and be formed around the ungauged site of interest (Rahman *et al.* 2019). There is no clear consensus on the best method of regionalisation in hydrology (Oudin *et al.* 2008, He *et al.* 2011, Blöschl *et al.* 2013) and is dependent on region and climate (Razavi and Coulibaly 2013), but spatial proximity has been found to offer the best solution for regionalisation (Merz and Blöschl 2005, Oudin *et al.* 2008).

The index flood-based procedure developed by Hosking and Wallis (1993, 1997) and which utilises L-moments is a robust procedure and has been applied in a number of studies. A cluster analysis of site descriptors is used to identify potential homogeneous regions, which allows for independent testing of the at-site data for homogeneity. Methods based on L-moments are used for frequency estimation, screening for discordant data and testing clusters for homogeneity (Hosking and Wallis 1993, 1997). The Index Flood method has been successfully applied in a number of studies including the UK Flood Estimation Handbook (Kjeldsen *et al.* 2008), South Africa (HRU 1972, Kovács 1988, Van Bladeren 1993, Mkhanda and Kachroo 1997, Kachroo *et al.* 2000, Mkhanda *et al.* 2000, Kjeldsen *et al.* 2001, 2002, Görgens 2007, Haile 2011) and Australia for data poor regions (Rahman *et al.* 2015)

Where insufficient streamflow data are available for FFA, design rainfall with event-based methods are commonly used for DFE. The most widely used rainfall based method for DFE in small to medium sized catchments is the Rational Method (RM) (Hodgkins *et al.* 2007), which was originally developed by Mulvaney (1850, cited by Stephenson 1981, Shaw 1994,

Thompson 2007). The RM relies on the subjective estimation of a runoff coefficient (*C*-value) to estimate a design flood event. Van Vuuren *et al.* (2013) performed a survey of the DFE methods used in South African practice and, although the number of responses (35) was limited, the results provide valuable insight into the methodologies adopted in practice. The survey was circulated at several DFE related courses and conferences, with respondents varying in qualification and experience. It was found that the deterministic methods, and in particular the RM, is still the most widely used DFE method applied in South Africa. Deterministic methods, however, assume that the T% Annual Exceedance Probability (AEP) design rainfall will produce the T% AEP design flood event, which has been identified by Ben-Zvi (1989), Pilgrim (1989) and Alexander (2002), to mention a few, as being incorrect as a number of additional factors, such as antecedent soil moisture, have a significant impact on catchment responses during extreme rainfall events.

Several modifications have been made to the RM in attempts to reduce the deterministic nature of the model. These modifications range from the development of modified runoff coefficient tables (Caltrans 2006, Kasserchun 2008) to the development of probabilistic approaches to the use of the RM, such as the Probabilistic RM (PRM) (Pilgrim 1989) in Australia and the Standard Design Flood (SDF) (Alexander 2002) in South Africa. Many texts recommend maximum (approximately 15 km<sup>2</sup>) and minimum catchment areas when applying the deterministic RM (Caltrans 2006, Kasserchun 2008, SANRAL 2013). Pegram (2003) investigated the use of a Modified Rational Method (MRM) for catchments ranging from 100 to 100 000 km<sup>2</sup>. Young *et al.* (2009) determined the RM *C* values for 72 gauged catchments in Kansas and identified that the *C* values did not exhibit dependence on the catchment areas, which further supports the use of the method for catchments exceeding 15 km<sup>2</sup>.

Pilgrim (1989) recommends the use of probabilistic methods rather than deterministic methods for DFE. Probabilistic methods derive a direct link between the T% AEP design rainfall and the T% AEP design flood event. Pilgrim (1989) developed a PRM for Australia, which was included in the 1987 Australian Rainfall and Runoff (ARR) guide for flood estimation (Pilgrim 2001) and became a widely recognised method for flood estimation in Australia. Probabilistic methods are generally not limited by catchment sizes and are recommended for large ranges of catchment areas. The latest revision of the ARR (Rahman *et al.* 2019) has, however, recommended an alternative approach based on a RFFA which yields improved results.

In the South African context, the SDF method developed by Alexander (2002) is a locally developed PRM. However, the method has been recommended for review in a number of studies (Görgens 2002, Smithers and Schulze 2003, Van Bladeren 2005, Gericke 2010, Van Vuuren *et al.* 2013).

Görgens (2002) found that when estimating the 2% AEP floods the SDF estimates could be up to 210% of the observed estimates. In the development of the SDF, Alexander (2002) does state that conservative “upper envelope” coefficients were derived, which could cause the over-estimation, but are within the uncertainty levels related to hydrological estimation. Smithers and Schulze (2003) expressed the need to assess the SDF method and provide further refinement. Van Bladeren (2005) proposed modifications to the SDF method, but in the C5 secondary drainage region these only resulted in improved estimates in 26% of the catchments assessed. Gericke (2010) reviewed the SDF method and found that the SDF over-estimated design floods by up to 230% in the DWS C5 secondary drainage region. Gericke (2010) also determined correction factors for the SDF method. The corrected SDF method provided the most accurate results in the majority of the study area (Gericke 2010). The ratios of calibrated SDF:FFA ranged between 0.85 and 1.15, and resulted in a major improvement on the standard SDF results. Van Vuuren *et al.* (2013) identified inconsistencies in the estimation of catchment parameters during the development of the SDF as one of the potential problems that needs further research and refinement.

For the SDF method, Alexander (2002) performed a subjective regionalisation based on the DWS drainage regions and climatic conditions. Smithers and Schulze (2003) and Van Bladeren (2005) both recommend that a more rigorous statistical based approach to regionalisation be adopted. Other attempts at regionalisation for floods in South Africa have been performed by HRU (1972), Kovács (1988), Mkhandi *et al.* (2000), Kjeldsen *et al.* (2001) for the KwaZulu-Natal province and Haile (2011) but, with the exception of HRU (1972), have not been widely adopted for local use. The above highlight the need for a review of the SDF or the development of a new DFE approach for implementation in South Africa.

Calitz (2016) developed a PRM for primary DWS Drainage Regions A, C and U in South Africa and successfully regionalised the flood distributions in ten homogeneous regions, which were used to derive PRM *C* value relationships for the estimation of the design floods.

From the above, the original aims of this study was to develop an improved and refined regionalised PRM for South Africa, and this objective was expanded to include the development of a Regional Index Flood (RIF) method and a comparison of the performance of the two approaches was undertaken. Specific objectives include the following:

- (a) Collation and quality control of selected gauged flow data in South Africa.
- (b) Produce at-site flood frequency curves for selected stations.
- (c) Compilation of catchment descriptors database.
- (d) Identify and verify homogeneous flood producing regions.
- (e) Calibration of the Rational Method within homogeneous regions.
- (f) Regional flood model development.
- (g) Assessment of the performance of the proposed methodology.
- (h) Develop a DFE utility for application of the newly proposed methodologies by design practitioners
- (i) Development of a RIF method for DFE and comparison of performance with the regionalised PRM developed.

In this report Chapter 2 contains a review of literature on regionalisation for DFE, the general methodology is outlined in Chapter 3 and is followed by the development of a national parameter database in Chapter 4 and streamflow data used in the study is summarised in Chapter 5. The identification of the most suitable probability distribution for FFA in South Africa is detailed in Chapter 6. Chapter 7 contains details the regionalisation done for FFA and the model development and results of the application are reported in Chapter 8. The development of the draft design flood estimation utility is summarised in Chapter 9 and provides a link for users to follow the development of the utility. The study is discussed in Chapter 10 which includes conclusions and recommendations for future research.

## **2 REVIEW OF REGIONALISATION METHODS FOR DESIGN FLOOD ESTIMATION**

The reasoning for using a regional model is to have more reliable design events by supplementing at-site data with data from neighbouring or hydrologically similar catchments (Kjeldsen *et al.* 2014). A Regional Flood Frequency Analysis (RFFA) requires the identification of hydrologically homogeneous regions, and the application of a regional estimation method within each delineated homogeneous group (Gado and Nguyen 2016).

RFFA generally requires two steps. The first step is the identification of hydrologically homogeneous regions where the standardised flood frequency curves are similar and can be combined to improve estimates in the region. The second step is the application of the regional method in the regions (Gado and Nguyen 2016).

### **2.1 Formation of Regions**

Contiguous fixed region, non-contiguous fixed region, and hydrologic neighbourhood type are approaches used for regionalisation (Gado and Nguyen 2016). Geographical locations and/or administrative and political boundaries have traditionally been used for regionalisation and more recent techniques include cluster analysis (e.g. Tasker 1982), discriminant analysis (e.g. Wiltshire 1986) and discordancy measures (e.g. Hosking and Wallis 1993), all of which require subjectivity in region formation and are dependent on the similarity measures and classification techniques employed (Ilorme and Griffis 2013, Gado and Nguyen 2016). Hydrological homogeneity is generally determined by statistical homogeneity (Ilorme and Griffis 2013). In order to overcome the subjectivity involved, Ilorme and Griffis (2013) introduced a new statistical metric to identify physically discordant sites and a new methodology to identify the physical attributes that are the most indicative of extreme hydrologic response. Sites which were both hydrologically discordant, as determined by the Hosking and Wallis (1993) *H*-test, and physically discordant, determined using principal component analysis performed on all available physical variables, were discarded from a region. A combination of cluster analyses, principal component analyses, canonical correlation analyses and multiple discriminant analyses applied to flood statistics and physical variables were used as an intermediary step to identify the most relevant physical variables to use in a cluster analysis for the regionalisation

process (Ilorme and Griffis 2013). When this approach was compared to physically-based regionalisation procedures typically employed in practice, it resulted in more homogeneous regions and more efficient quantile estimation at ungauged sites and also enabled the flood regime and estimated quantiles to be inferred at sites outside the extent of the area used for model development (Ilorme and Griffis 2013).

When performing regionalisation, it is necessary to determine what information is best transferred, how to transfer the information and what catchments are used to derive the information. The selection of catchments to use is generally based on spatial proximity or hydrological similarity, which are often based on catchment descriptors (e.g. catchment size, land use, geology, elevation, soil characteristics as well as climate variables such as MAP) as surrogates for hydrological response (Merz and Blöschl 2005). However, a number of studies have shown that catchment descriptors are not necessarily a good indicator of hydrological response from a catchment.

The formation of regions aims to group hydrologically similar catchments, using either fixed regions or varying regions. Conventional regionalisation techniques form groups of fixed regions that only have an interdependence with the catchments within their respective regions (Burn 1990). However, Burn and Goel (2000) investigated the use of overlapping fixed regions in areas with limited hydrological data availability with promising results.

From a review of studies in the literature to approaches to regionalisation, Ridolfi *et al.* (2016) identify fixed region and region of influence as the most widespread approaches to regionalisation. However, there is no clear consensus on the best method of regionalisation in hydrology (Blöschl *et al.* 2013). Similarly, both Oudin *et al.* (2008) and He *et al.* (2011) concluded that no single method was the best solution to regionalisation, but studies have shown the need to improve both the understanding and quantification of catchment hydrological responses (He *et al.* 2011).

Rahman *et al.* (2012) noted that the formation of regions can be performed on both geographic or attribute space proximity, indicating that geographic proximity may not equate to hydrological similarity. This was also identified by Dalrymple (1960) who highlights that within a single state in the United States there may be a number of homogeneous flood producing regions. However, these regions may be grouped across states and could potentially

lead to pockets of homogeneous regions spread across a large area. Non-contiguous regionalisation has also been adopted in the UK (Robson and Reed 1999, Kjeldsen *et al.* 2008).

Rahman *et al.* (2012) found that when considering regionalisation using the attribute space approach the regional placement of an ungauged catchment may be difficult, however, the catchment can still be placed in a regional grouping based on the attribute space locality. Merz and Blöschl (2005) performed a comparison between the use of geographic and attribute space for use in regionalisation and found that the model which produced the most accurate results was when a combination of the geographic and attribute variables were used to form the regions.

Rao and Srinivas (2008) list the following common approaches to regionalise catchments which are grouped according to space and regional definitions, as illustrated in Figure 2.1:

- (a) index flood method,
- (b) Method of Residuals (MOR),
- (c) Canonical Correlation analysis (CCA),
- (d) Region of Influence (RoI),
- (e) hierarchical,
- (f) cluster analysis, and
- (g) geostatistical methods.

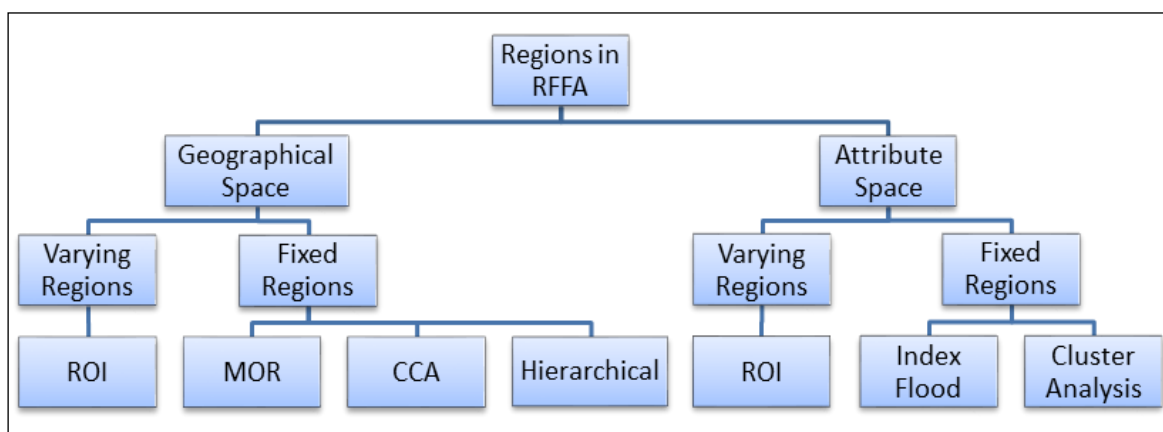


Figure 2.1 RFFA methods used in the formation of regions (after Rahman *et al.* 2012)

The index flood method has been included as a regionalisation method as an index flood based method requires the identification of homogeneous regions, as presented by Langbein

(Dalrymple 1960). A number of RFFA studies that have been performed in Southern Africa based on different grouping regions. (e.g. HRU 1972, Kovács 1988, Mkhandi and Kachroo 1997, Mkhandi *et al.* 2000, Kjeldsen *et al.* 2001, Alexander 2002, Kjeldsen *et al.* 2002, Görgens 2007, Haile 2011). The majority of these regionalisation studies use regions identified in previous studies (HRU 1972, Kovács 1988) as a base or an initial regionalisation scheme. HRU (1972) and Kovács (1988) performed hydrological analysis on available data sets and derived dimensionless 1-h unit hydrographs and Franco-Rodier K values, respectively. These parameters were then utilised in conjunction with physiographical maps to manually delineate homogeneous flood regions. A number of studies have recommended that the number of regions be increased to accommodate for the hydrological diversity of South Africa (Van Bladeren 2005, Gericke 2010, Smithers 2012, Van Dijk *et al.* 2013). Hosking and Wallis (1997) identifies that a balance between the number of stations in a region or clusters must be found, as clusters that are too large may bias the data set, whereas too small a cluster may add little benefit over at-site FFA.

The MOR, Hierarchical and CCA methods are not currently adopted in practice, nor have they been tested within Southern Africa and hence only brief descriptions of these methods are provided, with the remaining methods described in further detail in the following sections.

### **2.1.1 Index flood**

Dalrymple (1960) describes the methodology for Index Flood regionalisation and divides the approach into two distinct parts:

- (a) the development of a dimensionless scaled growth curve for a hydrologically homogeneous region, which relates scaled at-site flood peaks to exceedance probability or return period, and
- (b) determining relationships between catchment descriptors and the scaling variable used, e.g. the Mean Annual Flood (MAF).

The dimensional growth curve is derived by scaling the at-site values by an index flood. The scaling in the original Index Flood approach used the MAF and another commonly used index flood is the Median Flood (MEF) (Robson and Reed 1999, Kjeldsen *et al.* 2001, 2002, Nobert *et al.* 2014).

In terms of the Index Flood method, the approach groups at-site growth curves that have similar slopes or steepness. The homogeneity testing method uses the ratio between the 10% AEP and the MAFs as a slope and tests whether the range of slopes can be attributed to chance within the population. Dalrymple (1960) used the standard deviation of the Gumbel (GUM) distribution to estimate whether the variations were due to natural chance. Additional division of the population may be required should the range exceed two times the standard deviation, which was used as the homogeneous limits.

The growth curve is used as shown in Equation 2.1, whereby the desired T% AEP flood event ( $Q_T$ ) is related to the index flood ( $Q_{IND}$ ) by means of a growth factor ( $GF_T$ ). Alternatively, a parameter estimation approach can be followed where the scaled regional descriptive statistics are estimated and which are used to estimate a site specific statistical growth curve (Rahman *et al.* 2015).

$$Q_T = Q_{IND} \times GF_T \quad (2.1)$$

Relating the index flood to catchment descriptors enables the user to estimate the index flood at an ungauged site. The Index Flood method has been successfully applied in a number of studies including the UK Flood Engineering Handbook (Kjeldsen *et al.* 2008), South Africa (HRU 1972, Kovács 1988, Van Bladeren 1993, Mkhandi and Kachroo 1997, Kachroo *et al.* 2000, Mkhandi *et al.* 2000, Kjeldsen *et al.* 2001, 2002, Görgens 2007, Haile 2011) and Australia for data poor regions (Rahman *et al.* 2015). A number of these studies adopted the estimation procedure as shown in Equation 2.1, but relied on more statistically robust methods than the method described by Langbein (Dalrymple 1960) for the identification of homogeneous regions.

### **2.1.2 Method of residuals**

Choquette (1988) describes the MOR as a regionalisation method whereby a regression for the entire set of available records is performed as an initial step. Thereafter the residuals, i.e. the difference between the estimated flows calculated from the regressions and the actual flows, are investigated to identify any regions where consistent over- or under-estimation occurs. The regions that are deemed to be of similar over- or under-estimation are then isolated and the process is repeated on the separated regions until no further refinement can be achieved.

Thomas and Benson (1970), Glatfelter (1984) and Choquette (1988) are some of the studies that have used the MOR approach.

### 2.1.3 Canonical correlation analysis

GREHYS (Groupe de recherche en hydrologie (1996) provide an outline of the CCA method developed by Cavadias (1990), which is described as a multivariate statistical method used to reduce the dimensionality of linear dependence problems in two groups of variables. The hydrological parameters include quantiles or statistical information, and the catchment parameters. Ribeiro-Corréa *et al.* (1995), Cavadias *et al.* (2001), Ouarda *et al.* (2001) and Tsakiris *et al.* (2011) are some of the studies that used the CCA.

### 2.1.4 Hierarchical

Gabriele and Arnell (1991) proposed a hierarchical regionalisation approach for fixed regions. The approach assumes that growth curve parameters of a higher order require a larger set of donor catchments to improve the accuracy of the estimates. This was achieved by sub-dividing regions for estimation of the different order parameters.

### 2.1.5 Region of influence

Burn (1990) deviated from conventional fixed regions methods and details the RoI approach which produces a unique region for each catchment or station that is being assessed. The development of the RoI approach has also been attributed to Acreman (1987) and Acreman and Wiltshire (1987). The approach groups the regions based on a Euclidian distance ( $D_{jk}$ ), with the aim being to minimise the combined distance between  $p$  number of parameters ( $C^i$ ) of different sites ( $j$  and  $k$ ), be it geographical or attribute related. The Euclidian distance is estimated using Equation 2.2

$$D_{jk} = \sqrt{\sum_{i=1}^p (C_j^i - C_k^i)^2} \quad (2.2)$$

The region requires a threshold distance ( $THL$ ), which provides an upper bound allowable distance to be accepted. Burn (1990) highlighted the importance of selecting an appropriate

*THL* as it affects the number, size and homogeneity of the proposed regions. Considering that the donor sites will not all be equally close in Euclidian measure to the site being considered, a weighting factor between sites  $j$  and  $k$  ( $WF_{jk}$ ) is proposed by Burn (1990) which considers a  $D_{jk}$  based weighting, as shown in Equation 2.3.

$$WF_{jk} = 1 - \left( \frac{D_{jk}}{THL} \right)^n \quad (2.3)$$

The value of  $WF_{jk}$  can thus vary between zero and one. The  $n$  value can be used to control the rate of decreased influence based on the distance measure. Eng *et al.* (2005) investigated the use of an alternative approach whereby the number of closest stations was predetermined which, in some instances, allows for stations of a distance in excess of the initial *THL* to form part of the region. Robson and Reed (1999) recommend as a rule of thumb that the record length of the donor sites be five times the required AEP being estimated, i.e. a 1:20 year (5% AEP) flood estimate requires a donor set that has a combined record length of at least 100 years. This is referred to as the *5T* rule and, if it is not possible to achieve a data set of five times the return period, then a minimum of two times (*2T*) is recommended. Zrinji and Burn (1996) provide a revised RoI approach, combining it with the Hierarchical approach which uses a number of RoIs per catchment being investigated, depending on the variable being estimated. Haddad *et al.* (2015) compared the RoI approach to fixed region approaches in Tasmania and identified that the RoI methods generally presented improved results over the fixed region approaches. The methodology adopted by Haddad *et al.* (2015) is detailed by Haddad *et al.* (2012) and Reis *et al.* (2003).

Noteworthy studies that use the RoI approach for the formation of homogeneous regions are the UK FEH (Robson and Reed 1999, Kjeldsen *et al.* 2008) and the ARR Regional Flood Frequency Estimation (RFFE) (Rahman *et al.* 2015), both of which have been adopted in national DFE guidelines.

### **2.1.6 Cluster analysis**

Cluster analysis is one of the methods that does not require the restriction of contiguous regions. Both Hosking and Wallis (1997) and Blöschl *et al.* (2013) regard it as the most practical method of forming regions. Cluster analysis groups catchments that have similar

characteristics and hence is performed in the attribute space. Each cluster will therefore contain catchments with similar characteristics, which emphasises the importance of the selection of similarity parameters and their respective weighting. Cluster analysis aims to minimise the total Euclidian distance for the entire study by ensuring that the Euclidian distance for each region is minimised. The method can thus be seen as a fixed region approach to the RoI.

Clustering aims to group stations with stations with similar traits into clusters. Two commonly used approaches are hierarchical and k-means, both of which require the selection of an appropriate number of clusters ( $k$ ). Hierarchical clustering initially assumes that each station being considered is its own cluster, after which clusters are grouped by Euclidian distance until only a single overall cluster remains. Due to the Euclidian distances remaining constant between sites the process is easily reproducible.

Alternatively,  $k$ -means clustering requires the definition of the number of clusters prior to undertaking the division into clusters, the initial cluster centroids are randomly generated and iteratively refined until no further reduction in the overall Euclidian distance is achieved. Due to the random generation of the initial centroids the results of  $k$ -means clustering can vary between simulations. It is therefore common practice to use clusters defined through Hierarchical clustering as an initial estimate of the centroids, followed by refining the clusters through  $k$ -means clustering.

Hosking and Wallis (1997) noted that the results from the clustering analysis should not be considered final and that subjective adjustments may improve the homogeneity of the identified regions, and listed potential subjective adjustments that can be made. Wiltshire (1986) used an iterative relocation algorithm to adjust the clusters, which iteratively increases or reduces the number of clusters and adjusts the included stations to achieve the lowest total Euclidian distance. Alternatively, Smithers (1998) and Smithers and Schulze (2003) used a more subjective approach to refine extreme rainfall clusters and Kjeldsen *et al.* (2002) recommends further investigation into the use of clustering for the formation of homogeneous regions in South Africa.

The JPV method (Görgens 2007) uses a framework that is similar to both Clustering and RoI approaches. The stations used for the regionalisation were grouped based on the existing veld-type regions (HRU 1972) and the Kovács (1988) RMF K-regions, which in the initial

estimation are treated as fixed regions. Should a practitioner wish to perform a more detailed analysis, Görgens (2007) suggests an approach similar to the RoI and provides the relevant catchment descriptors for use in a “narrow” pooling exercise which allows the selection of the most appropriate donor sites.

### **2.1.7 Geostatistical methods**

Kottegoda and Rosso (2008) describe the function of spatial correlation as a technique for relating measured geographical data and using this relationship to estimate the variables at unmeasured locations. Tools such as a correlation function or a semi-variogram are used to form the required relationships.

Pilgrim (1989) used Kriging analysis methods, attributed to DG Krige by Kottegoda and Rosso (2008), which is a form of spatial correlation multivariate geostatistical analysis and is widely accepted in Australia. In the PRM adopted methodology in Australia, Kriging was used as the preferred geostatistical method for application.

In the South African context, Lynch (2004) investigated the use of Kriging, Inverse Distance Weighting (IDW), Thiessen polygons and regression techniques for the development of a national Mean Annual Precipitation (MAP) raster database. Lynch (2004) adopted the use of Geographically Weighted Regressions (GWR) due to the inclusion of further explanatory variables for use in the technique.

### **2.1.8 Performance**

Merz and Blöschl (2005) evaluated the predictive performance of various flood regionalisation methods in 575 ungauged catchments in Austria and found that spatial proximity is a significantly better predictor of regional flood frequencies than catchment attributes and a combination of spatial proximity and catchment attributes yielded the best predictive performance. When comparing a regression-based approach, an approach based on physical similarity and the spatial proximity approach to regionalisation, it was found that the spatial proximity, offers the best solution for regionalization (Oudin *et al.* 2008), confirming the findings by Merz and Blöschl (2005).

Generally non-contiguous fixed region, and hydrologic neighbourhood type (RoI) regionalisation approaches provide more accurate flood estimation than contiguous fixed region approaches (Gado and Nguyen 2016).

From a review of the literature in regionalisation in modelling, Razavi and Coulibaly (2013) conclude that variability in catchment physical attributes and climatic variability result in different performances for different regionalisation methods, but that generally spatial proximity and physical similarity have shown satisfactory performance in arid to warm temperate climate (e.g. Australia) and in cold and snowy regions (e.g. Canada), while spatial and regression-based methods have performed better in in warm temperate regions (e.g. most European countries).

The performance of regionalisation using scaling of catchment area, RoI and canonical correlation analysis (CCA) approaches to regionalisation was assessed at 57 catchments in Québec, Canada and the results indicate that flood quantiles estimated using the scaling approach were more accurate and more robust than those estimated by the RoI or CCA methods (Gado and Nguyen 2016).

## 2.2 Homogeneity Testing

Homogeneity testing refers to the calculation of test statistics to validate the assumption of homogeneity for a grouping of donor catchments in a region or cluster. Hosking and Wallis (1993) provide test statistics that may be used during homogeneity testing, namely  $H$  and L-moment Discordance ( $D_i$ ). The  $H$  statistics are derived using LMs ( $\lambda_r$ ) and LM ratios ( $\tau_r$ ), of order  $r$  and the estimation procedures are detailed in Eqs 2.4-2.6 using an observation set  $X$  of length  $n$ , with an expected value  $E(X)$ .

$$\lambda_r = r^{-1} \sum_{j=0}^{r-1} (-1)^j \binom{r-1}{j} E(X_{r-j:r}) \quad (2.4)$$

$$\tau_r = \frac{\lambda_r}{\lambda_2}, r = 3, 4, \dots \quad (2.5)$$

$$\tau_1 = \frac{\lambda_2}{\lambda_1} \quad (2.6)$$

$H$ , calculated using Eqs. 2.7 and 2.8, uses Monte Carlo simulations to create simulated homogeneous regions based on the Kappa distribution with regional record length weighted averaged LMs ( $\bar{\tau}_r$ ), which Hosking and Wallis (1997) use to emulate all distributions.  $H$  compares the observed weighted standard deviation ( $V$ ) of the at-site ( $i$ ) LM coefficient of variations (L-CV) ( $\tau_1^i$ ) with the mean ( $\mu_V$ ) and standard deviation ( $\sigma_V$ ) of the L-CV of the simulated homogeneous regions. If the value of  $H$  is less than one, a region is considered to be homogeneous. A value between one and two is relatively heterogeneous and a value in excess of two is considered heterogeneous. The  $H$  statistic described below, however, does not provide insight into the homogeneity of individual sites within the proposed region.

$$V = \frac{\sum_{i=1}^k n_i (\tau_1^i - \bar{\tau}_1)^2}{\sum_{i=1}^k n_i} \quad (2.7)$$

$$H = \frac{V - \mu_V}{\sigma_V} \quad (2.8)$$

Hosking and Wallis (1997) therefore, developed a discordancy measure, shown in Eqs 2.9-2.11, as a means to screen the selected sites. Considering a group of  $n$  sites, the discordancy measure ( $D_i$ ) provides a parametric measure of relative proximity of an individual site,  $i$ , relative to the remaining sites by comparing the site specific LM vectors ( $U_i$ ) with the regional mean matrix ( $U_m$ ) and the covariance matrix  $S$ . A site with a  $D_i$  in excess of three is considered to be discordant.

$$D_i = \frac{1}{3} (U_i - U_m)^T S^{-1} (U_i - U_m) \quad (2.9)$$

$$U_m = \frac{1}{n} \sum_{i=1}^n U_i \quad (2.10)$$

$$S = \frac{1}{n-1} \sum_{i=1}^n (U_i - U_m) (U_i - U_m)^T \quad (2.11)$$

Kachroo *et al.* (2000) described a regional “graphical” homogeneity testing methodology used by Mkhandi *et al.* (2000) which, similar to the  $H$  statistics, relies on synthetically generated regions to test against. The simulated regions used by Kachroo *et al.* (2000), however, utilised the selected parent distributions rather than only the Kappa distribution. The “graphical” method identifies whether the regional  $t_3$  falls within the simulated maximum and minimum simulated values, and an additional more stringent check is to identify whether the historical data lies within the approximate 95% bounds, which are estimated using the standard deviation.

Kachroo *et al.* (2000) compared the proposed approach to that of Hosking and Wallis (1997) for twelve regions identified in Tanzania and found that the stringent “graphical” approach provided similar results.

Viglione *et al.* (2007) compared some of the common homogeneity tests for RFFA, including  $H$ , the Bootstrap Anderson Darling (BAD) test (Scholz and Stephens 1987) and the Durbin and Knott test (Durbin and Knott 1972). It was suggested that the homogeneity testing be performed based on the location of a site and the L-moment  $t_3$  vs  $t_4$  plot. Where the  $t_3^R$  value is less than 0.23 the  $H$  measure is to be used for homogeneity testing, however, if  $t_3^R$  is larger than 0.23, the bootstrap Anderson Darling test is to be used. The  $H$  measure was also noted for its performance and its extensive use in hydrology.

### **2.3 Selection of an appropriate parent distribution**

Flood frequency analysis requires the selection and fitting of a probability distribution to an AMS of peak events (Stedinger *et al.* 1993), either graphically or analytically (Basson and Pegram 1994, Smithers and Schulze 2000, Alexander 2002, Smithers and Schulze 2003, Gericke 2010, SANRAL 2013, Van der Spuy and Rademeyer 2018). In order to perform FFA the following aspects need to be considered:

- (a) Selection of a parent distribution.
- (b) Selection of a parameter estimation method.
- (c) Validation of appropriateness of selections.

The approach listed above has been adopted in this study, where a range of statistical measures are applied to judge the quality of distribution fits. Selection of a suitable distribution is a task that is often open to interpretation, even though there are numerous methods available to assess the quality of fit for different distributions. Similarly, validation of the appropriateness of the selected distribution is often difficult as multiple distributions may statistically fit the data but may appear less well suited when interpreted graphically and result in very different estimates of high return period floods.

### 2.3.1 Parent distributions

The choice of distribution can have a considerable impact on the estimated peaks. For example, Alexander (2002) demonstrated that the design flood estimate of a 0.5% annual exceedance probability flood obtained using different distributions fitted to the same dataset could result in variations of up to 38%. For conducting flood frequency analysis in South African catchments, Alexander (1990, 2000) recommended using the Log-Pearson Type 3 (LP3) distribution. Gericke (2010) proposed that the best distributions for use in South Africa are the three parameter Log-Normal (LNO), LP3 and Generalised Extreme Value (GEV). Van der Spuy and Rademeyer (2018) describe the LNO, LP3 and GEV distributions as the most suitable distributions for FFA but provide no evidence to support these. Görgens (2007) used both the LP3 and GEV distribution in South Africa, simply stating that the methods are commonly used in practise, and no further motivation for their use is provided. Görgens (2007) found that the LP3 distribution showed significant variation in its estimation, whereas, the GEV provided improved results. In addition to these distributions, Haile (2011) found that the Generalised Pareto (GPA), LNO and Pearson Type 3 (PE3) distributions were the best suited distributions in South Africa. However, Haile (2011) only utilised 73 flow-gauging stations within South Africa, where the DWS currently has 1458 registered river gauges. Kjeldsen *et al.* (2002) found that the infrequent occurrence of very extreme events resulting from cyclone activity in the coastal region of KZN resulted in poor performance of standard distributions. However, for the inland region of KZN the Generalised Normal (GNO), PE3 and GPA distributions were all suitable candidates. Mkhandi *et al.* (2000) reviewed seven distributions and two parameter estimation methods in southern Africa and found that the most suitable distribution was PE3 in 12 of the 13 regions considered, with LP3 being most suitable for the last remaining region.

Internationally, numerous scientific studies have been undertaken to validate and substantiate the selection of suitable flood distributions, primarily in Europe, United States of America (USA), and Australia. Although the hydrological climates and responses vary significantly from prevailing conditions in South Africa, experience can still be drawn from the studies.

Castellarin *et al.* (2012) compiled the first inventory of streamflow data and statistical methods used for FFA across Europe. The study compiled data received from 17 countries, which includes PD selection, FFA and regional FFA procedures. Across Europe, a number of different distributions are recommended, including: GEV, GPA, LP3, LNO, PE3, GUM, Weibull (WEI)

and Two Component Extreme Value (TCEV). Salinas *et al.* (2014) investigated the applicability of the GEV distribution as a pan-European distribution and found that the GEV cannot fully describe the differences in flood series characteristics between catchments. However, not enough statistical evidence was found to reject the hypothesis for general applicability of the GEV. Kjeldsen *et al.* (2017) tested the application of the four parameter Kappa (KAP) distribution at a regional scale in the UK, motivated by the fact that several of the commonly used three parameter distributions are special cases of the KAP distribution (Hosking 1994). Kjeldsen *et al.* (2017) proposed the application of a national KAP distribution, by reducing the KAP distribution to a 3-parameter distribution (KAP3) through estimation of a national shape parameter. The KAP3 improved the description of the regional distribution compared to both the GLO and GEV distributions. Given the high hydrological variability evident in South Africa, the use of distributions with increased flexibility may provide improved estimates.

In the USA, two predominant studies focussed on the identification of a suitable distribution for design flood estimation. Benson (1968) details testing performed on six different distributions (LP3, GUM, Gamma (GAM), log-GUM, LNO, Hazen), these were tested at 10 stations with record lengths ranging from 40 to 97 years. Recommendations of the methods were based on deviations between design flood estimates, as opposed to statistical methods. From the distributions reviewed, the LNO, LP3 and Hazen methods resulted in the smallest deviations and bias. The LP3 was, however, recommended based on popularity of use, the use of a skew parameter thus increasing its flexibility, and its rigorous mathematical backing. Six years later Beard (1974) tested eight distributions at 300 sites and the two distributions deemed to perform best were the LNO and LP3 with a regional skew (LPR). Apart from these studies there has been little further investigation into the selection of an appropriate PD in USA. Emphasis has rather been placed on improving the moment estimations for use with the LP3 through the use of moment adjustments as presented by Cohn *et al.* (2013).

South Eastern Australia presents the most climatologically similar region to South Africa. Haddad and Rahman (2008) investigated the performance of twelve distributions and fitting combinations at 18 sites in South-East Australia and concluded that GPA with the use of Linear moment (LM) fitting (Hosking 1990) (GPA-L) and the GEV with the use of LH-moments (LHM) (Wang 1997) (GEV-LH), a generalisation of LM (Wang 1997), fitting provided the best fits to the data, which was not consistent with the recommendations of the 1987 Australian

Rainfall and Runoff (ARR) manual (ARR 1987). Haddad and Rahman (2011) revisited the assessment of distribution selection in Tasmania to possibly modify the selection criteria. They considered seven distributions and identified that the most suitable model for use in Tasmania was the LNO distribution combined with Bayesian Markov Chain Monte Carlo (MCMC) fitting. The climate and hydrological responses in Tasmania are, however, different to conditions in most parts of South Africa. In the latest revision of the ARR guidelines, it is noted that the GEV and LP3 are reasonable initial choices for flood frequency analysis, and it is recommended that a single distribution is not prescribed due to the potential sampling variability of the relatively short record lengths (Rahman *et al.* 2019). In addition, it is recommended that a review of the data at a regional scale can be used to identify the best fit distribution through the use of an L-moment diagram (Rahman *et al.* 2019).

### **2.3.2 Parameter estimation methods**

Some of the methods available for parameter estimation include: the Method of Moments (MM), LM (Hosking 1990), LHM (Wang 1997), Probability Weighted Moments (PWM) (Greenwood *et al.* 1979) and Maximum Likelihood procedure (ML) (R.A. Fisher 1912 as referenced in Aldrich 1997). In South Africa, Gørgens (2007) used both the MM and PWM methods, whereas SANRAL (2013) and Van der Spuy and Rademeyer (2018) recommend the use of MM. England *et al.* (2018) prescribes the use of MM in simple cases, where data are not censored, and where data censoring is present the Expected Moment Algorithm (EMA) is recommended. In Australia a number of studies were undertaken to identify both the best fit distribution and best fitting procedure. The most notable study was undertaken by Haddad and Rahman (2008), who reviewed twelve distribution/fitting combinations and the LP3, N, LNO, GUM, GEV and GPA were fitted using the MM, LM, LHM and Bayesian Maximum Likelihood (BML) fitting procedures and identified that the three top performing combinations are GPA-LM, GEV-LHM and LP3-BML.

The method of L-moments (Hosking and Wallis 1993), detailed in Eqs. 2.4, 2.5 and 2.6, parameter estimation techniques have gained in popularity and proven successful locally and internationally (e.g. Pearson 1991, Vogel *et al.* 1993, Zrinji and Burn 1996, Mkhanda and Kachroo 1997, Kjeldsen *et al.* 2001, Smithers and Schulze 2003, Chen *et al.* 2007, Borujeni and Sulaiman 2009, Castellarin *et al.* 2011, Haile 2011, Hassan and Ping 2012, Rutkowska *et al.* 2016, Cassalho *et al.* 2018, Mostofi Zadeh and Burn 2019). In addition, the LM technique

is theoretically superior to the MM due to lower weighting being applied to the larger values within the dataset and LM are therefore more robust for use in the presence of high outliers.

### **2.3.3 Validation of selections**

Selection of a distribution can be based on three types of assessment: (i) Goodness-of-Fit (GoF) tests, (ii) model selection criterion, and (iii) graphical methods. Based on the literature reviewed the most widely used approach for selection of distribution types in South Africa are graphical methods in isolation, whereas internationally graphical, GoF and model selection criterion are commonly applied in combinations.

#### **2.3.3.1 Graphical methods**

Graphical methods are often employed to identify the most suitable flood distributions. The simplest graphical test is the use of plotting positions for observed data on an at-site basis. The observed data is plotted against the calculated distributions to provide a graphical comparison of the distribution to the observed data. The plotting positions identified by DWS (Van der Spuy and Rademeyer 2018) and SANRAL (2013) are the Weibull, Blom, Gringörten, Cunane, Beard and Greenwood methods. SANRAL (2013) describe these in further detail. Bulletin 17C (England *et al.* 2018) proposes the use of the plotting positions described by Stedinger *et al.* (1993).

Product Moment Diagrams (PMD) are an additional graphical measure that can be used; however, Vogel and Fennessey (1993) recommend the use of LM Ratio Diagrams (LMRDs) as developed by Hosking (1990) in favour of PMDs due to the LM being nearly unbiased. LMRDs have become a common method for the identification of best fit regional flood distribution and have been used by numerous authors for this purpose (e.g. Vogel *et al.* 1993, Zafirakou-Koulouris *et al.* 1998, Peel *et al.* 2001, Castellarin *et al.* 2012, Salinas *et al.* 2014, Kjeldsen *et al.* 2017). LMRDs are constructed by plotting the L-kurtosis ( $\tau_4$ ) versus the L-skew ( $\tau_3$ ).

Predominantly the assessment of the most suitable distribution is undertaken using two methods: (i) plotting the mean of the LMs of the region, and (ii) plotting a best fit line and

comparing the result to the theoretical distributions for a set of standard 3 parameter distributions (GLO, GEV, GNO, LP3). Kjeldsen and Prosdocimi (2015) proposed a modification to the use of LMRD, referred to as KP test hereafter, by applying the assumption that  $\tau_3$  and  $\tau_4$  share a bivariate normal relationship, this allows for the derivation of a 90% confidence ellipse. The confidence ellipse identifies the suitable PDs for the estimated LMs, and a selection is then undertaken through the use of a Mahalanobis distance.

### 2.3.3.2 Goodness-of-fit tests

The purpose of a GoF test is to identify, in a statistical manner, the most suitable distribution for the data being fitted. Zeng *et al.* (2015) reviewed the Chi-squared (CS) (Pearson 1900), Kolmogorov-Smirnov (KS) (Massey 1951) and Anderson-Darling (AD) (Anderson and Darling 1952) GoF tests for use in flood frequency analysis considering the PE3, Uniform, GNO and Weibull distributions. Zeng *et al.* (2015) concluded that most powerful GoF tests for the PE3, GNO and Weibull are the AD, KS and AD. Haddad and Rahman (2008) applied two additional GoF tests, Cramer von-Mises (CvM) (Cramér 1928, von Mises 1928) and the Filliben Correlation Coefficient (FCC) test (Filliben 1975),. Laio (2004) tested the power of the AD, CS, CvM, KS, FCC and LM based GoF tests for the GUM, WEI, GNO, GEV, GAM, LNO, and LP3 distributions. For the GEV, GAM and GUM distributions the power of the GoF tests were consistently below 50%, whereas the AD and CvM had power exceeding 80% for the LP3 and LNO distributions. The variation in the power of the GoF tests can be attributed to the fact that the tests apply larger weighting to different components (tail, head or entire curve) of the distribution functions (Kottegoda and Rosso 2008) and it is therefore recommended that multiple GoF tests be considered simultaneously AD applies additional weighting to the tails of distributions, favouring the higher or lower observations, whereas CvM weights the centre of the distribution more heavily. Lastly KS can be considered an intermediate test between AD and CvM and weights the entire distribution more evenly. The GoF tests listed above are generally applied on an at-site scale, but when reviewing regional data, can be used to identify the distribution through identifying the percentage of sites that are accepted for each test.

The Chi-Squared test, Eq. 2.12, is a measure of the difference between the observed ( $O$ ) and the expected ( $E$ ) frequencies of ordered observations ( $x_i, \dots, x_n$ ) in a sample of size  $n$ . The KS

test indicated in Eq. 2.13 measures the GoF, in relation to a distribution with a parameter vector  $\theta$ , through the maximum variance between the hypothetical ( $F(x_i, \theta)$ ) and Empirical Distribution Functions ( $F_n(x)$ ).

$$X^2 = \sum_{i=1}^n \frac{(O_i - E_i)^2}{E_i} \quad (2.12)$$

$$KS = \max_x |F_n(x) - F(x_i, \theta)| \quad (2.13)$$

Alternatively, quadratic statistics, Eq. 2.14, can be utilised, from which the AD and CvM, Eqs. 2.15 and 2.16 respectively, are derived (Cramér 1928, von Mises 1928, Anderson and Darling 1952).

$$Q^2 = n \int_{all\ x} [F_n(x) - F(x_i, \theta)]^2 \Psi(x) dF(x) \quad (2.14)$$

$$AD = -n - \frac{1}{n} \sum_{i=1}^n \left[ \left[ F(x_i, \theta) - \frac{2i-1}{2n} \right] + (2n+1-2i) \ln[1 - F(x_i, \theta)] \right] \quad (2.15)$$

$$CvM = \sum_{i=1}^n \left[ F(x_i, \theta) - \frac{2i-1}{2n} \right]^2 + \frac{1}{12n} \quad (2.16)$$

where  $\Psi(x)$  is a weighting function, which is 1 for CvM and  $[F(x_i, \theta)(1 - F(x_i, \theta))]^{-1}$  for AD.

Hosking and Wallis (1993) also provide a regional GoF measure,  $Z$ , shown in Eq. 2.17. The test statistics  $Z$  is a measure of the difference between regional sample ( $\bar{\tau}_4$ ) and theoretical L-kurtosis ( $\tau_4^D$ ), in relation to the standard deviation of theoretical L-kurtosis ( $\sigma_4$ ) estimated using Monte-Carlo simulations. An absolute value of less than 1.64 signifies a suitable distribution, and the distribution (Dist) with the lowest  $Z$  is often accepted.

$$Z^{Dist} = (\bar{\tau}_4 - \tau_4^{Dist}) / \sigma_4 \quad (2.17)$$

The test relies on the assumption that the regional values used are from a homogeneous region.

### 2.3.3.3 Model selection criterion

Laio *et al.* (2009) investigated the use of model selection criterion for use with flood frequency analysis, which was also adopted by Haddad and Rahman (2011). The criterion chosen were the Akaike Information Criterion (AIC, Eq 2.18) (Akaike 1974), second order AIC (AICc, Eq 2.19) (Sugiura 1978), Bayesian Information Criterion (BIC, Eq 2.20) (Schwarz 1978), and a modified Anderson-Darling Criterion (ADC) (Laio *et al.* 2009). The ADC requires distribution dependent coefficients to be applied, however, these parameters have only been derived for seven of the more commonly used hydrological distributions and has therefore not been include. Model criterion consider relative fit of models to data by measuring the information lost in the process of fitting through the likelihood function ( $L(\hat{\theta})$ ). Models ( $j$ ) are penalised for the number of parameters ( $p$ ) utilised, and as such a lower value indicates a better model fit.

$$AIC_j = -2\ln\left(L_j(\hat{\theta})\right) + 2p_j \quad (2.18)$$

$$AICc_j = AIC_j + \frac{2p_j^2 + 2p_j}{n - p_j - 1} \quad (2.19)$$

$$BIC_j = -2\ln\left(L_j(\hat{\theta})\right) + \ln(n)p_j \quad (2.20)$$

The criterion are applied at an at-site level to identify the distribution that provides the best model fit per site. The at-site results are summarised at a regional scale by calculating the percentage of sites where each distribution provides the best fit providing an indication of the regional distribution.

### 2.3.3.4 Model uncertainty

In the application of FFA, it is generally assumed that the data being used, after pre-processing of the data, are free of errors. In contrast the model errors can be quantified and are represented by the error introduced by misrepresentation of the actual events by the fitted parent distribution. As such it is assumed that the sample data is accurate and that the selected distributions introduce uncertainty into the estimates, which can be determined. Typical approaches used to determine the uncertainty associated with distributions are, (i) Analytical methods (e.g. Kjeldsen and Jones 2006); (ii) Monte Carlo simulations (e.g. Silva *et al.* 2012); and (iii) Bootstrapping (e.g. Burn 2003).

Taylor approximations attempt to approximate non-linear functions with a linear function within a set of known parameters. The performance is linked with the degree of non-linearity of the function in question and a critical assumption for its use is that the known parameters are true reflections of the population parameters.

Similarly, Monte Carlo (MC) simulations assume that the parameters estimated from the sample are a true reflection of the population parameters. However, instead of undertaking an analytical approach, a resampling approach is used. MC simulations resample from a known distribution and generate a number of iterations (N) of random samples with each sample containing the same record length as the original sample. The T-year runoff event is then generated for each of the N samples generated and the variance in relation to the original dataset calculated and used to estimate the confidence bands.

Bootstrapping refers to a resampling method where N number of iterations are considered to identify the variation in estimates, whereby the confidence intervals (uncertainty) can be determined. To determine the variation of a T% event a synthetic record is created from the existing record using resampling with replacement. This process involves the random selection of flood events from the observed records until the synthetic record length matches the observed record length, and FFA of the synthetic record is performed, which is considered a single iteration. Bootstrapping can be undertaken in a balanced or an unbalanced approach. The balanced approach ensures that the mean of the overall sample set is maintained as each sample can only be reproduced N number of times, whereas for unbalanced bootstrapping no limitation is applied to the number of occurrences of any sample. When considering 5% and 1% confidence intervals it is recommended to use N=1000 and N=10000 respectively.

## **2.4 Information transfer**

Reviewing the available literature has revealed that the most common method of regional flood information transfer is the use of regression analysis. Weisberg (2005) describes regressions as the “study of dependence”, i.e. the dependence of the response variable on predictor variables. Two regression techniques currently in use in a number of studies are the Quantile Regression Technique (QRT) and the Parameter Regression Technique (PRT) (e.g. Görgens 2007, Rahman *et al.* 2015).

QRT uses the catchment parameters as predictor variables to estimate the expected peak flow ( $Q_x$ ) event using predictor variables ( $B, C, D, \dots$ ) and regression parameters ( $a, b, c, d, \dots$ ). The regression equations generally take the form of Eqs. 2.21 or 2.22.

$$Q_x = a B^b C^c D^d \dots \quad (2.21)$$

$$Q_x = a + b*B + c*C + d*D \dots \quad (2.22)$$

PRT estimates the descriptive statistics of the selected growth curve for the required site. For example, when considering the LP3 distribution, the standard deviation ( $S$ ), mean ( $M$ ) and coefficient of skewness ( $SK$ ) are required and each of these parameters are individually estimated for a selected site using separate regressions. Rahman *et al.* (2012) list the following advantages that the PRT has over the QRT:

- (a) QRT may lead to an inconsistent curve. PRT eliminates this by estimating the entire growth curve, hence providing a smooth increase with increased AEP.
- (b) PRT can estimate floods for any AEP and is not limited to the derived QRT relationships.

A number of methods exist for the estimation of the regression parameters, some of these methods are (Kottegoda and Rosso 2008, Rahman *et al.* 2009, Haddad *et al.* 2012): (i) Ordinary Least Squares (OLS); (ii) Weighted Least Squares (WLS); (iii) General Least Squares (GLS); and (iv) Bayesian GLS (BGLS). Rahman *et al.* (2015) recommend the use of BGLS and state that the method provides more accurate results in comparison to OLS and WLS.

Comparisons between QRT and PRT was undertaken on 53 catchments in Tasmania (Haddad *et al.* 2012). Catchment area and design rainfall intensity were found to be the most important predictor variables in the QRT and four predictor variables were used in the PRT (Haddad *et al.* 2012). The QRT was found to provide more accurate flood quantile estimates for the higher return periods while the PRT resulted in relatively better flood estimates for smaller return periods (Haddad *et al.* 2012).

A similar comparison between QRT and PRT was undertaken on 237 catchments in North-Eastern USA and the PRT is recommended due to its accuracy, computational simplicity and ability to estimate design floods for any return period, even though the QRT gave a slightly better performance for all return periods (Ahn and Palmer 2016). From a study in 1 535

catchments in France, Odry and Arnaud (2017) found that inconsistencies between floods estimated for different return periods were possible when the QRT approaches was used and therefore recommend the use of the PRT.

The assessment of the performance of different approaches to regionalisation found that the spatially smooth estimation approach where the parameters of the regional model vary continuously along the space was the most robust approach and less sensitive to different patterns of heterogeneity and the impacts of short records (Ganora and Laio 2016).

Regionalised flood models can be developed that describe the flood producing characteristics in order to have the capability of transferring them to ungauged catchments. These models can take a number of forms, can be used to predict a number of variables and their development is based on the (i) the selection of response and predictor variables, and (ii) regional flood relationship identification (Kjeldsen *et al.* 2001, Nobert *et al.* 2014, Rahman *et al.* 2015).

#### **2.4.1 Response variable selection**

The response variable refers to the variable(s) required to apply the regional flood model and can vary depending on the application method of the RFFA. Some of the response variables used in flood studies include, but are not limited to:

- (a) peak flow (Riggs 1982),
- (b) growth curve Frequency |Factors ( $FF_T$ ) (Riggs 1982, Kjeldsen *et al.* 2002, Rahman *et al.* 2015),
- (c) distribution descriptive statistics (Rahman *et al.* 2015),
- (d) MEF (Robson and Reed 1999),
- (e) MAF (Dalrymple 1960, Kjeldsen *et al.* 2001), and
- (f) average rainfall intensity (McDermott and Pilgrim 1982).

The selection of appropriate predictor variables to estimate the ungauged site response variables are described in further detail in the following sections.

## 2.4.2 Predictor variables

Predictor variables are used to establish the relationship between the response variable and the local catchment descriptors. McDermott and Pilgrim (1982) divided catchment descriptors into two groupings, natural and introduced. Natural variables refer to descriptors such as area, soil, rainfall and topography, whereas introduced variables consider man-made effects such as land use and urbanisation. Since introduced variables change more rapidly than natural variables, they are often difficult to quantify. It is evident from regionalisation studies that the use of natural variables is widely adopted (Dalrymple 1960, McDermott and Pilgrim 1982, Riggs 1982, Pilgrim 1989, Mkhani and Kachroo 1997, Mkhani *et al.* 2000, Kjeldsen *et al.* 2001, 2002, Smithers and Schulze 2003, Merz and Blöschl 2005, Görgens 2007, Rao and Srinivas 2008, Rahman *et al.* 2015). Rahman *et al.* (2009, 2012) identified that increasing the number of predictor variables does not necessarily increase the accuracy of the flood model and has a diminishing returns effect. Out of a pool of ten potential predictor variables, five were used for the final RFFE and the selected variables are listed below (Rahman *et al.* 2015):

- (a) catchment area ( $A$ ),
- (b) 6-hour 50% AEP (2-year return period) rainfall intensity at the catchment centroid ( $I_{6,2}$ ),
- (c) 6-hour 2% AEP (50-year return period) rainfall intensity at the catchment centroid ( $I_{6,50}$ ),
- (d)  $I_{6,2} / I_{6,50}$  ratio, and
- (e) shape factor ( $SHF$ ) computed as shown in Equation 2.23, using  $A$  and the shortest distance between catchment centroid and outfall ( $L_c$ ).

$$SHF = \frac{L_c}{\sqrt{A}} \quad (2.23)$$

Alexander (2002) utilised eight predictor variables to estimate the required design flood, as listed below:

- (a) catchment area ( $\text{km}^2$ ),
- (b) length of main channel (km),
- (c) average watercourse slope (m/m),
- (d) time of concentration,  $T_c$  estimated using the Bransby-Williams formula (hours),
- (e) point design rainfall (mm),
- (f) daily rainfall maxima (Adamson 1981) (mm),
- (g) number of days on which thunder was heard, and

- (h) rainfall intensity (mm.h<sup>-1</sup>).

Additional predictor variables that are utilised in other studies include, but are not limited to, the following:

- (a) MAP (Kjeldsen and Jones 2007),
- (b) upstream reservoir attenuation (Kjeldsen and Jones 2007),
- (c) runoff percentage (Kjeldsen and Jones 2007),
- (d) veld zone types (HRU 1972),
- (e) RMF K-regions (Kovács 1988),
- (f) potential evaporation (Mediero and Kjeldsen 2014), and
- (g) soil water retention capacity.

## 2.5 Performance Assessment

Rahman *et al.* (2012) detailed a number of statistics to assess the performance of the methods developed. Prior to application of the methods on a national scale, the method that yields the best performance statistics needs to be identified. The performance statistics to be utilised to assess the performance of the regionalisation methods are those adopted by Gado and Nguyen (2016). In addition to these statistics, Rahman *et al.* (2012) utilised the ratio of modelled vs estimated values and categorised the ratio of modelled and at-site values into the three distinct categories provided in Table 2.1. An additional measure used for the estimation of model accuracy is the Nash-Sutcliffe model efficiency coefficient (NSE) (Nash and Sutcliffe 1970). The NSE is generally used for the estimation of the efficiency of continuous models and when considering regression analysis is equivalent to the coefficient of determination ( $R^2$ ). Equations 2.24-2.29 provide six performance statistics used in RFFA studies.

Table 2.1 Categories of modelled vs at-site ratios Rahman *et al.* (2012)

Category	Under-estimation	Acceptable	Over-estimation
Ratio	< 0.5	0.5-2	> 2

$$RMSE^{CI,T} = \sqrt{\left(\frac{1}{n}\right) \sum (Q_m - Q_o)^2} \quad (2.24)$$

$$RMSE_r^{Cl,T} = \sqrt{\left(\frac{1}{n}\right) \Sigma \frac{(Q_m - Q_o)^2}{(Q_o)}} \quad (2.25)$$

$$BIAS^{Cl,T} = \left(\frac{1}{n}\right) \Sigma |Q_m - Q_o| \quad (2.26)$$

$$BIAS_r^{Cl,T} = \left(\frac{1}{n}\right) \Sigma \left(\frac{|Q_m - Q_o|}{Q_o}\right) \quad (2.27)$$

$$NSE = 1 - \frac{\Sigma_{i=1}^n (Q_m^i - Q_o^i)^2}{\Sigma_{i=1}^n (Q_o^i - \bar{Q}_o)^2} \quad (2.28)$$

$$Ratio^{S,T} = \frac{Q_{mod}}{Q_{AMS}} \quad (2.29)$$

where,

$RMSE^{Cl,T}$  = root mean squared error ( $m^3.s^{-1}$ ) for each cluster/region ( $Cl$ ) and AEP% ( $T$ ),

$BIAS^{Cl,T}$  = bias for each cluster/region ( $Cl$ ) and AEP% ( $T$ ),

$Ratio^{S,T}$  = ratio of modelled and at-site values for each site ( $S$ ) and AEP% ( $T$ ),

$n$  = number of sites,

$r$  = indicates relative values ( $BIAS_r$  and  $RMSE_r$ ),

$Q_m$  = modelled design peak flow ( $m^3.s^{-1}$ ), and

$Q_o$  = at-site design peak flow computed from the observed AMS ( $m^3.s^{-1}$ ).

Rahman *et al.* (2012) described the “Leave-one-out” (LOO) methodology, which is an alternative name for Jack-knife resampling, to assess the performance of models. This approach “hides” each gauging station from the model development for a single iteration per cluster, hence creating a number of models equal to the number of stations being considered, plus an iteration including all gauging stations (Overall). This facilitates a statistical test of proof of concept, which thereafter allows for the use of all sites in the final RFFA. After the LOO simulations, the evaluation statistics can be computed for the final  $Q_T$  values estimated using the developed models.

Rahman *et al.* (2012) notes that the limits presented above are arbitrary limits but provide a guide with regards to relative accuracy between models, however Naidoo (In Preparation) proposed the refined set of categories shown in Table 2.2.

Table 2.2 Revised categories of modelled vs at-site ratios

<b>Category</b>	<b>Under-estimation</b>	<b>Potentially Acceptable</b>	<b>Acceptable</b>	<b>Potentially Acceptable</b>	<b>Over-estimation</b>
<b>Ratio</b>	< 0.50	0.50-0.75	0.75 1.25	1.25-1.50	> 1.50

## 2.6 Conclusions

Generally non-contiguous fixed region, and hydrologic neighbourhood type (RoI) regionalisation approaches provide more accurate flood estimation than contiguous fixed region approaches, but spatial proximity has also been found in a number of studies to be important and the performance of the approaches has been found to be variable, dependent on the region and climate. In particular, the RoI approach has been found to be the preferred approach to regionalisation in recent studies. However, the subjectivity in regionalisation has also been highlighted as an issue which should be minimised.

The above studies have also highlighted the general preference for PRT rather than QRT to transfer information from gauged to ungauged sites.

Razavi and Coulibaly (2013) question the relevance and validity of regionalisation given the emerging issue of non-stationarity in hydrological time series and the impact of non-stationary data on regionalisation needs to be kept in mind.

### 3 METHODOLOGY

Based on the literature reviewed in Chapter 2, the methodology adopted required the completion of: (i) collation and assessment of observed streamflow data, (ii) the formation of homogeneous flood producing regions, (iii) selection of an appropriate parent distribution for flood frequency analysis, (iv) RM calibration, and (v) regional model development and assessment.

#### 3.1 Streamflow Data Assessment and Screening

The study utilised the stations identified by Nathanael (2015) and extended the data from December 2013 to September 2017 where possible. Primary flow data up to 2017 were obtained from the DWS. The data were then assessed both in terms of length of record and data quality using a number of criteria. In order to provide reliable design values, long records of data are required. Hence, selecting a minimum record length of 20 years for inclusion in the analysis reduced the number of stations that could potentially be utilised. The second screening process required the identification of human impacts on flow, such as dams, abstractions and urban development. Data from the WR2012 (de Groen *et al.* 2015) study, which contains registers of dams and abstractions, was used for the identification of potentially impacted stations, and secondary manual checks were also performed using aerial imagery to verify and supplement the WR2012 data. A number of dams that were not registered on the WR2012 database were identified during the manual checks.

The last criterion utilised was the quality of data. The DWS flow data contain many quality flags ranging from user errors to technical errors. Examples of this include the incorrect capture of data and hardware malfunction. The data set prepared by Van Bladeren (1993), which includes historical peak flow measurements, was included in the study and the data was extended to the 2017 hydrological year for the available sites and a combined data set was used in the study. Table 3.1 provides a summary of the screening criteria, similar to the methodology developed by described by Nathanael (2015), and data errors which were used to exclude stations from this study.

Table 3.1 Data errors and recommendations

<b>Screening Criteria and Data Error</b>	<b>Recommendation*</b>
Records shorter than 20 years	Exclusion of site for at-site FFA
Negative/null records	Exclusion of erroneous data
Recorded depth of flow exceeded discharge rating table at flow-gauging station (i.e. “Over-topping”)	Possible extension of the rating tables, otherwise exclusion of erroneous data
Missing periods	Annual records were assessed based on the number of records/days of missing data with possible exclusion of the year

As the national available data sets contain many thousands of years data, it was deemed to be impractical to assess the screening criteria and data errors manually. Therefore, as part of the study the above selection and quality criteria were automated, and recommendations generated based on the data received from DWS.

In some instances, the recorded river stage exceeded the available discharge rating curves for the flow-gauging stations. Where the rating curve of a station was exceeded, the viability of extending the existing rating curve was assessed. For example, as shown in Figure 3.1, the maximum rated level is 0.96 m, however, the maximum recorded water level for the station is approximately 3.20 m. In such cases simple extension of the rating curve could potentially produce major under- or over-estimation of peak flow events. Due to the nature of flow gauging weirs, as shown in Figure 3.2, an accurately extended rating curve would require an extensive survey and calibration beyond the structural limit. A general rule was therefore adopted that a rating curve may only be extended up to a maximum of 20% of the original maximum stage, as shown in Figure 3.1. In addition a limitation of 20% increase in flow discharge exceedance was adopted similar to Gericke and Smithers (2015). Where a rating curve is extended, a small grouping of 5% of the total number of points located at the upper end of the rating table was considered and a best-fit linear extension was applied. Although the number of stations that required extensions was not excessive, these values still need to be used with caution due to the uncertainty in the estimation of flow from the recorded stage.

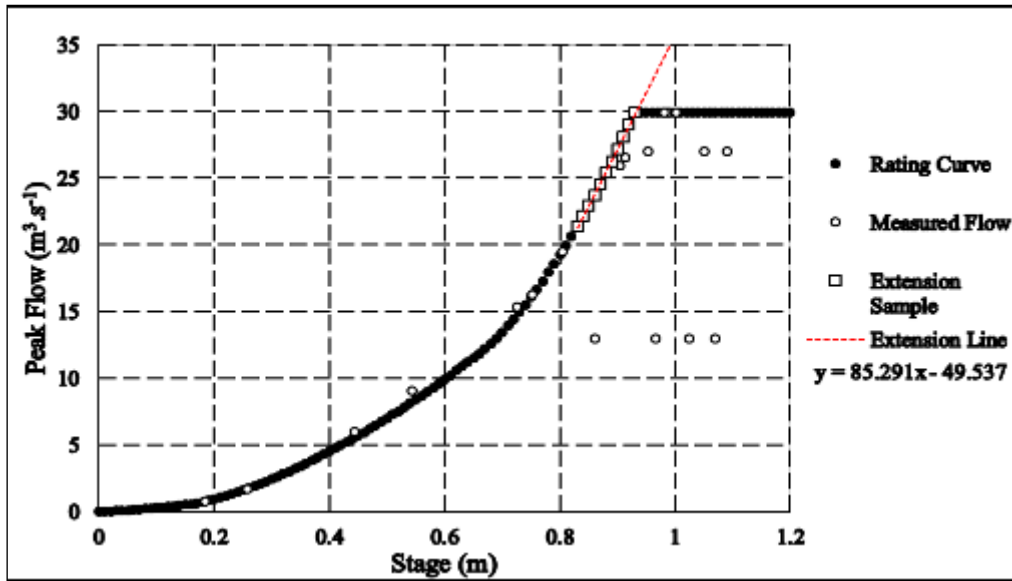


Figure 3.1 Example of a rating curve exceedance and extension the adopted extension methodology



Figure 3.2 Example of a flow gauging weir on the Tongati River at Riet Kuil (DWS 2015)

### 3.2 Selection of an Appropriate Parent Distribution

As is evident from a review of the literature, both in South Africa and internationally there are numerous differences between the recommendations and applications of distributions and the parameters estimation methods for flood frequency analysis. The distributions most commonly recommended in literature for use in South Africa are the GEV and LP3, in addition the popularity of the GPA and PE3 internationally and the findings by Kjeldsen *et al.* (2002) and Haile (2011) substantiate further investigation into its application within South Africa. In addition Kjeldsen *et al.* (2017) have provided a methodology to utilise the KAP distribution on a regional scale by determining a regional  $h$  shape parameter value, reducing the four parameter distribution to the three parameter KAP3. The cumulative distribution function of the KAP distribution is given in Eq. 3.1.

$$F(x) = \left\{ 1 - h[1 - k(x - \xi)/\alpha]^{1/k} \right\}^{1/h} \quad (3.1)$$

where  $\alpha$  is the scale parameter,  $\xi$  the location parameter, and  $k$  and  $h$  are shape parameters. Eight other distributions are special cases of the KAP distribution for fixed values of the  $h$  and  $k$  parameters, including the GPA ( $h = 1$ ), GEV ( $h = 0$ ) and Generalised Logistic (GLO) ( $h = -1$ ) distributions (Hosking 1994). The additional flexibility may be better suited to describe the hydrological variability of flood series across the contrasting geographical and climatological regions of South Africa. Thus, the KAP3 distribution utilising a national record length weighted mean  $h$  value was included in the assessment.

South African guidelines recommend the use of MM for parameter estimation, which are sensitive to the presence of outliers in the data. LM are theoretically less sensitive to the presence of outliers and have been adopted in numerous studies. South African hydrology is highly variable, which results in the inclusion of potential outliers in the datasets. Hence a total of five PDs (GEV, GPA, KAP3, LP3 and PE3) fitted using LM were assessed to identify the most suitable method in South Africa.

It has been shown that the selection of a distribution can be based on three types of assessment: (i) graphical methods, (ii) Goodness-of-Fit (GoF) tests, and (iii) model selection criterion. The most widely used approach for selection of distribution types in South Africa are graphical

methods used in isolation, whereas internationally graphical, GoF and model selection criterion are commonly applied in combinations. In this study, the model uncertainty was used as an additional selection criterion. To assess the PD uncertainty the bootstrapping methodology was selected as it is not reliant on the assumption that the sample parameters represent the population and that no distribution needs to be assumed. Given that it is recommended that the tests are not used in isolation the following methods were selected for use: The adopted selection approach is summarised in Figure 3.3

Table 3.2 List of test categories and the selected methods for selection of an appropriate Parent Distribution

Test Category	Methods
Graphical	KP method
Goodness-of-fit	AD, CS, CvM, KS
Model Selection Criterion	AIC, AICc, BIC
Model Uncertainty	Balanced bootstrapping

### 3.3 Regionalisation

Both RoI and K-means clustering were utilised for regionalisation. This allows for a comparison between the methods prior to implementation on a national scale. The methods utilise the Euclidian distance computed as shown in Equation 2.2, which is an indication of the relative distances between the stations in the attribute space. Given that the attributes utilised for the study vary in order of magnitude, parameter normalisation ( $x_n$ ) was undertaken to reduce the bias towards a single parameter. The normalisation adopted and used in Eq. 3.2 ensured that all parameters at site  $i$  ( $x_i$ ) were within the range of 0-1 by scaling them within the maximum and minimum range of each parameter ( $x$ ).

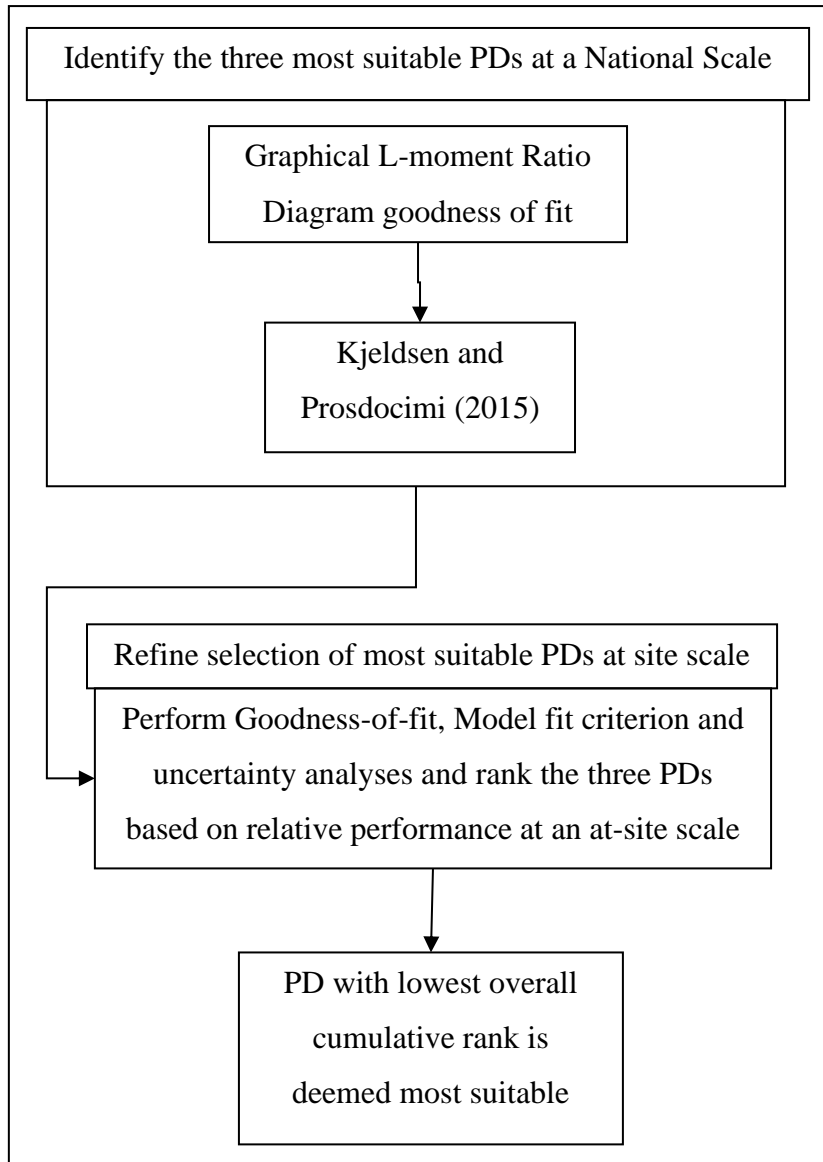


Figure 3.3 Methodology flow diagram for the selection of a suitable parent distribution

The location parameters, latitude and longitude were double weighted in comparison with the remaining catchment descriptors due to the findings by Merz and Blöschl (2005).

$$x_n = \frac{x_i - \min(x)}{\max(x) - \min(x)} \quad (3.2)$$

The clustering approach requires that the number of clusters be defined as one of the input parameters. The size of clusters was motivated by the 2/5T rule, with emphasis placed on the 1% AEP. This ensures that each cluster has a combined minimum record length of 200 years, fulfilling the 2T rule for the 1% AEP. The RoI approach creates unique regions for each site

investigated, with the 2T rule applied to ensure that the defined region satisfies the 2T rule for the 1% AEP.

The  $H$  testing statistic (Eq. 2.8) was used in conjunction with the discordancy measure, as described by Hosking and Wallis (1993), for homogeneity testing. Although the measure defined by Hosking and Wallis (1993) considers a region to be homogeneous if the value is less than one, it is considered relatively homogeneous with an  $H$  value of between one and two and relatively homogeneous regions are anticipated to provide more accurate DFE than single site FFA. As such an  $H$  value less than 2 was deemed suitable for application in this study.

### 3.3.1 Clustering

An iterative process was used in the identification of relatively homogeneous clusters, whereby the grouping of the full data set, and a set divided into the DWS regions were initially tested for homogeneity. The initial groupings were then assessed for homogeneity and adjusted as needed using the clustering of site descriptors, which allows for the formation of fixed clusters within which regional flood relationships can be developed.

The clustering efficiency was tested by performing the clustering multiple times to assess the impact of the chosen descriptor(s). Nine descriptors, listed below, and further described in Section 4.2, were tested in an iterative fashion ensuring that every possible unique combination of descriptors was used. The entire data set was used for the clustering for each iteration by initially dividing the data set into a maximum of 90 clusters, which allows for an average cluster size exceeding 200 years. This process also included the use of a minimum record length of 500 years, which equates to a maximum of 37 clusters. The descriptors used were:

- (a) outlet latitude,
- (b) outlet longitude,
- (c) outlet elevation,
- (d) catchment area,
- (e) areal mean SCS soil classification ( $SCS_{mean}$ ),
- (f) mean catchment runoff percentage ( $RO_{mean}$ ),
- (g) Mean Annual Precipitation ( $MAP_{mean}$ )
- (h) 10-year design rainfall intensity ( $I_{10yr}$ ), and
- (i) 100 vs 2-year design rainfall depth ratio ( $DRR_{100-2}$ ).

The clustering process is outlined in a flow diagram shown in Figure 3.4.

### **3.3.2 Region of influence**

Similarly, to the clustering approach adopted, the descriptors for formation of regions were not predetermined. Therefore, an iterative process of ensuring all parameter combinations were assessed using the  $H$  measure, was also applied. The RoI approach used by the UK FEH (1999), was applied and allows for the determination of regions based on the required record length, using the  $2/5T$  rule. The RoI process is outlined in a flow diagram shown in Figure 3.5.

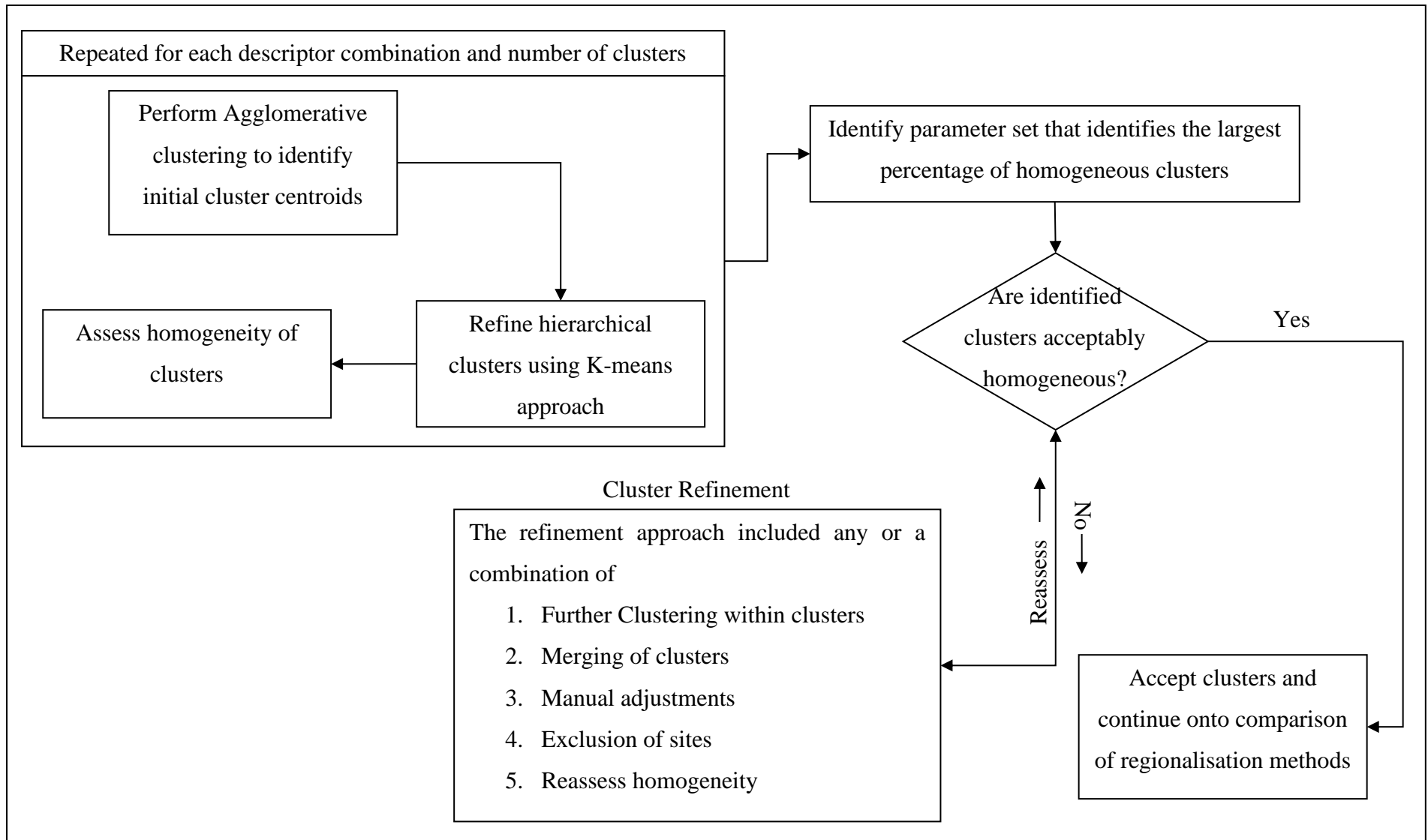


Figure 3.4 Clustering methodology flow diagram

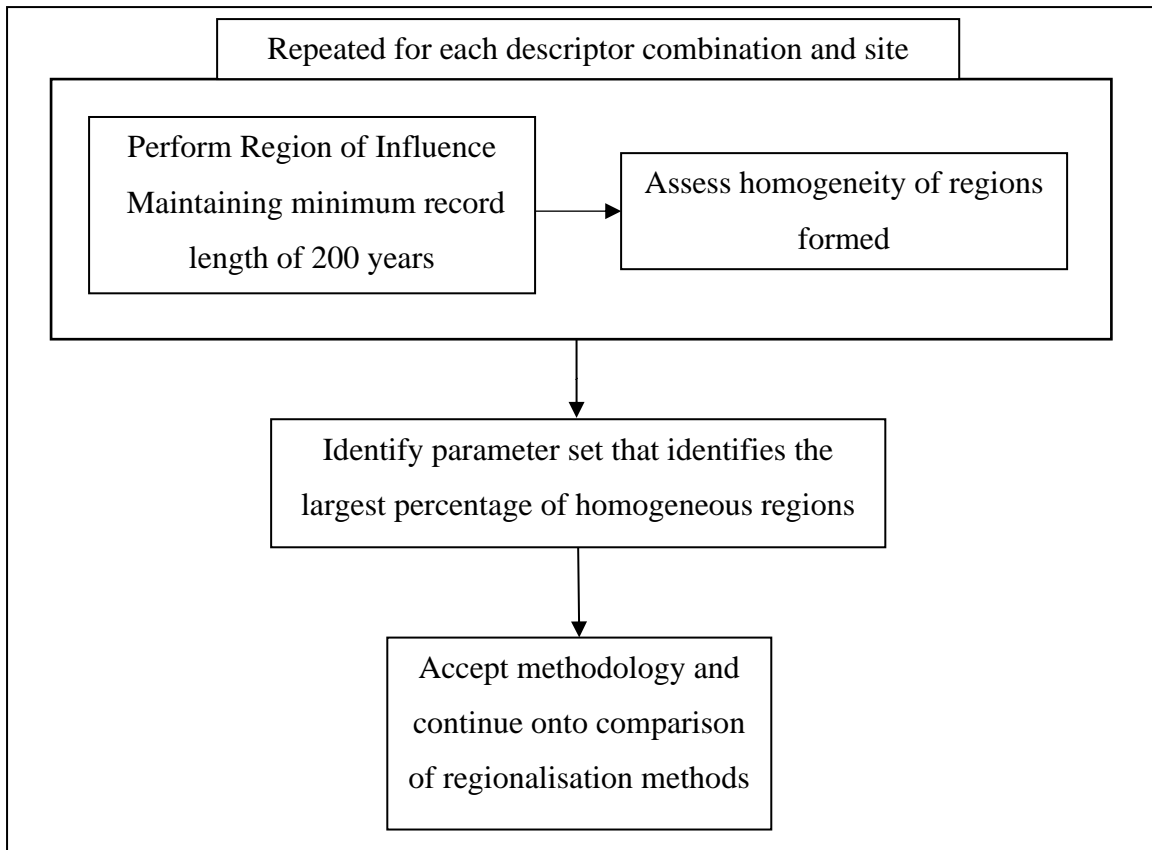


Figure 3.5 Region of Influence methodology flow diagram

### 3.4 Rational Method Calibration

The RM takes the form shown in Eq 3.3 and relates the  $T\%$  AEP peak flow ( $Q_T$ ) to the  $A$ , design rainfall intensity for a known  $T_c$  ( $I_{(T_c, T)}$ ) and the runoff coefficient  $C_T$ . A unit factor ( $U_F$ ) is also incorporated to convert peak flows to the desired units. To calibrate the RM, the relationship between the runoff coefficient  $C_T$  and the remaining parameters needs to be defined for each AEP and is provided in Eq 3.4.

$$Q_T = U_F C_T I_{(T_c, T)} A \quad (3.3)$$

$$C_T = \frac{Q_T}{U_F A I_{(T_c, T)}} \quad (3.4)$$

This allows for the derivation of a C value growth curve for each site being considered.

### 3.5 Model Development and Performance Assessment

The model development and performance assessment process was coupled and undertaken using the LOO approach. This allowed for the calculation of the six performance statistics identified in Section 2.5 for each iteration of the LOO process.

Two approaches to the model development have been implemented. Calitz (2016) showed that the use of a  $C$ -value index flood approach proved partially successful in Regions A, C and U. This approach utilises regressions to estimate  $C_{10}$ , and a growth curve, scaled using  $C_{10}$ , is used to estimate  $C_T$  for the remaining AEPs utilising the median values of the sites in the clusters. The  $C_{10}$  growth curve is a series of growth factors ( $GF_T$ ) for  $AEP = T\%$ . Considering that the approach has already proven partially successful locally, it was adopted for the study, with the intent to improve the estimates. This approach is a PRT that estimates the one of the parameters ( $C_T$  values) used to estimate the design floods. In addition, a regional index flood approach, which has been widely adopted internationally, was investigated to identify whether not requiring the additional step of converting the design quantiles to  $C$ -values improves the estimates.

Both of the model approaches were developed at two scales, National and homogeneous cluster. Kjeldsen *et al.* (2008) performed the development of a national scale model which increases the number of stations used in the development of the regressions, which theoretically provides an improved model for estimating ungauged catchments. Rahman *et al.* (2019), however, developed regional regression models for Australia due to the hydrological variability and variation in station density.

## 4 HYDROLOGICAL PARAMETER DATABASE

The development of a unified hydrological parameter database for use across multiple studies is a critical requirement for the development and application of methods for DFE in South Africa. A unified database would move much of the focus of flood studies from the development of parameter sets to the methods to be applied, thus providing a standard basis of comparison.

To ensure the reproducibility of the parameters, Python scripts were developed to extract the catchment parameters. This will also allow for the extraction of revised parameters as and when new datasets become available, e.g. improved Digital Elevation Model (DEM). All scripts and data utilised for the development of the database are open source and available on request.

### 4.1 Base Data Collation

Estimation of the hydrological parameters required the collection and collation of base datasets.

The base datasets required for the derivation of the selected parameters are:

- (a) DEM,
- (b) rainfall data, and
- (c) DWS data.

#### 4.1.1 Digital elevation model

The Shuttle Radar Topography Mission (SRTM) data was utilised for the development of the DEM. A hydrological conditioning process adjusts the DEM to ensure that flow directions derived from the surface define expected flow directions. A common methodology followed for hydrological conditioning is filling (Fernandez *et al.* 2016), whereby the DEM is assessed for any potential voids or impressions that could prevent the derivation of natural flow lines. After the voids or impressions have been identified, the elevations are increased until the water would flow along a natural pathway. Fernandez *et al.* (2016) identified that, although alternative methods are available for hydrological conditioning, the filling procedure maintained the slope descriptors of the catchment.

The 30 x 30 m SRTM grid was used and, where necessary, infilling was undertaken using the 90 x 90m grid. Infilling was, however, limited to a small region in primary drainage Region J. Nine DEM regions were created which divides South Africa into distinct catchment boundaries.

#### **4.1.2 Rainfall**

Three sets of rainfall data were utilised for the study, the Mean Annual Precipitation (MAP), the patched daily rainfall dataset (Lynch 2004) and design rainfall depths (Smithers and Schulze 2003).

The MAP dataset utilised was extracted from the Water Resources 2012 study (de Groen *et al.* 2015) and consists of a national MAP depth grid with a minute by minute grid spacing. The minute by minute design rainfall grid developed by Smithers and Schulze (2003) was utilised to derive the design rainfall depths.

#### **4.1.3 DWS data**

The DWS data utilised in the study included river networks, primary to quaternary catchment boundaries and gauging station locations. This data was utilised for verification and location purposes. Flow data was also acquired from DWS, as detailed in Section 3.1.

### **4.2 Parameter Estimation**

As identified in previous studies (McDermott and Pilgrim 1982, Robson and Reed 1999, Mkhandi *et al.* 2000, Alexander 2002, Van Bladeren 2005, Görgens 2007, Kjeldsen *et al.* 2008, Gericke 2010, Haile 2011, Rahman *et al.* 2015), the geographical location, rainfall intensity, MAP and catchment area are potential parameters used for the regionalisation of the peak flow estimation methods. Considering previous studies and the requirement of ease of application by practitioners, the following descriptors that are readily available, or simple to estimate, were selected for inclusion in the study:

- (a) outlet location,
- (b) outlet elevation,
- (c) catchment area ( $A$ ),

- (d) catchment centroid,
- (e) catchment perimeter,
- (f) rainfall region,
- (g) rainfall seasonality ( $R_s$ ),
- (h) catchment runoff percentage ( $C_{ro}$ ),
- (i) SCS soil classifications (SCS),
- (j) distance from the coast ( $D_c$ ),
- (k) hydraulic length / longest flow path ( $L$ ),
- (l) length to centroid ( $L_c$ ),
- (m) slope ( $S_{10-85}$ ,  $S_{ea}$ ,  $S_c$ ),
- (n) time of concentration ( $T_c$ ),
- (o) Areal Reduction Factor (ARF),
- (p) Mean Annual Precipitation ( $MAP$ ),
- (q) Design rainfall depths ( $DR_{2-100yr}$ ).

Further investigation identified that the use of catchment perimeter may lead to variability due to the fractal nature of the parameter. Bardossy and Schmidt (2002) highlight this and note that a number of methods to account for its fractal dimension have been proposed. The perimeter was therefore excluded from use but was still calculated for reference purposes.

#### **4.2.1 Catchment area**

The catchment areas were delineated using the TauDEM toolbox. The toolbox was chosen due to it being freely available and can be used outside of commercial GIS packages.

A problem was encountered with the delineation of catchment areas for the DWS gauging station locations, where the gauging stations were not located on the drainage paths defined by the hydrological conditioning, as explained in Section 4.1.1. This was corrected by manual manipulation of the gauging station locations to coincide with the defined drainage paths. On a national scale this will, however, not be an issue as the parameters will be derived on a 30 x 30 m grid. The drainage paths will be available for practitioners to assess the location of the ungauged site relative to the drainage path to ensure the correct catchment parameters can be extracted. A comparison of the catchment areas automatically calculated from the corrected

DEM and the catchment areas from DWS are shown in Figure 4.1. Due to the values ranging from 1 to 160 000 km<sup>2</sup> the values are presented on a log scale.

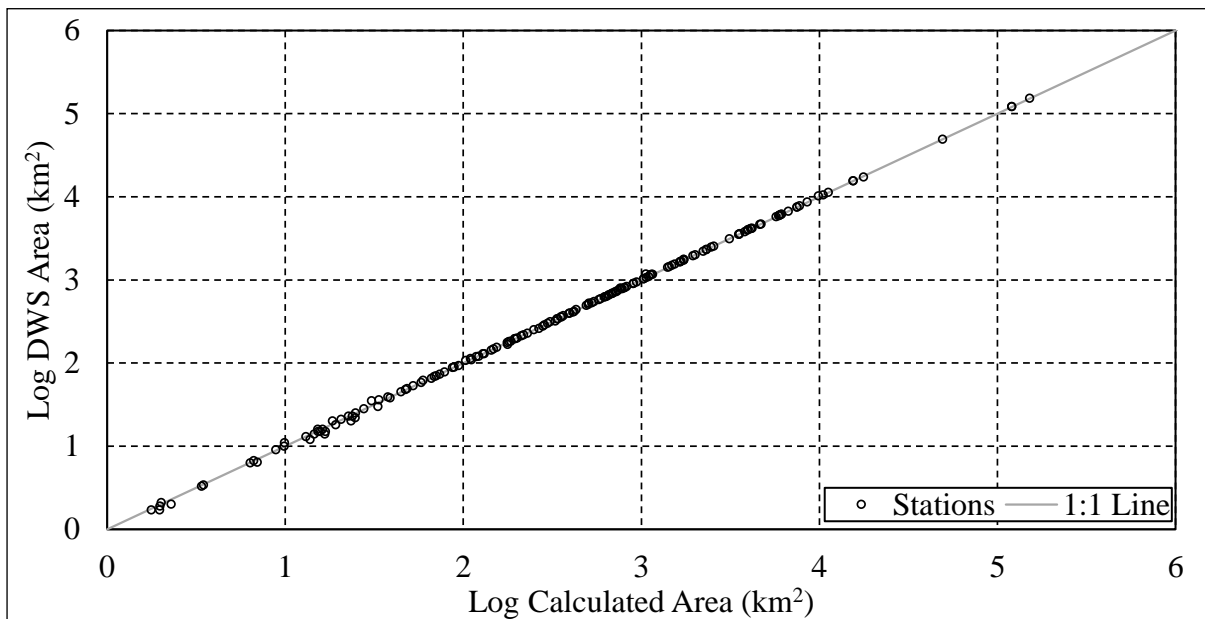


Figure 4.1 Catchment area comparison

#### 4.2.2 Longest flow path

A custom Python script, which utilises the Geospatial Data Abstraction Library (Team 2017) was developed that traces the longest flow path along the contributing area raster developed as part of the hydrological DEM corrections. Comparisons to previous studies undertaken has yet to be performed.

#### 4.2.3 Slope

SANRAL (2013) details three methods for the estimation of slope, all of which were calculated for each of the sites investigated:

- (a) 10-85 ( $S_{10-85}$ );
- (b) equal area ( $S_{ea}$ ); and
- (c) average catchment ( $S_c$ ).

$S_{10-85}$  and  $S_{ea}$  are considered average slope estimations, whereas  $S_c$  is considered a catchment slope estimator.  $S_{10-85}$  and  $S_{ea}$  are recommended as alternative methods. A comparison of the slopes, as shown in Figure 4.2, was undertaken to assess the variability of the estimates.

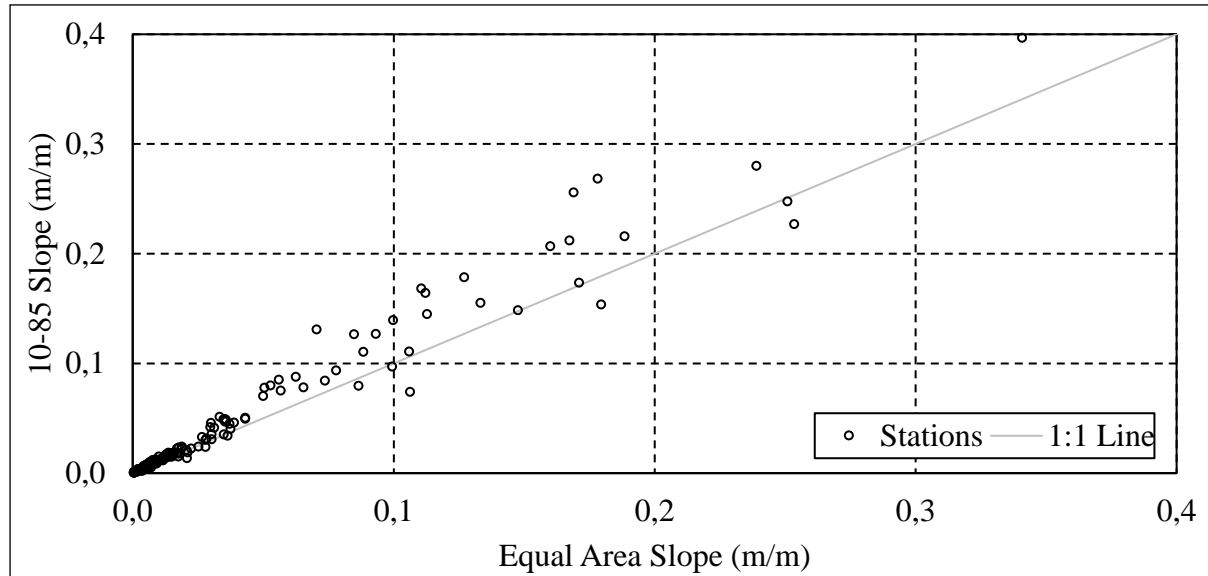


Figure 4.2 Average slope comparison

What is evident from Figure 4.2 is that there is a large variation of up to 86% between the estimation methods, with  $S_{10-85}$  consistently estimating steeper slopes than  $S_{ea}$  by an average of 15%. This will lead to estimates of shorter  $T_c$  and increased peak flows, which could be considered a more conservative approach. Therefore,  $S_{10-85}$  was utilised in this study.

A comparison of the slopes calculated in this study and slopes calculated in previous studies has not been undertaken.

#### 4.2.4 Time of concentration

Similar to the estimation of ARF, studies are currently underway to derive local relationships for  $T_c$  estimation. The studies are yet to be finalised and thus the recommended SANRAL (2013) drainage manual methods were selected for use in this study. The method utilised was the defined watercourse method developed by the US Bureau of Reclamation (USBR 1973) and is shown in Equation 4.1

$$T_c = \left( \frac{0.87 L^2}{1000 S_{10-85}} \right)^{0.385} \quad (4.1)$$

Although the USBR  $T_c$  method was not developed locally, the locally developed methods have been isolated to selected DWS drainage regions, as such the USBR method has been adopted for the estimation of  $T_c$ .

#### 4.2.5 Areal reduction factor

Although work is currently being undertaken to develop new  $ARF$  relationships for South Africa, the results are not yet available for use in this study. Therefore, the method proposed by Alexander (2001), as shown in Equation 4.2, which relates the  $A$  and  $T_c$  to the  $ARF$  was adopted.

$$ARF = (90\,000 - 12\,800 \ln A + 9\,830 \ln(60T_c))^{0.4} \quad (4.2)$$

#### 4.2.6 Rainfall based parameters

The MAP and design rainfall values were calculated at a catchment scale by averaging the gridded values over the catchment. For smaller catchments which contained no grid points within the catchment, the grid point closest to the catchment centroid was utilised to estimate the rainfall parameters.

Similarly,  $MAP_{max}$ ,  $MAP_{min}$  and  $MAP_{mean}$ , which represent the maximum, minimum and mean MAP values within the catchment, were derived. The use of the 30 x 30 m grid allows for the identification of the variation of the MAP within a catchment.

Rainfall seasonality was estimated using circular statistics as described by Burn (1997), by developing a monthly rain rose, as shown in Figure 4.3, per rainfall station being considered. A national plot of the mean seasonality direction is shown Figure 4.4. For this study the Lynch (2004) dataset was adopted due to the data being patched, removing any additional pre-processing.

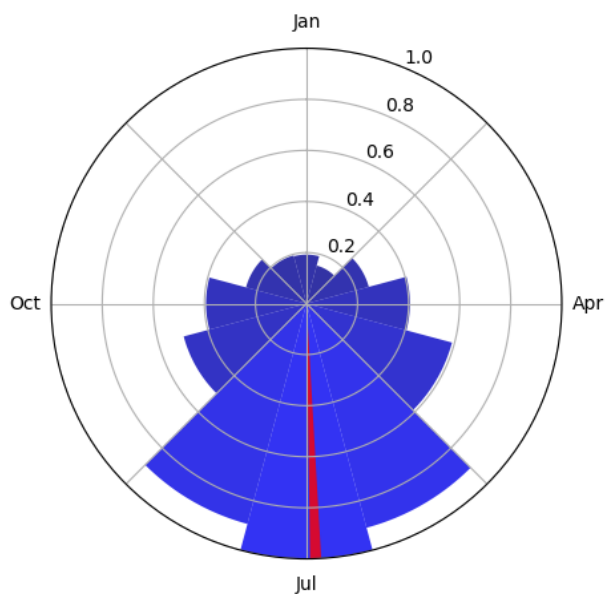


Figure 4.3 Normalised rainfall seasonality for station 0004816AW indicating the monthly (blue) and average (red) rainfall seasonality

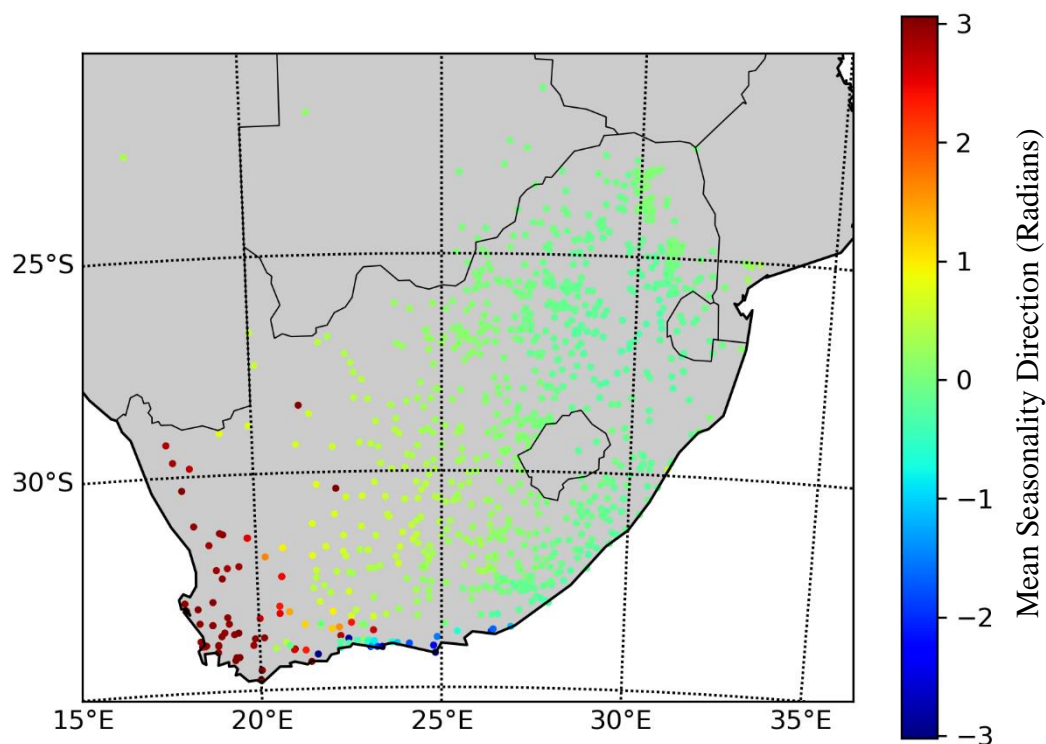


Figure 4.4 National rainfall seasonality indicating the mean direction (radians) of each site investigated

The rainfall regions utilised in the study consisted of the long term rainfall (Smithers and Schulze 2003), relatively homogeneous daily extreme rainfall (Smithers and Schulze 2000)

and short duration rainfall clusters (Smithers and Schulze 2000). The outlet position dictated the cluster for each gauging station considered.

#### **4.2.7 Catchment runoff**

Schulze (2011) developed catchment runoff percentages for naturalised land cover conditions using the ACRU model and simulating 50 years of runoff from daily rainfall data. The catchment runoff percentage was developed at a quinary level and incorporated into this study as a potential regionalisation parameter. Similarly, Schulze and Schütte (In Preparation)/. developed SCS soil characteristics for South Africa at a Terrain unit level.

## 5 STREAMFLOW DATA

The DWS currently has 1 458 streamflow gauging stations within South Africa. A total of 383 gauging stations remained after screening, assessment and cleaning and were utilised in the study. The gauging station locations are shown in Figure 5.1. The gauging stations are divided into 296 river gauges and 87 synthetic dam inflow records.

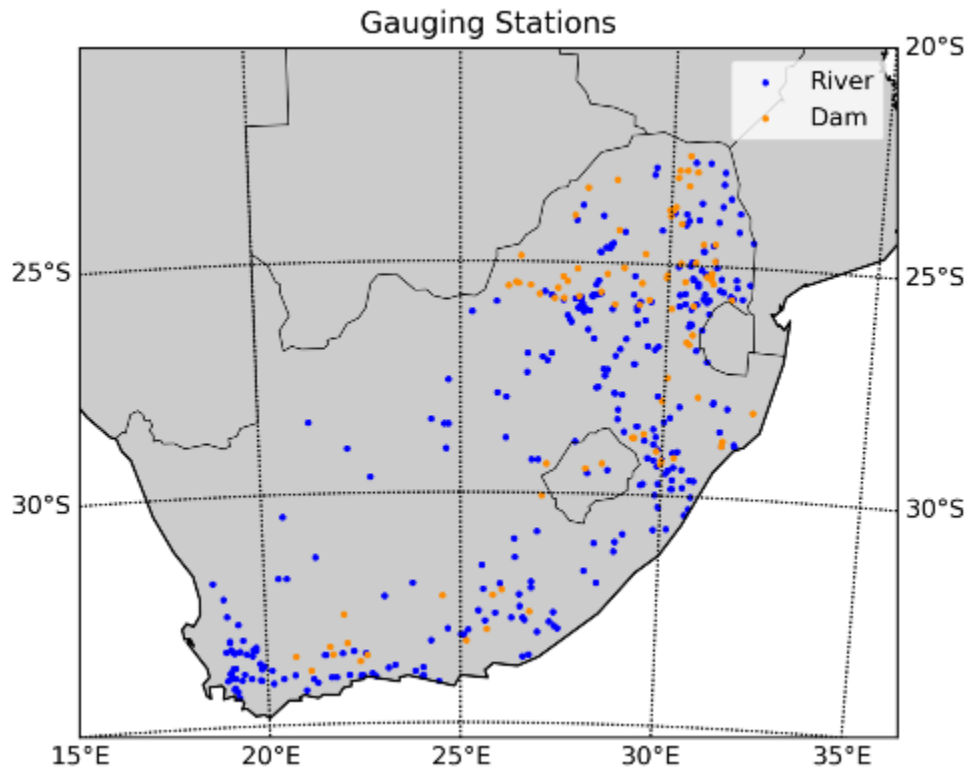


Figure 5.1 Map indicating the DWS gauging stations (blue) and the synthetic dam stations (orange) selected for application

### 5.1 Record Lengths

Table 5.1 and Figure 5.2 contains the breakdown of records lengths per DWS drainage region before and after data cleaning. Figure 5.3 shows the distribution of the record lengths per gauging station.

Table 5.1 Number of DWS flow-gauging stations and record lengths

DWS Drainage Region	No. of Gauging Stations	Cumulative Record Length (years)		Average Record Length (years)	
		Raw	Cleaned	Raw	Cleaned
A	62	3347	3314	54	53
B	47	2265	2253	48	48
C	34	1636	1432	48	42
D	20	1147	981	57	49
E	5	290	229	58	46
G	21	868	800	41	38
H	19	791	760	42	40
J	19	1091	1043	57	55
K	10	518	475	52	48
L	5	263	252	53	50
N	4	294	263	74	66
P	2	99	92	50	46
Q	14	635	628	45	45
R	4	176	146	44	37
S	3	179	171	60	57
T	13	782	625	60	48
U	12	619	570	52	48
V	28	1297	1511	46	54
W	19	916	890	48	47
X	42	2039	1914	49	46
TOTAL	383	19252	18349	50	48

## 5.2 Station Information

A summary of the raw data was generated for each station, as shown in Figure 5.4, which provides the DWS information for the station (Station number, catchment area, location, start and end date), a map layout of the station indicating the catchment boundary, longest flow path and the topography. In addition, the annual peak flow series available from DWS and the annual peak flow series generated from the primary flow data and the rating tables, including rating table extensions, are also shown.

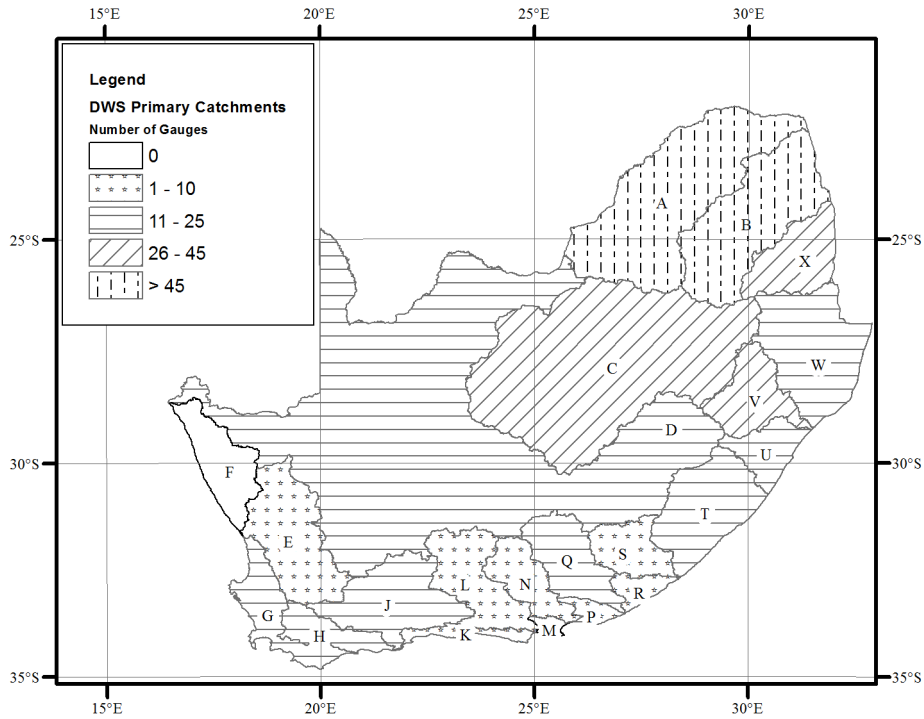


Figure 5.2 Number of gauging stations per DWS primary drainage region across South Africa

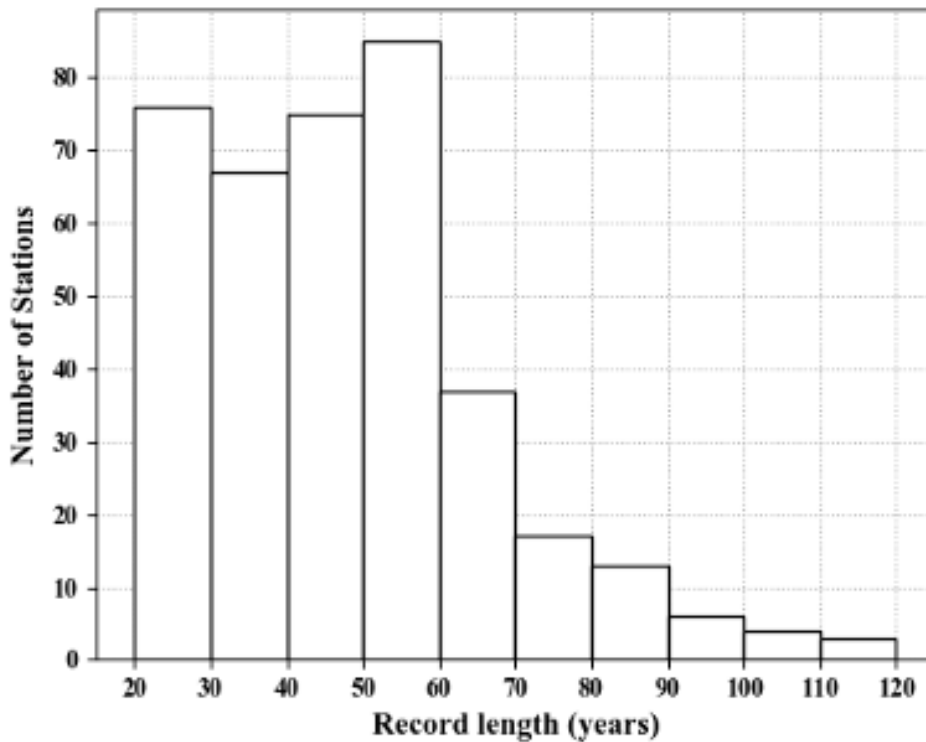


Figure 5.3 Histogram depicting the distribution of the station record lengths for the selected 383 gauging and synthetic dam stations

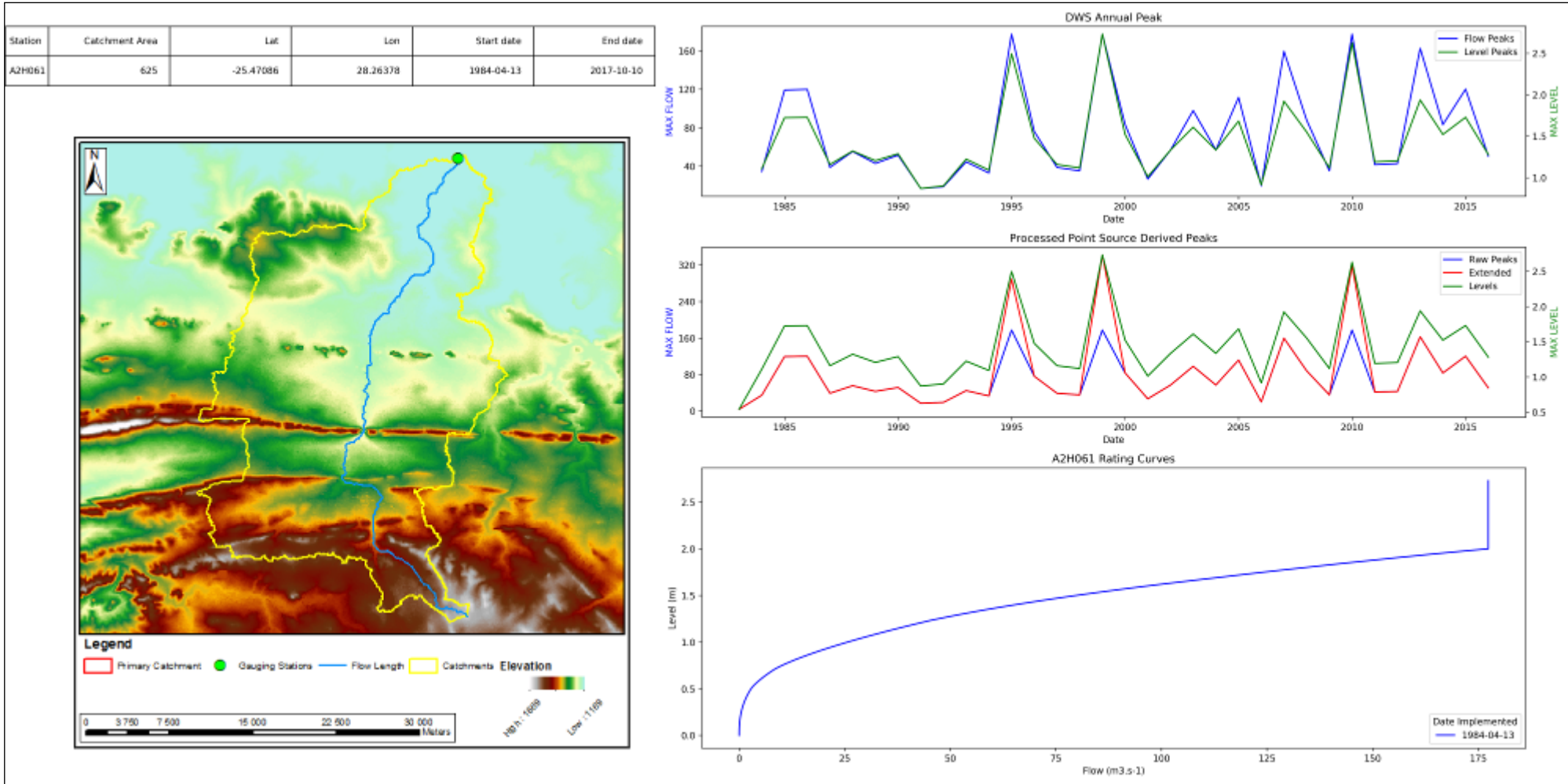


Figure 5.4 Catchment information for Gauging Station A2H061

## 6 IDENTIFICATION OF A PARENT DISTRIBUTION SUITABLE FOR FLOOD FREQUENCY ANALYSIS IN SOUTH AFRICA

In order to estimate design floods using observed flow data, it is necessary to select the best parent probability distribution to use in a flood frequency analysis. The design value computed from the observed data is then the best estimate of the design flood at the site and the performance of the other methods of estimating design floods at the site can be assessed using the design flood estimated from the observed data. During the course of this study an investigation was undertaken to identify the most suitable parent distribution for FFA in South Africa. Four categories of model selection methods were applied: (i) Graphical methods, (ii) Goodness-of-fit tests, (iii) model selection criterion, and (iv) model uncertainty.

### 6.1 National Kappa $h$ Value Estimation

Prior to undertaking the selection process the estimation of the national KAP3 distribution  $h$  value was required. Figure 6.1 shows the LMRD with the KAP  $h$  value contours, ranging from -1 to 1 at 0.25 intervals, and the record length weighted mean L-skew and L-kurtosis. From the mean coordinates the  $h$  value was estimated to be 0.77. Having established the national  $h$  value, the number of distributions being assessed increased to five: (i) GEV, (ii) GPA, (iii) KAP3 ( $h = 0.77$ ), (iv) LP3, and (v) PE3.

### 6.2 Graphical Methods

When considering the graphical approach all PDs considered were ranked for the performance at a national scale. The ranked order of selection are the KAP3 ( $h = 0.77$ ), GPA, LP3, GEV and PE3 distributions. When considering the graphical data representation using LMRD, as shown in Figure 6.2, the most suitable regional distributions are the LP3, GPA or KAP3 due to the close fit of the weighted moving average line to the theoretical lines. Table 6.1 provides the geometric rank of the GEV, GPA, KAP3, LP3 and PE3 distributions based on the KP test (Kjeldsen and Prosdocimi 2015).

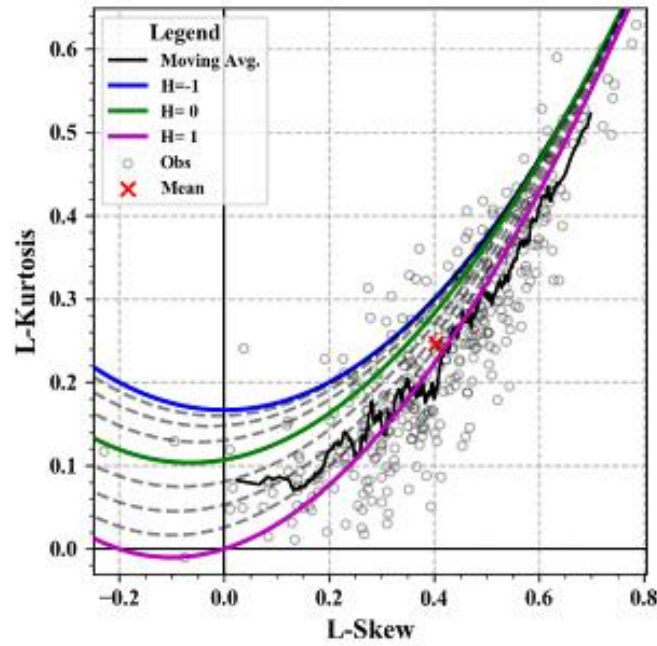


Figure 6.1 L-moment ratio diagram for all 383 selected sites using untransformed data indicating the KAPPA distribution  $h$  value contours at 0.25 intervals and the record length weighted mean L-skew and L-kurtosis.

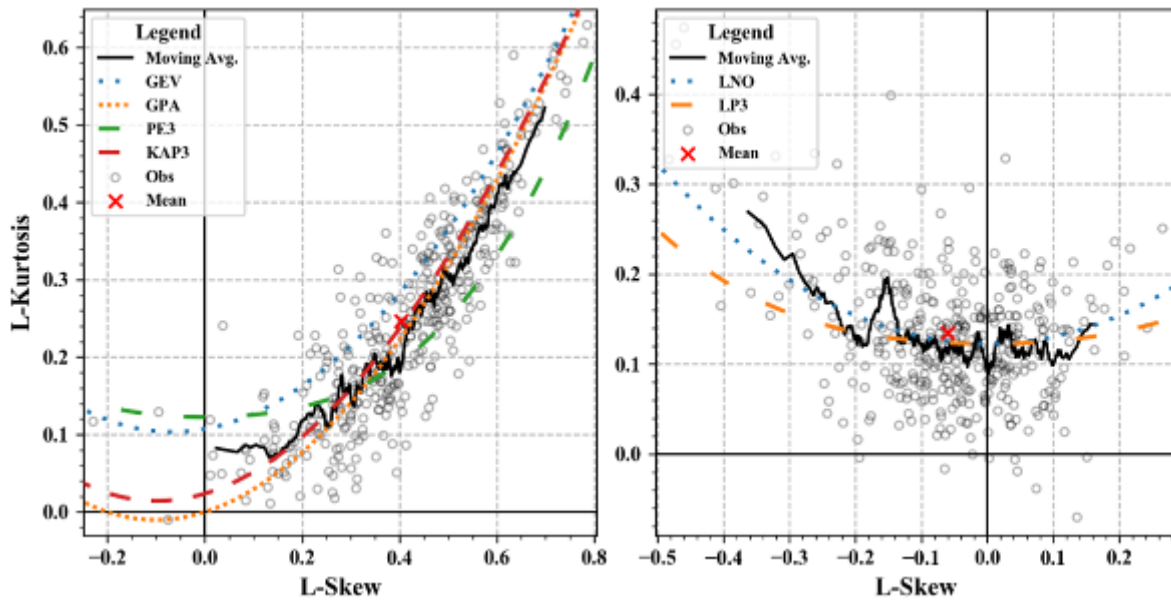


Figure 6.2 L-moment ratio diagram for all 383 selected sites using untransformed (left) and log transformed (right) data. The record length weighted mean (red cross) and moving average line are indicated (solid) in relation to the GEV, GPA, GNO, PE3, LNO and LP3 distributions.

Table 6.1 Rank of distributions based on the KP test in relation to the theoretical GEV, GPA, KAP3 ( $h = 0.77$ ), LP3, and PE3 distributions and the KP test

Distribution	Rank
GEV	4
GPA	2
KAP3	1
LP3	3
PE3	5

A LMRD indicating the DWS drainage region averages is presented in Figure 6.3, and it is evident that the regional averages are largely clustered around the GPA/KAP3 theoretical distributions for natural data, whereas the variation of the log transformed regional averages does not provide a clear fit around any distribution.

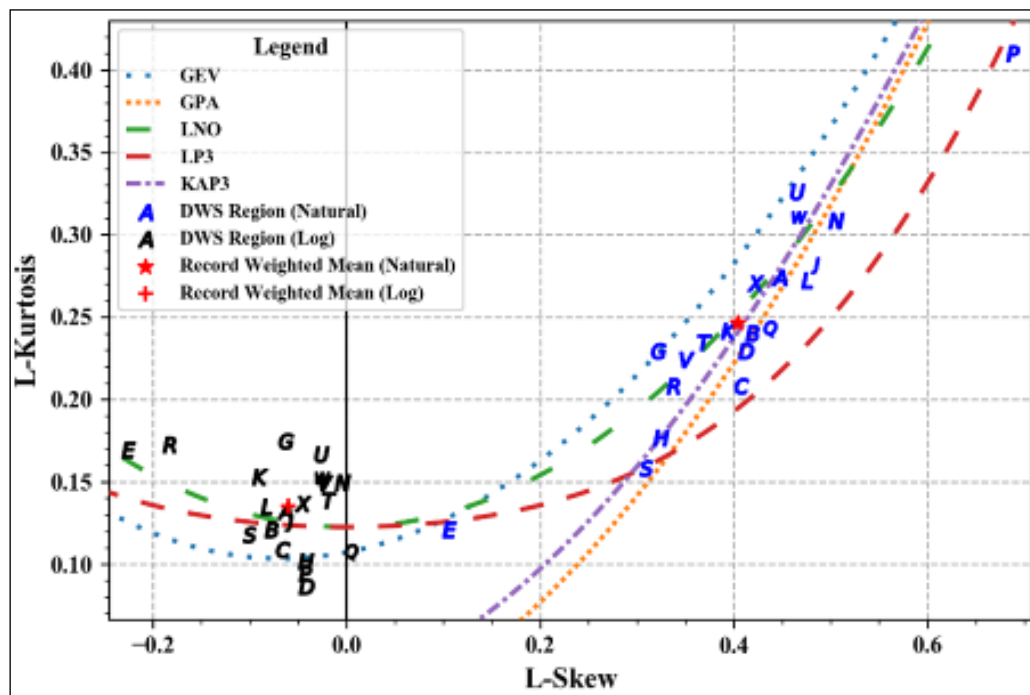


Figure 6.3 L-moment ratio diagram indicating the position of the record length weighted mean L-skew and L-kurtosis per DWS drainage region, represented by the relevant alphabetic numeral, for natural (blue) and log transformed (black) data as well as the record length weighted means of the entire dataset

### 6.3 Goodness-of-fit

The GoF tests applied consisted of the AD, CS, CvM and KS tests. Table 6.2 contains a summary of the number of sites (%) that were accepted for each GoF test and distribution considered. It is evident from the GoF test acceptance that the distribution that is accepted most frequently is the LP3. However, all distributions under consideration can be considered suitable options for the use in South Africa as an average GoF acceptance in excess of 80% is achieved by all distributions. The GPA and KAP acceptance levels are, however, only 49.9% and 68.4%, respectively for the AD test.

Table 6.2 Summary of the Anderson-Darling, Chi-squared, Cramer-von-Mises and Kolmogorof-Smirnov GoF test results for 383 sites in South Africa\*.

Distribution	GoF Test Acceptance (% of sites)					Rank
	AD	CS	CvM	KS	Average	
GPA	49.9	81.5	91.9	98.2	80.4	3
KAP3	68.4	79.4	90.6	98.2	84.2	2
LP3	<b>89.8</b>	<b>85.6</b>	<b>97.7</b>	<b>99.7</b>	<b>93.2</b>	<b>1</b>

\*Distribution with the highest acceptance rate is highlighted in bold

### 6.4 Model Uncertainty

The final consideration for the selection of a suitable distribution was estimating the uncertainty associated with the distributions being considered. Figure 6.4 shows the 90% confidence limits, calculated as a percent variance in relation to the original flood frequency analysis using the original dataset. The assessment of the uncertainty associated with the distributions was based on the 1% AEP due to its common application in practice and requirement in regulatory documents and the rank of the distributions is shown in Table 6.4.

### 6.5 Model Selection Criterion

The next assessment utilised the model fit criteria, which provide selections based on the relative best fits by comparing the information lost in the model fitting procedure for each distribution. The model fit criteria considered were the AIC, AICc and BIC. Table 6.3 contains the results of the best relative fit test, undertaken in an iterative manner due to the criterion providing relative fit results. Each iteration eliminates the distribution/s that is selected for the

lowest percentage of sites. From the model fit criterion, it is evident that the GPA, KAP, KAP3 and LP3 PDs are better suited for application in South Africa. The KAP was applied in the four-parameter format and hence was penalised more harshly by the model fit criterion, yet still retained a high selection rate. However, KAP could not be fitted to approximately 10% of sites considered, which eliminated the distribution in the penultimate iteration. Similar to the KAP distribution, the LNO distribution could also not be fitted to the all the stations. Based on the process undertaken, the GPA and LP3 distributions are selected for 54.2% and 45.8% of sites respectively. An investigation into the relationship between catchment descriptors and selected distribution provided no suitable descriptor to describe the variance in selection. In addition, the GPA distribution selection is only 10% more than the LP3 selection, which does not suggest that either of the distributions out performs the other at a national scale.

Table 6.3 Summary of iterations of model criterion test selections for South Africa, the distribution with the highest selection rate for each iteration is indicated in bold

Iteration	Distribution	Model Fit Criteria Selection (% of sites)			Rank
		AIC	AICc	BIC	
1	GPA	55.1	55.1	55.4	-
	KAP3	0.3	0.3	0	3
	LP3	44.6	44.6	44.6	-
2	GPA	<b>55.4</b>	<b>55.4</b>	<b>55.4</b>	<b>1</b>
	LP3	44.6	44.6	44.6	2

\* KAP eliminated due to lack of fit at 10% of sites considered

## 6.6 Distribution Ranking

Each distribution was ranked based on the performance for each test undertaken and is shown in Table 6.5. The GPA ranks highest in two of the approaches undertaken, followed by the KAP3 and LP3 both performing best in one of the two remaining approaches.

Table 6.4 Rank of distributions based on the uncertainty associated with the 1% AEP for 383 sites in South Africa

Distribution	Rank
GPA	1
KAP3	2
LP3	3

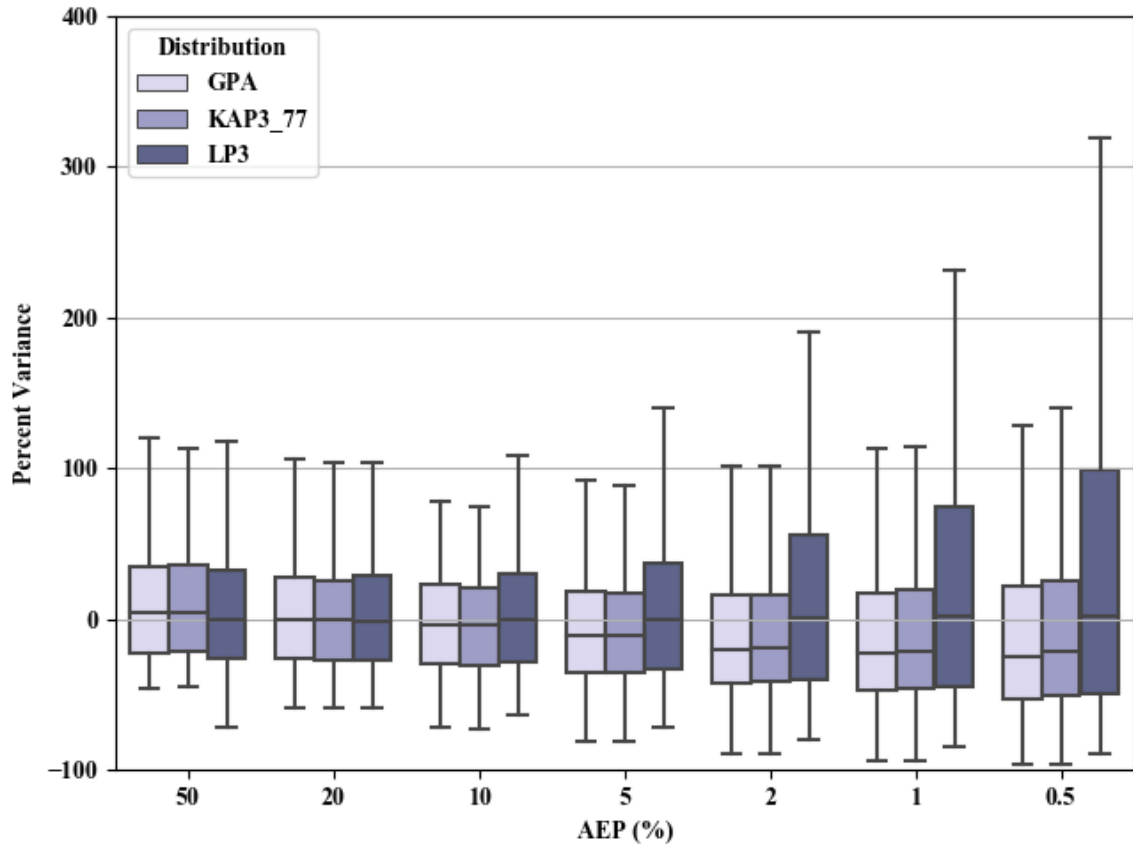


Figure 6.4 Variation of the 90% confidence bands presented as percentage variance of the balanced bootstrap confidence bands for the GPA, KAP3 ( $h = 0.77$ ), and LP3 distributions

Table 6.5 Rank of distributions for the Goodness-of-fit, model fit criterion, graphical and uncertainty tests. The best performing distribution is highlighted in bold.

Distribution	Graphical	GoF	Model Fit Criterion	Uncertainty	Total
GPA	2	3	<b>1</b>	<b>1</b>	7
KAP3	<b>1</b>	2	3	2	8
LP3	3	<b>1</b>	2	3	9

## 6.7 Discussion and Conclusions

The literature indicates that a large number of distributions for FFA are available and are prescribed internationally. However, in South Africa, little scientifically justifiable investigation has been undertaken into the most suitable distributions to use. This identified the need for a detailed scientific investigation in order to identify the most suitable distribution for use based on South African flow data.

Four separate approaches were applied at 383 locations, consisting of 296 river gauges and 87 synthetic dam inflows, for the selection of the most suitable distributions using graphical LMRD, GoF tests, model fit criterion and model uncertainty. The GoF tests indicated that the distribution with the highest acceptance rate is the LP3. However, given the high acceptance rates of all of the candidate distributions, little clarity was provided as nearly all the candidate distributions considered were accepted at the majority of the sites for all tests applied (AD, CS, CvM, and KS). To refine the results, model fit criterion (AIC, AICc, and BIC) were utilised to identify the relative best fit of the distributions under consideration. The model fit criterion refined the results, and the best fit models were the GPA and LP3.

The graphical method employed LMRDs and GoF was based on the KP test. Assessing the distributions using the KP test identified that the KAP3 was most suitable, followed by the GPA and LP3 distributions.

The final consideration for distribution selection was the estimation of the uncertainty associated with the distributions. Although the uncertainty is not traditionally used for the selection of a distribution, it has become an important consideration in hydrological modelling. Balanced bootstrapping was used to determine the uncertainty bands associated with each distribution for each site considered and it was evident that the most uncertain distribution was the LP3. The least uncertain distributions were the GPA, GEV and KAP3 respectively.

Based on the assessment undertaken it is recommended that the GPA, which is a special case of the KAP, is the most suitable PD to use when applying FFA on a national scale in South Africa.

## 7 REGIONALISATION

A summary of the regionalisation undertaken is presented in this chapter. Based on the literature reviewed, RoI and clustering methods were identified as applicable approaches to regionalisation for application in South African conditions. Each method has a unique set of benefits, e.g. the RoI method is often used in data rich regions, whereas clustering is often utilised in data poor regions.

### 7.1 Region of Influence

At each site being analysed the full set of potential descriptor combinations were tested in order to identify the best parameters for use in the selection of donor catchments in the RoI Approach. Enforcing the 5T rule, reduced the homogeneity of the regions in many instances and resulted in an increase of  $H$  beyond the adopted maximum value of 2. The best performing single parameter set was the Latitude, Longitude, Distance from the Coastline and mean runoff percentage which generated 16% and 51% homogeneous regions for 500- and 200-year minimum record lengths approaches, respectively.

In an attempt to increase the number of relatively homogenous regions identified through the use of the RoI the best combination of two parameter sets was considered. The best performing combination of two parameter sets was the combination of Area, Elevation, 24-hour 10-year design rainfall, latitude, longitude, mean SCS value and MAP combined with Distance from the coastline, Kovacs region, latitude, longitude and mean runoff percentage. By combining the two sets, 71% of regions formed were deemed to be relatively homogeneous.

### 7.2 Clustering

As an initial approach to cluster size selection, an analysis was undertaken to identify the relative homogeneity of all the stations used in the study and for stations per primary drainage regions. Table 7.1 indicates the improvement of the  $H$  measure when discordant sites have been removed from the data sets. However, it is still evident that even with the removal of the discordant stations the homogeneity requirement ( $H < 2$ ) is generally not met. The number of

discordant sites removed was determined by iteration after each exclusion, which required the further exclusion of additional sites.

Removal of the discordant sites from the entire data set and from Regions A and B caused additional sites to become discordant, doubling the required number of sites to be excluded. With the exception of Regions L, N, P, R and S, the regions were heterogeneous. Due to the lack of homogeneity in the remaining regions, and the need to exclude sites to achieve homogeneity, further division of the clusters was performed. All sites were considered for the cluster analysis in an attempt to maximise the number of sites used and ensure that cross catchment homogeneity was considered.

As highlighted in Section 2.4.2, various catchment parameters have been used in different studies as clustering variables. It is important to note that the growth curve descriptive statistics were excluded from the regionalisation to ensure that the homogeneity testing and cluster formation remain independent. All potential combinations of clustering variables were investigated and the combination that generated the largest number of homogeneous regions without manual intervention was adopted. The parameter combination used for further investigation was therefore Latitude, Longitude and Distance from the Coastline, which generated relatively homogeneous clusters in 44.4% of clusters as indicated in Table 7.2.

Table 7.3 provides the final accepted clusters. Clusters were adjusted using a combination of manual adjustments such as: (i) further clustering within clusters, (ii) merging of clusters, (iii) manual adjustment of clusters to improve spatial variations, and (iv) exclusion of sites. The final number of sites utilised in the relatively homogeneous clusters is 332. The formation of the relatively homogeneous clusters therefore required the exclusion of 51 sites (13%).

It is evident that a total of 42 relatively homogeneous clusters were created that all satisfy the  $H < 2$  requirement, however, in some instances the minimum record length of 200 years was relaxed with a minimum accepted record length of 129 in Cluster 18. The spatial representation of the accepted clusters is shown in Figure 7.1.

Table 7.1 Homogeneity testing for national and drainage regions

<b>Region</b>	<b>No. of Stations</b>	<b>Cumulative Record Length (years)</b>	<b><i>H</i> (Including Discordant Sites)</b>	<b><i>H</i> (Excluding Discordant Sites)</b>	<b>Total No. of Discordant Sites Removed</b>
National	411	18965	36.33	28.01	42
A	66	3626	10.87	8.64	4
B	52	2548	9.38	6.89	7
C	37	1679	5.62	5.62	0
D	20	1148	4.66	4.66	0
E	5	247	9.16	9.16	0
G	21	850	10.99	9.13	1
H	23	899	15.44	15.44	0
J	21	1083	6.99	4.95	3
K	10	504	10.18	10.18	0
L	6	295	0.25	0.25	0
N	6	326	0.00	0.00	0
P	2	100	0.29	0.29	0
Q	16	722	5.80	5.80	0
R	4	166	1.81	1.81	0
S	4	214	0.23	0.23	0
T	13	676	5.37	5.37	0
U	14	636	4.72	4.72	0
V	28	1554	3.36	2.60	2
W	20	957	4.91	4.91	0
X	43	2045	6.38	6.38	0

Table 7.2 Initial clustering

Cluster No.	No. of Stations	No. of Discordant Sites	$H_I^*$	Record Length (years)
1	29	1	9.1	1445
2	4	0	4.6	172
3	8	0	1.1	340
4	8	0	2.9	457
5	12	0	1.5	540
6	4	0	2.4	230
7	9	0	1.4	437
8	14	0	6.3	685
9	17	1	10.6	775
10	5	0	7.3	217
11	7	0	1.6	393
12	7	0	2.9	264
13	13	0	1.8	660
14	8	0	1.8	405
15	15	1	1.3	777
16	4	0	0.3	199
17	10	0	0.8	424
18	7	0	1.2	296
19	6	0	0.4	254
20	18	0	4.2	959
21	14	1	7.8	634
22	11	0	4.0	482
23	19	0	10.7	648
24	2	0	0.9	124
25	3	0	1.5	219
26	12	0	3.0	718
27	9	0	1.1	407
28	15	0	9.0	841
29	19	0	4.5	1043
30	28	0	6.7	1279
31	10	0	1.5	371
32	9	0	5.2	456
33	8	0	8.2	297
34	5	0	0.9	136
35	6	0	1.9	368
36	8	0	2.3	397

\* Shaded cells indicate relatively homogeneous clusters

Table 7.3 Accepted relatively homogeneous clusters

Cluster No.	No. of Stations	No. of Discordant Sites	$H_1$	Record Length (years)
1	10	0	1.5	357
2	15	0	1.6	860
3	5	0	1.0	325
4	11	0	1.9	530
5	12	0	1.5	540
6	6	0	1.2	329
7	5	0	1.8	184
8	7	0	1.5	431
9	10	0	0.8	424
10	8	0	1.9	424
11	9	0	1.8	389
12	6	0	1.3	198
13	8	0	1.8	405
14	12	0	1.3	517
15	8	0	1.1	340
16	7	0	0.6	276
17	3	0	0.6	191
18	4	0	1.0	129
19	7	0	1.2	296
20	6	0	0.4	240
21	8	0	1.8	230
22	8	0	1.9	263
23	5	0	1.3	182
24	5	0	1.0	192
25	6	0	1.9	368
26	5	0	1.5	299
27	6	0	1.9	280
28	5	0	0.2	252
29	8	0	2.0	400
30	5	0	1.9	241
31	8	0	0.1	374
32	7	0	1.5	317
33	11	0	1.4	507
34	9	0	2.0	387
35	18	0	0.7	1015
36	6	0	1.6	301
37	9	0	1.1	407
38	3	0	0.2	192
39	8	0	2.0	440
40	9	0	1.4	437
41	13	0	1.8	660
42	10	0	1.5	371

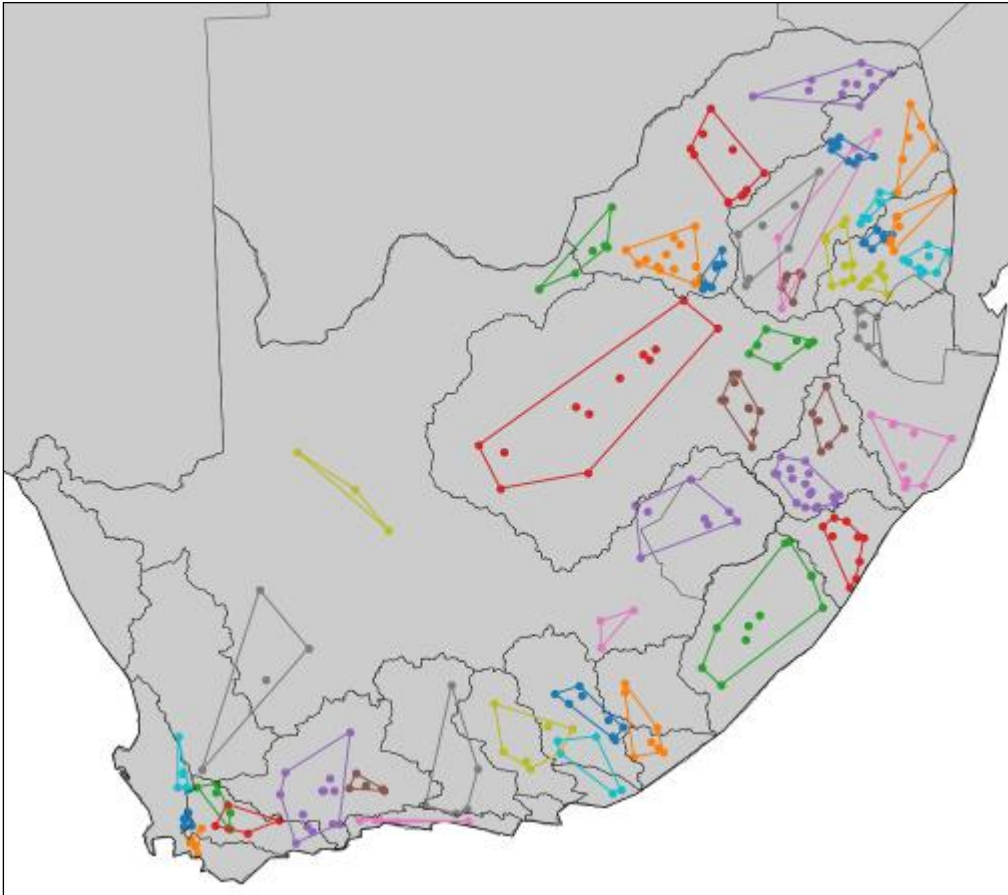


Figure 7.1 Distribution of the 42 relatively homogeneous clusters identified

### 7.3 Discussion and Conclusions

The RoI approach is flexible to the needs of the user, however once the rules of application are defined adjusting regions becomes difficult due to each site defining a unique region. The rigid nature, coupled with the low level of identification of homogeneous regions, in particular when considering the use of a single parameter set, results in a difficult to apply method, which could limit the uptake of the developed models.

In contrast, the Clustering approach has developed 42 relatively homogeneous regions that are distributed geographically. The simpler definition and geographic distribution of the regions provide an approach that has a higher probability of acceptance with practitioners. The 42 homogeneous clusters have therefore been adopted for the RM calibration and model development.

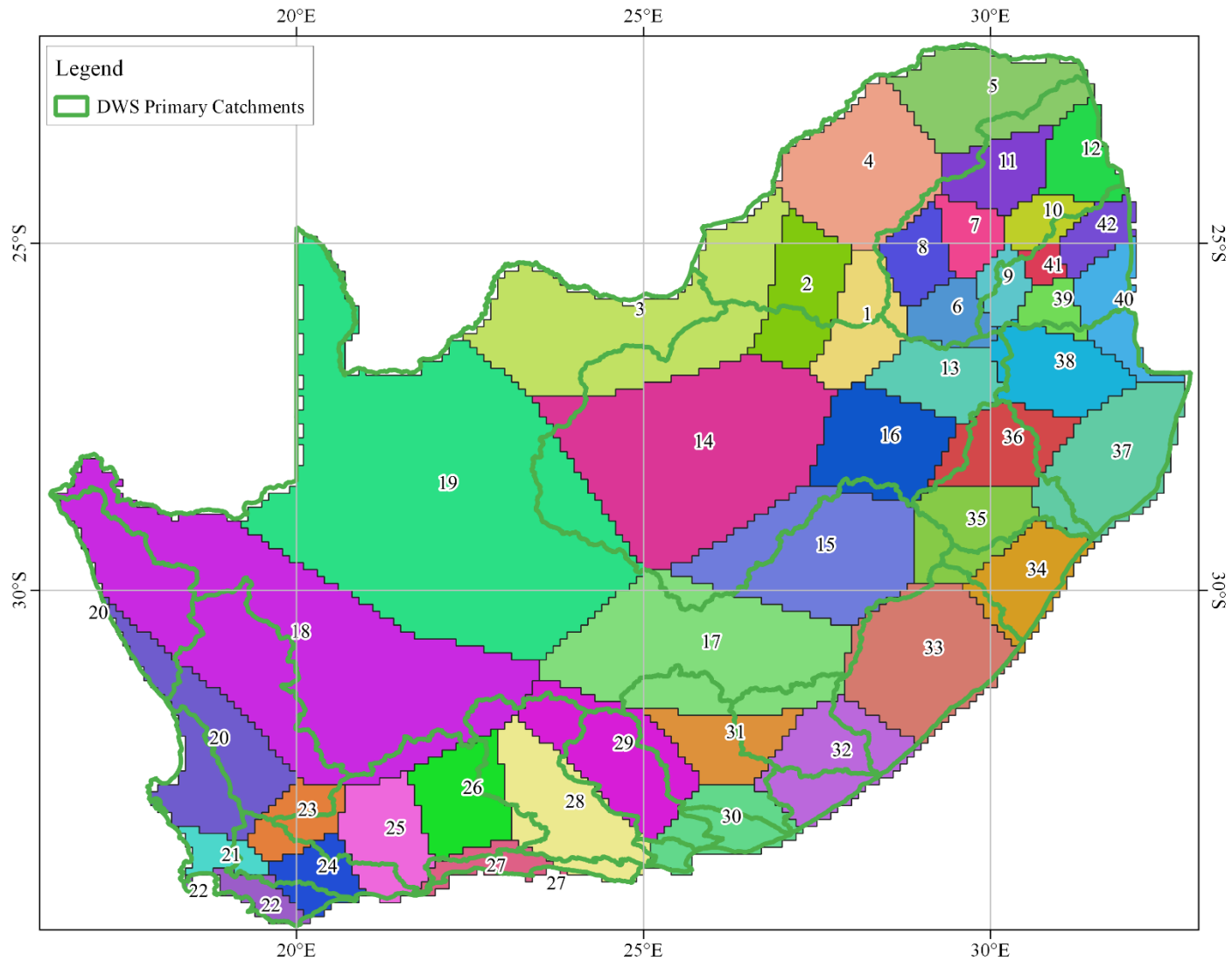


Figure 7.2 Delineation of national cluster association based on location and distance in relation to the DWS primary drainage regions (green) from the sea at a scale of 0.1 degrees

## 8 MODEL DEVELOPMENT AND ASSESSMENT

This chapter contains a summary of the development of models to for DFE at ungauged sites and assessment of the performance of the models.

Two distinct approaches were adopted for the development of models for the estimation of design floods at ungauged sites: (i) Regional Index Flood approach (RIF), and (ii) Calibrated PRM ( $C_T$ ) method. The RIF approach was adopted in an attempt to reduce the uncertainty identified when using the Calibrated  $C_T$  approach by Calitz (2016). It is believed that the conversion from quantile estimates to the  $C_T$ -values introduces additional uncertainty due to an increase in the number of parameters being considered, as well as the increase in complexity of the estimation of the  $C_T$  values. The  $C_T$  value approach is retained due to the simplicity of the application and current level of integration into current practice within South Africa.

The modelling process therefore follows the following steps:

- (a) identify the cluster that the sites belong to,
- (b) estimate the scaling factor based on the developed regressions, and
- (c) estimate the  $Q_T$  values using the regional dimensionless growth curves.

### 8.1 Regional Growth Curve Development

Utilising the 42 relatively homogeneous clusters developed in Chapter 6, regional growth curves were developed for each cluster. This required that the growth curves for each station in each cluster be converted to a dimensionless growth curve for the sites within the cluster, and this required the selection of a suitable scaling factor, commonly referred to as an index flood. This was followed by calculating the representative scaled (dimensionless) growth curve for each cluster. Thereafter, regressions were developed to estimate the scaling factor (index value) at ungauged sites in each cluster.

### 8.1.1 Quantile Growth Curves

Considering the results presented in Chapter 6, the GPA distribution was utilised for the estimation of the design values using the observed data and hence quantile growth curves at each site.

### 8.1.2 RM Calibration

The calibrated  $C_T$  values were found to have varied properties, as summarised in Table 8.1 for each relatively homogeneous cluster. Similar to the findings of Parak and Pegram (2006), the calibrated  $C_T$  values were found at some sites to not be consistent with the assumption that the  $C_T$  values should increase with a decrease in AEP. This occurred at 79 of the sites investigated. Parak and Pegram (2006) identified that the calibrated  $C_T$  values used in their study were within reasonable bounds when compared to Chow *et al.* (1988) and hence tentatively included the inconsistent results for the remainder of the study. Similarly, the sites with a decrease of  $C_T$  with AEP have been tentatively included in this study. It should also be noted that AEP's lower than 5% contain  $C_T$  values in excess of 1 at six sites for the 0.5% AEP and at a single site for 5% AEP. These values could have been the result of design rainfall estimates being restricted to use of the median values. Smithers and Schulze (2003) do, however, provide upper and lower 90% confidence bounds for estimates and these bounds could be investigated to restrict the  $C$ -values to not exceed 1.

Table 8.1 Summary of calibrated  $C_T$  values per AEP for the 42 homogeneous clusters

Cluster	Statistic	AEP (%)						
		50	20	10	5	2	1	0.5
1	Max	0.326	0.327	0.345	0.377	0.402	0.412	0.415
	Min	0.003	0.008	0.012	0.015	0.019	0.019	0.018
	Median	0.167	0.217	0.234	0.237	0.205	0.184	0.178
	Average	0.166	0.211	0.219	0.218	0.210	0.202	0.192
2	Max	0.052	0.094	0.124	0.152	0.212	0.273	0.350
	Min	0.003	0.008	0.012	0.015	0.019	0.019	0.018
	Median	0.030	0.060	0.082	0.109	0.137	0.166	0.201
	Average	0.031	0.060	0.081	0.104	0.138	0.168	0.202
3	Max	0.030	0.063	0.097	0.143	0.230	0.326	0.462
	Min	0.003	0.008	0.012	0.015	0.019	0.019	0.018
	Median	0.028	0.048	0.072	0.092	0.120	0.144	0.171
	Average	0.025	0.049	0.070	0.095	0.140	0.187	0.251

Cluster	Statistic	AEP (%)						
		50	20	10	5	2	1	0.5
4	Max	0.036	0.080	0.118	0.161	0.230	0.294	0.372
	Min	0.003	0.008	0.012	0.015	0.019	0.019	0.018
	Median	0.025	0.063	0.078	0.096	0.109	0.117	0.123
	Average	0.023	0.050	0.069	0.091	0.123	0.152	0.188
5	Max	0.135	0.247	0.299	0.391	0.533	0.663	0.818
	Min	0.003	0.008	0.012	0.015	0.019	0.019	0.018
	Median	0.030	0.062	0.087	0.114	0.165	0.215	0.266
	Average	0.047	0.090	0.120	0.152	0.201	0.248	0.307
6	Max	0.084	0.174	0.237	0.300	0.385	0.454	0.528
	Min	0.003	0.008	0.012	0.015	0.019	0.019	0.018
	Median	0.054	0.099	0.129	0.157	0.196	0.220	0.251
	Average	0.055	0.107	0.141	0.173	0.215	0.248	0.283
7	Max	0.146	0.182	0.176	0.162	0.157	0.158	0.156
	Min	0.003	0.008	0.012	0.015	0.019	0.019	0.018
	Median	0.082	0.112	0.115	0.111	0.102	0.094	0.088
	Average	0.089	0.120	0.123	0.121	0.114	0.108	0.101
8	Max	0.062	0.119	0.159	0.199	0.254	0.298	0.345
	Min	0.003	0.008	0.012	0.015	0.019	0.019	0.018
	Median	0.040	0.072	0.100	0.130	0.172	0.207	0.247
	Average	0.044	0.080	0.104	0.127	0.158	0.183	0.211
9	Max	0.123	0.181	0.194	0.195	0.186	0.178	0.213
	Min	0.003	0.008	0.012	0.015	0.019	0.019	0.018
	Median	0.050	0.078	0.090	0.111	0.142	0.162	0.164
	Average	0.055	0.088	0.104	0.117	0.130	0.138	0.146
10	Max	0.226	0.361	0.413	0.440	0.451	0.446	0.434
	Min	0.003	0.008	0.012	0.015	0.019	0.019	0.018
	Median	0.060	0.106	0.134	0.152	0.173	0.186	0.198
	Average	0.070	0.118	0.145	0.165	0.188	0.202	0.216
11	Max	0.071	0.150	0.207	0.268	0.358	0.437	0.655
	Min	0.003	0.008	0.012	0.015	0.019	0.019	0.018
	Median	0.024	0.053	0.074	0.104	0.140	0.171	0.208
	Average	0.030	0.060	0.084	0.112	0.158	0.206	0.270
12	Max	0.160	0.314	0.434	0.567	0.772	0.960	1.185
	Min	0.003	0.008	0.012	0.015	0.019	0.019	0.018
	Median	0.065	0.123	0.161	0.198	0.251	0.292	0.322
	Average	0.071	0.138	0.184	0.231	0.296	0.353	0.417
13	Max	0.238	0.397	0.462	0.499	0.519	0.521	0.515
	Min	0.003	0.008	0.012	0.015	0.019	0.019	0.018
	Median	0.080	0.151	0.198	0.239	0.266	0.307	0.377
	Average	0.116	0.196	0.238	0.271	0.308	0.334	0.361

Cluster	Statistic	AEP (%)						
		50	20	10	5	2	1	0.5
14	Max	0.123	0.252	0.343	0.434	0.561	0.663	0.776
	Min	0.003	0.008	0.012	0.015	0.019	0.019	0.018
	Median	0.045	0.083	0.101	0.118	0.143	0.170	0.186
	Average	0.054	0.106	0.138	0.168	0.205	0.233	0.263
15	Max	0.435	0.632	0.712	0.786	0.885	0.945	0.996
	Min	0.003	0.008	0.012	0.015	0.019	0.019	0.018
	Median	0.115	0.180	0.211	0.233	0.258	0.274	0.299
	Average	0.172	0.276	0.329	0.368	0.408	0.432	0.454
16	Max	0.114	0.239	0.343	0.459	0.638	0.801	0.995
	Min	0.003	0.008	0.012	0.015	0.019	0.019	0.018
	Median	0.081	0.139	0.177	0.213	0.263	0.309	0.360
	Average	0.082	0.146	0.192	0.238	0.304	0.361	0.426
17	Max	0.150	0.266	0.365	0.478	0.660	0.830	1.036
	Min	0.003	0.008	0.012	0.015	0.019	0.019	0.018
	Median	0.084	0.145	0.170	0.208	0.290	0.366	0.458
	Average	0.095	0.173	0.230	0.290	0.381	0.463	0.562
18	Max	0.068	0.135	0.184	0.236	0.316	0.387	0.469
	Min	0.003	0.008	0.012	0.015	0.019	0.019	0.018
	Median	0.021	0.049	0.074	0.105	0.159	0.216	0.293
	Average	0.033	0.070	0.098	0.129	0.178	0.226	0.286
19	Max	0.041	0.065	0.075	0.089	0.107	0.120	0.132
	Min	0.003	0.008	0.012	0.015	0.019	0.019	0.018
	Median	0.032	0.058	0.074	0.080	0.091	0.098	0.103
	Average	0.035	0.060	0.073	0.083	0.094	0.100	0.106
20	Max	0.425	0.534	0.552	0.546	0.519	0.494	0.467
	Min	0.003	0.008	0.012	0.015	0.019	0.019	0.018
	Median	0.166	0.204	0.205	0.198	0.183	0.172	0.161
	Average	0.208	0.265	0.276	0.274	0.263	0.251	0.239
21	Max	0.388	0.501	0.544	0.585	0.673	0.733	0.787
	Min	0.003	0.008	0.012	0.015	0.019	0.019	0.018
	Median	0.098	0.124	0.141	0.153	0.170	0.184	0.197
	Average	0.162	0.226	0.258	0.283	0.306	0.321	0.332
22	Max	0.059	0.134	0.187	0.242	0.321	0.387	0.460
	Min	0.003	0.008	0.012	0.015	0.019	0.019	0.018
	Median	0.025	0.049	0.073	0.098	0.122	0.160	0.209
	Average	0.030	0.057	0.078	0.101	0.139	0.174	0.219
23	Max	0.107	0.161	0.174	0.177	0.172	0.165	0.157
	Min	0.003	0.008	0.012	0.015	0.019	0.019	0.018
	Median	0.047	0.063	0.069	0.071	0.072	0.071	0.069
	Average	0.062	0.085	0.089	0.089	0.086	0.082	0.077

Cluster	Statistic	AEP (%)						
		50	20	10	5	2	1	0.5
24	Max	0.159	0.251	0.312	0.391	0.534	0.665	0.819
	Min	0.003	0.008	0.012	0.015	0.019	0.019	0.018
	Median	0.117	0.218	0.284	0.303	0.312	0.310	0.304
	Average	0.089	0.153	0.192	0.229	0.277	0.316	0.359
25	Max	0.225	0.401	0.479	0.528	0.565	0.578	0.682
	Min	0.003	0.008	0.012	0.015	0.019	0.019	0.018
	Median	0.050	0.102	0.142	0.185	0.228	0.301	0.379
	Average	0.072	0.130	0.166	0.199	0.245	0.282	0.325
26	Max	0.112	0.203	0.266	0.328	0.412	0.481	0.602
	Min	0.003	0.008	0.012	0.015	0.019	0.019	0.018
	Median	0.045	0.118	0.177	0.221	0.238	0.245	0.248
	Average	0.059	0.118	0.156	0.195	0.249	0.297	0.352
27	Max	0.264	0.388	0.453	0.500	0.546	0.571	0.588
	Min	0.003	0.008	0.012	0.015	0.019	0.019	0.018
	Median	0.140	0.212	0.240	0.253	0.259	0.256	0.249
	Average	0.167	0.236	0.262	0.275	0.280	0.279	0.274
28	Max	0.392	0.707	0.879	1.021	1.176	1.276	1.365
	Min	0.003	0.008	0.012	0.015	0.019	0.019	0.018
	Median	0.123	0.216	0.267	0.310	0.358	0.390	0.420
	Average	0.148	0.272	0.345	0.411	0.491	0.551	0.611
29	Max	0.074	0.114	0.155	0.213	0.312	0.414	0.547
	Min	0.003	0.008	0.012	0.015	0.019	0.019	0.018
	Median	0.046	0.085	0.115	0.136	0.157	0.173	0.194
	Average	0.050	0.087	0.111	0.136	0.171	0.203	0.241
30	Max	0.072	0.164	0.248	0.345	0.506	0.662	0.859
	Min	0.003	0.008	0.012	0.015	0.019	0.019	0.018
	Median	0.045	0.106	0.153	0.219	0.325	0.390	0.518
	Average	0.048	0.115	0.170	0.235	0.343	0.451	0.590
31	Max	0.060	0.110	0.143	0.173	0.210	0.238	0.267
	Min	0.003	0.008	0.012	0.015	0.019	0.019	0.018
	Median	0.039	0.064	0.083	0.098	0.126	0.146	0.163
	Average	0.039	0.067	0.085	0.103	0.127	0.145	0.165
32	Max	0.128	0.180	0.235	0.289	0.362	0.419	0.481
	Min	0.003	0.008	0.012	0.015	0.019	0.019	0.018
	Median	0.081	0.149	0.142	0.164	0.199	0.227	0.255
	Average	0.081	0.130	0.154	0.174	0.197	0.213	0.230
33	Max	0.293	0.413	0.461	0.487	0.498	0.502	0.583
	Min	0.003	0.008	0.012	0.015	0.019	0.019	0.018
	Median	0.148	0.200	0.211	0.209	0.213	0.216	0.235
	Average	0.151	0.219	0.250	0.270	0.287	0.295	0.301

Cluster	Statistic	AEP (%)						
		50	20	10	5	2	1	0.5
34	Max	0.137	0.294	0.429	0.589	0.853	1.109	1.430
	Min	0.003	0.008	0.012	0.015	0.019	0.019	0.018
	Median	0.053	0.101	0.108	0.124	0.154	0.214	0.286
	Average	0.075	0.135	0.176	0.217	0.278	0.333	0.400
35	Max	0.256	0.361	0.397	0.411	0.410	0.471	0.574
	Min	0.003	0.008	0.012	0.015	0.019	0.019	0.018
	Median	0.108	0.177	0.220	0.245	0.268	0.307	0.339
	Average	0.116	0.173	0.206	0.233	0.266	0.291	0.318
36	Max	0.179	0.266	0.300	0.318	0.325	0.323	0.317
	Min	0.003	0.008	0.012	0.015	0.019	0.019	0.018
	Median	0.104	0.152	0.176	0.194	0.211	0.213	0.211
	Average	0.109	0.158	0.178	0.190	0.198	0.201	0.201
37	Max	0.217	0.445	0.614	0.793	1.060	1.296	1.569
	Min	0.003	0.008	0.012	0.015	0.019	0.019	0.018
	Median	0.086	0.139	0.174	0.215	0.280	0.360	0.461
	Average	0.093	0.173	0.234	0.300	0.401	0.494	0.606
38	Max	0.103	0.157	0.177	0.187	0.190	0.187	0.189
	Min	0.003	0.008	0.012	0.015	0.019	0.019	0.018
	Median	0.050	0.078	0.094	0.106	0.121	0.129	0.138
	Average	0.053	0.081	0.095	0.106	0.117	0.125	0.132
39	Max	0.124	0.216	0.297	0.394	0.558	0.715	0.914
	Min	0.003	0.008	0.012	0.015	0.019	0.019	0.018
	Median	0.049	0.082	0.110	0.129	0.165	0.194	0.226
	Average	0.057	0.096	0.125	0.155	0.202	0.246	0.302
40	Max	0.099	0.159	0.207	0.256	0.320	0.368	0.419
	Min	0.003	0.008	0.012	0.015	0.019	0.019	0.018
	Median	0.036	0.065	0.093	0.124	0.149	0.167	0.186
	Average	0.045	0.081	0.105	0.128	0.159	0.186	0.216
41	Max	0.048	0.063	0.071	0.078	0.085	0.090	0.093
	Min	0.003	0.008	0.012	0.015	0.019	0.019	0.018
	Median	0.015	0.023	0.025	0.025	0.030	0.034	0.039
	Average	0.020	0.028	0.032	0.035	0.038	0.040	0.042
42	Max	0.049	0.096	0.131	0.166	0.218	0.260	0.308
	Min	0.003	0.008	0.012	0.015	0.019	0.019	0.018
	Median	0.033	0.070	0.091	0.118	0.164	0.194	0.227
	Average	0.035	0.067	0.089	0.112	0.145	0.173	0.204

### 8.1.3 Scaling factor

For both adopted modelling approaches, a choice had to be made for the selection of the most appropriate scaling variable for the developed regional growth curves. The ARR (Pilgrim 2001)

and Calitz (2016) both adopted the  $C_{10}$  value to scale the RM growth curves, which proved successful, and was therefore adopted in this study for the calibrated  $C_T$  method. For the development of a regional index flood approach, the use of the MAF or MEF, as defined in Section 2.1.1, are widely reported in the literature. Hence, both the MAF and MEF values were assessed for use in the study, however, the MAF value proved to be most representative and reduced the spread of the dimensionless growth curves within a cluster.

#### 8.1.4 Dimensionless growth curves

Having calibrated the RM at each site, cluster based dimensionless growth curves were developed using the  $C_{10}$  value to scale the individual at-site curves. Similarly, the at-site growth curves and the site MAF were used to derive at-site dimensionless growth curves for the development of the RIF approach. An example of the dimensionless growth curves for a cluster is shown in Figure 8.1 and the growth curves for all clusters are included in Appendix A, reference can be made to Figure 7.2 to identify curves. Table 8.2 and Table 8.3 show the cluster based  $C_T$  and RIF dimensionless growth factors, respectively.

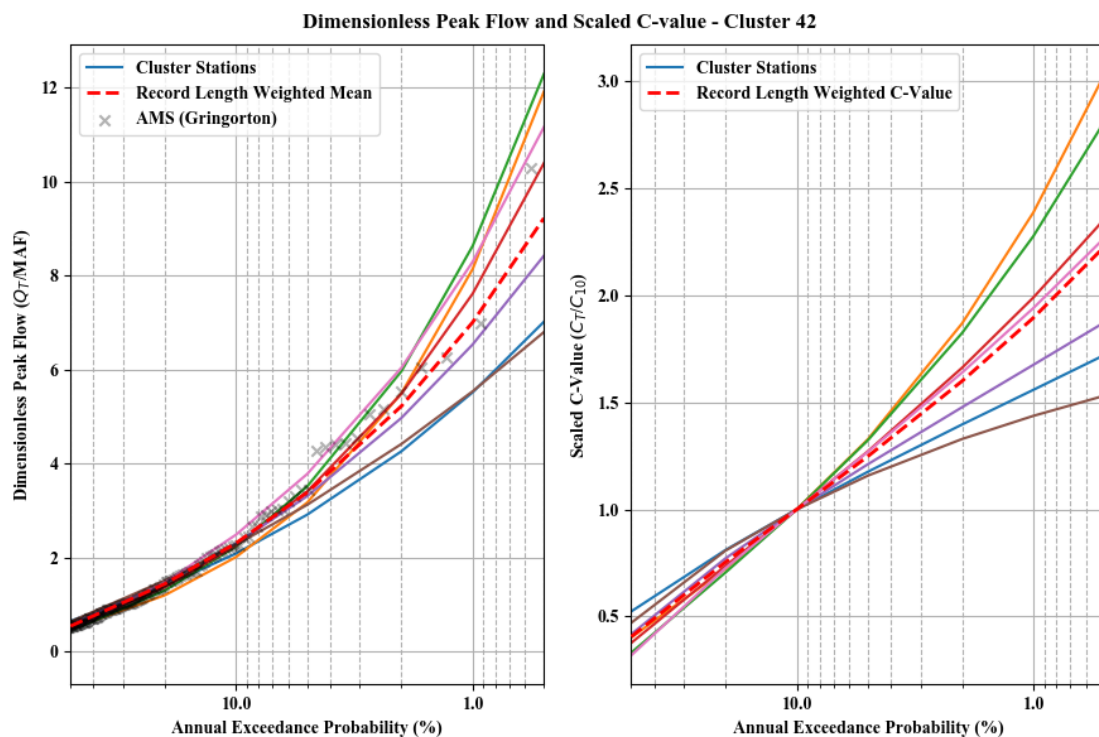


Figure 8.1 Dimensionless Peak flow (left) and Scaled  $C_T$  growth curves (right) for Cluster 42 indicating the record length weighted average curves (red dash) in relation to the sites within the cluster (coloured lines)

Table 8.2 Dimensionless  $C_T$  curves for each relatively homogeneous cluster

Cluster	Growth Factor ( $GF_T$ ) per AEP (%)						
	50	20	10	5	2	1	0.5
1	0.75	0.96	1.00	1.00	0.97	0.93	0.89
2	0.39	0.74	1.00	1.27	1.68	2.03	2.45
3	0.37	0.71	1.00	1.34	1.93	2.54	3.36
4	0.31	0.70	1.00	1.33	1.85	2.34	2.97
5	0.39	0.74	1.00	1.28	1.72	2.13	2.65
6	0.40	0.77	1.00	1.22	1.50	1.72	1.94
7	0.72	0.97	1.00	0.98	0.93	0.89	0.84
8	0.44	0.78	1.00	1.20	1.48	1.70	1.95
9	0.51	0.83	1.00	1.14	1.28	1.38	1.47
10	0.46	0.80	1.00	1.17	1.37	1.51	1.65
11	0.38	0.73	1.00	1.31	1.83	2.35	3.05
12	0.40	0.77	1.00	1.21	1.50	1.72	1.97
13	0.46	0.80	1.00	1.18	1.40	1.58	1.77
14	0.39	0.77	1.00	1.21	1.47	1.66	1.87
15	0.49	0.81	1.00	1.17	1.37	1.52	1.67
16	0.44	0.77	1.00	1.23	1.54	1.81	2.12
17	0.41	0.76	1.00	1.24	1.60	1.92	2.30
18	0.32	0.71	1.00	1.32	1.83	2.33	2.97
19	0.47	0.82	1.00	1.14	1.29	1.38	1.45
20	0.76	0.97	1.00	0.99	0.94	0.89	0.84
21	0.61	0.86	1.00	1.11	1.24	1.33	1.41
22	0.40	0.73	1.00	1.31	1.81	2.30	2.92
23	0.71	0.95	1.00	1.00	0.96	0.91	0.86
24	0.42	0.77	1.00	1.23	1.54	1.81	2.11
25	0.43	0.78	1.00	1.21	1.50	1.74	2.01
26	0.37	0.75	1.00	1.26	1.64	1.97	2.36
27	0.67	0.92	1.00	1.03	1.03	1.00	0.97
28	0.41	0.77	1.00	1.22	1.51	1.74	1.99
29	0.43	0.77	1.00	1.23	1.56	1.85	2.18
30	0.28	0.67	1.00	1.39	2.06	2.73	3.62
31	0.47	0.79	1.00	1.20	1.45	1.66	1.88
32	0.55	0.86	1.00	1.11	1.22	1.30	1.37
33	0.61	0.88	1.00	1.08	1.16	1.20	1.24
34	0.48	0.80	1.00	1.19	1.48	1.73	2.05
35	0.56	0.83	1.00	1.15	1.34	1.49	1.65
36	0.64	0.90	1.00	1.06	1.09	1.10	1.10
37	0.41	0.75	1.00	1.27	1.67	2.03	2.47
38	0.52	0.83	1.00	1.15	1.33	1.47	1.62
39	0.46	0.79	1.00	1.22	1.53	1.82	2.19
40	0.43	0.77	1.00	1.23	1.55	1.82	2.14
41	0.60	0.86	1.00	1.11	1.22	1.29	1.36

Cluster	Growth Factor ( $GF_T$ ) per AEP (%)						
	50	20	10	5	2	1	0.5
42	0.41	0.75	1.00	1.25	1.60	1.89	2.23

Table 8.3 Dimensionless RIF growth curves for each relatively homogeneous cluster

Cluster	Growth Factor ( $GF_T$ ) per AEP (%)						
	50	20	10	5	2	1	0.5
1	0.85	1.54	1.95	2.28	2.63	2.83	2.99
2	0.53	1.41	2.28	3.38	5.30	7.20	9.61
3	0.44	1.27	2.19	3.45	5.89	8.57	12.28
4	0.45	1.40	2.38	3.66	5.96	8.32	11.40
5	0.50	1.40	2.31	3.48	5.56	7.65	10.33
6	0.59	1.52	2.35	3.30	4.76	6.07	7.56
7	0.83	1.67	2.15	2.52	2.89	3.10	3.27
8	0.56	1.44	2.29	3.32	5.04	6.69	8.69
9	0.70	1.55	2.21	2.89	3.81	4.54	5.29
10	0.64	1.53	2.28	3.11	4.33	5.37	6.51
11	0.44	1.32	2.27	3.56	5.98	8.57	12.09
12	0.56	1.55	2.44	3.47	5.11	6.58	8.29
13	0.63	1.52	2.28	3.14	4.42	5.53	6.77
14	0.59	1.59	2.44	3.39	4.81	6.01	7.35
15	0.64	1.51	2.25	3.08	4.33	5.40	6.59
16	0.62	1.49	2.25	3.13	4.50	5.72	7.11
17	0.55	1.45	2.30	3.35	5.10	6.77	8.82
18	0.44	1.41	2.40	3.69	6.01	8.38	11.46
19	0.69	1.61	2.31	3.02	3.97	4.70	5.44
20	0.92	1.52	1.80	1.99	2.14	2.22	2.27
21	0.78	1.46	1.97	2.46	3.09	3.56	4.02
22	0.52	1.40	2.29	3.40	5.35	7.30	9.76
23	0.88	1.58	1.94	2.21	2.45	2.57	2.66
24	0.57	1.46	2.30	3.32	4.99	6.56	8.46
25	0.55	1.49	2.37	3.42	5.14	6.75	8.68
26	0.46	1.39	2.34	3.59	5.86	8.20	11.26
27	0.76	1.56	2.12	2.64	3.29	3.74	4.16
28	0.56	1.50	2.37	3.39	5.03	6.54	8.32
29	0.54	1.42	2.29	3.37	5.23	7.04	9.31
30	0.34	1.20	2.20	3.65	6.62	10.06	15.05
31	0.64	1.49	2.23	3.07	4.37	5.50	6.79
32	0.69	1.58	2.27	2.97	3.94	4.68	5.45
33	0.76	1.50	2.05	2.60	3.32	3.86	4.39
34	0.56	1.40	2.21	3.23	4.99	6.71	8.86
35	0.71	1.45	2.06	2.74	3.73	4.56	5.47
36	0.80	1.52	2.01	2.44	2.94	3.27	3.57
37	0.47	1.32	2.23	3.45	5.74	8.17	11.45

Cluster	Growth Factor ( $GF_T$ ) per AEP (%)						
	50	20	10	5	2	1	0.5
38	0.67	1.49	2.19	2.95	4.07	5.01	6.05
39	0.61	1.45	2.23	3.14	4.61	5.96	7.56
40	0.55	1.42	2.27	3.31	5.09	6.81	8.94
41	0.72	1.47	2.08	2.71	3.61	4.32	5.08
42	0.54	1.43	2.30	3.38	5.22	7.00	9.22

## 8.2 Model Development

For both the  $C_{10}$  and the  $MAF$  the development of regressions for the estimation of the scaling parameters utilised three of eight catchment descriptors considered. The three parameters were selected by developing ordinary least squares models using all the available catchment descriptors and iteratively eliminating the descriptors with the highest p-values until only three descriptors remained. In addition to the removal of the highest p-values, only descriptors with p-values less than 0.05 were retained. For both the  $C_{10}$  and  $MAF$  the most significant, and therefore adopted, descriptors were the catchment area, MAP and the distance from the coastline and the adopted model equation is provided in Equation 8.1.

$$\ln(SF) = a * \ln(A) + b * \ln(MAP) + c * \ln(D_c) + Const \quad (8.1)$$

where

$SF$  = Scaling Factor ( $MAF$  or  $C_{10}$ )

a, b, c = model coefficients, and

$Const$  = intercept (constant).

Two approaches were used for the development of the regressions, one at a national scale estimation and the other a cluster based approach. The national approach pools all the data (332 sites) to develop the model for estimating the scaling variable. A review of the required number of stations to improve the overall model estimates was undertaken and it was found that using less than 30 sites affected the estimation of the scaling factor, whereas exceeding 30 sites reduced the benefit gained from increasing the number of sites. Thus the cluster based approach utilises a minimum of 30 stations for the development of the scaling variable model. Where clusters contain less than 30 stations, the closest geographic clusters were included until a minimum of 30 sites was reached. Geographic proximity was defined by the distance between cluster centroids. The adopted scaling variable model coefficients are contained in Table 8.4

and a comparison between the observed and estimated values are shown in Figure 8.2 and Figure 8.3 for the  $C_{10}$  and MAF models, respectively.

Similarly, plots were developed for the  $Q_T$  estimation of both the RIF and  $C_T$  approaches when estimating the SF using national- and a cluster based scales and are shown in Figure 8.4 to Figure 8.7.

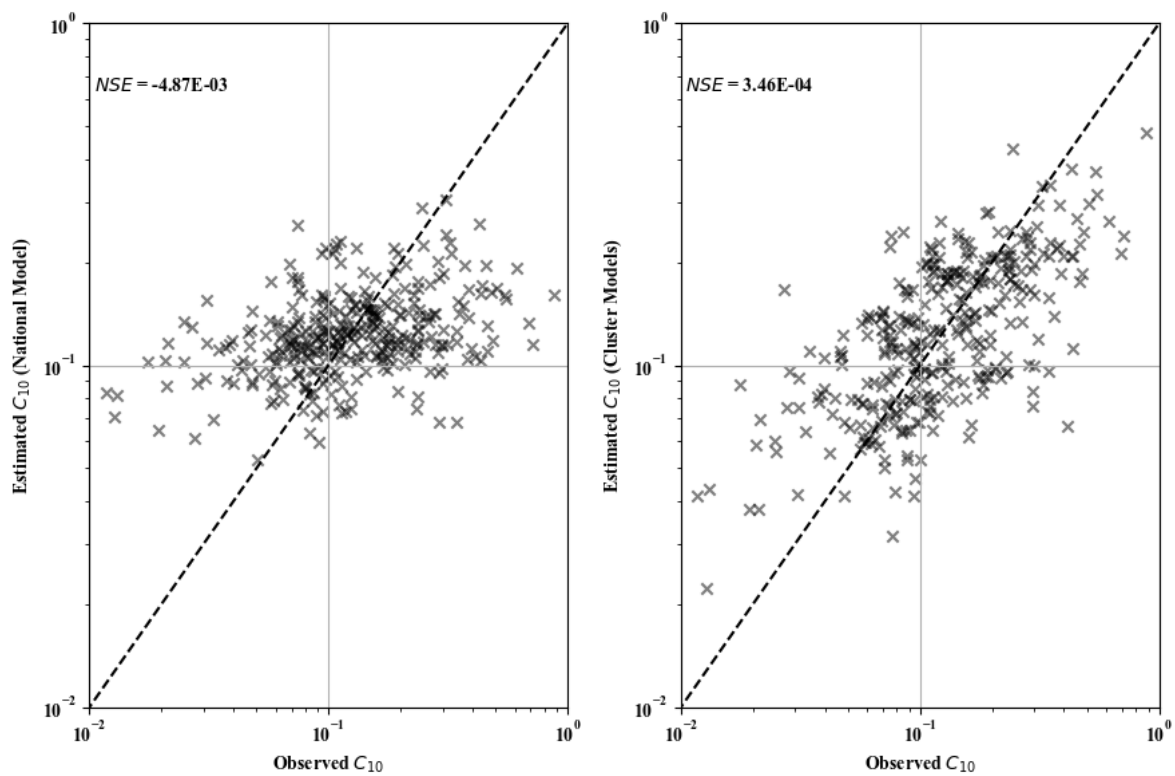


Figure 8.2 Observed versus estimated  $C_{10}$  for the national- (left) and cluster based (right) models

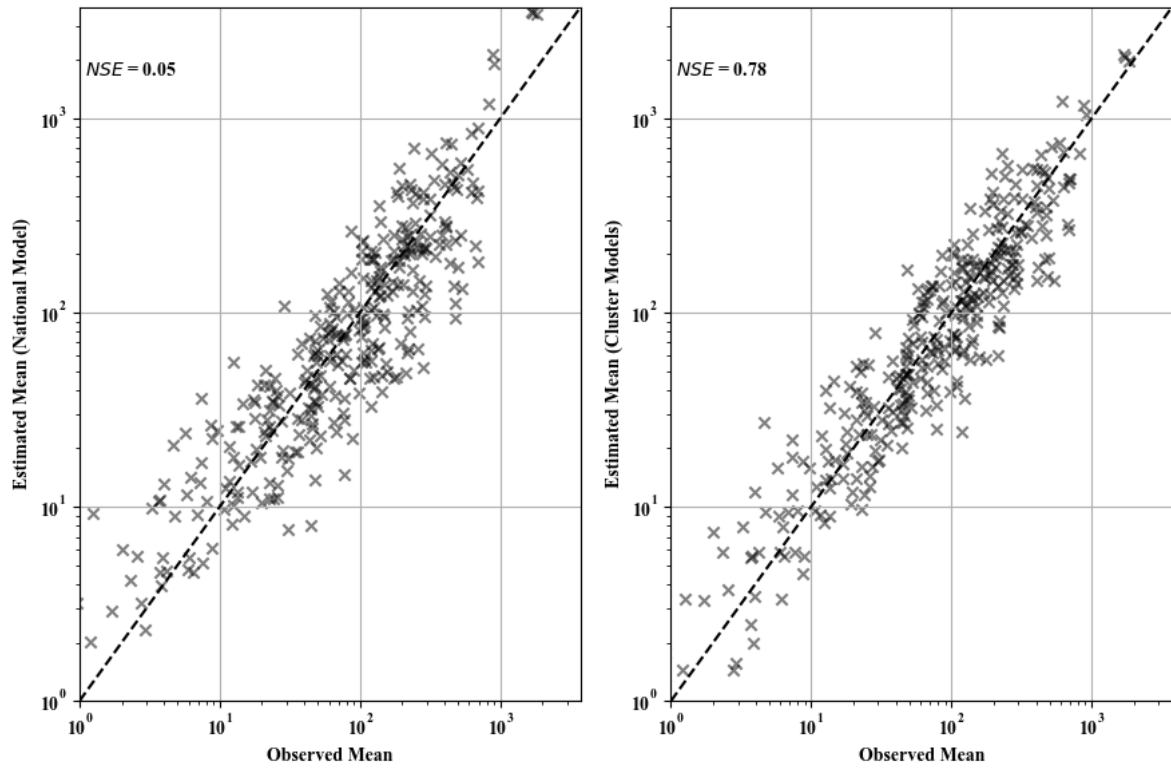


Figure 8.3 Observed versus estimated MAF for the national- (left) and cluster based (right) models

Table 8.4 Scaling parameter model coefficients

Model	<i>MAF</i>					<i>C<sub>10</sub></i>				
	Constant	Area	MAP	Distance from Coast	R <sup>2</sup>	Constant	Area	MAP	Distance from Coast	R <sup>2</sup>
National	-5.88	0.69	0.90	-0.24	0.79	-4.26	0.11	0.24	-0.26	0.13
Cluster 1	-18.32	0.49	3.19	-0.82	0.76	-12.99	-0.11	2.09	-1.39	0.33
Cluster 2	2.34	0.50	0.43	-2.52	0.68	12.02	-0.14	-1.37	-2.82	0.45
Cluster 3	2.34	0.50	0.43	-2.52	0.68	12.02	-0.14	-1.37	-2.82	0.45
Cluster 4	-39.34	0.63	6.03	0.23	0.83	-39.39	0.06	5.67	-0.10	0.34
Cluster 5	-6.01	0.64	1.00	-0.30	0.64	-5.78	0.13	0.51	-0.71	0.13
Cluster 6	-21.52	0.66	3.09	1.13	0.85	-8.92	0.08	0.85	0.65	0.11
Cluster 7	-18.34	0.70	2.60	0.79	0.86	-11.35	0.10	1.21	0.46	0.15
Cluster 8	-35.46	0.64	5.10	1.96	0.85	-18.84	0.02	2.32	1.24	0.29
Cluster 9	-6.40	0.80	0.76	0.52	0.83	3.67	0.19	-1.08	0.02	0.40
Cluster 10	-8.67	0.85	1.08	0.28	0.79	-6.82	0.29	0.29	1.02	0.30
Cluster 11	-6.01	0.64	1.00	-0.30	0.64	-5.78	0.13	0.51	-0.71	0.13
Cluster 12	-5.23	0.74	0.73	0.16	0.73	-3.47	0.16	0.05	-0.12	0.16
Cluster 13	-10.59	0.51	1.77	0.20	0.59	-5.55	-0.03	0.51	0.65	0.05
Cluster 14	-8.95	0.62	1.41	-0.17	0.90	4.82	0.04	-0.79	-1.52	0.21
Cluster 15	-8.45	0.63	1.37	-0.15	0.75	-0.17	0.09	-0.29	-0.17	0.09
Cluster 16	-8.38	0.57	1.40	0.02	0.69	1.06	0.04	-0.44	-0.06	0.05
Cluster 17	-11.82	0.70	1.83	-0.03	0.74	-7.39	0.07	0.82	-0.01	0.03
Cluster 18	-9.27	0.82	1.37	-0.32	0.80	-9.08	0.24	0.90	-0.40	0.28
Cluster 19	-3.36	0.66	0.54	-0.52	0.89	-4.76	0.06	0.38	-0.35	0.22
Cluster 20-24	-13.04	1.02	1.87	0.39	0.88	-11.03	0.36	1.16	0.08	0.45
Cluster 25	-5.17	0.74	0.77	-0.32	0.85	-4.81	0.14	0.27	-0.50	0.37
Cluster 26-27	-2.16	0.69	0.30	-0.50	0.82	-2.56	0.08	-0.03	-0.55	0.29
Cluster 28	-3.21	0.67	0.50	-0.38	0.84	-3.97	0.08	0.22	-0.38	0.30
Cluster 29	0.15	0.47	0.17	-0.41	0.71	3.53	-0.21	-0.65	-0.36	0.15

Model	<i>MAF</i>					<i>C<sub>10</sub></i>				
	Constant	Area	MAP	Distance from Coast	R <sup>2</sup>	Constant	Area	MAP	Distance from Coast	R <sup>2</sup>
Cluster 30-32	-7.48	0.68	1.16	-0.16	0.84	-3.44	-0.01	0.26	-0.13	0.02
Cluster 33	-2.45	0.67	0.45	-0.05	0.74	4.72	0.10	-1.03	-0.05	0.13
Cluster 34	4.42	0.68	-0.55	-0.05	0.80	8.71	0.09	-1.60	-0.08	0.21
Cluster 35	2.34	0.61	-0.20	-0.02	0.70	10.03	0.03	-1.75	-0.02	0.13
Cluster 36	-6.21	0.60	1.06	0.10	0.70	2.85	0.04	-0.71	-0.01	0.10
Cluster 37	4.15	0.66	-0.50	-0.06	0.79	8.23	0.07	-1.52	-0.08	0.16
Cluster 38-39	-4.41	0.77	0.53	0.05	0.82	5.48	0.17	-1.30	-0.34	0.35
Cluster 40	-7.92	0.78	1.05	-0.09	0.85	-6.23	0.20	0.36	-0.26	0.32
Cluster 41	-10.56	0.90	1.38	-0.22	0.79	-9.58	0.34	0.75	0.06	0.32
Cluster 42	-11.46	0.85	1.48	0.32	0.83	-10.36	0.27	0.88	0.20	0.28

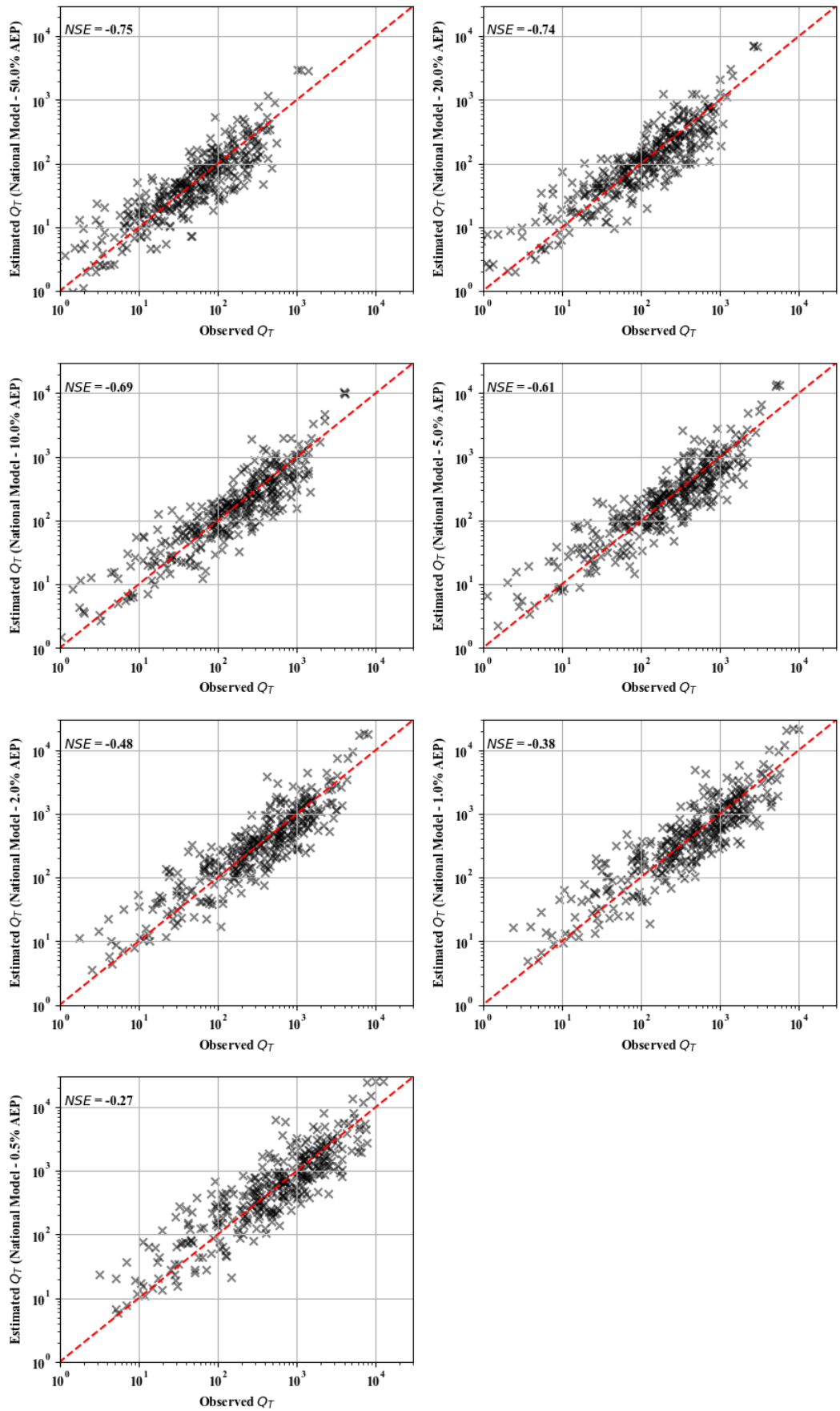


Figure 8.4 Estimated vs observed  $Q_T$  using the  $C_T$  National based approach for the 50, 20, 10, 5, 2, 1 and 0.5% annual exceedance probabilities

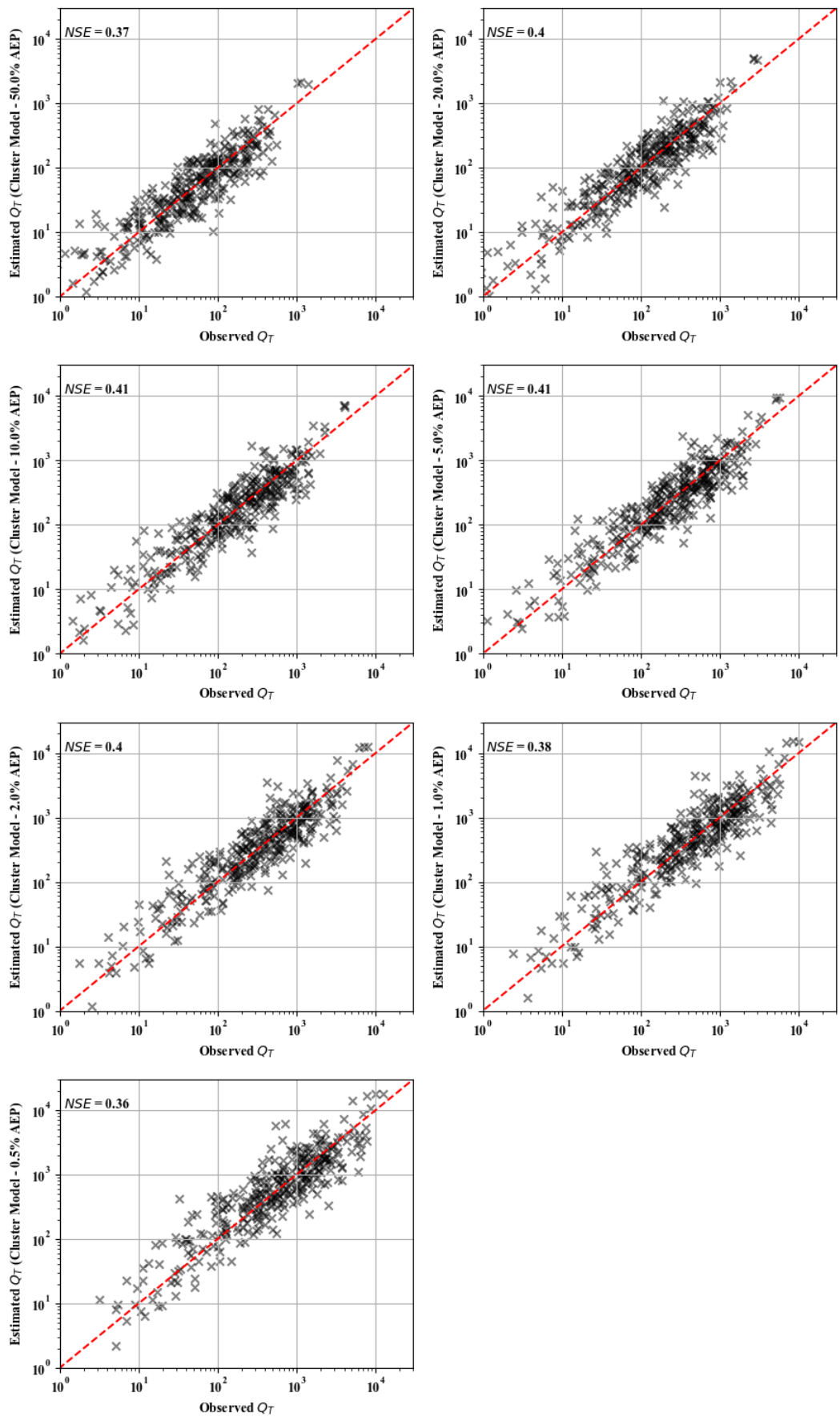


Figure 8.5 Estimated vs observed  $Q_T$  using the  $C_T$  Cluster based approach for the 50, 20, 10, 5, 2, 1 and 0.5% annual exceedance probabilities

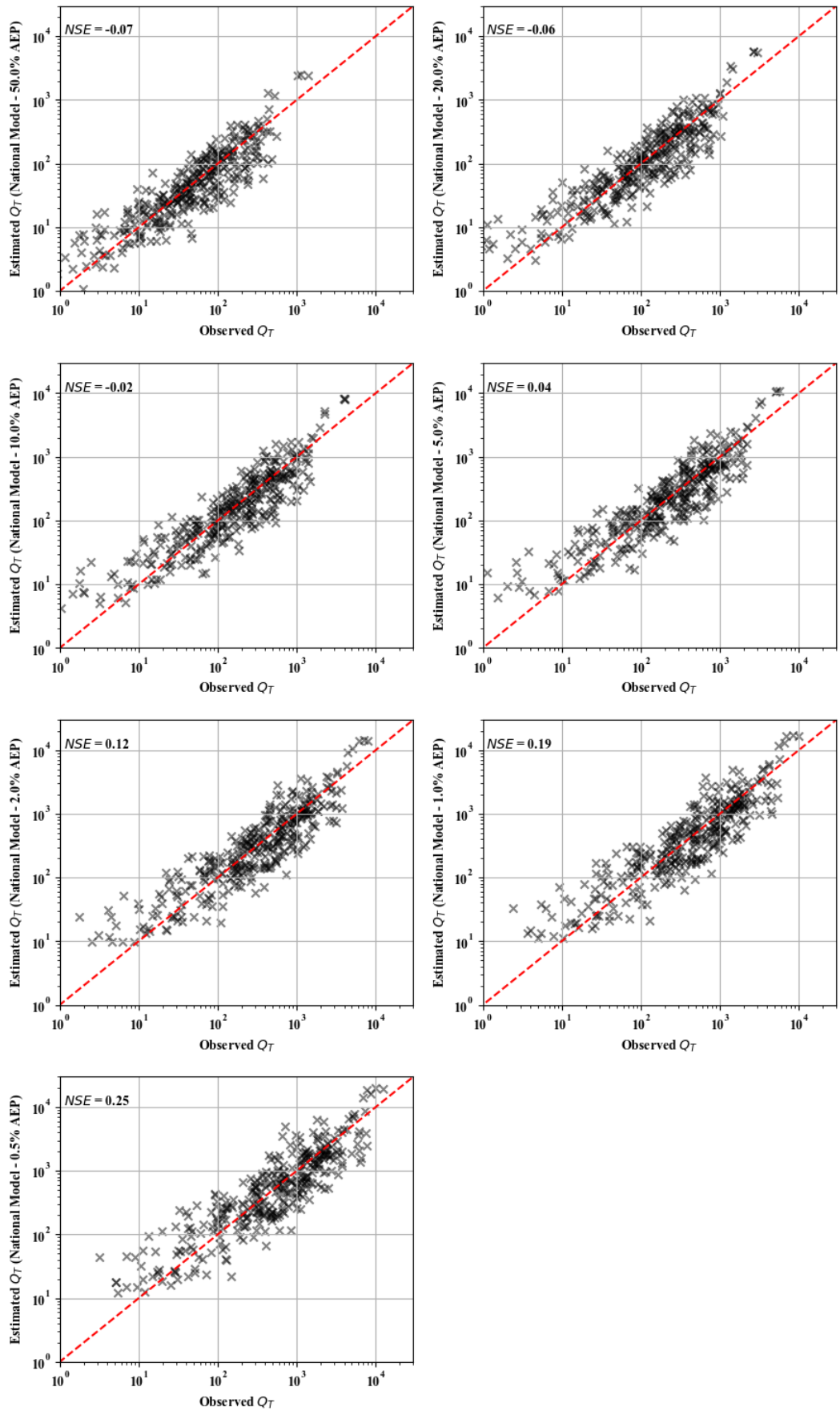


Figure 8.6 Estimated vs observed  $Q_T$  using the RIF National based approach for the 50, 20, 10, 5, 2, 1 and 0.5% annual exceedance probabilities

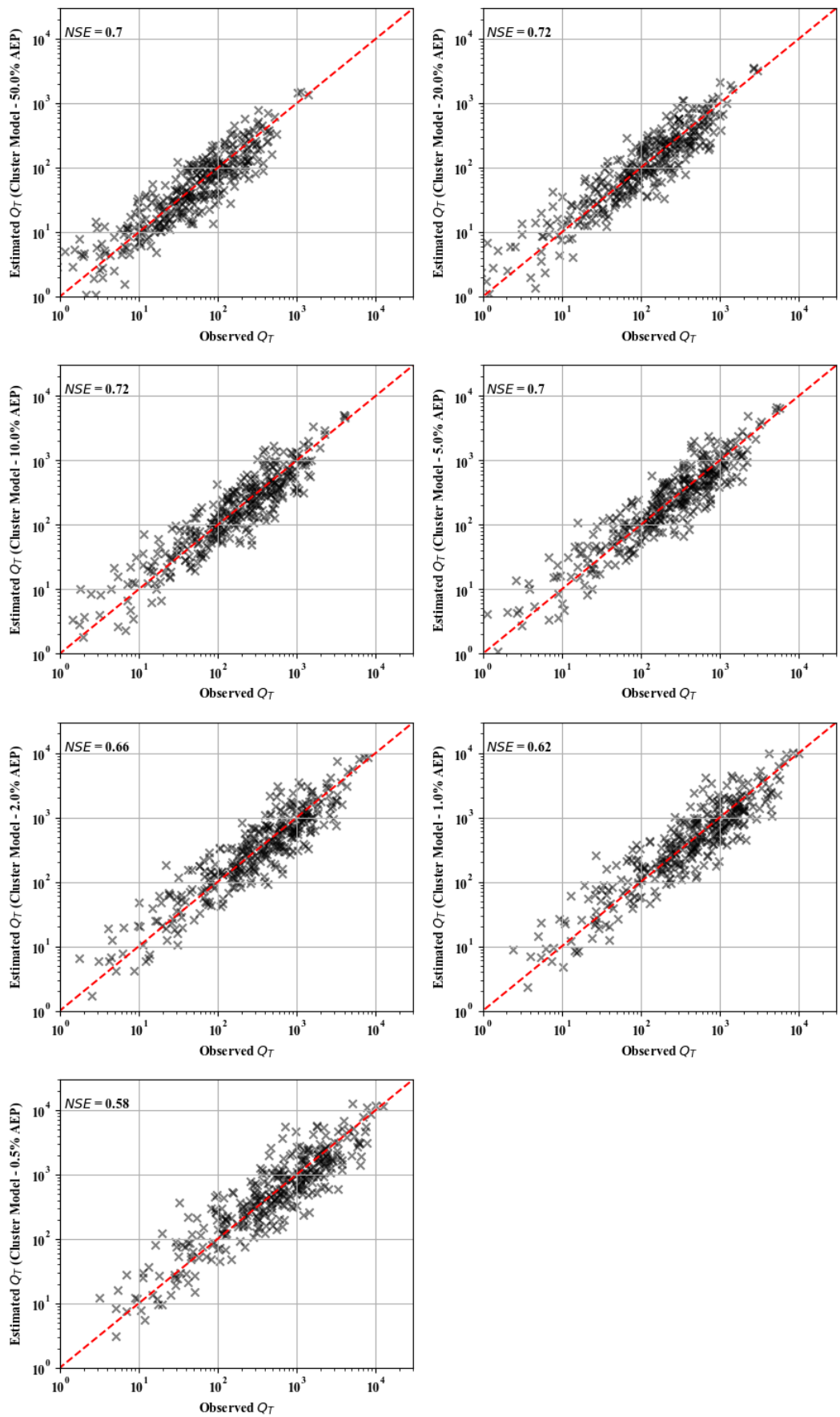


Figure 8.7 Estimated vs observed  $Q_T$  using the RIF Cluster based approach for the 50, 20, 10, 5, 2, 1 and 0.5% annual exceedance probabilities

### 8.3 Performance Assessment

Having developed both regional dimensionless growth curves and models to estimate the scaling factors for the  $C_T$  and RIF approach (Eq 8.1 and Table 8.4), an assessment of the model performance could be undertaken. All results presented in this section are based on the LOO analyses, as described in Section 3.5. Figure 8.8 and Figure 8.9 provides a breakdown of the percentage of estimates that are within, under or in excess of the desirable ratio prescribed by Rahman *et al.* (2012) and Naidoo (In Preparation) respectively. It is evident that the RIF model, at a cluster scale, marginally outperforms the remaining models when considering only the ratios. The percentage of sites within the desirable range varies between 69 and 74%. The worst performing model was the  $C_T$  based national model achieving a minimum percentage within the desirable ratio of 62%.

When considering the RMSE and BIAS values presented in Table 8.5, on a national scale the RIF approach outperforms the  $C_T$  approach. However, when performing the modelling at a cluster level the models perform equally well with the RIF approach outperforming the  $C_T$  approach by only 0.4%.

However, when considering the NSE values, shown in Table 8.6, the results are significantly different. The National based models are outperformed by the cluster based models for both the RIF and  $C_T$  approaches, where the national models score negative NSE values. The RIF approach outperforms the  $C_T$  approach, where the  $C_T$  approach scored maximum values of -0.27 and 0.41 for the national- and cluster based approaches respectively. The RIF approach was the best performing model with the cluster based approach scoring a maximum NSE of 0.72.

As an additional check, the slopes of the regressions of the estimated versus observed  $Q_T$  values were calculated. The slopes were estimated forcing the regression intercept to zero. The slopes indicate that the national approaches tend to over-estimate the  $Q_T$ , whereas the cluster based  $C_T$  approach over-estimates the higher AEPs and are within reasonable bounds for the 1% and 0.5% AEPs. The cluster based RIF approach is within reasonable bounds for all AEPs, except for the 0.5% AEP, which tends to an under-estimation.

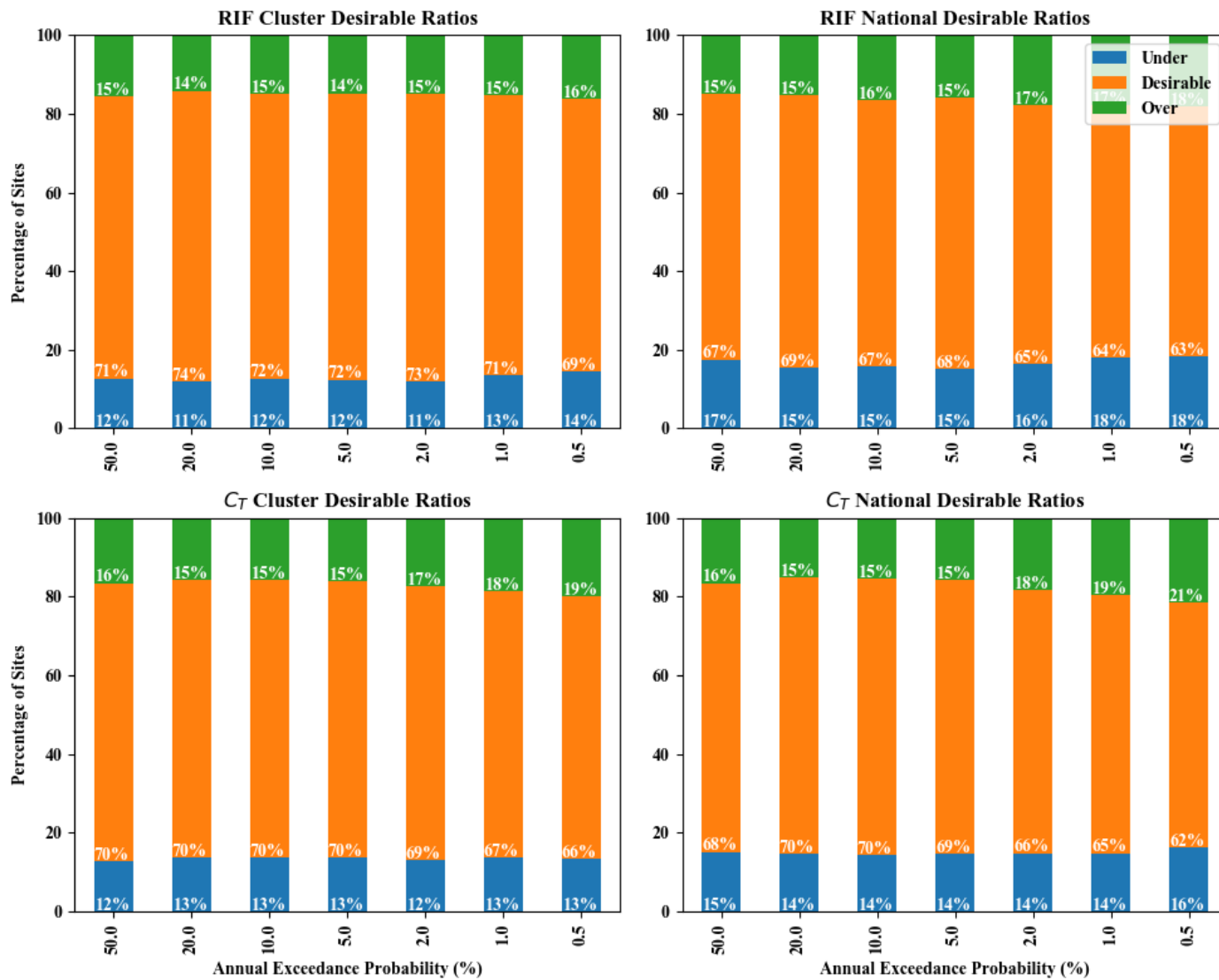


Figure 8.8 Percentage of  $Q_T$  estimates within the desirable ratio defined by Rahman *et al.* (2012) using the RIF (top) and  $C_T$  (bottom) approaches for both Cluster based and National based scaling factor estimation methods

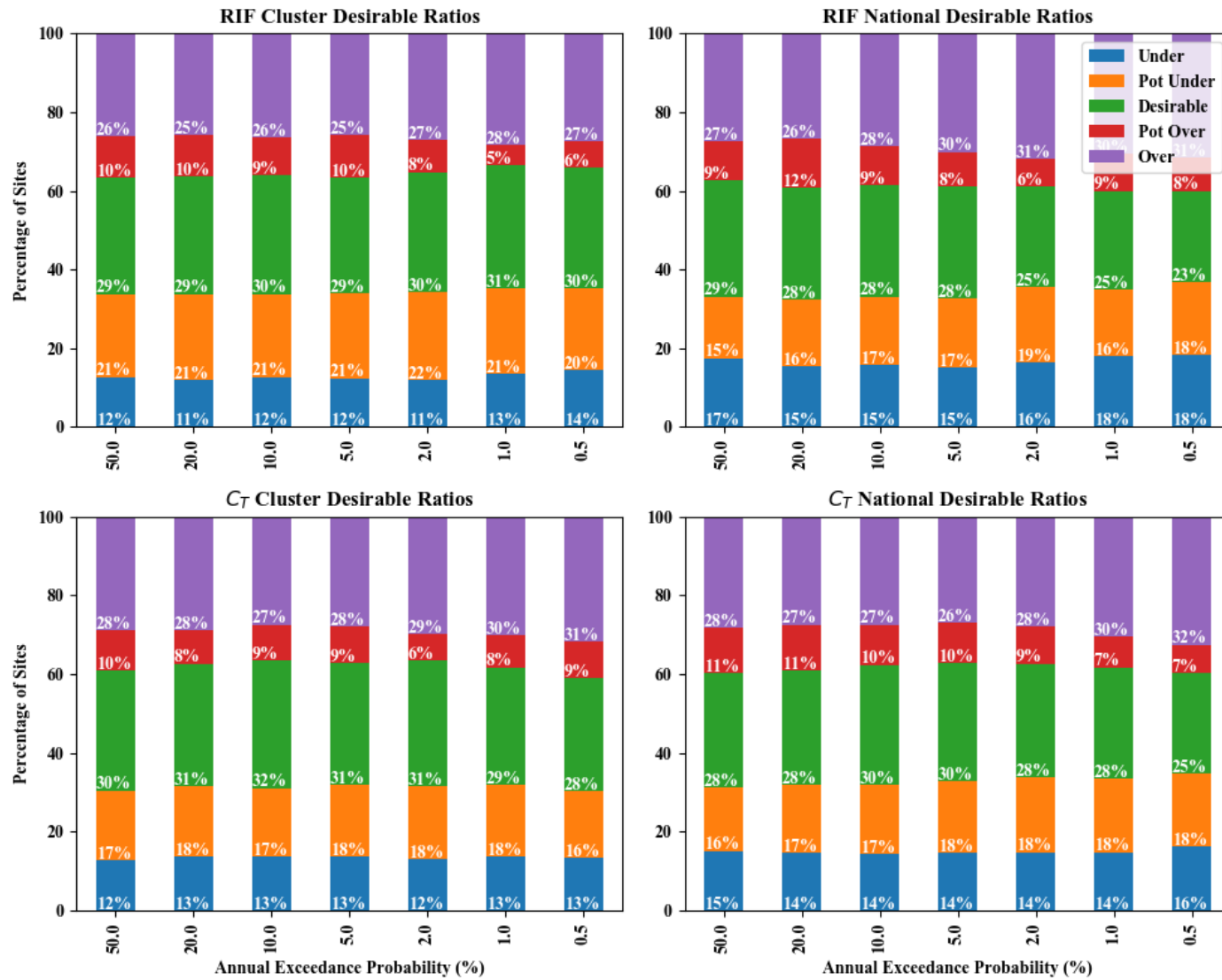


Figure 8.9 Percentage of  $Q_T$  estimates within the desirable ratio defined by Naidoo (In Preparation) using the RIF (top) and  $C_T$  (bottom) approaches for both Cluster based and National based scaling factor estimation methods

Table 8.5 Performance statistics of  $Q_T$  estimation using the RIF and  $C_T$  approaches\* for 10% and 1% AEP

	RIF								$C_T$							
	10% AEP				1% AEP				10% AEP				1% AEP			
	RMSE	RMSEr	BIAS	BIASr	RMSE	RMSEr	BIAS	BIASr	RMSE	RMSEr	BIAS	BIASr	RMSE	RMSEr	BIAS	BIASr
National	516.07	22.72	191.56	0.69	1181.06	34.37	509.55	0.77	663.51	25.76	210.53	0.67	1541.53	39.26	572.40	0.79
Cluster 1	80.57	8.98	62.67	0.41	109.38	10.46	86.78	0.36	87.34	9.35	67.72	0.43	117.62	10.85	88.96	0.37
Cluster 2	111.03	10.54	67.69	0.39	335.33	18.31	230.78	0.50	102.61	10.13	58.33	0.42	361.81	19.02	227.32	0.52
Cluster 3	63.71	7.98	55.79	0.46	307.72	17.54	270.53	0.92	40.09	6.33	33.07	0.21	402.36	20.06	350.37	0.58
Cluster 4	60.50	7.78	35.31	0.78	282.26	16.80	160.42	0.70	76.90	8.77	49.59	0.91	321.37	17.93	197.75	0.83
Cluster 5	387.30	19.68	262.59	0.75	1444.60	38.01	993.64	1.00	310.61	17.62	203.09	0.55	1165.82	34.14	801.84	0.76
Cluster 6	141.41	11.89	122.75	0.79	481.08	21.93	422.07	0.96	122.70	11.08	111.91	0.63	373.15	19.32	301.33	0.74
Cluster 7	110.85	10.53	89.26	0.44	205.42	14.33	135.49	0.45	95.80	9.79	84.53	0.43	185.22	13.61	143.84	0.33
Cluster 8	230.50	15.18	174.68	0.52	578.20	24.05	476.83	0.82	192.44	13.87	169.66	0.56	609.42	24.69	498.61	0.87
Cluster 9	81.68	9.04	53.59	0.41	147.66	12.15	99.63	0.45	77.32	8.79	53.36	0.41	157.42	12.55	104.67	0.46
Cluster 10	117.65	10.85	85.27	0.43	235.59	15.35	178.34	0.40	125.28	11.19	86.06	0.39	235.13	15.33	178.14	0.39
Cluster 11	103.90	10.19	58.95	0.57	440.94	21.00	314.67	1.04	80.49	8.97	44.54	0.39	340.97	18.47	246.95	0.81
Cluster 12	317.37	17.81	277.76	0.80	1146.97	33.87	974.08	0.98	287.21	16.95	221.16	0.66	1302.24	36.09	1085.67	0.94
Cluster 13	358.98	18.95	328.29	0.68	709.98	26.65	633.09	0.55	260.80	16.15	237.09	0.57	411.21	20.28	372.20	0.41
Cluster 14	357.12	18.90	272.45	0.32	900.40	30.01	685.08	0.36	497.76	22.31	346.52	0.34	1230.28	35.08	867.91	0.36
Cluster 15	428.86	20.71	300.70	0.85	817.02	28.58	610.29	0.72	474.77	21.79	343.65	0.95	892.36	29.87	641.87	0.72
Cluster 16	224.20	14.97	189.26	0.41	773.32	27.81	647.79	0.55	195.86	14.00	163.35	0.37	786.61	28.05	631.50	0.56
Cluster 17	268.79	16.39	191.53	0.30	1141.70	33.79	798.53	0.34	582.92	24.14	367.50	0.40	2075.78	45.56	1347.47	0.48
Cluster 18	234.97	15.33	155.32	0.71	680.69	26.09	550.31	1.14	104.86	10.24	80.44	0.50	403.79	20.09	367.32	0.88
Cluster 19	896.07	29.93	863.48	0.22	1780.00	42.19	1469.06	0.19	3028.13	55.03	3019.28	0.75	6491.66	80.57	6406.33	0.79
Cluster 20	176.56	13.29	107.93	0.32	262.82	16.21	158.96	0.33	180.61	13.44	100.41	0.36	249.40	15.79	147.01	0.38
Cluster 21	54.64	7.39	32.68	0.38	71.82	8.47	47.06	0.35	55.14	7.43	36.26	0.39	77.89	8.83	50.11	0.43
Cluster 22	9.75	3.12	6.56	0.94	38.72	6.22	19.87	0.81	6.89	2.62	4.07	0.69	46.38	6.81	23.60	0.82
Cluster 23	12.41	3.52	9.64	0.33	17.96	4.24	14.68	0.38	16.46	4.06	12.16	0.45	22.74	4.77	16.93	0.47
Cluster 24	22.73	4.77	19.88	1.08	171.41	13.09	115.07	0.84	131.78	11.48	83.60	1.76	527.92	22.98	295.09	1.45

	RIF								Cr							
	10% AEP				1% AEP				10% AEP				1% AEP			
	RMSE	RMSEr	BIAS	BIASr	RMSE	RMSEr	BIAS	BIASr	RMSE	RMSEr	BIAS	BIASr	RMSE	RMSEr	BIAS	BIASr
Cluster 25	525.36	22.92	245.35	0.83	1696.30	41.19	864.75	1.00	531.41	23.05	242.27	0.90	1844.62	42.95	891.35	1.18
Cluster 26	80.29	8.96	59.85	0.40	141.30	11.89	103.15	0.34	147.63	12.15	92.66	0.51	404.70	20.12	246.75	0.51
Cluster 27	55.14	7.43	34.38	0.59	113.71	10.66	74.89	0.77	65.10	8.07	36.48	0.41	130.85	11.44	78.56	0.57
Cluster 28	104.78	10.24	79.97	0.34	360.97	19.00	307.83	0.39	113.17	10.64	90.53	0.33	157.52	12.55	127.87	0.21
Cluster 29	110.42	10.51	82.40	0.20	706.77	26.59	444.05	0.41	91.89	9.59	73.85	0.39	671.67	25.92	377.05	0.64
Cluster 30	83.61	9.14	68.58	0.40	340.84	18.46	283.35	0.28	84.49	9.19	66.54	0.40	330.25	18.17	254.42	0.28
Cluster 31	141.88	11.91	106.05	0.50	257.26	16.04	200.63	0.39	559.35	23.65	349.76	1.47	1515.96	38.94	898.37	1.79
Cluster 32	85.08	9.22	59.46	0.42	298.52	17.28	201.48	0.75	89.85	9.48	56.84	0.42	261.91	16.18	202.58	0.86
Cluster 33	242.49	15.57	183.08	0.30	760.20	27.57	514.72	0.38	310.00	17.61	257.02	0.43	873.98	29.56	663.57	0.51
Cluster 34	400.78	20.02	262.53	0.95	1520.18	38.99	986.35	1.50	370.11	19.24	233.99	0.85	1487.41	38.57	930.69	1.43
Cluster 35	245.12	15.66	173.92	0.47	352.95	18.79	193.90	0.31	255.84	15.99	160.08	0.38	351.59	18.75	255.88	0.35
Cluster 36	451.08	21.24	250.56	0.67	806.75	28.40	437.63	0.90	423.44	20.58	226.46	0.61	769.64	27.74	412.62	0.86
Cluster 37	342.62	18.51	203.69	0.93	1531.57	39.14	895.58	1.22	326.72	18.08	182.80	0.90	1442.19	37.98	838.54	1.30
Cluster 38	67.19	8.20	54.42	1.11	153.59	12.39	92.22	0.73	52.69	7.26	41.59	0.79	115.23	10.73	78.58	0.58
Cluster 39	435.22	20.86	214.04	0.59	1197.92	34.61	683.92	0.69	216.46	14.71	112.45	0.38	730.47	27.03	463.64	0.59
Cluster 40	483.54	21.99	381.58	0.72	1451.23	38.09	1083.67	0.75	428.57	20.70	321.67	0.60	1283.05	35.82	906.72	0.61
Cluster 41	27.00	5.20	19.50	1.05	56.06	7.49	38.63	1.02	33.87	5.82	22.75	1.15	75.84	8.71	52.27	1.26
Cluster 42	88.51	9.41	58.33	0.35	321.75	17.94	220.11	0.42	75.05	8.66	52.38	0.32	270.23	16.44	201.89	0.41

\* Shaded blocks indicate best performance of the two methods

Table 8.6 NSE and regression slope of observed and estimated  $Q_T$  for the RIF and  $C_T$  approaches at national and cluster scale.

		AEP (%)	50	20	10	5	2	1	0.5
RIF	National	NSE	-0.07	-0.06	-0.02	0.04	0.12	0.19	0.25
		Slope	1.38	1.46	1.45	1.41	1.32	1.23	1.12
	Cluster	NSE	0.70	0.72	0.72	0.70	0.66	0.62	0.58
		Slope	1.03	1.07	1.06	1.04	0.99	0.94	0.87
$C_T$	National	NSE	-0.75	-0.74	-0.69	-0.61	-0.48	-0.38	-0.27
		Slope	1.55	1.61	1.59	1.55	1.45	1.36	1.26
	Cluster	NSE	0.37	0.40	0.41	0.41	0.40	0.38	0.36
		Slope	1.25	1.28	1.26	1.23	1.16	1.09	1.02

Figure 8.10 indicates the reason for the low NSE values achieved by the National models, using the  $C_{10}$  approach. What is evident is that there are three sites (D7H002, D7H005, D7H008) that are significantly over estimated by the approach, which negatively affect the results.

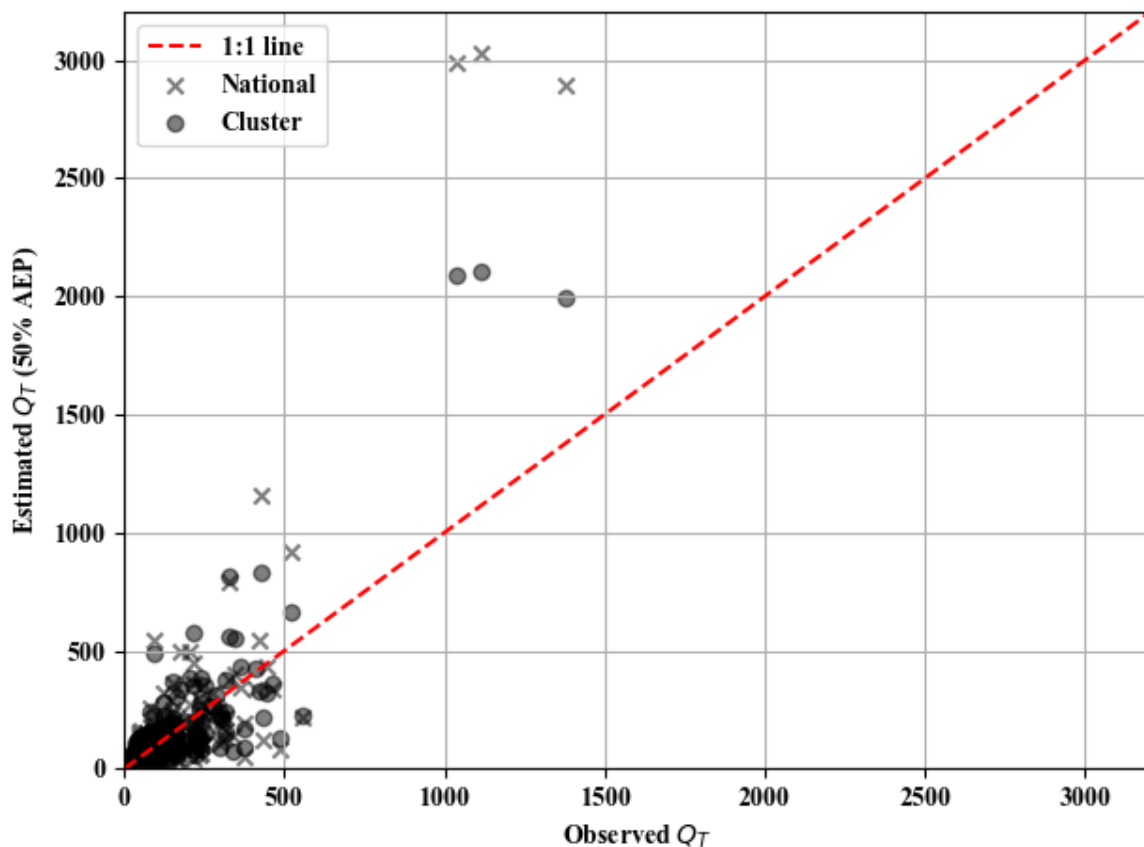


Figure 8.10 Estimated vs observed  $Q_T$  using the  $C_{10}$  approach for the 50% AEP

Given the above results of the performance assessment of the RIF and  $C_T$  methods, it is recommended that the RIF cluster based approach be adopted.

#### **8.4 Comparison to Standard Design Flood Method**

Considering that the purpose of the project was the development of an improved PRM for South Africa, a comparison to the SDF method was undertaken using the same performance metrics to compare the RIF and  $C_T$  approaches. Figure 8.11 and Figure 8.12 compares the spread of the estimated vs observed ratios for the cluster based RIF and  $C_T$ , and the SDF. It is evident that the SDF estimation method over estimates the design flood values.

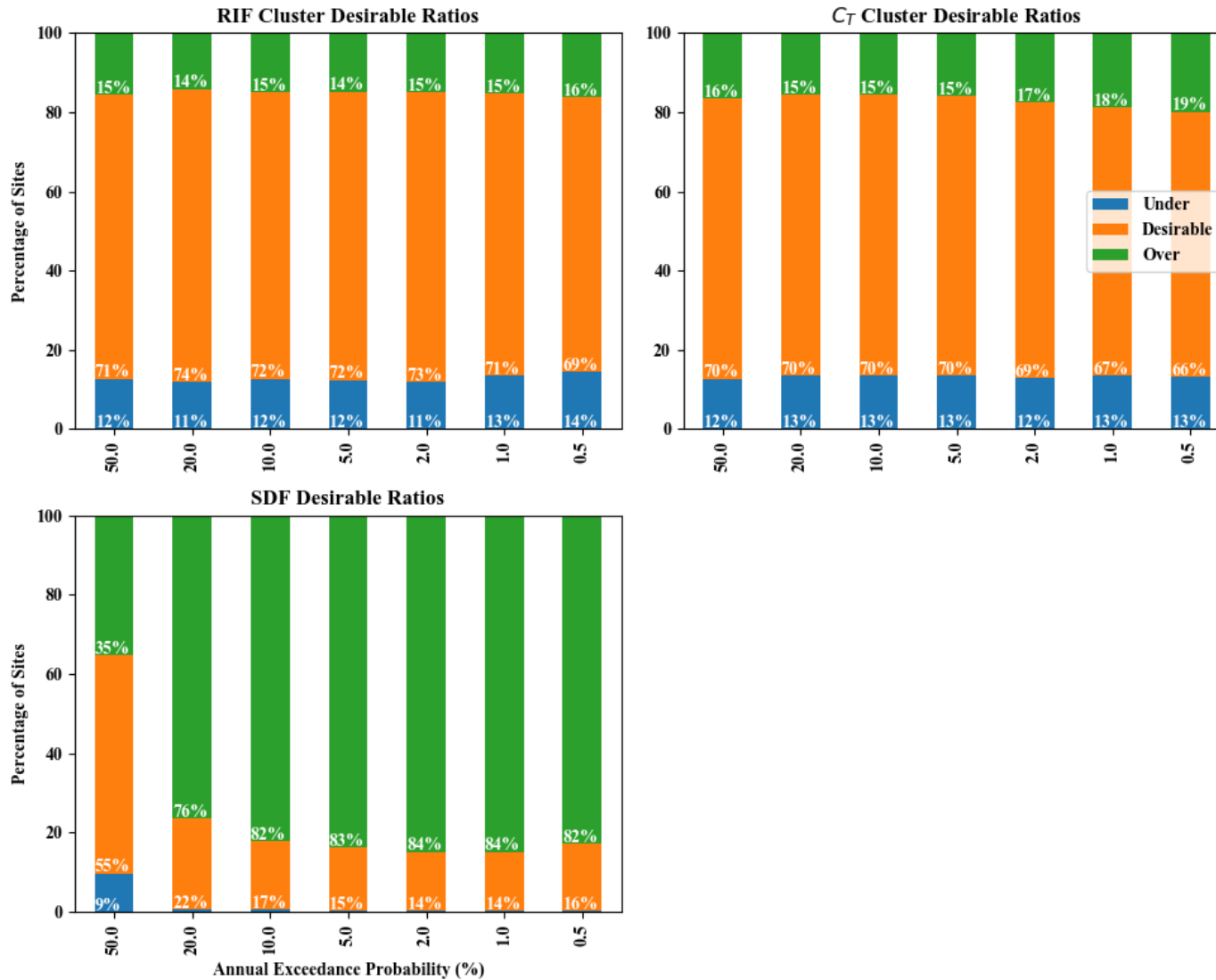


Figure 8.11 Comparison of the percentage of  $Q_T$  estimates within the desirable ratio defined by Rahman *et al.* (2012), between the RIF (top left),  $C_T$  (top right) and the SDF (bottom left) approaches

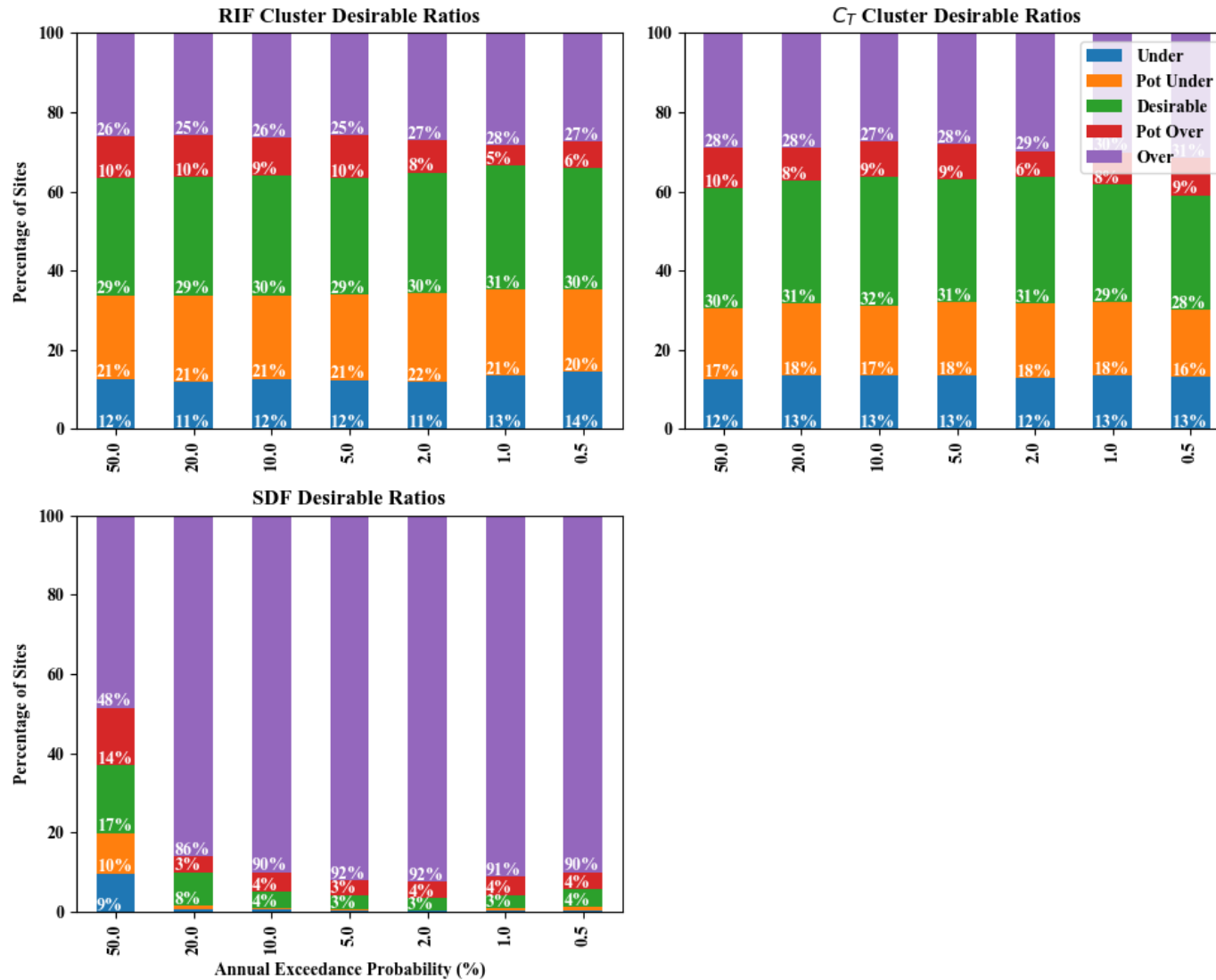


Figure 8.12 Comparison of the percentage of  $Q_T$  estimates within the desirable ratio defined by Naidoo (In Preparation), between the RIF (top left),  $C_T$  (top right) and the SDF (bottom left) approaches

## 9 DEVELOPMENT OF A DESIGN FLOOD ESTIMATION UTILITY

Accessibility to design flood data and hydrological parameters is limited in South Africa, with both practitioners and students often having difficulty obtaining, cleaning and compiling datasets. This leads to duplication of effort and inconsistent estimation of model input parameters by practitioners working in the same catchment. Similarly, for researchers and students, there is much duplication of effort to access data required for different research projects and consequently less time is spent on the research. The National Flood Studies Programme (NFSP) has identified the need for the development of a freely available hydrological database containing information pertinent to national flood studies (Smithers *et al.* 2014).

The National Flood Studies Application (NaFSApp) which has been developed is considered a pilot study for the development of an online database which contains an interface to extract catchment data and parameters for design flood estimation, thus limiting duplication of effort and improving consistency in application of the methods.

The interface was developed with the “Three-click-rule” in mind, which attempts to ensure that the users are able to access the desired information within three clicks. Additionally, a mobile first approach was adopted, whereby the application was developed with accessibility in mind.

### 9.1 Technical specifications

The Interface was developed using the following technologies:

- (i) Web framework: Python 3.7 and Django 2.2
- (ii) Server Provider: Heroku
- (iii) Database: PostgreSQL + PostGIS
- (iv) Mapping: Leaflets
- (v) Basemaps: OpenStreetMaps, ESRI Imagery and Stamen Design Terrain
- (vi) Graphing: Bokeh – Interactive graphing functionality
- (vii) Progressive Web App functionality, as shown in Figure 9.1.

Progressive web app functionality has been integrated into the application which allows mobile users to save an app-like shortcut to their mobile phones. This allows for the use of the entire screen as well as the use of push notifications. Web app functionality is currently limited on iOS devices due to technical requirements of the SSL certificates, however, it is anticipated that this functionality will become available in the near future.

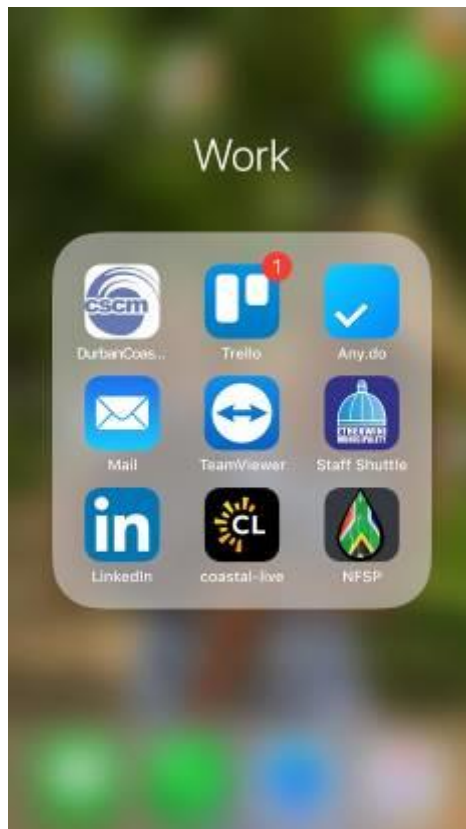


Figure 9.1 Progressive web app

## 9.2 User guide

The NaFSApp is currently hosted on the NFSP website (<https://www.nfsp.co.za>). Please refer to the NFSP website for the user guide and any future developments.

## 10 DISCUSSION, CONCLUSIONS AND RECOMMENDATIONS

The aim of this study is to develop a refined regionalised, probabilistic approach to the application of the RM for design flood estimation in South Africa. The objectives of the study listed in Chapter 1 can be summarised as follows:

- (a) Collation and quality control of selected gauged flow data in South Africa.
- (b) Produce at-site flood frequency curves for selected stations.
- (c) Compilation of catchment descriptors database.
- (d) Identify and verify homogeneous flood producing regions.
- (e) Calibration of the Rational Method within homogeneous regions.
- (f) Regional flood model development.
- (g) Assessment of the performance of the proposed methodology.
- (h) Develop a DFE utility for application of the newly proposed methodologies by design practitioners
- (i) Development of a RIF method for DFE and comparison of performance with the regionalised PRM developed.

### 10.1 Data Collection and Screening

The collection of the required data for the study was considered to be a two phased approach, whereby both the catchment specific parameters, and the hydrological streamflow data were collated.

#### 10.1.1 Catchment specific parameters

The methods used in this study are based on internationally accepted DFE procedures. This was used to ensure familiarity in the approach and ease of application. These methods require nearly identical catchment parameters to be estimated for use in the two DFE methods developed and range from meteorological parameters to topographic and land use parameters.

The SDF method (Alexander 2002), which is a PRM, has been criticised for the use of an outdated rainfall data set and broad regionalisation (Smithers and Schulze 2003) and the use of incorrect catchment parameters (Van Vuuren *et al.* 2013). In this study, the derived

catchment parameters were verified against DWS data sets. The selected catchment parameters, including the estimation method, for inclusion into the study were:

- (a) outlet location (from DWS),
- (b) outlet elevation (derived from DEM),
- (c) catchment area (derived from DEM),
- (d) catchment centroid (derived from area),
- (e) longest flow path (L),
- (f) length to centroid (L<sub>c</sub>),
- (g) distance from the coast ( $D_c$ ),
- (h) slope ( $S_{10-85}$ ,  $S_{ea}$ ,  $S_c$ ),
- (i) time of concentration ( $T_c$ ),
- (j) Areal Reduction Factor (ARF),
- (k) catchment runoff percentage ( $C_{ro}$ ),
- (l) SCS soil classifications (SCS),
- (m) arid region,
- (n) Mean Annual Precipitation ( $MAP_{max}$ ,  $MAP_{min}$  and  $MAP_{mean}$ ),
- (o) rainfall region,
- (p) rainfall seasonality ( $R_s$ ),
- (q) design rainfall depths (2 to 200-year return period), and
- (r) Design rainfall intensities (2 to 200-year return period).

A number of Python scripts were developed to automate the process of determining the catchment parameters on a national scale. In addition, the conditioning of the DEM data has been undertaken for South Africa.

### **10.1.2 Development of a quality-controlled streamflow dataset**

The DWS is the custodian for streamflow data for all of the sites across South Africa. In addition, the data set compiled by Van Bladeren *et al.* (2007) was used to supplement the available data. Considering that the entire data set received consisted of 474 flow-gauging stations with a total record length exceeding 15 000 years, Python scripts were developed to process the point source data, identifying potential errors and to summarise the primary data into annual, monthly, weekly and daily peak values. This processing procedure allowed for the

inclusion of additional years that would conventionally have been excluded due to the extent of missing information and the time at which these occurred.

The screening process considered multiple steps. Firstly, the selection of a minimum record length of 20 years, secondly, identifying stations impacted by upstream developments and, lastly, data quality assessment. The quality assessment included the identification of missing data, verification of the regional occurrence of floods, error identification and quality control. Some of the stations considered also required rating curve extensions to be performed, and this was limited to a maximum of 20% increase in the currently maximum rated stage and flow. After the screening, a total number of 383 sites remained for further processing and calibration of the model.

## **10.2 Selection of Parent Distribution**

At-site design peak discharges were required to form the basis of the calibration and performance assessment processes. It was identified that a number of methods have been suggested to fit probability distributions to the data in South Africa, ranging from standard Method of Moments estimation techniques to L-moments. The wide use of L-moments both locally (Smithers and Schulze 2003) and internationally (Kjeldsen *et al.* 2008, Castellarin *et al.* 2012) resulted in the adoption of L-moments to fit probability distribution to the data used in this study.

An integral part of the FFA is the selection of an appropriate parent distribution. The importance of this selection is highlighted by Smithers and Schulze (2000). A review of the literature indicated that the distributions most commonly applied in South Africa for design flood estimation are the GEV and LP3 distributions. Calitz (2016) found that the LP3 distribution had a larger variation in the calibrated  $C_T$  values and over-estimated flood events compared to the GEV distribution. Calitz (2016) also considered the GPA as a potential distribution due to the preferential fit to the overall data set. GOF, model fit criterion and L-moment ratio diagrams, as developed by Hosking and Wallis (1997), were applied for the selection of the most suitable PD. On a national scale it was identified that when considering the entire data set, the best-fit distributions is the GPA followed by the KAP3 and LP3 distributions. Hence the GPA distribution was utilised for the study.

### **10.3 Regionalisation**

Clustering and RoI regionalisation approaches were applied, with both methods requiring multiple adjustments and further refinement of the regional delineation. The regionalisation, modification and recommendations are discussed below.

#### **10.3.1 Region of Influence**

A RoI approach which enforces a minimum required record length was investigated, which allowed for an assessment of whether the enforcement of the 2/5T rule generates homogeneous flood regions. Initial investigations using the minimum record length requirement of 500 years indicated that the majority of the regions formed are not homogeneous, with a maximum of 195 homogeneous regions expected out of 383.

Using a single parameter set approach resulted 16% and 51% homogeneous regions for 500- and 200-year minimum record lengths approaches respectively. With a combination of two parameter sets, 71% of regions formed were deemed to be relatively homogeneous. Further manual adjustment of regions for the RoI approach is not practically feasible due to each site generating a unique region and as such no further adjustments were undertaken.

#### **10.3.2 Clustering**

K-means clustering aims to estimate the minimum overall Euclidian distance for all clusters being considered. The identified clusters were also required to adhere to homogeneity requirements as stipulated by Hosking and Wallis (1997) as well as the 2T or 5T rule. The homogeneity measures adopted in the study were the  $H_I$  statistic and the discordancy measure ( $D$ ).

Using the overall and primary drainage regions as a starting point, the homogeneity testing identified that three of the regions contained discordant sites, which would need to be moved, replaced or excluded to improve the homogeneity. After removing the discordant sites for the entire data set, homogeneity was still not achieved. Following the same approach further discordant sites were excluded when the primary drainage regions were considered independently of each other. Removal of the discordant sites did not improve the homogeneity

of the primary drainage regions. Therefore, a re-clustering approach was adopted in order to identify relatively homogeneous clusters within the entire data set.

The clustering was performed in the attribute space and the attributes were normalised to a range of 0 to 1. This reduced the bias of large values such as the MAP that may unduly influence the clustering. An iterative cluster analysis process was followed, whereby each potential parameter combinations was included for a cycle of cluster analyses. The homogeneity measures were also calculated for each iteration and each iteration ranked based on the level of homogeneity achieved. Clustering was performed using site descriptors, whereas the homogeneity of the clusters was assessed using the site specific quantitative FFA descriptive statistics.

The parameter sets that were able to identify the highest percentage of homogeneous clusters were largely meteorological and geographical parameters, with the combination of latitude longitude and distance from the coastline being deemed as the most suitable parameters for clustering. It should be noted that the additional rainfall descriptive statistics can be used, such as the growth curve slope, rainfall seasonality, and rainfall clusters, and further investigation is required into the validity of their use.

The preferred number of clusters was determined using the  $2/5T$  approach adopted by Robson and Reed (1999) as a minimum criteria for the sizing of clusters. This specifies the absolute minimum required record length for RFFA as two times the design event being estimated, with five times being preferable. As an initial estimate a maximum of 36 clusters was adopted, which provides an average of approximately 500 years per cluster. The initial clustering identified 17 homogeneous clusters. The remaining heterogeneous clusters were further analysed using the same clustering approach to ensure continuity and prevent any potential subjectivity. The initial selection of the number of clusters was such that the clusters varied in size from two to twenty-nine sites. Hosking and Wallis (1997) noted that there is no set standard for the selection of the cluster sizes and that the size will affect the model's capabilities to identify regional differences or bias.

A total of 42 relatively homogeneous clusters were identified through adjusting the initial 36 clusters. The process, however, required the exclusion of 51 sites due to discordancy and inconsistencies with geographic variance.

The use of the quantitative FFA for the homogeneity testing produced additional uncertainty as the aim of the regionalisation was the estimation of calibrated  $C_T$  values. The calibration of  $C_T$  values was only performed after the homogeneity verification and site clustering.

#### **10.4 RM Calibration**

The calibrated  $C_T$ -values, derived from the design rainfall determined by Smithers and Schulze (2003) and design peak discharges determined from the observed flow data using the GPA parent distribution, resulted in some  $C_T$ -values in excess of one, with a maximum and minimum of 1.569 and 0.002, respectively. In theory the  $C_T$  value will increase as the AEP% decreases. Twenty sites, however, had negative  $C_T$  value growth curves after the regional calibration process was undertaken. Although the stations potentially introduce errors into the derived models, it is anticipated that due to the use of regional analysis that the effect will be limited. However, further investigation is necessary to resolve this inconsistency.

#### **10.5 Model Development**

Two distinct approaches were adopted for the estimation of  $Q_T$ , i.e. the  $C_T$  and the RIF approaches, in addition each approach was developed on a national- and a cluster based scale. The national- and cluster based scale models refer to the estimation of the  $SF$ , with the  $C_T$  and RIF approaches having adopted the  $C_{10}$  and the  $MAF$  as scaling values, respectively. Models were developed for the estimation of the  $SF$  at a national and a cluster scale.

#### **10.6 Model Performance**

The models were assessed using the  $BIAS$ ,  $RMSE$ , ratio and the  $NSE$  values. The cluster based approaches performed best for both the  $C_T$  and the RIF approaches and when, excluding the  $NSE$  results, the cluster based approaches performed at a similar level. However, the cluster based RIF approach significantly outperformed the other approaches when considering the  $NSE$  results.

Additionally the ratio for the cluster based CT and RIF approaches were compared to the SDF estimates. It was evident that the SDF method consistently over-estimated peak flows, which confirms the findings in the literature reviewed.

Given the overall performance of the RIF cluster based approach, it is recommended for application in South Africa.

## 10.7 Conclusions

Reviewing the objectives of the study it is evident that the study was capable of collating and undertaking quality control on the 411 selected sites. FFA was undertaken at each of the 383 sites deemed adequate for use utilising tools developed during the course of the study. Additionally, to identify homogeneous flood regions the RoI approach was investigated for use in South Africa with limited success, however, a clustering approach resulted in the identification of 42 relatively homogeneous clusters. In addition, the RM was successfully calibrated at the 332 sites that encompass the 42 relatively homogeneous clusters.

Two modelling approaches were adopted, the use of a PRM, referred to as  $C_T$  hereafter, approach and a Regional Index Flood (RIF) approach, which required the identification of suitable  $SF$  for application with the dimensionless growth curves. The  $C_{10}$  value was used for the  $C_T$  approach and both the MAF and MEF were investigated for use with the RIF approach, however the MAF was used due to the reduction in variance in the dimensionless growth curves when using the MAF. Regressions were developed for the estimation of the  $SFs$  at national and cluster scale, however the cluster scale regression development outperformed the national scale as is evident from the  $NSE$  scores achieved. The  $SF$  regressions were used to estimate  $Q_T$ .

When comparing the  $Q_T$  estimated on a LOO basis a minimum number of thirty sites was used for the development of the regressions, which reduced the  $BIAS$  and  $RMSE$  for the  $SF$  estimates. The best performing model was the cluster based RIF approach, although the cluster based  $C_T$  and national based  $C_T$  and RIF models performed at a similar level when considering only the  $BIAS$ ,  $RMSE$  and ratio. The  $NSE$  value and regression slopes favoured the cluster based RIF approach and it is therefore recommended for application.

The final objective of the study was the development of a design flood estimation utility. The structure of an on-line system has been developed that will allow users to seamlessly apply the developed methods on a national scale. News on advancements on the development of the tool will be available on the NFSP website (<https://www.nfsp.co.za>)

## **10.8 Recommendation for Future Research**

The following recommendations for future research and development are made:

1. Investigation into the impacts of non-stationarity on regionalisation
2. Investigation into the applicability of Bayesian statistics in South African hydrology
3. Compilation of a national hydrological descriptor database, beyond flood estimation, similar to the databases implemented internationally,
4. Further development of the NaFSApp to integrate additional models and techniques currently available,
5. Refinement of the estimation of aerial reduction factors,
6. Improvement of time of concentration estimation at a national scale

## 11 REFERENCES

- Acreman, MC. 1987. *Regional Flood Frequency Analysis in the UK: Recent Research – New Ideas*. Report No. None. Institute of Hydrology, Wallingford, UK.
- Acreman, MC and Wiltshire, SE. 1987. Identification of Regions for Regional Flood Frequency Analysis. *EOS* 68(44):1262
- Adamson, PT. 1981. *Southern African Storm Rainfall*. Department of Environment Affairs, Pretoria, South Africa.
- Ahn, K-H and Palmer, R. 2016. Regional Flood Frequency Analysis Using Spatial Proximity and Basin Characteristics: Quantile Regression Vs. Parameter Regression Technique. *Journal of Hydrology* 540(Supplement C):515-526
- Akaike, H. 1974. A New Look at the Statistical Model Identification. *IEEE Transactions on Automatic Control* 19(6):716-723
- Aldrich, J. 1997. R.A. Fisher and the Making of Maximum Likelihood 1912-1922. *Statist. Sci.* 12(3):162-176
- Alexander, WJR. 1990. *Flood Hydrology for Southern Africa*. SANCOLD, Pretoria, RSA.
- Alexander, WJR. 2000. *Flood Risk Reduction Measures*. University of Pretoria, Pretoria, South Africa.
- Alexander, WJR. 2002. The Standard Design Flood. *Journal of the South African Institution of Civil Engineering* 44(1):26-30
- Alexander, WJR. 2002. Statistical Analysis of Extreme Floods. University of Pretoria, Pretoria, South Africa.
- Anderson, TW and Darling, DA. 1952. Asymptotic Theory of Certain "Goodness of Fit" Criteria Based on Stochastic Processes. *Ann. Math. Statist.* 23(2):193-212
- Aronica, GT and Candela, A. 2007. Derivation of Flood Frequency Curves in Poorly Gauged Mediterranean Catchments Using a Simple Stochastic Hydrological Rainfall-Runoff Model. *Journal of Hydrology* 347(1):132-142
- Basson, MS and Pegram, GGS. 1994. *Probabalistic Management of Water Resource and Hydropower Systems*. Water Resources Publications, Highlands Ranch, Colo., USA.
- Beard, LR. 1974. *Flood Flow Frequency Techniques*. Report No. CRWR-119. University of Texas, Texas, USA.
- Ben-Zvi, A. 1989. Toward a New Rational Method. *Journal of Hydraulic Engineering* 115(9):1241-1255
- Benson, MA. 1968. Uniform Flood-Frequency Estimating Methods for Federal Agencies. *Water Resources Research* 4(5):891-908
- Blöschl, G, Sivapalan, M, Wagener, T, Viglione, A and Savenije, H. 2013. *Runoff Prediction in Ungauged Basins: Synthesis across Processes, Places and Scales*. Cambridge University Press, Cambridge, UK.
- Borujeni, SC and Sulaiman, WNA. 2009. Development of L-Moment Based Models for Extreme Flood Events. *Malaysian Journal of Mathematical Sciences* 3(2):281-296

- Burn, D. 1997. Catchments Similarity for Regional Flood Frequency Analysis Using Seasonality Measures. *Journal of Hydrology* 202(1):212-230
- Burn, DH. 1990. An Appraisal of the "Region of Influence" Approach to Flood Frequency Analysis. *Hydrological Sciences Journal* 25(2):149-165
- Burn, DH. 2003. The Use of Resampling for Estimating Confidence Intervals for Single Site and Pooled Frequency Analysis / Utilisation D'un Rééchantillonnage Pour L'estimation Des Intervalles De Confiance Lors D'analyses Fréquentielles Mono Et Multi-Site. *Hydrological Sciences Journal* 48(1):25-38
- Burn, DH and Goel, NK. 2000. The Formation of Groups for Regional Flood Frequency Analysis. *Hydrological Sciences Journal* 45(1):97-112
- Calitz, JP. 2016. Development and Assessment of a Probabilistic Rational Method for Design Flood Estimation in Selected Primary Drainage Regions in South Africa. Unpublished Bioresources Engineering, University of KwaZulu Natal, Pietermaritzburg, RSA.
- Caltrans. 2006. Chapter 810: Hydrology. In: ed. Transport, CDo, *Highway Design Manual*, California Department of Transport, California, USA.
- Cassalho, F, Beskow, S, de Mello, CR and de Moura, MM. 2018. Regional Flood Frequency Analysis Using L-Moments for Geographically Defined Regions: An Assessment in Brazil. *Journal of Flood Risk Management* 2018(e12453):1-13
- Castellarin, A, Domeneghetti, A and Brath, A. 2011. Identifying Robust Large-Scale Flood Risk Mitigation Strategies: A Quasi-2d Hydraulic Model as a Tool for the Po River. *Physics and Chemistry of the Earth, Parts A/B/C* 36(7-8):299-308
- Castellarin, A, Kohnova, S, Gaal, L, Fleig, A, Salinas, JL, Toumazis, A, Kjeldsen, TR and Macdonald, N. 2012. *Review of Applied-Statistical Methods for Flood-Frequency Analysis in Europe*. Report No. ES0901. Centre for Ecology & Hydrology, Wallingford, UK.
- Cavadias, GS. 1990. The Canonical Correlation Approach to Regional Flood Estimation. In: eds. *Regionalization in Hydrology*, International Association of Hydrological Sciences, Ljubljana, Slovenia.
- Cavadias, GS, Ouarda, TBMJ, Bobèe, B and Girard, C. 2001. A Canonical Correlation Approach to the Determination of Homogeneous Regions for Regional Flood Estimation of Ungauged Basins. *Hydrological Sciences Journal* 46(4):499-512
- Chadwick, A, Morfett, J and Borthwick, M. 2004. *Hydraulics in Civil and Environmental Engineering*. Spon, London, England.
- Chen, Y, Wang, Q, Wang, L, Pieter, VG and Chen, M. 2007. Regional Flood Frequency Analysis by L-Moments for the Middle and Lower Reaches Region of the Yangtze River. *Water Resources and Environment* 1(2007):204-209
- Choquette, AF. 1988. *Regionalisation of Peak Discharges for Streams in Kentucky*. Report No. 87-4209. US Geological Survey, Kentucky, USA.
- Chow, VT, Maidment, DR and Mays, LR. 1988. *Applied Hydrology*. McGraw-Hill, New York, USA.
- Cohn, TA, England, JF, Berenbrock, CE, Mason, RR, Stedinger, JR and Lamontagne, JR. 2013. A Generalized Grubbs-Beck Test Statistic for Detecting Multiple Potentially Influential Low Outliers in Flood Series. *Water Resources Research* 49(8):5047-5058

- Cramér, H. 1928. On the Composition of Elementary Errors. *Scandinavian Actuarial Journal* 1928(1):13-74
- Dalrymple, T. 1960. *Manual of Hydrology: Part 3 Flood Flow Techniques. Flood Frequency Analyses*. Report No. 1543-A. US Geol. Survey Water Supply, USA.
- Davies, R. 2017. *South Africa – Storm Leaves 8 Dead, Record Rain in Durban*. Date Accessed: 27/08/2018, Floodlist, <http://floodlist.com/africa/kwazulu-natal-durban-flood-october-2017>.
- de Groen, M, Bailey, A and Commission, WR. 2015. *Water Resources of South Africa 2012*. Date Accessed: 2 February 2016, Water Research Commission, <http://waterresourceswr2012.co.za>.
- Durbin, J and Knott, M. 1972. Components of Cramer-Von Mises Statistics. I. *Journal of the Royal Statistical Society. Series B (Methodological)* 34(2):290-307
- DWS. 2015. *U3h001*. Date Accessed: 01/05/2015, Department of Water and Sanitation, <https://www.dwa.gov.za/Hydrology/HyImage.aspx?Station=U3H001>.
- Eng, K, Tasker, GD and Milly, PCD. 2005. An Analysis of Region-of-Influence Methods for Flood Regionalisation in the Gulf-Atlantic Rolling Plains. *Journal of the American Water Resources Association* 41(1):135-143
- England, JF, Cohn, TA, Faber, BA, Stedinger, JR, Thomas Jr, WO, Veilleux, AG, Kiang, JE and Mason Jr, RR. 2018. *Guidelines for Determining Flood Flow Frequency—Bulletin 17c*. Report No. 4-B5. Reston, VA, USA.
- Filliben, JJ. 1975. The Probability Plot Correlation Coefficient Test for Normality. *Technometrics* 17(1):111-117
- Gabriele, S and Arnell, N. 1991. A Hierarchical Approach to Regional Flood Frequency Analysis. *Water Resources Research* 27(6):1281-1289
- Gado, T and Nguyen, V. 2016. Comparison of Homogenous Region Delineation Approaches for Regional Flood Frequency Analysis at Ungauged Sites. *Journal of Hydrologic Engineering* 21(3):441-495
- Ganora, D and Laio, F. 2016. A Comparison of Regional Flood Frequency Analysis Approaches in a Simulation Framework. *Water Resources Research* 52(7):5644-5661
- Gericke, OJ. 2010. Evaluation of the Sdf Method Using a Customised Design Flood Estimation Tool. Unpublished MScEng Thesis, Department of Civil Engineering, Stellenbosch University, Stellenbosch, RSA.
- Gericke, OJ and Smithers, JC. 2015. An Improved and Consistent Approach to Estimate Catchment Response Time Parameters: Case Study in the C5 Drainage Region, South Africa. *Journal of Flood Risk Management* 11(S1):S284-S301
- Glatfelter, DR. 1984. *Techniques for Estimating Magnitude and Frequency of Floods on Streams in Indiana*. Report No. 84-4134. US Geological Survey, Indiana, USA.
- Görgens, AHM. 2002. Design Flood Hydrology. In: ed. Basson, G, *Design and Rehabilitation of Dams*, 460-524. Institute for Water and Environmental Engineering, Department of Civil Engineering, University of Stellenbosch, South Africa.
- Görgens, AHM. 2007. *Joint Peak-Volume (Jpv) Design Flood Hydrographs for South Africa*. Report No. 1420/3/07. Water Research Commission, Gezina, South Africa.

- Görgens, AHM. 2007. *Modernised South African Design Flood Practice in the Context of Dam Safety*. Report No. 1420/2/07. Water Research Commission, Gezina, South Africa.
- Greenwood, JA, Landwehr, JM, Matalas, NC and Wallis, JR. 1979. Probability Weighted Moments: Definition and Relation to Parameters of Several Distributions Expressable in Inverse Form. *Water Resources Research* 15(5):1049-1054
- GREHYS (Groupe de recherche en hydrologie, s. 1996. Presentation and Review of Some Methods for Regional Flood Frequency Analysis. *Journal of Hydrology* 186(1-4):63-84
- Haddad, K and Rahman, A. 2008. Investigation on at-Site Flood Frequency Analysis in South-East Australia. *The institution of engineers, Malaysia* 69(3):59-64
- Haddad, K and Rahman, A. 2011. Selection of the Best Fit Flood Frequency Distribution and Parameter Estimation Procedure: A Case Study for Tasmania in Australia. *Stochastic Environmental Research and Risk Assessment* 25(3):415-428
- Haddad, K, Rahman, A and Ling, F. 2015. Regional Flood Frequency Analysis Method for Tasmania, Australia: A Case Study on the Comparison of Fixed Region and Region-of-Influence Approaches. *Hydrological Sciences Journal* 60(12):2086-2101
- Haddad, K, Rahman, A and Stedinger, JR. 2012. Regional Flood Frequency Analysis Using Bayesian Generalized Least Squares: A Comparison between Quantile and Parameter Regression Techniques. *Hydrological Processes* 26(7):1008-1021
- Haile, AT. 2011. Regional Flood Frequency Analysis in Southern Africa. Unpublished MSc Thesis, Department of Geosciences, University of Oslo, Oslo, Norway.
- Hassan, BGH and Ping, F. 2012. Formation of Homogenous Regions for Luanhe Basin – by Using L-Moments and Cluster Techniques. *International Journal of Environmental Science and Development* 3(2):205-210
- He, Y, Bárdossy, A and Zehe, E. 2011. A Review of Regionalisation for Continuous Streamflow Simulation. *Hydrol. Earth Syst. Sci.* 15(11):3539-3553
- Hodgkins, GA, Hebson, C, Lombard, PJ and Mann, A. 2007. *Comparison of Peak-Flow Estimation Methods for Small Drainage Basins in Maine*. Report No. 2007-5170. U.S. Geological Survey, Maine, USA.
- Holloway, A, Fortune, G and Chasi, V. 2010. *Risk and Development Annual Review: Western Cape*. Report No. 2010. University of Cape Town, Cape Town, South Africa.
- Hosking, JRM. 1990. L-Moment – Analysis and Estimation of Distributions Using Linear-Combinations of Order-Statistics. *Journal of the Royal Statistical Society* 52(1):105-124
- Hosking, JRM. 1994. The Four-Parameter Kappa Distribution. *IBM Journal of Research and Development* 38(3):251-258
- Hosking, JRM and Wallis, JR. 1993. Some Statistics Useful in Regional Frequency Analysis. *Water Resources Research* 29(2):271-281
- Hosking, JRM and Wallis, JR. 1997. *Regional Frequency Analysis: An Approach Based on L-Moments*. Cambridge University Press, Cambridge, UK.
- HRU. 1972. *Design Flood Determination in South Africa*. Report No. 1/72. University of the Witwatersrand, Department of Civil Engineering, Johannesburg, South Africa.

- Ilorme, F and Griffis, VW. 2013. A Novel Procedure for Delineation of Hydrologically Homogeneous Regions and the Classification of Ungauged Sites for Design Flood Estimation. *Journal of Hydrology* 492(2013):151-162
- Kachroo, RK, Mkhandi, SH and Parida, BP. 2000. Flood Frequency Analysis of Southern Africa: I. Delineation of Homogeneous Regions. *Hydrological Sciences Journal* 45(3):437-447
- Kasserchun, R. 2008. *Design Manual: Guidelines for the Design of Stormwater Drainage and Stormwater Management Systems*. Report No. None. Coastal Stormwater and Catchment Management Department, eThekweni Municipality, Durban, South Africa.
- Kjeldsen, T, Jones, D, Bayliss, A, Spencer, P, Surendran, S, Stefan, L, Webster, P and McDonald, D. 2008. Improving the Feh Statistical Method. Environment Agency/Defra, University of Manchester, UK.
- Kjeldsen, TR, Ahn, H and Prosdocimi, I. 2017. On the Use of a Four-Parameter Kappa Distribution in Regional Frequency Analysis. *Hydrological Sciences Journal* 62(9):1354-1363
- Kjeldsen, TR and Jones, D. 2007. Estimation of an Index Flood Using Data Transfer in the Uk. *Hydrological Sciences Journal* 52(1):86-98
- Kjeldsen, TR and Jones, DA. 2006. Prediction Uncertainty in a Median-Based Index Flood Method Using L Moments. *Water Resources Research*, 42. doi: 10.1029/2005WR004069.
- Kjeldsen, TR, Jones, DA and Bayliss, AC. 2008. *Improving the Feh Statistical Procedures for Flood Frequency Estimation*. Report No. SC050050. Environment Agency, Bristol, UK.
- Kjeldsen, TR, Lamb, R and Blazkova, SD. 2014. Uncertainty in Flood Frequency Analysis. In: ed. Beven, K and Hall, J, *Applied Uncertainty Analysis for Flood Risk Management*, 684. IMPERIAL COLLEGE PRESS, London, UK.
- Kjeldsen, TR and Prosdocimi, I. 2015. A Bivariate Extension of the Hosking and Wallis Goodness-of-Fit Measure for Regional Distributions. *Water Resources Research* 51(2):896-907
- Kjeldsen, TR, Smithers, JC and Schulze, RE. 2001. Flood Frequency Analysis at Ungauged Sites in the Kwazulu-Natal Province, South Africa. *Water SA* 27(3):315-324
- Kjeldsen, TR, Smithers, JC and Schulze, RE. 2002. Regional Flood Frequency Analysis in the Kwazulu-Natal Province, South Africa, Using the Index-Flood Method. *Journal of hydrology* 2002(255):194-211
- Kottegoda, NT and Rosso, R. 2008. *Applied Statistics for Civil and Environmental Engineers*. McGraw-Hill, West Sussex, UK.
- Kovács, ZP. 1988. *Regional Maximum Flood Peaks in Southern Africa*. Department of Water Affairs, Pretoria, South Africa.
- Laio, F. 2004. Cramer-Von Mises and Anderson-Darling Goodness of Fit Tests for Extreme Value Distributions with Unknown Parameters. *Water Resources Research*, 40. doi: 10.1029/2004WR003204.
- Laio, F, Di Baldassarre, G and Montanari, A. 2009. Model Selection Techniques for the Frequency Analysis of Hydrological Extremes. *Water Resources Research*, 45. doi: 10.1029/2007WR006666.

- Lynch, SD. 2004. *Development of a Raster Database of Annual, Monthly and Daily Rainfall for Southern Africa*. Report No. 1156-1-04. Water Research Commission, Gezina, South Africa.
- Massey, FJ. 1951. The Kolmogorov-Smirnov Test for Goodness of Fit. *Journal of the American Statistical Association* 46(253):68-78
- McDermott, GE and Pilgrim, DH. 1982. *Design Flood Estimation for Small Catchments in New South Wales*. Department of National Development and Energy, Canberra, Australia.
- Mediero, L and Kjeldsen, TR. 2014. Regional Flood Hydrology in a Semi-Arid Catchment Using a Gls Regression Model. *Journal of Hydrology* 514(2014):158-171
- Merz, R and Blöschl, G. 2005. Flood Frequency Regionalisation – Spatial Proximity Vs. Catchment Attributes. *Journal of hydrology* 302(1):283-306
- Mkhandi, SH and Kachroo, RK. 1997. *Regional Flood Frequency Analysis for Southern Africa. Southern African Friend, Technical Documents in Hydrology 15*. UNESCO, Paris, France.
- Mkhandi, SH, Kachroo, RK and Gunsdeksrs, TAG. 2000. Flood Frequency Analysis for Southern Africa: Ii. Identification of Regional Distributions. *Hydrological Sciences Journal* 45(3):449-464
- Mostofi Zadeh, S and Burn, DH. 2019. A Super Region Approach to Improve Pooled Flood Frequency Analysis. *Canadian Water Resources Journal / Revue canadienne des ressources hydriques*, doi: 10.1080/07011784.2018.1548946.
- Mulvaney, TJ. 1850. On the Use of Self-Registering Rain and Flood Gauges in Making Observations on the Relationship of Rainfall and Runoff and of Flood Discharges in a Given Catchment. In: eds. *Transactions, Institute of Civil Engineers (Ireland)*, 10.
- Naidoo, J. In Preparation. An Assessment of the Performance of Deterministic and Empirical Design Flood Estimation Methods Used in South Africa. Pietermaritzburg, RSA.
- Nash, JE and Sutcliffe, JV. 1970. River Flow Forecasting through Conceptual Models Part I — a Discussion of Principles. *Journal of Hydrology* 10(3):282-290
- Nobert, J, Mugo, M and Gadain, H. 2014. Estimation of Design Floods in Ungauged Catchments Using a Regional Index Flood Method. A Case Study of Lake Victoria Basin in Kenya. *Physics and Chemistry of the Earth, Parts A/B/C* 67-69(2014):4-11
- Odry, J and Arnaud, P. 2017. Comparison of Flood Frequency Analysis Methods for Ungauged Catchments in France. *Geosciences* 7(3):88
- Ouarda, TBMJ, Girard, C, Cavadias, GS and Bobée, B. 2001. Regional Flood Frequency Estimation with Canonical Correlation Analysis. *Journal of Hydrology* 254(1-4):157-173
- Oudin, L, Andréassian, V, Perrin, C, Michel, C and Le Moine, N. 2008. Spatial Proximity, Physical Similarity, Regression and Ungauged Catchments: A Comparison of Regionalization Approaches Based on 913 French Catchments. *Water Resources Research*, 44. doi: 10.1029/2007WR006240.
- Parak, M and Pegram, GGS. 2006. Rational Formula from Runhydrograph. *Water SA* 32(2):163-180

- Pearson, CP. 1991. New Zealand Regional Flood Frequency Analysis Using L-Moments. *Journal of Hydrology (New Zealand)* 30(2):53-64
- Pearson, K. 1900. On the Criterion That a Given System of Deviations from the Probable in the Case of a Correlated System of Variables Is Such That It Can Be Reasonably Supposed to Have Arisen from Random Sampling. *The London, Edinburgh, and Dublin Philosophical Magazine and Journal of Science* 50(302):157-175
- Peel, MC, Wang, QJ, Vogel, RM and McMahon, TA. 2001. The Utility of L-Moment Ratio Diagrams for Selecting a Regional Probability Distribution. *Hydrological Sciences Journal* 46(1):147-155
- Pegram, GGS. 2003. Rainfall, Rational Formula and Regional Maximum Flood – Some Scaling Links. *Australian Journal of Water Resources* 7(1):29-39
- Pilgrim, D and Cordery, I. 1993. Flood Runoff. In: ed. Maidment, D, *Handbook of Hydrology*, 9, McGraw-Hill, New York, USA.
- Pilgrim, DH. 1989. Regional Methods for Estimation of Design Floods for Small to Medium Sized Drainage Basins in Australia. In: eds. *Baltimore Symposium*, 14. Baltimore, USA.
- Pilgrim, DH. 2001. *Australian Rainfall and Runoff : A Guide to Flood Estimation*. Institution of Engineers, Barton, A.C.T., Australia.
- Rahman, A, Haddad, K, Haque, MM, Kuczera, G and Weinmann, E. 2015. *Australian Rainfall and Runoff Revision Project 5: Regional Flood Methods (Stage 3)*. Report No. P5/S3/025. Engineers Australia, Australia.
- Rahman, A, Haddad, K, Kuczera, G and Weinmann, E. 2009. *Australian Rainfall and Runoff Revision Project 5: Regional Flood Methods (Stage 1)*. Report No. P5/SI/003. University of Western Sydney, Sydney, Australia.
- Rahman, A, Haddad, K, Kuczera, G and Weinmann, E. 2015. Regional Flood Methods. In: ed. Ball, J, *Australian Rainfall and Runoff: Book 3 Draft for Comment*, Engineers Australia, Australia.
- Rahman, A, Haddad, K, Kuczera, G and Weinmann, E. 2019. Book 3: Peak Flow Estimation. In: ed. Ball, J, *Australian Rainfall and Runoff: A Guide to Flood Estimation*, © Commonwealth of Australia (Geoscience Australia), Australia.
- Rahman, A, Haddad, K, Zaman, M, Ishak, E, Kuczera, G and Weinmann, E. 2012. *Australian Rainfall and Runoff Revision Project 5: Regional Flood Methods (Stage 2)*. Report No. P5/S2/015. University of Western Sydney, Sydney, Australia.
- Rao, AR and Srinivas, VV. 2008. *Regionalization of Watersheds : An Approach Based on Cluster Analysis*. Springer Science+Business Media B.V., Dordrecht, Netherlands.
- Razavi, T and Coulibaly, P. 2013. Streamflow Prediction in Ungauged Basins: Review of Regionalization Methods. *Journal of Hydrologic Engineering* 18(8):958-975
- Reis, DS, Stedinger, JR and Martins, ES. 2003. Bayesian GLS Regression with Application to Lp3 Regional Skew Estimation. *Water Resources Research* 41(10):1049-1058
- Ribeiro-Corréa, J, Cavadias, GS, Clément, B and Rousselle, J. 1995. Identification of Hydrological Neighborhoods Using Canonical Correlation Analysis. *Journal of Hydrology* 173(1-4):71-89

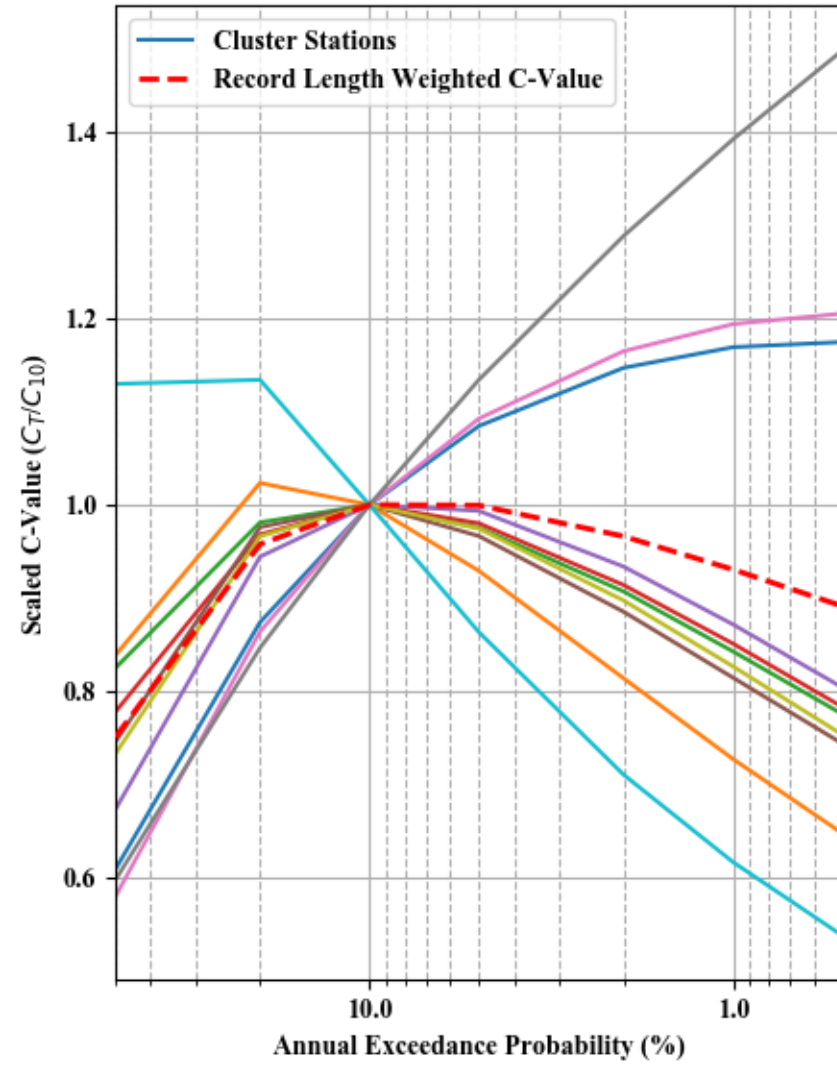
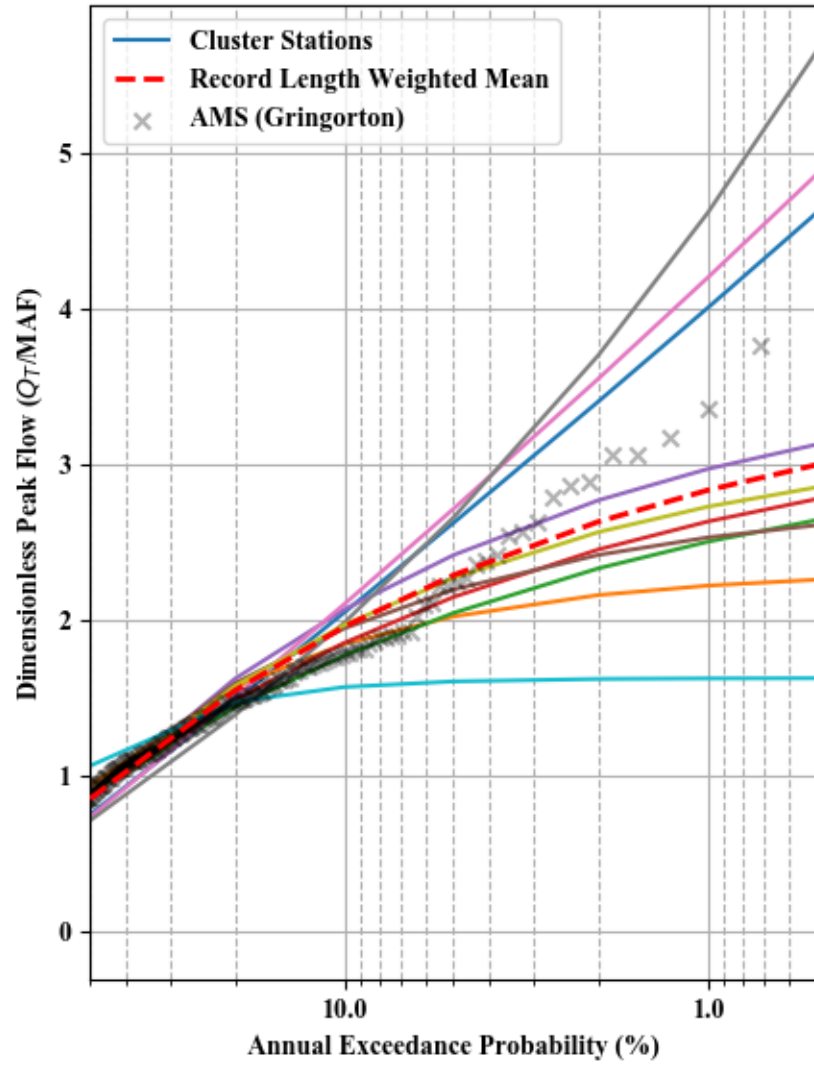
- Ridolfi, E, Rianna, M, Trani, G, Alfonso, L, Di Baldassarre, G, Napolitano, F and Russo, F. 2016. A New Methodology to Define Homogeneous Regions through an Entropy Based Clustering Method. *Advances in Water Resources* 96(Supplement C):237-250
- Riggs, HC. 1982. *Techniques of Water-Resources Investigations of the United States Geological Survey: Regional Analyses of Streamflow Characteristics*. United States Geological Survey, Washington, USA.
- Robson, A and Reed, D. 1999. *Flood Estimation Handbook Volume 3: Statistical Procedures for Flood Frequency Estimation*. Institute of Hydrology, Oxfordshire, UK.
- Rutkowska, A, Żelazny, M, Kohnová, S, Łyp, M and Banasik, K. 2016. Regional L-Moment-Based Flood Frequency Analysis in the Upper Vistula River Basin, Poland. *Pure and Applied Geophysics*, 174. doi: 10.1007/s00024-016-1298-8.
- Salinas, JL, Castellarin, A, Viglione, A, Kohnová, S and Kjeldsen, TR. 2014. Regional Parent Flood Frequency Distributions in Europe – Part 1: Is the Gev Model Suitable as a Pan-European Parent? *Hydrol. Earth Syst. Sci.* 18(11):4381-4389
- SANRAL. 2013. *Drainage Manual (6th Edition)*. South African National Roads Agency Limited, Pretoria, South Africa.
- Scholz, FW and Stephens, MA. 1987. K-Sample Anderson-Darling Tests. *Journal of the American Statistical Association* 82(399):918-924
- Schulze, RE. 2011. *A 2011 Perspective on Climate Change and the South African Water Sector*. Report No. WRC Report TT 518/12. Water Research Commission, Pretoria, RSA.
- Schulze, RE, Schmidt, EJ and Smithers, JC. 2004. *Visual Scs-Sa User Manual : Pc-Based Scs Design Flood Estimates for Small Catchments in Southern Africa*. University of KwaZulu-Natal, Pietermaritzburg, South Africa.
- Schulze, RE and Schütte, S. In Preparation. Mapping Scs Hydrological Soil Groups over South Africa at Terrain Unit Resolution.
- Schwarz, G. 1978. Estimating the Dimension of a Model. *The Annals of Statistics* 6(2):461-464
- Shaw, EM. 1994. *Hydrology in Practice*. Chapman & Hall, London, England.
- Shiceka, S. 2011. *Media Statement on the Declaration of a National Disaster as a Result of Flooding and Other Natural Disasters in the South Africa*. Ministry for cooperative governance and traditional affairs, Pretoria, South Africa.
- Silva, A, Portela, M, Baez, J and Naghettini, M. 2012. Construction of Confidence Intervals for Extreme Rainfall Quantiles. *WIT Transactions on information and Communication technologies*, 44. doi: 10.2495/RISK120251.
- Smithers, JC. 1998. Development and Evaluation of Techniques for Estimating Short Duration Design Rainfall in South Africa. Unpublished PhD, Agricultural Engineering, University of Natal, Pietermaritzburg, South Africa.
- Smithers, JC. 2012. Review of Methods for Design Flood Estimation in South Africa. *Water SA* 38(4):633-646
- Smithers, JC, Görgens, A, Gericke, OJ, Jonker, V and Roberts, CPR. 2014. The Initiation of a National Flood Studies Programme for South Africa. SANCOLD, Birchwood, Gauteng.

- Smithers, JC and Schulze, RE. 2000. *Development and Evaluation of Techniques for Estimating Short Duration Design Rainfall in South Africa*. Report No. 681/1/00. Water Research Commission, Pretoria, South Africa.
- Smithers, JC and Schulze, RE. 2000. *Long Duration Design Rainfall Estimates for South Africa*. Report No. 811/1/00. Water Research Commission, Pretoria, RSA.
- Smithers, JC and Schulze, RE. 2003. *Design Rainfall and Flood Estimation in South Africa*. Report No. 1060/1/03. Water Research Commission, Gezina, South Africa.
- Smithers, JC, Streatfield, J, Gray, RP and Oakes, EGM. 2015. Performance of Regional Flood Frequency Analysis Methods in Kwazulu-Natal, South Africa. *Water SA* 41(3):390-397
- Stedinger, JR and Griffis, VW. 2008. Flood Frequency Analysis in the United States: Time to Update. *Journal of Hydrologic Engineering* 13(4):199-204
- Stedinger, JR, Vogel, RM and Foufoula-Georgiou, E. 1993. Frequency Analysis of Extreme Events. In: ed. Maidment, DR, *Handbook of Hydrology*, 18, McGraw-Hill, Inc., New York.
- Stephenson, D. 1981. *Stormwater Hydrology and Drainage*. Elsevier Scientific, Amsterdam, Netherlands.
- Sugiura, N. 1978. Further Analysts of the Data by Akaike' S Information Criterion and the Finite Corrections. *Communications in Statistics – Theory and Methods* 7(1):13-26
- Tasker, GD. 1982. Comparing Methods of Hydrologic Regionalization. *Water Resources Bulletin* 18(6):965-970
- Gdal – Geospatial Data Abstraction Library: 1.7.2, 2017. Open Source Geospatial Foundation, <http://www.gdal.org>.
- Thomas, DM and Benson, MA. 1970. *Generalization of Streamflow Characteristics from Drainage-Basin Characteristics*. US Department of the Interior, Washington DC, USA.
- Thompson, DB. 2007. *The Rational Method*. R. O. Anderson Engineering, Minden, Nevada, USA.
- Tsakiris, G, Nalbantis, I and Cavadias, G. 2011. Regionalization of Low Flows Based on Canonical Correlation Analysis. *Advances in Water Resources* 34(7):865-872
- Van Bladeren, D. 1993. Application of Historical Flood Data in Flood Frequency Analysis, for the Natal and Transkei Region. In: eds. *Proceedings of Sixth South African National Hydrological Symposium*, 359-366. Department of Agricultural Engineering, University of Natal.
- Van Bladeren, D. 2005. *Verification of the Proposed Standard Design Flood (Sdf)*. Report No. 344512/1. SRK Consulting (Pty) Ltd, Pretoria, South Africa.
- Van Bladeren, D, Zawada, PKZ and Mahlangu, D. 2007. *Statistical Based Regional Flood Frequency Estimation Study for South Africa Using Systematic, Historical and Paleoflood Data – Pilot Study – Catchment Management Area 15*. Report No. 1260/1/07. WRC, Pretoria, RSA.
- Van der Spuy, D and Rademeyer, PF. 2018. Flood Frequency Estimation Methods as Applied in the Department of Water Affairs. Department of Water Affairs, Pretoria, South Africa.

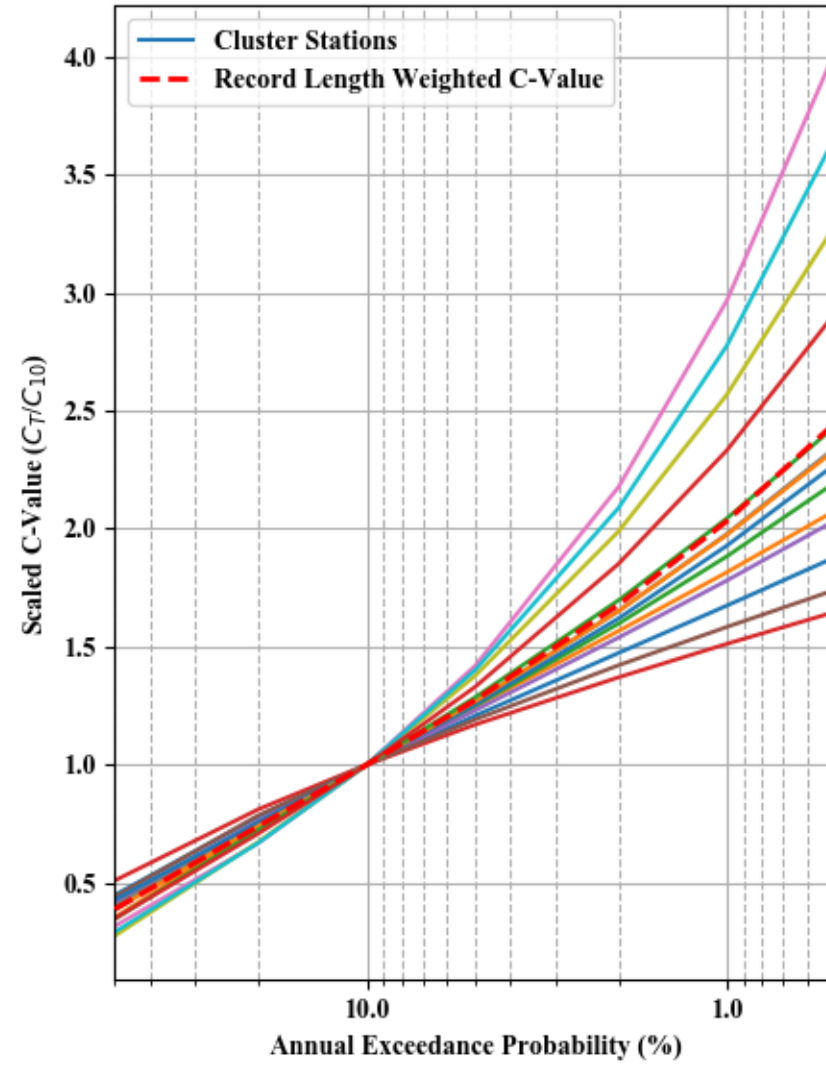
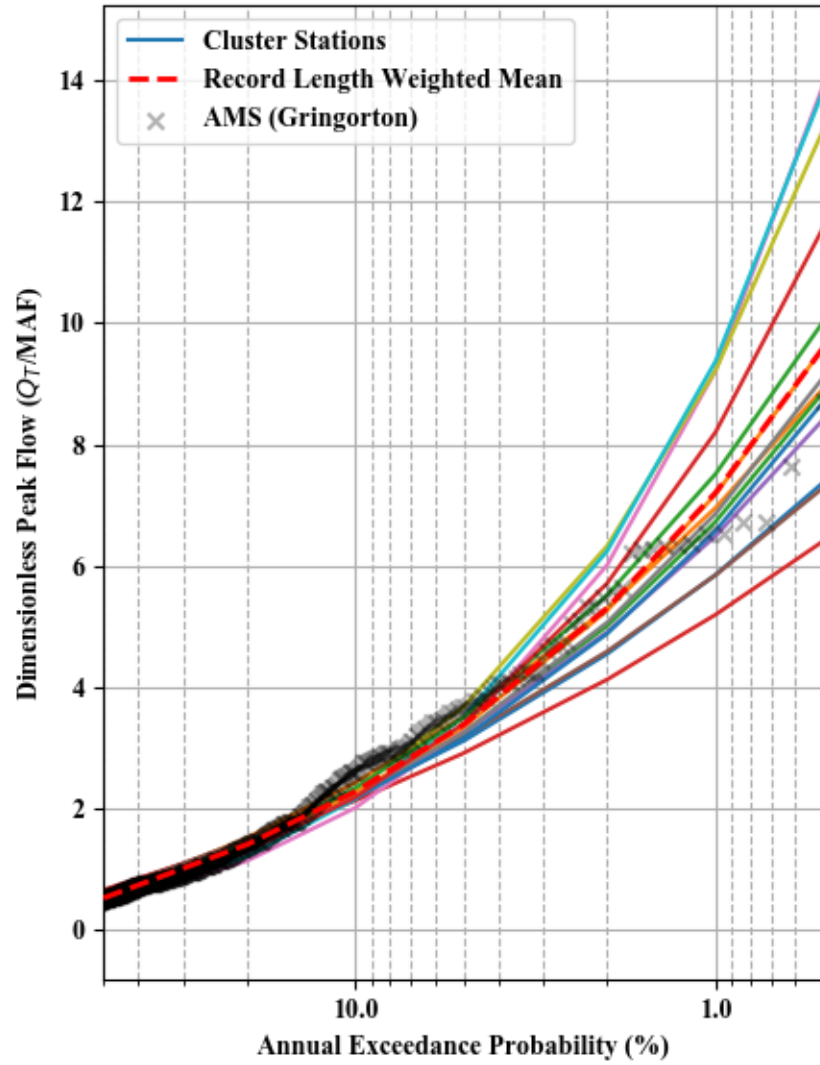
- Van Dijk, M, van Vuuren, SJ and Smithers, JC. 2013. Chapter 3: Flood Calculations. In: ed. Kruger, E, *Drainage Manual (Version 6)*, 3, 3.1-3.69. The South African Roads Agency SOC Limited, Pretoria, South Africa.
- Van Vuuren, SJ, Van Dijk, M and Coetzee, GL. 2013. *Status Review and Requirements of Overhauling Flood Determination Methods in South Africa*. Report No. TT563/13. WRC, Pretoria, RSA.
- Viglione, A, Laio, F and Claps, P. 2007. A Comparison of Homogeneity Tests for Regional Frequency Analysis. *Water Resources Research*, 43. doi: 10.1029/2006WR005095.
- Vogel, RM and Fennessey, NM. 1993. L Moment Diagrams Should Replace Product Moment Diagrams. *Water Resources Research* 29(6):1745-1752
- Vogel, RM, McMahon, TA and Chiew, FHS. 1993. Floodflow Frequency Model Selection in Australia. *Journal of Hydrology* 146(1993):421-449
- von Mises, RE. 1928. *Wahrscheinlichkeit, Statistik Und Wahrheit*. Julius Springer, Vienna, Austria.
- Wang, QJ. 1997. Lh Moments for Statistical Analysis of Extreme Events. *Water Resources Research* 33(12):2841-2848
- Weisberg, S. 2005. *Applied Linear Regression*. John Wiley and Sons, Inc., New Jersey, USA.
- Wiltshire, SE. 1986. Regional Flood Frequency Analysis Ii: Multivariate Classification of Drainage Basins in Britain. *Hydrological Sciences Journal* 31(3):335-346
- Wiltshire, SE. 1986. Regional Flood Frequency Analysis, I, Homogeneity Statistics. *Hydrological Sciences Journal* 31(3):321-333
- Young, CB, McEnroe, BM and Rome, A. 2009. Empirical Determination of Rational Method Runoff Coefficients. *ASCE Journal of Hydrologic Engineering* 14(12):1061-1067
- Zafirakou-Koulouris, A, Vogel, RM, Craig, SM and Habermeier, J. 1998. L Moment Diagrams for Censored Observations. *Water Resources Research* 34(5):1241-1249
- Zeng, X, Wang, D and Wu, J. 2015. Evaluating the Three Methods of Goodness of Fit Test for Frequency Analysis. *Journal of Risk Analysis and Crisis Response* 5(3):178-187
- Zrinji, Z and Burn, H. 1996. Regional Flood Frequency with Hierarchical Region of Influence. *Journal of Water Resources Planning and Management* 122(4):245-252

## **APPENDIX A: DIMENSIONLESS GROWTH CURVES**

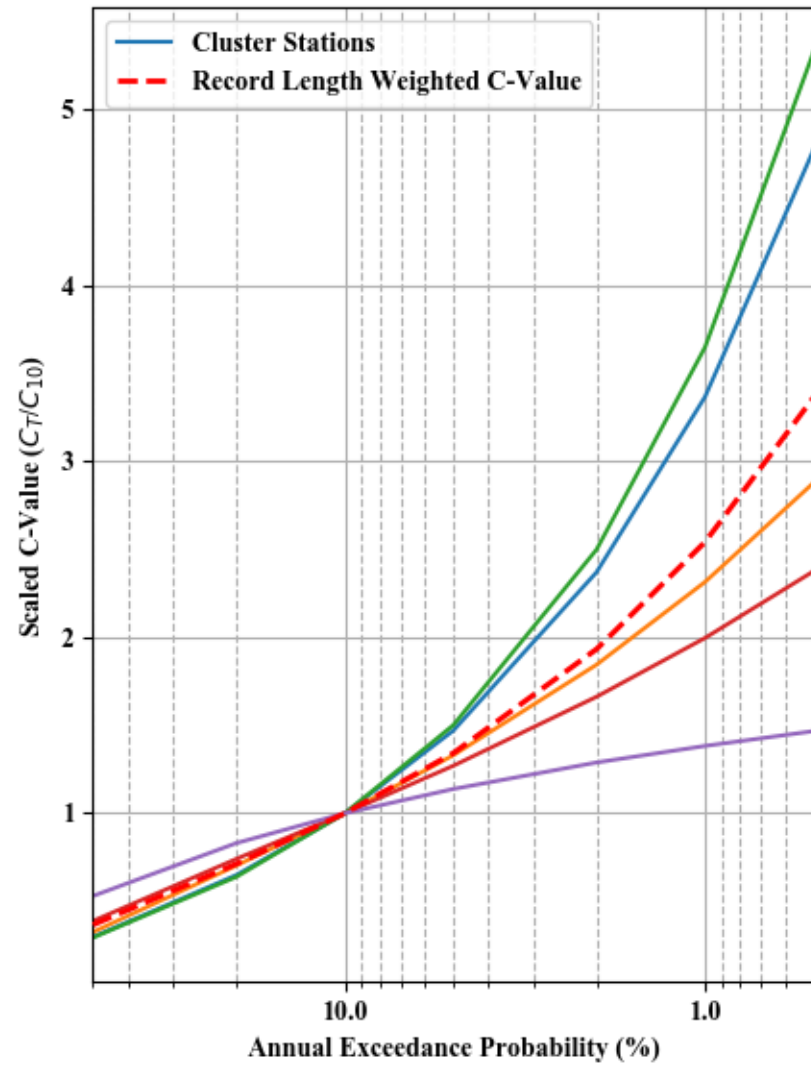
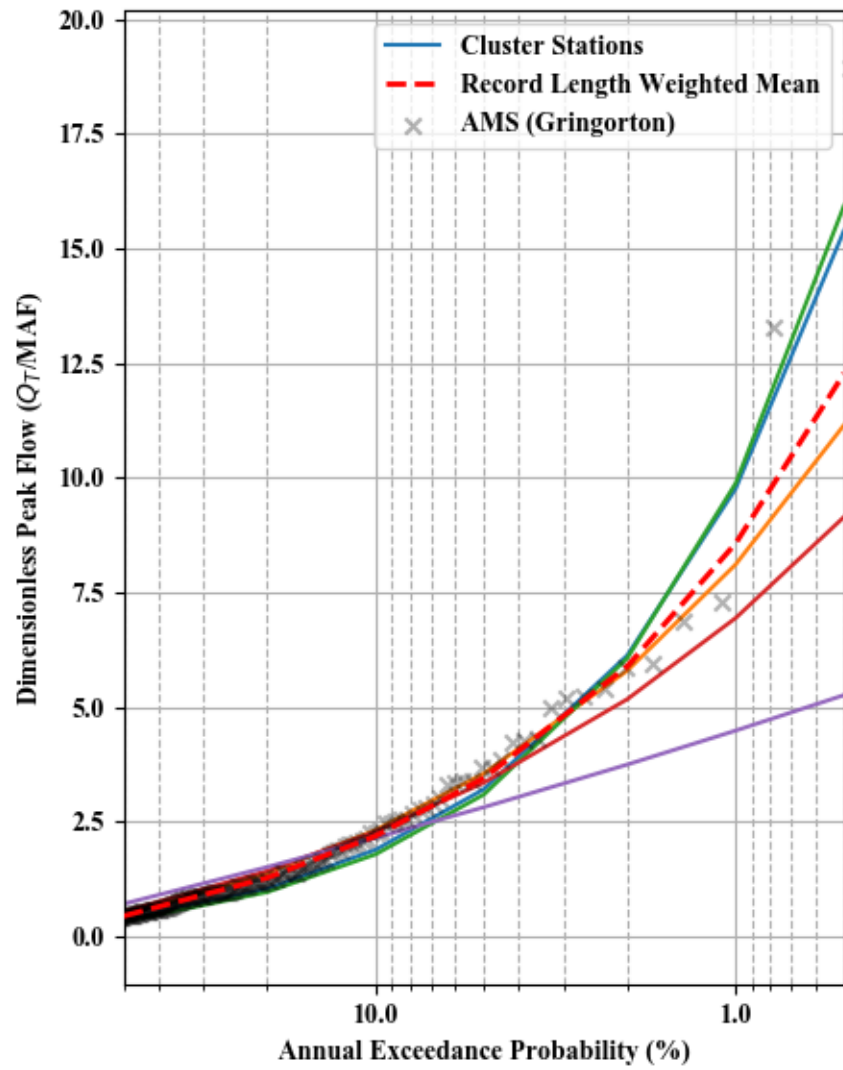
Dimensionless Peak Flow and Scaled C-value - Cluster 1



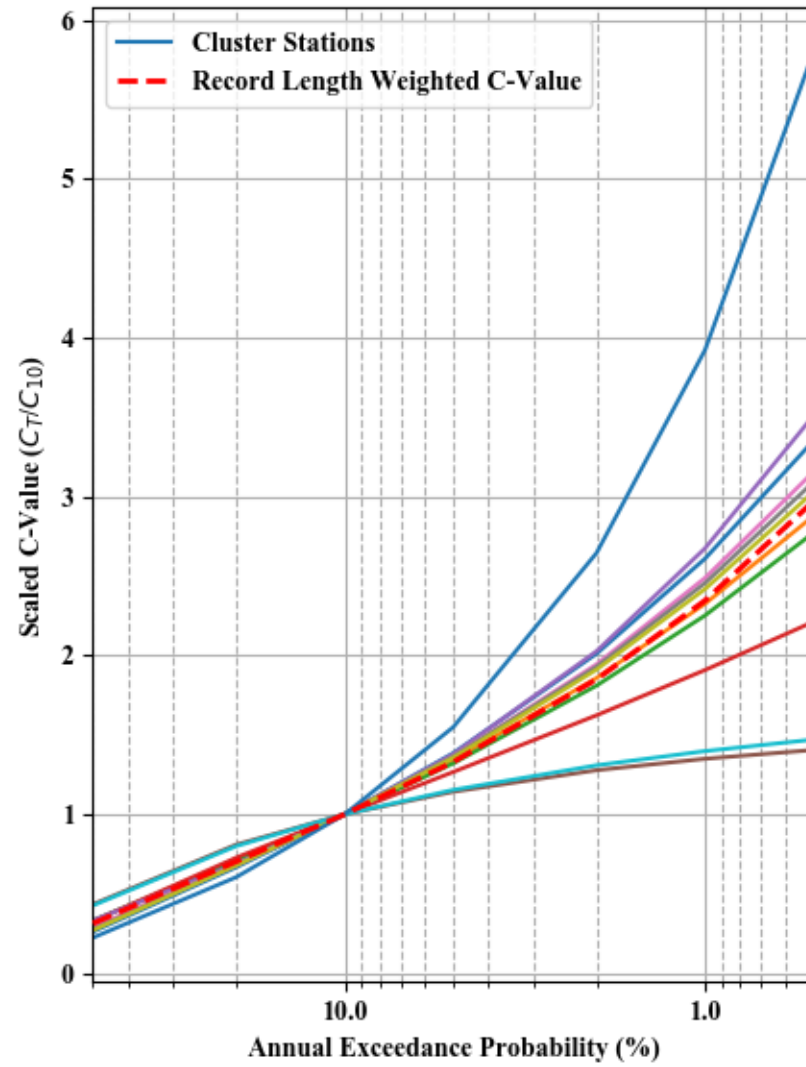
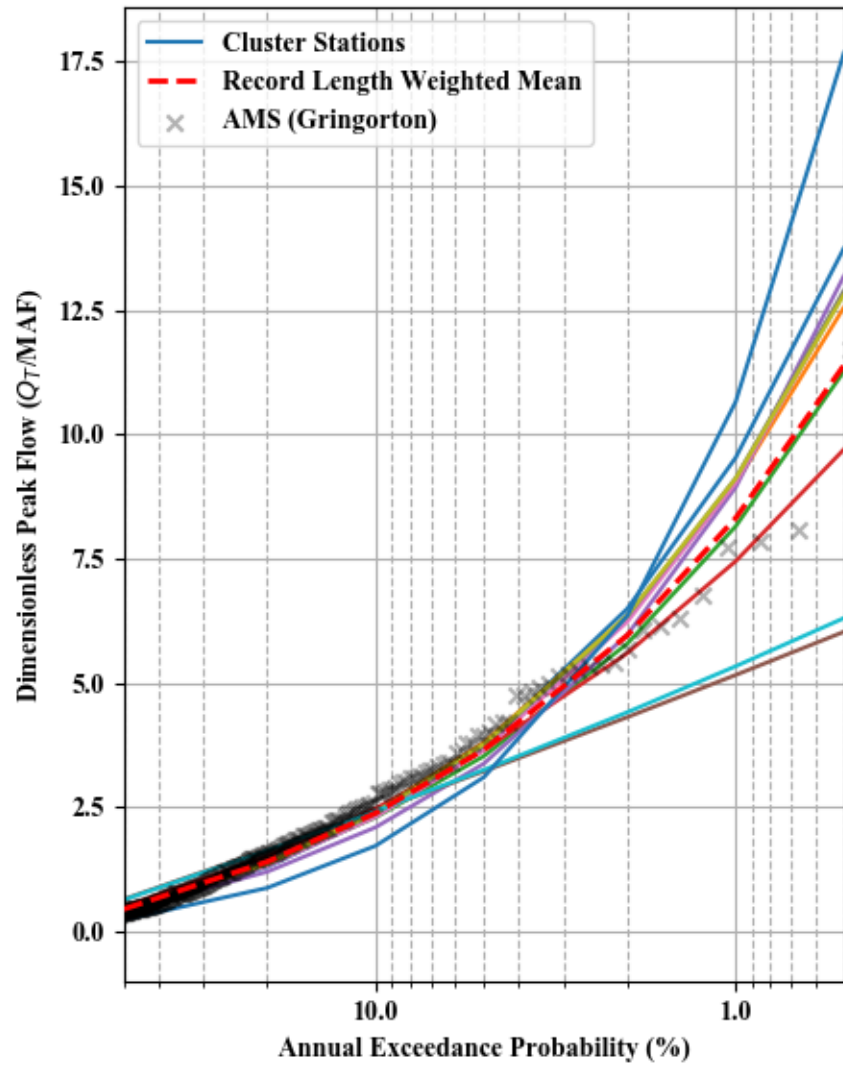
Dimensionless Peak Flow and Scaled C-value - Cluster 2



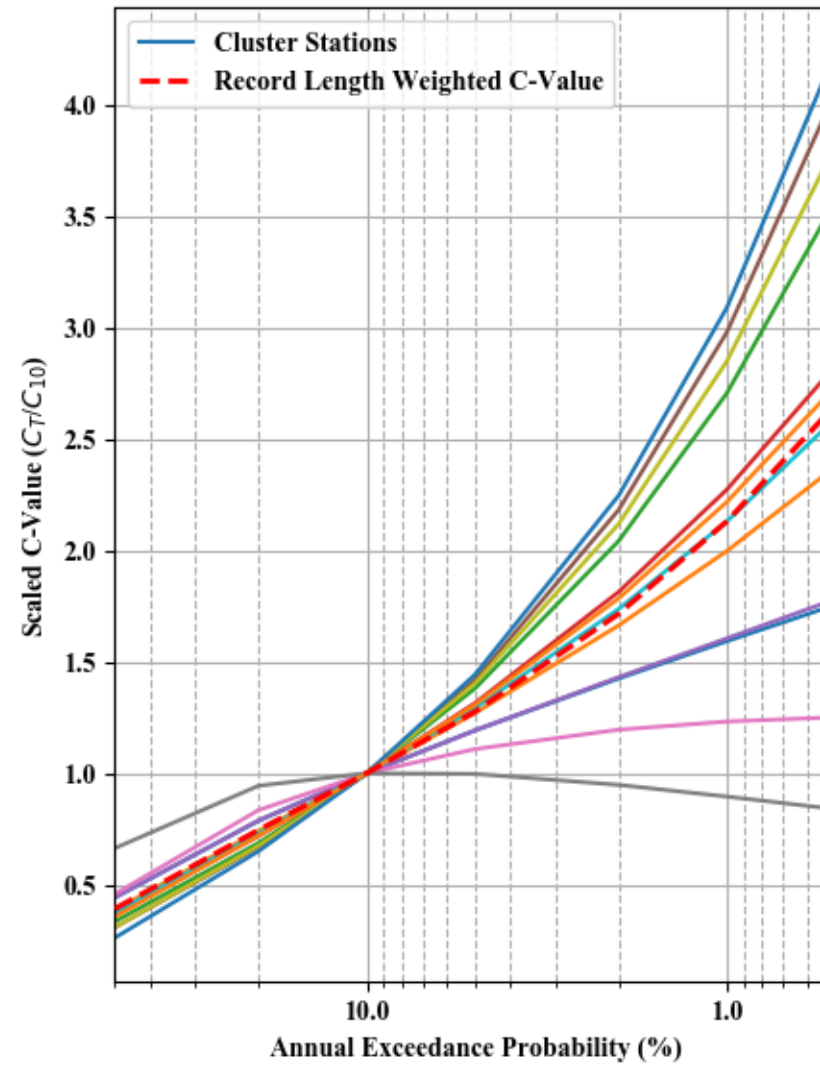
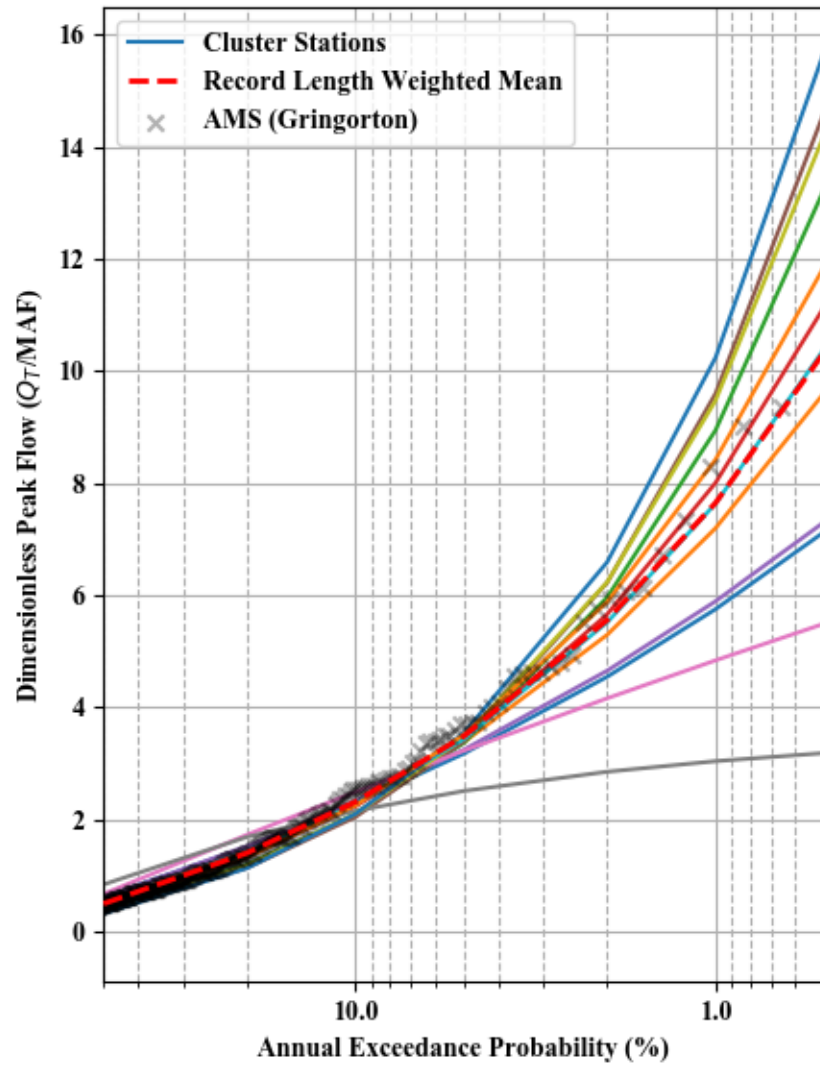
Dimensionless Peak Flow and Scaled C-value - Cluster 3



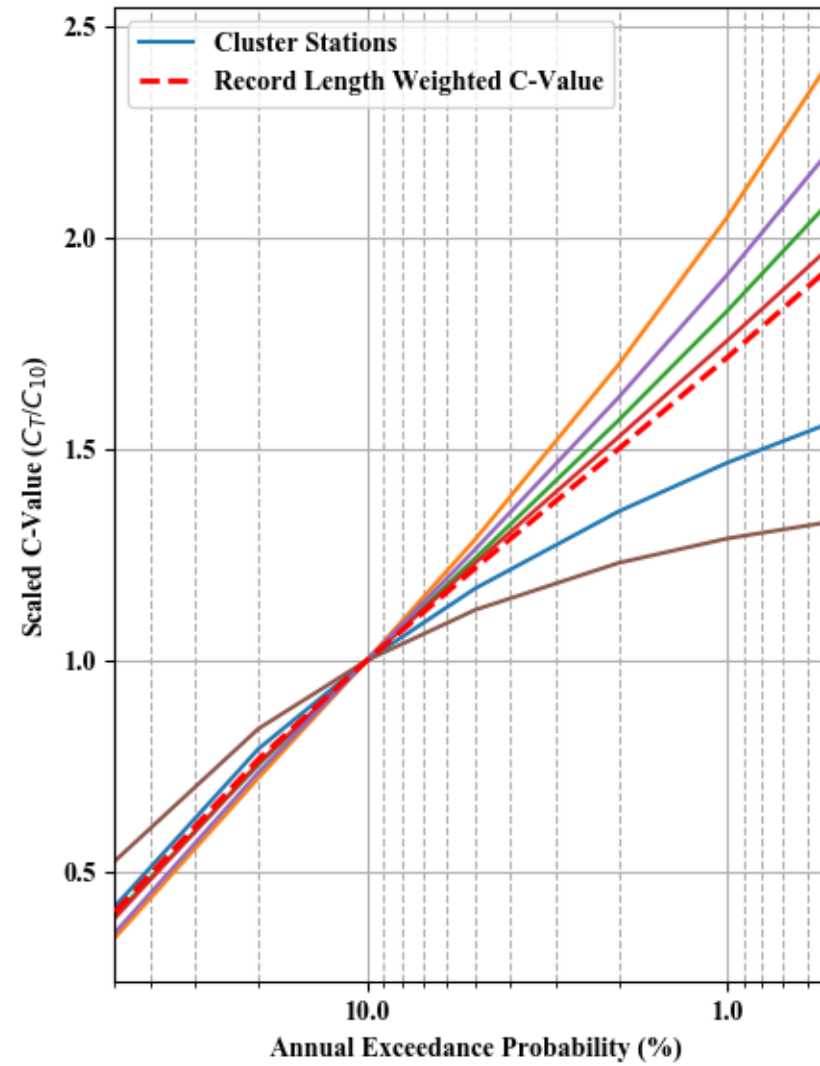
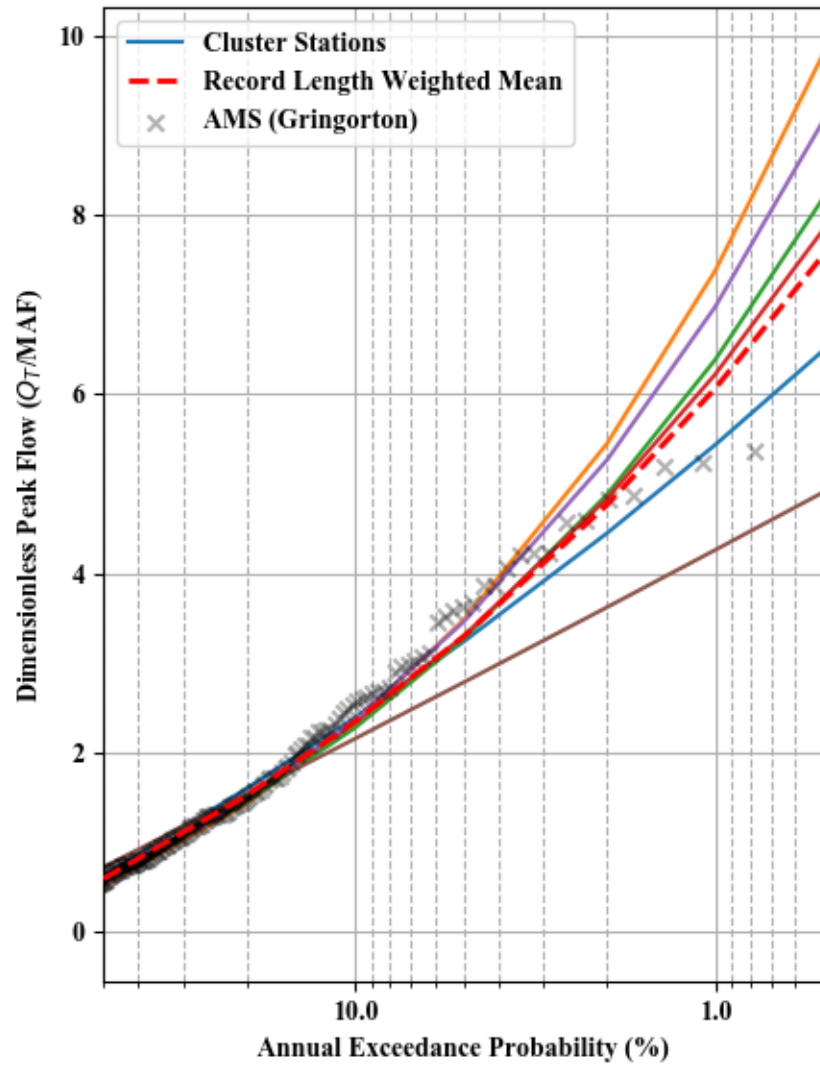
Dimensionless Peak Flow and Scaled C-value - Cluster 4



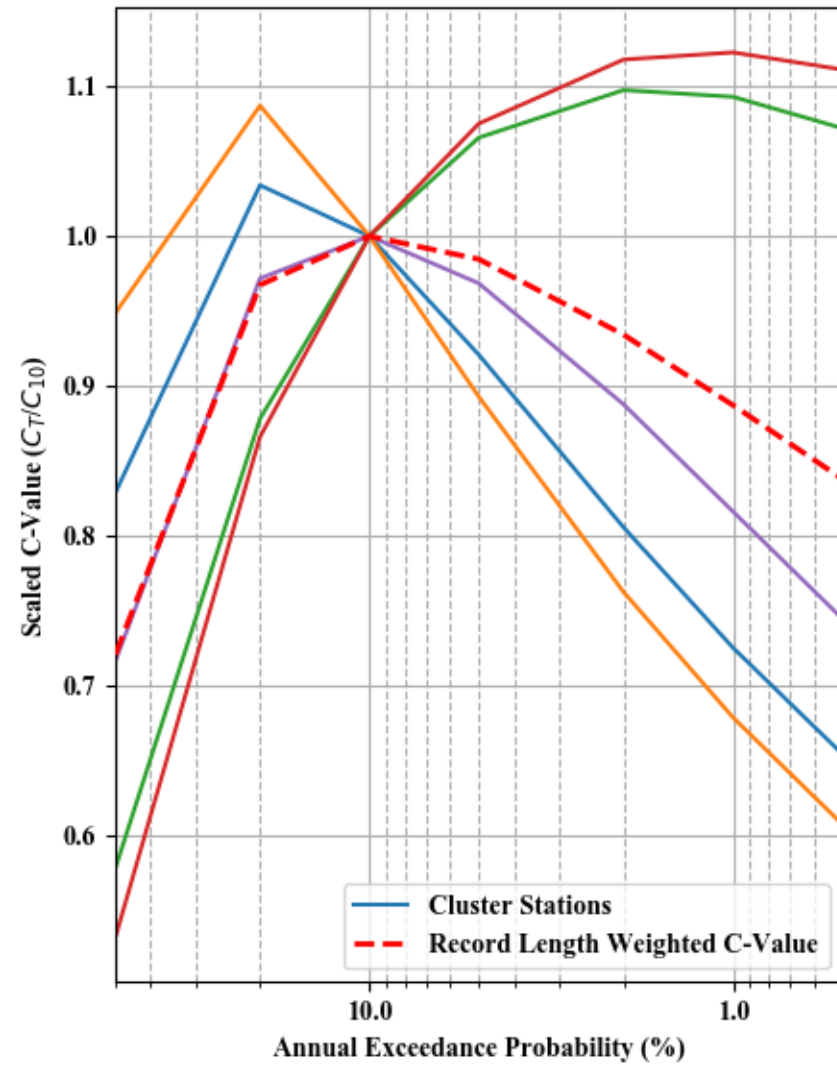
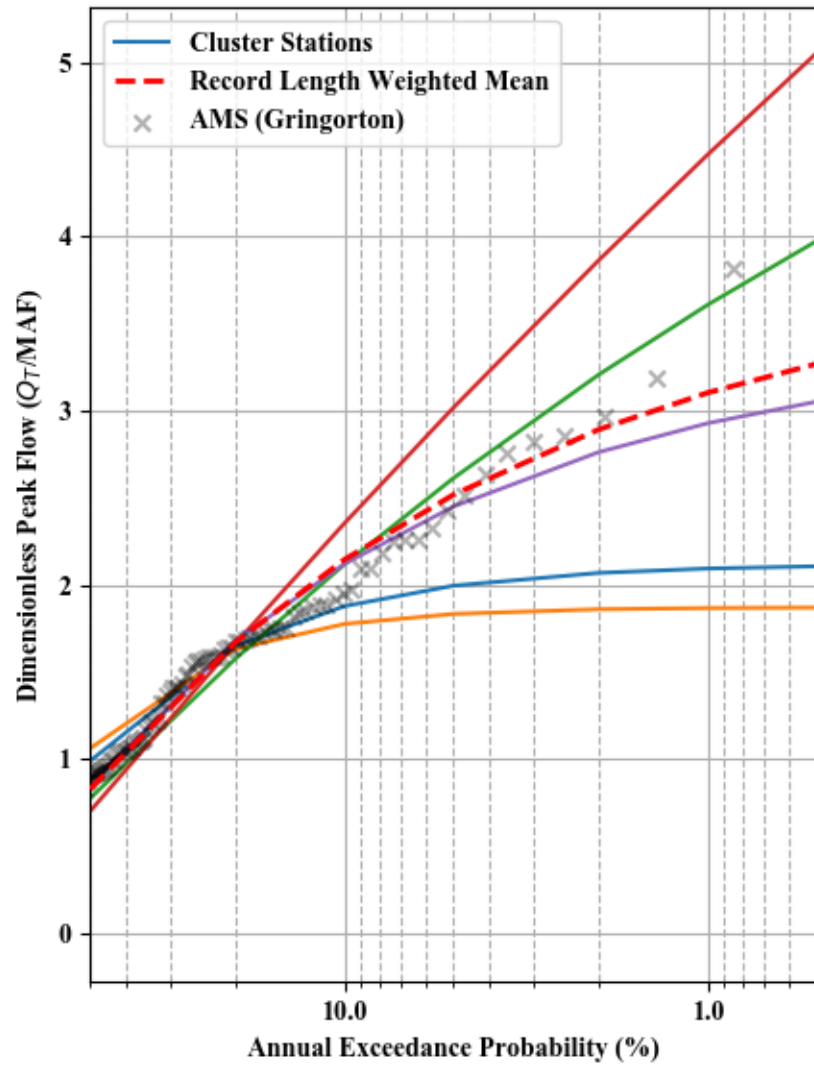
Dimensionless Peak Flow and Scaled C-value - Cluster 5



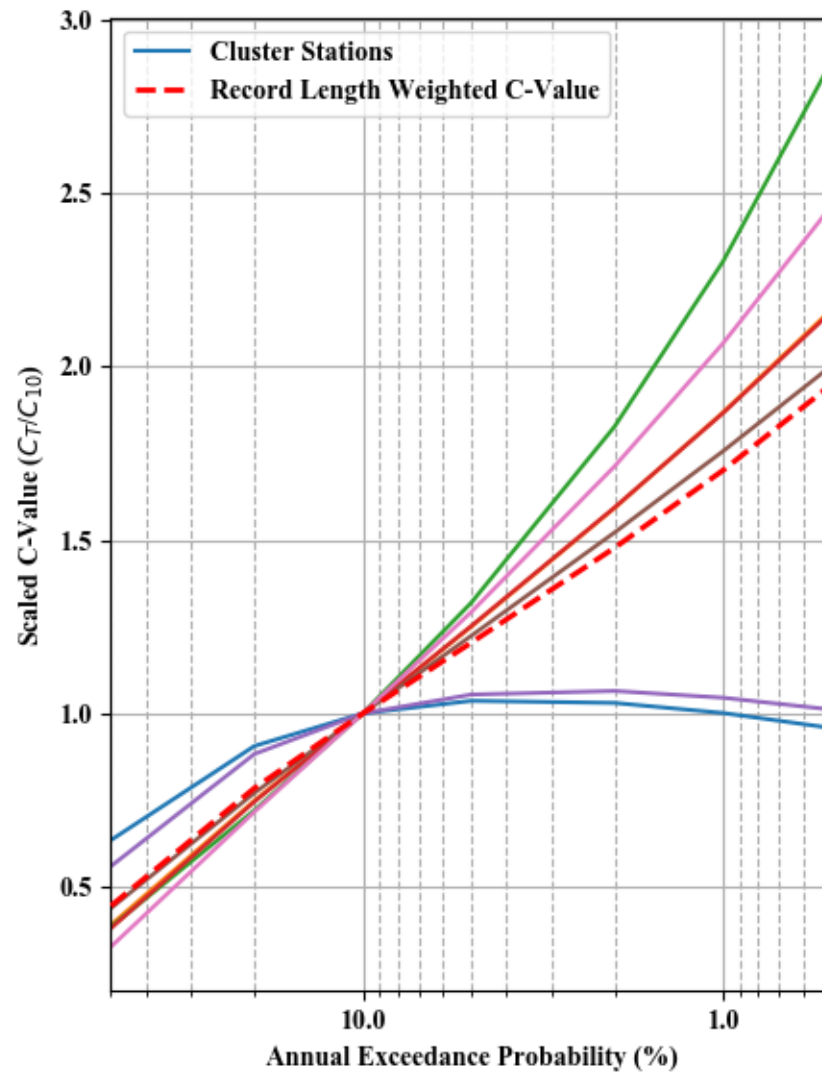
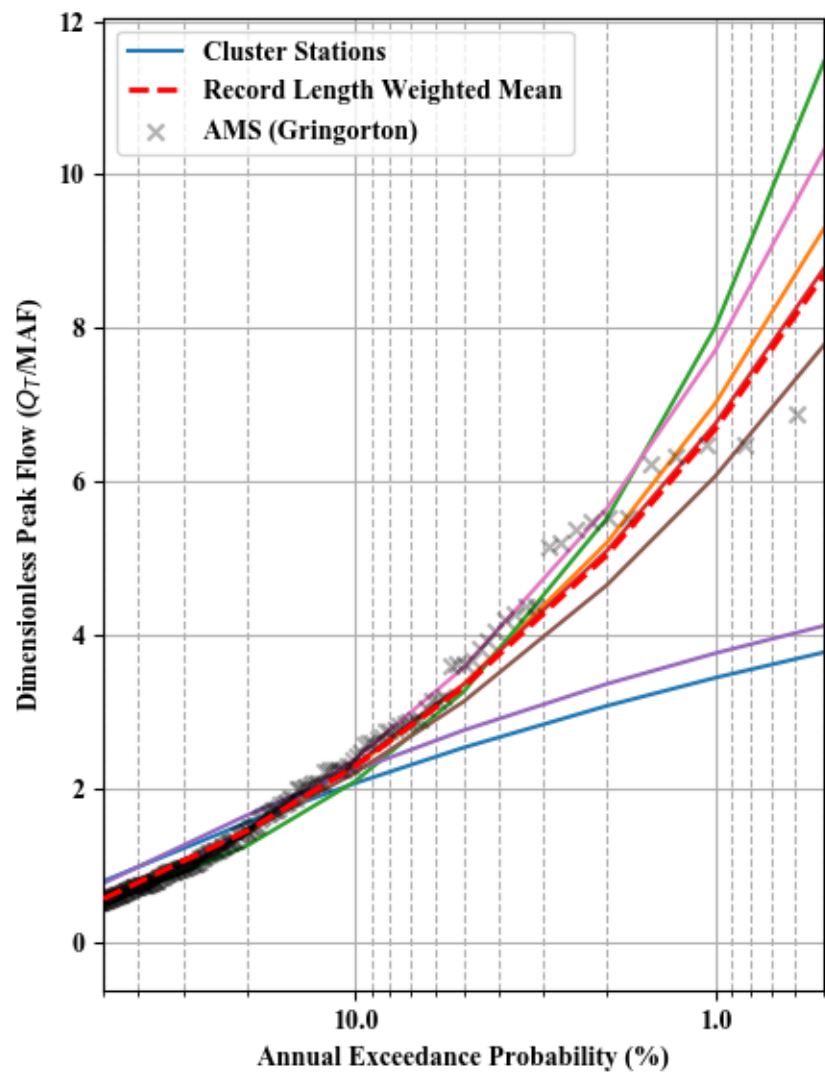
Dimensionless Peak Flow and Scaled C-value - Cluster 6



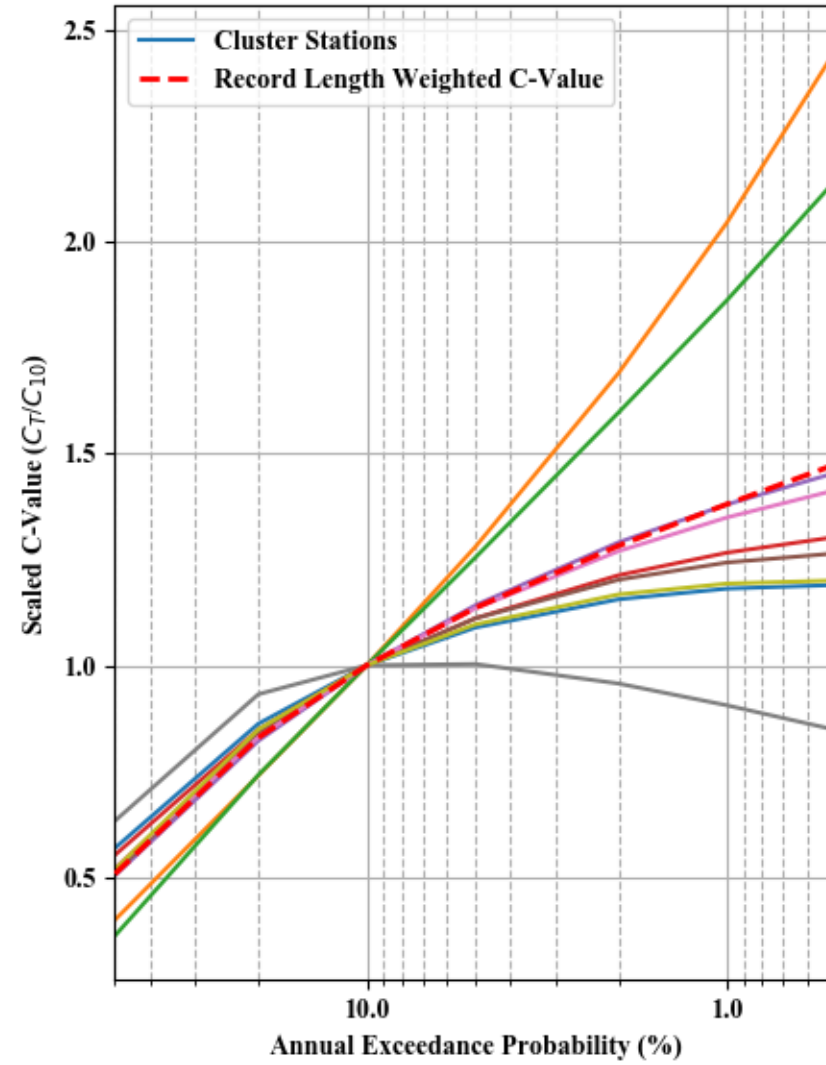
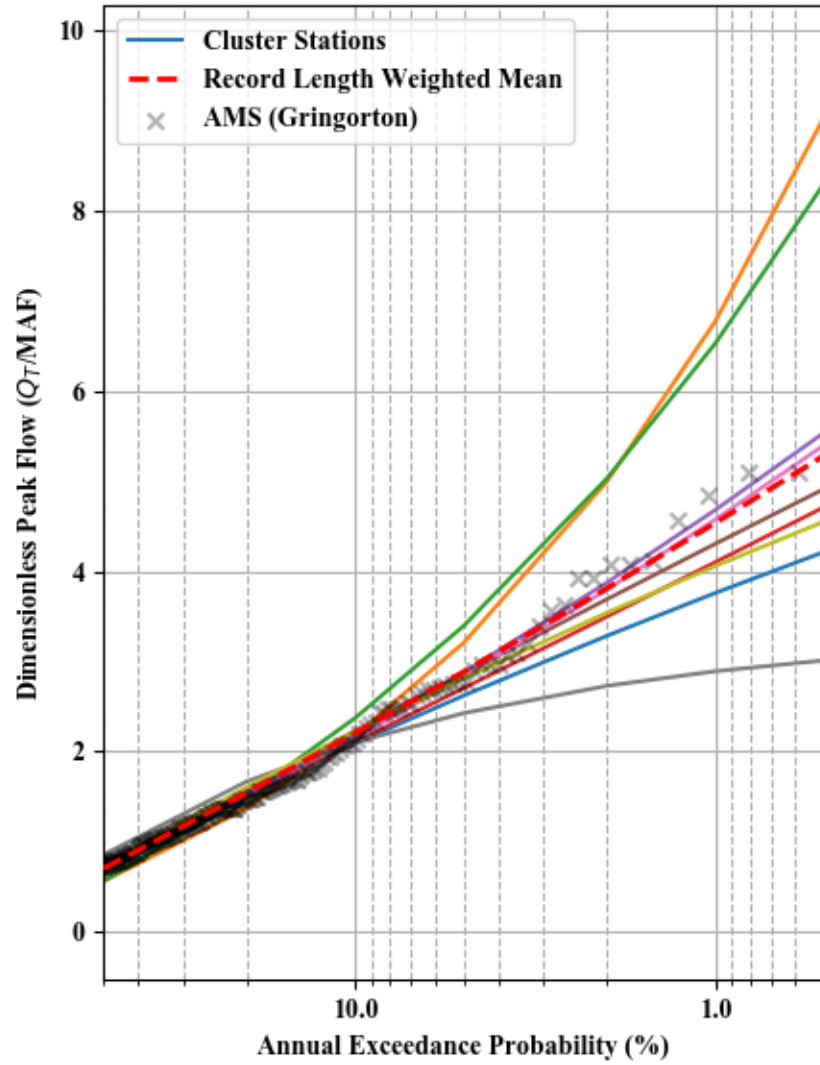
Dimensionless Peak Flow and Scaled C-value - Cluster 7



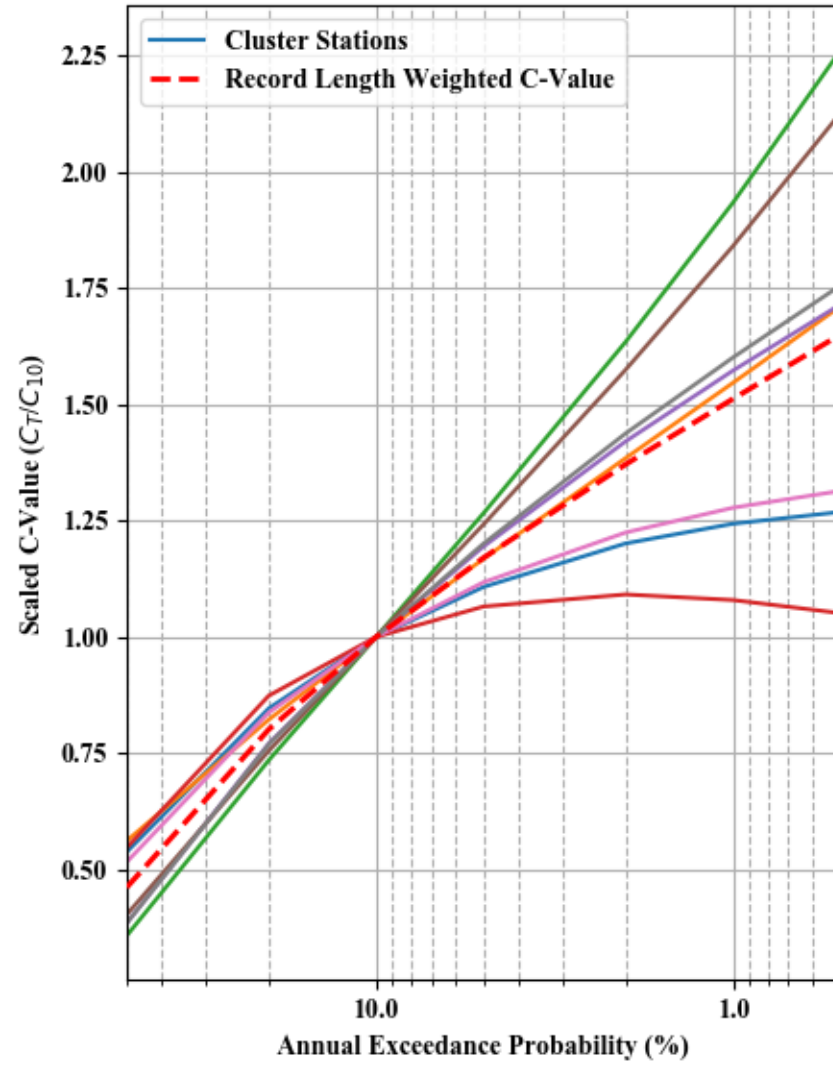
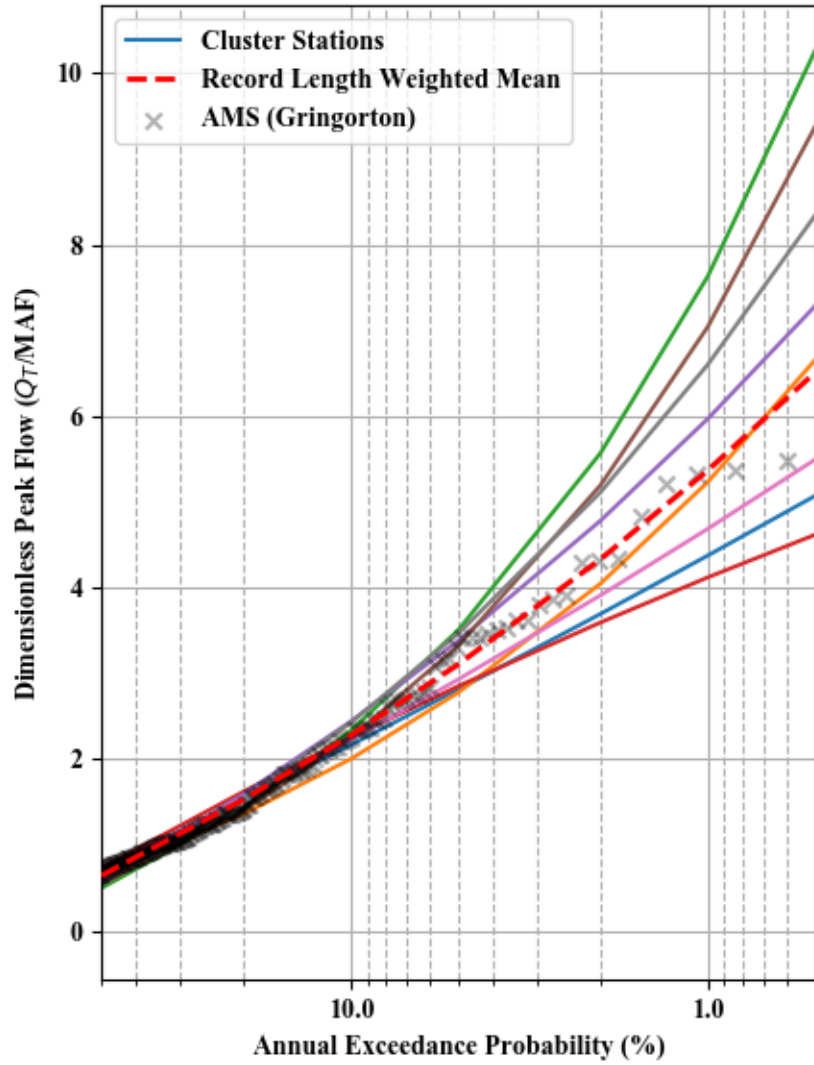
Dimensionless Peak Flow and Scaled C-value - Cluster 8



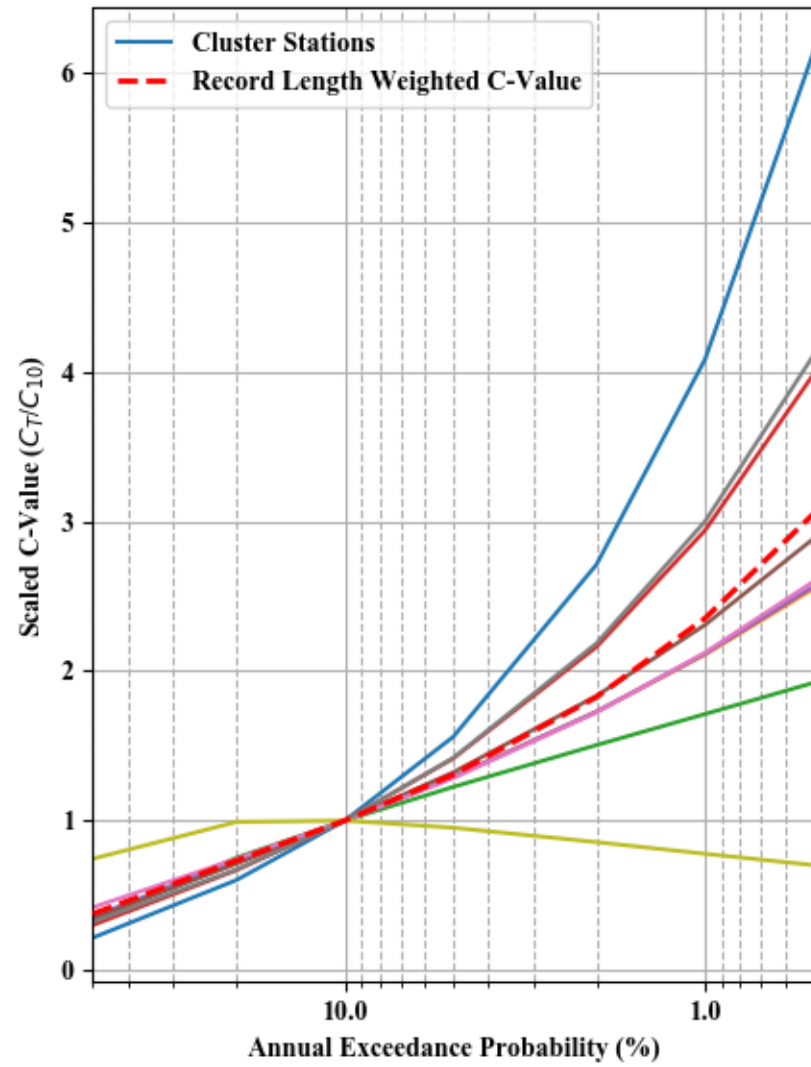
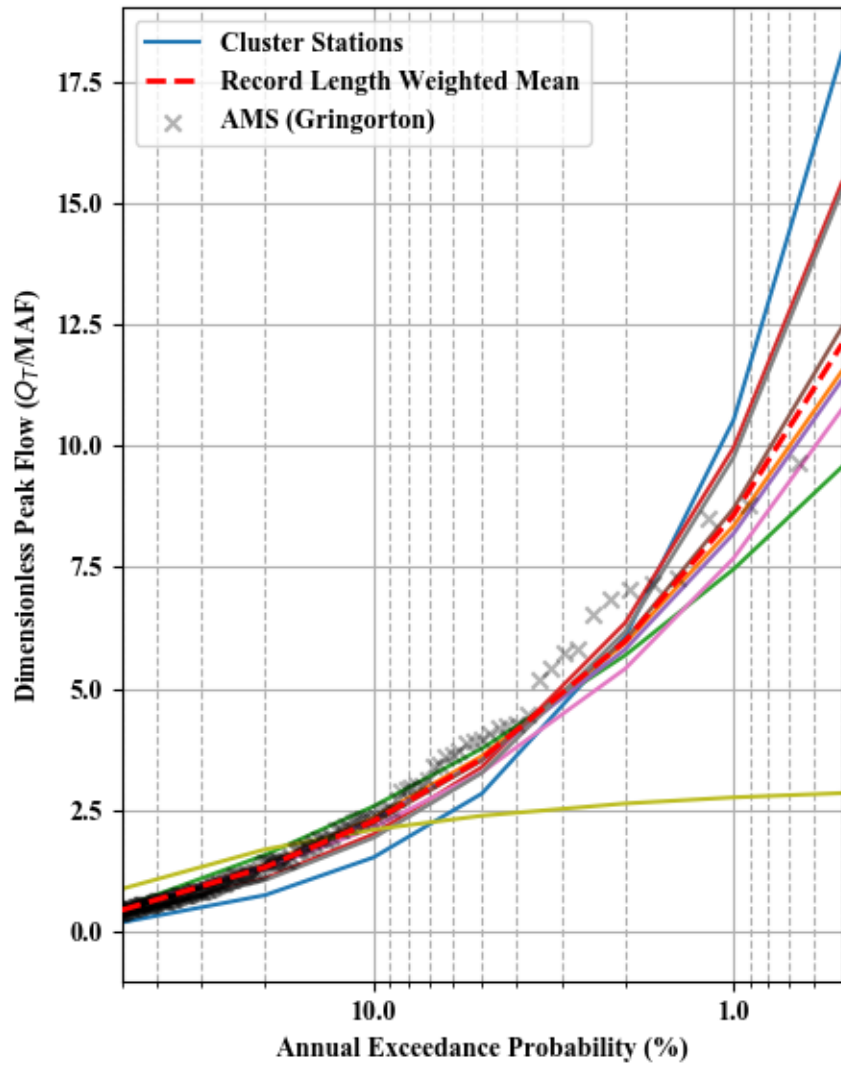
Dimensionless Peak Flow and Scaled C-value - Cluster 9



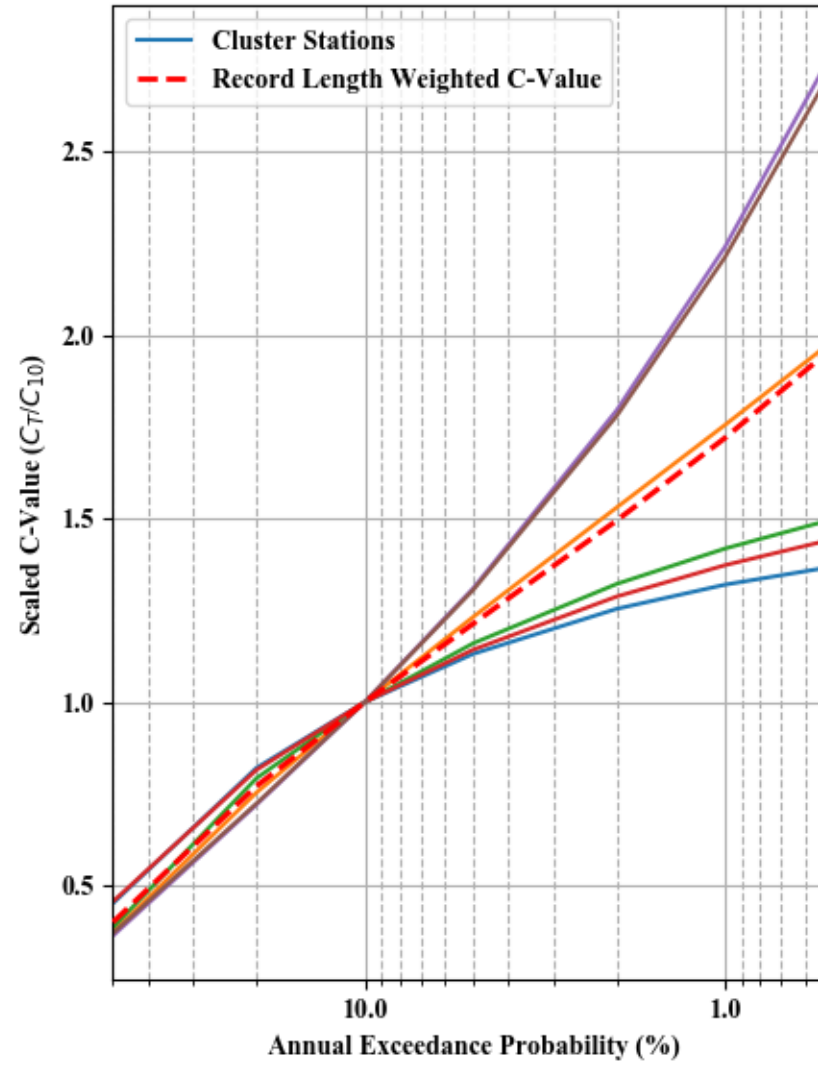
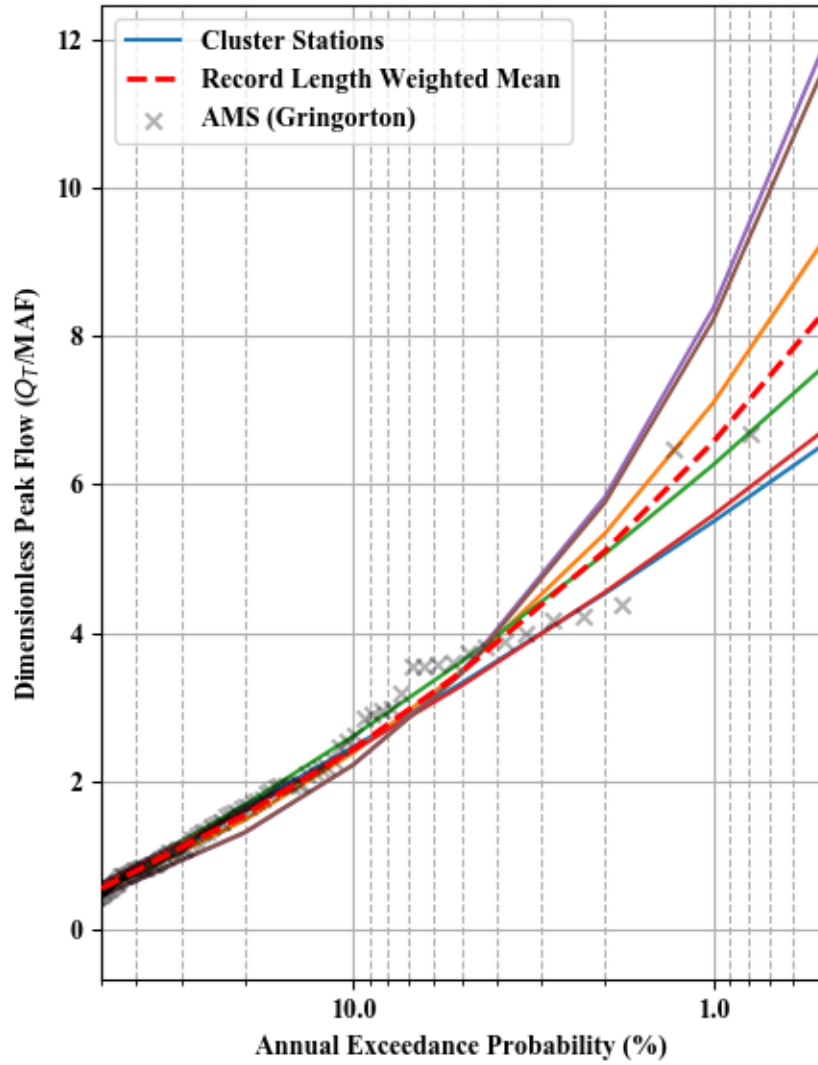
Dimensionless Peak Flow and Scaled C-value - Cluster 10



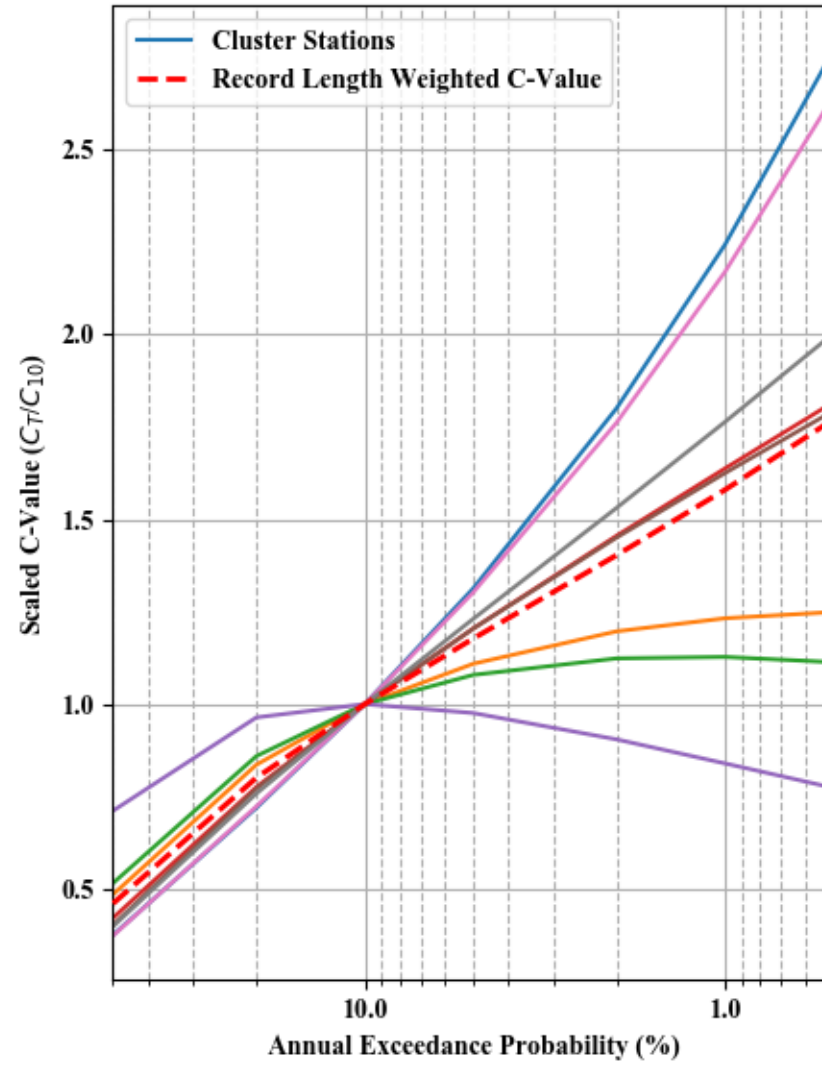
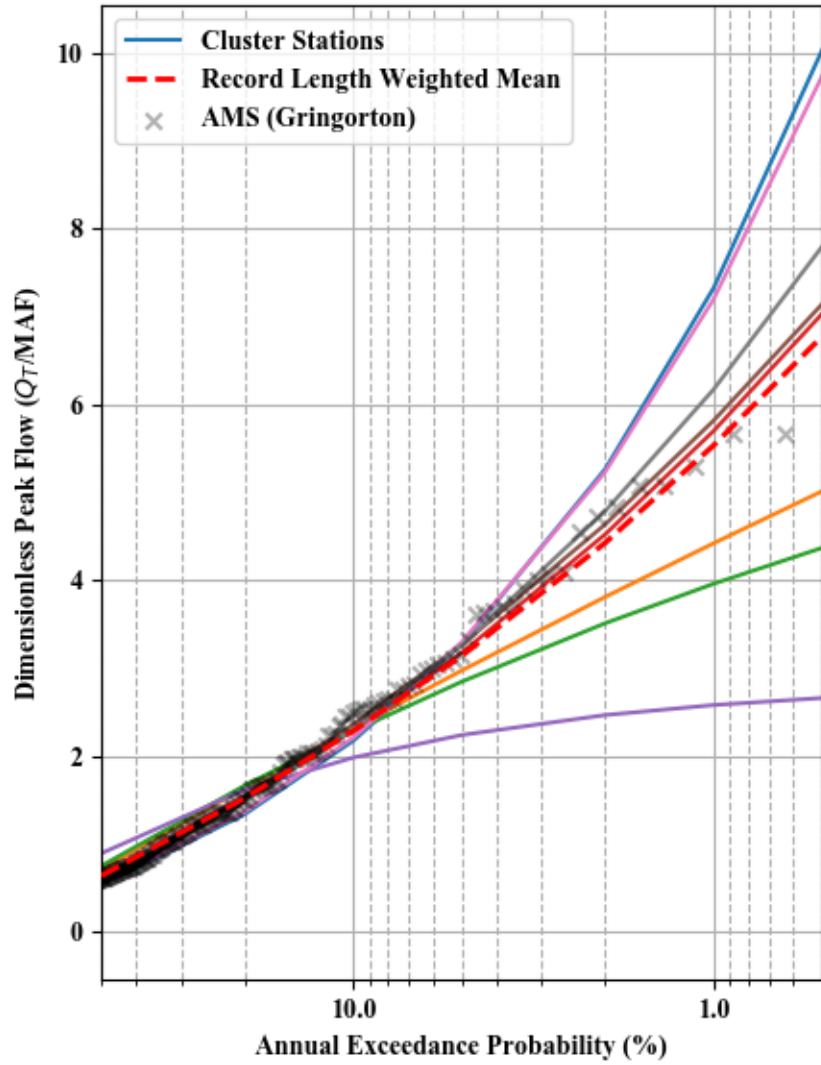
Dimensionless Peak Flow and Scaled C-value - Cluster 11



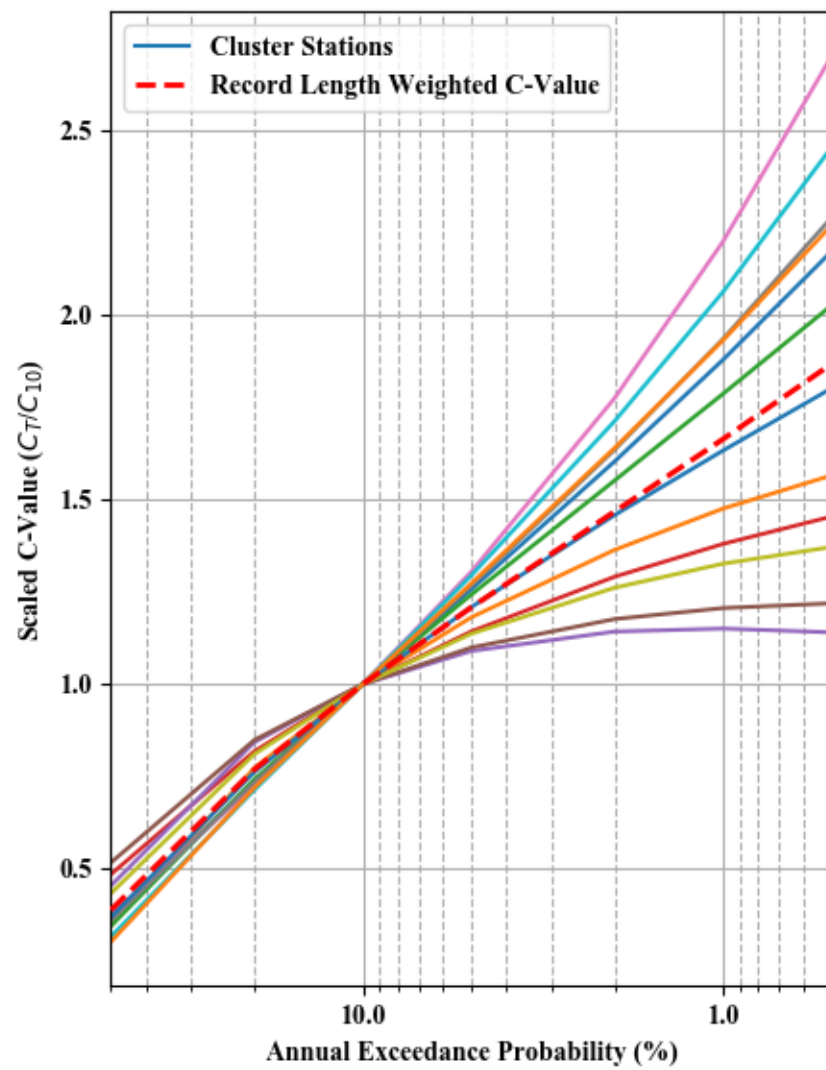
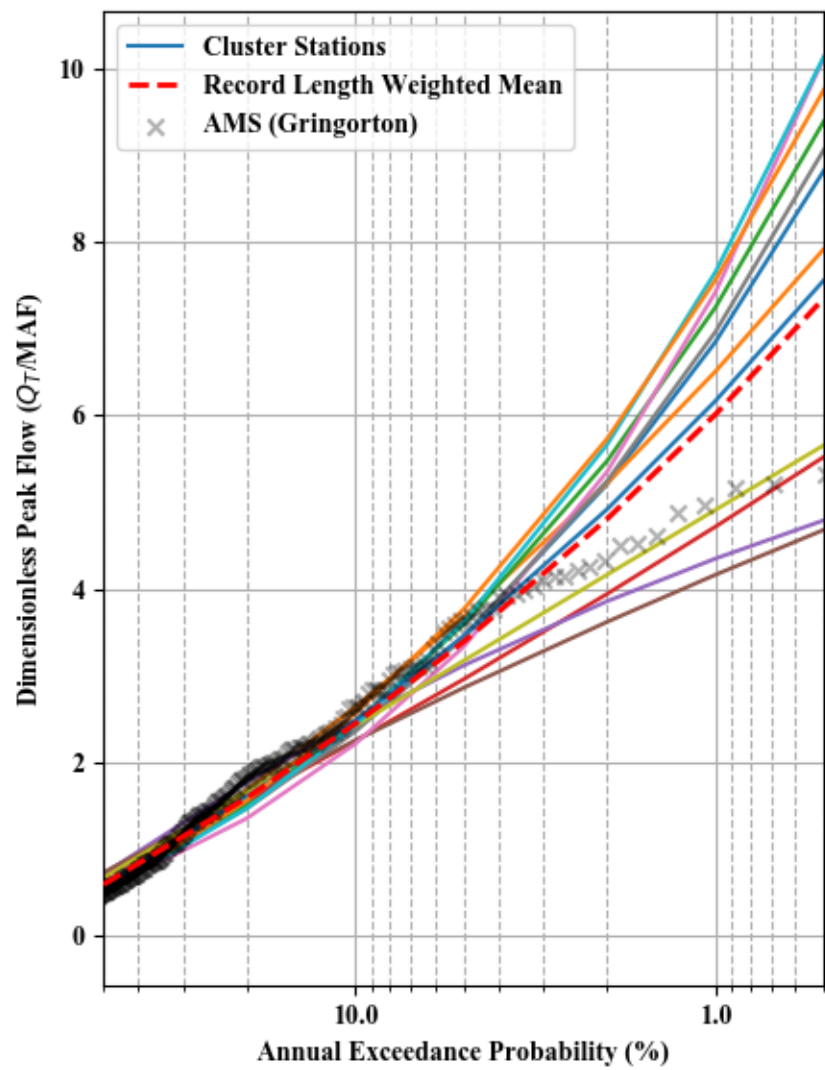
Dimensionless Peak Flow and Scaled C-value - Cluster 12



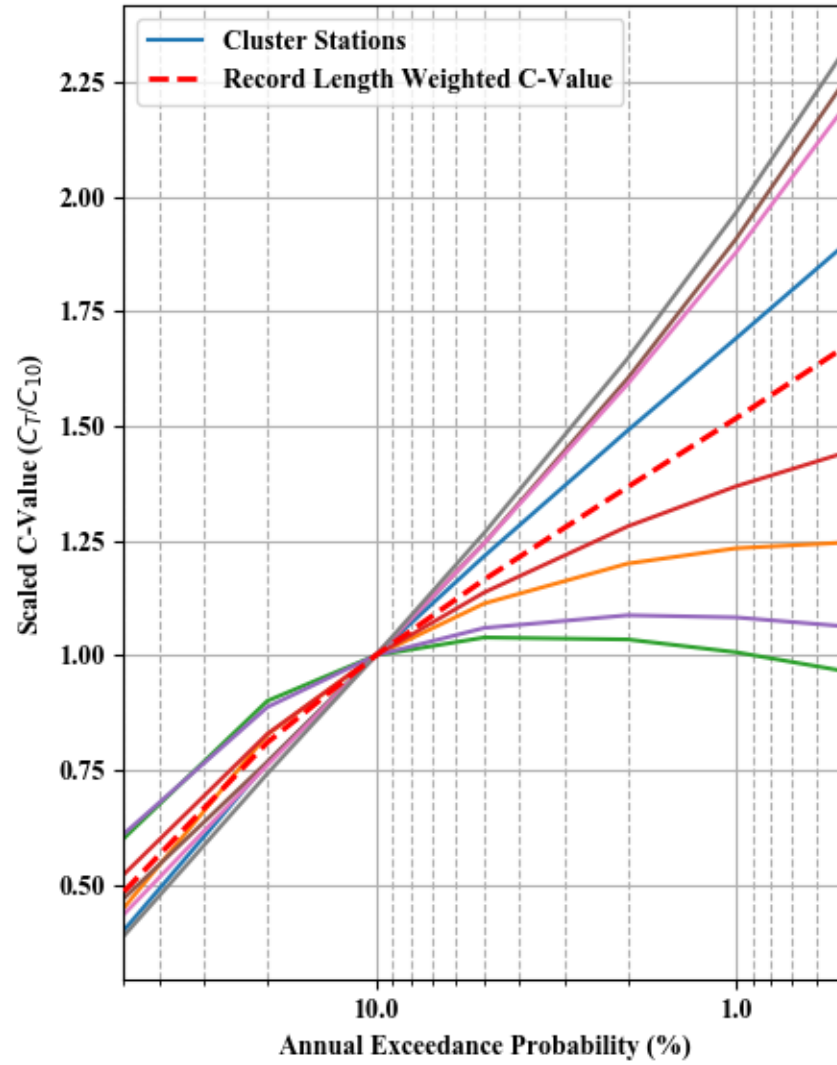
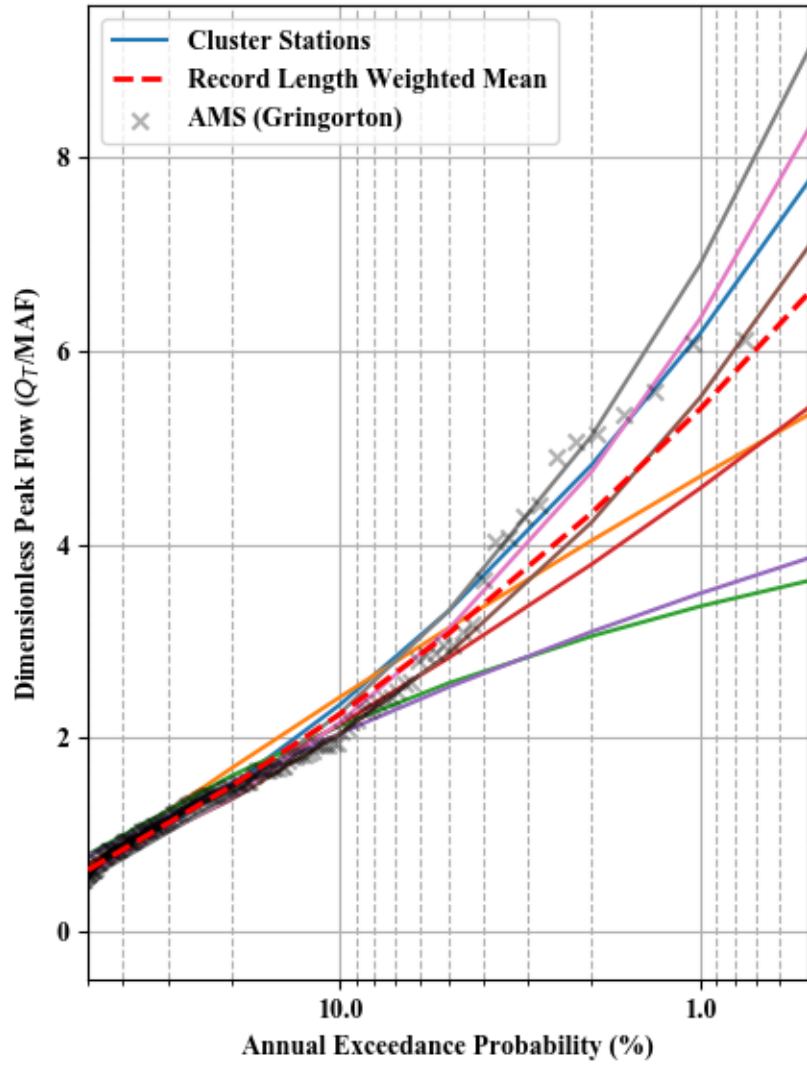
Dimensionless Peak Flow and Scaled C-value - Cluster 13



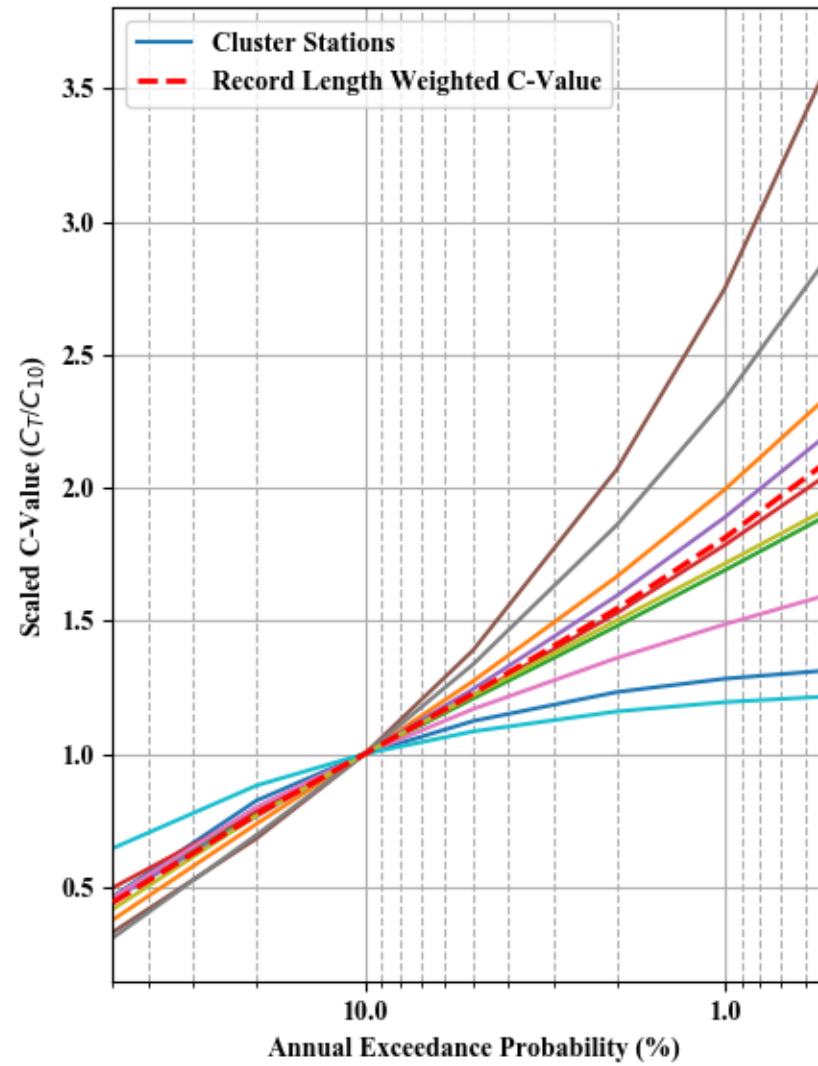
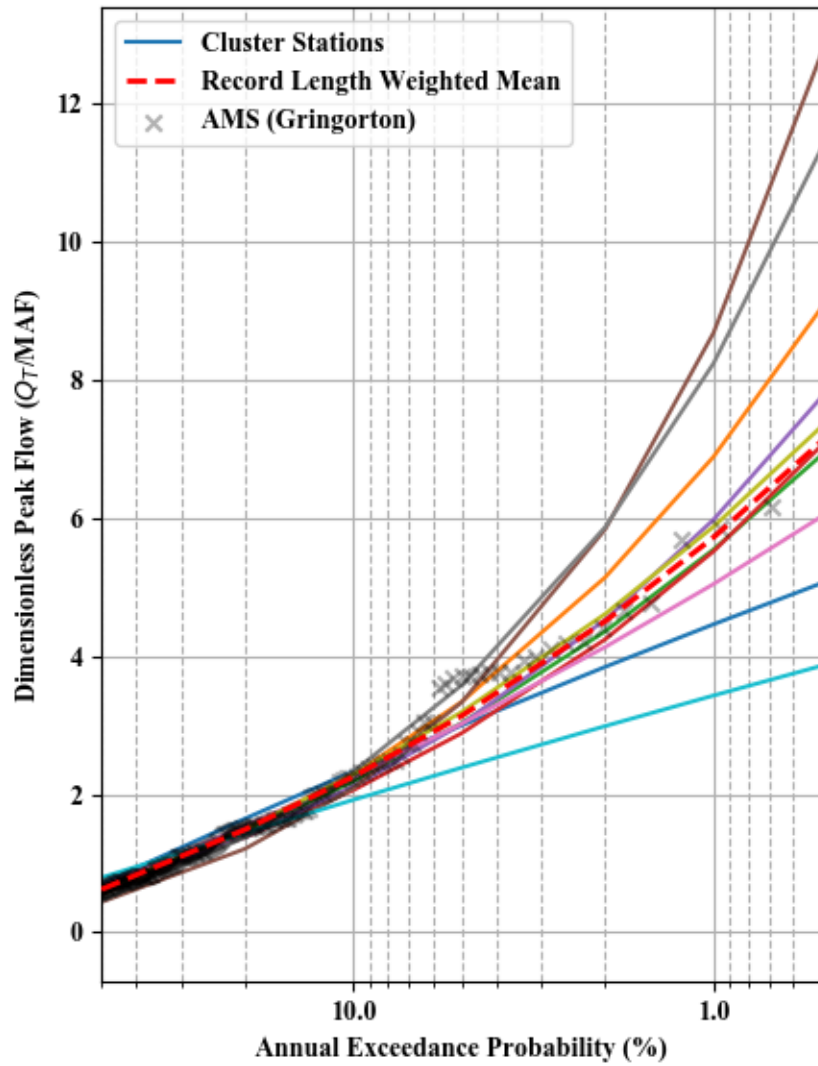
Dimensionless Peak Flow and Scaled C-value - Cluster 14



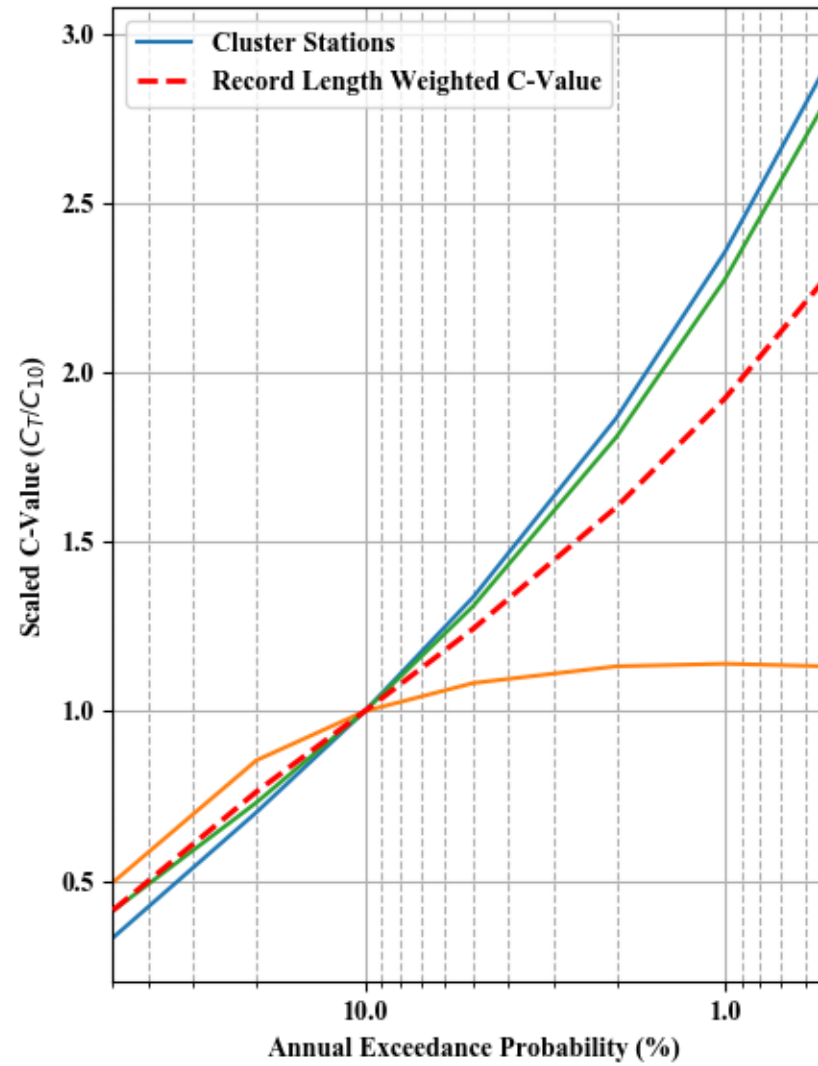
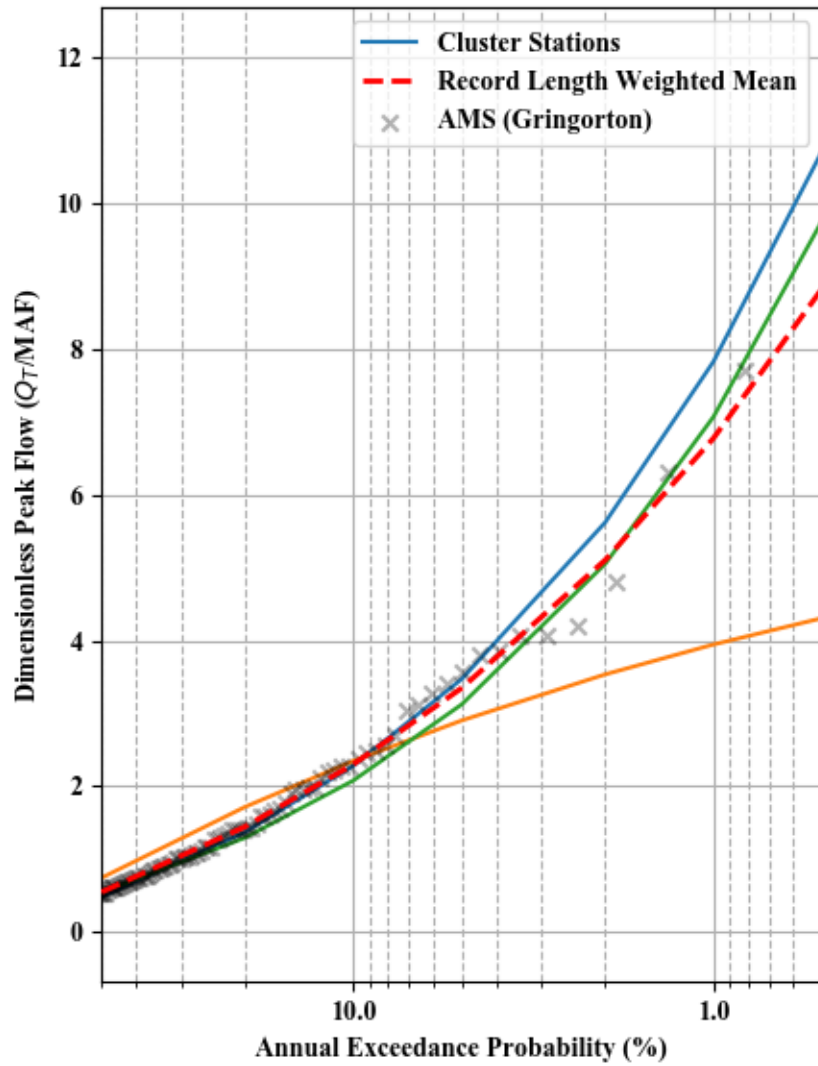
Dimensionless Peak Flow and Scaled C-value - Cluster 15



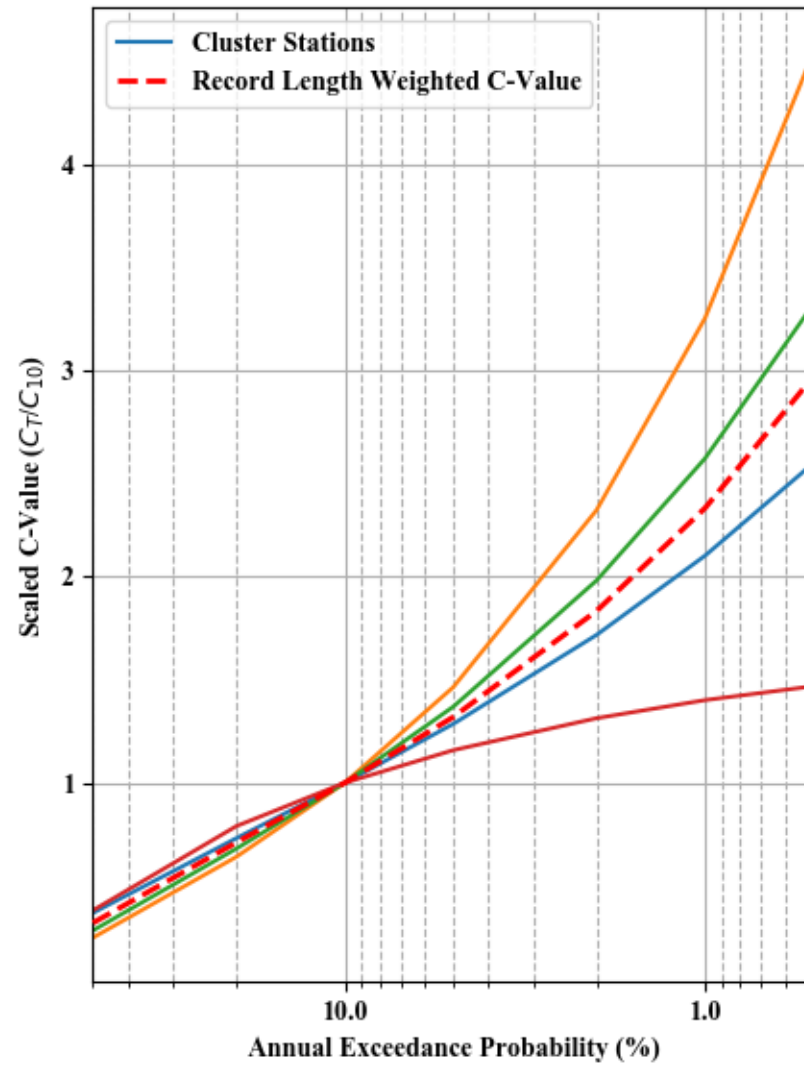
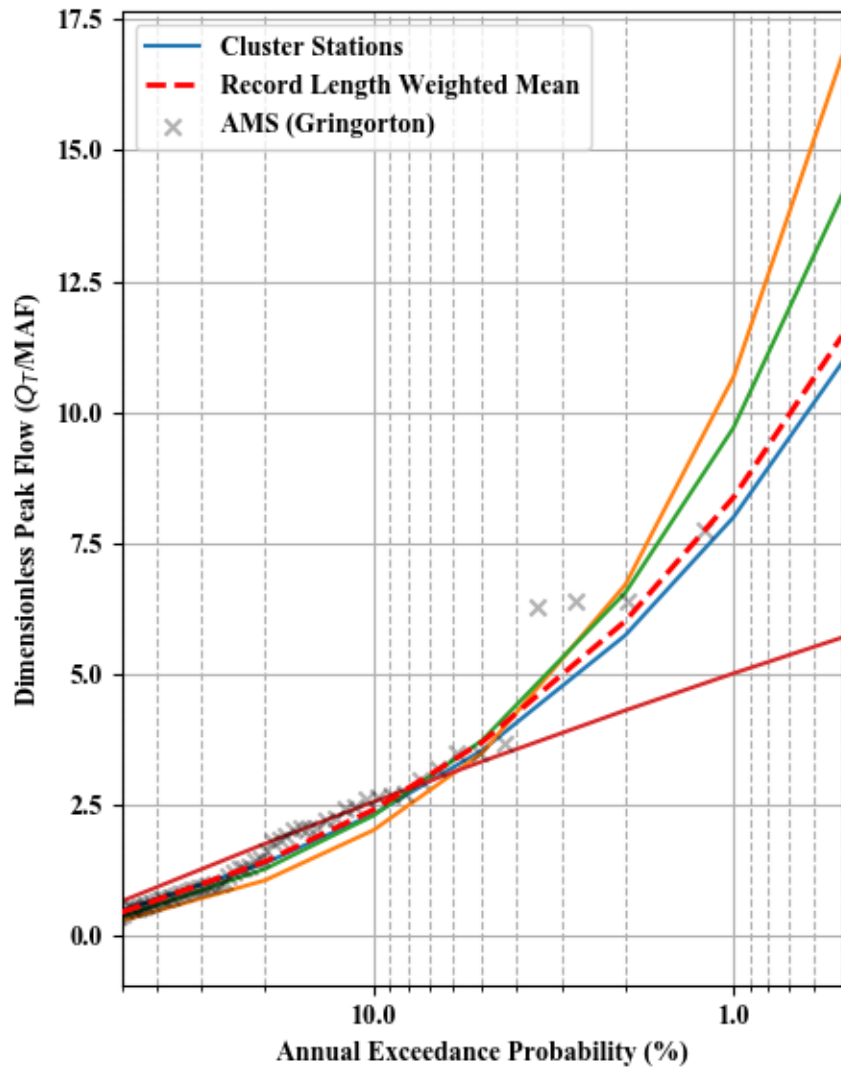
Dimensionless Peak Flow and Scaled C-value - Cluster 16



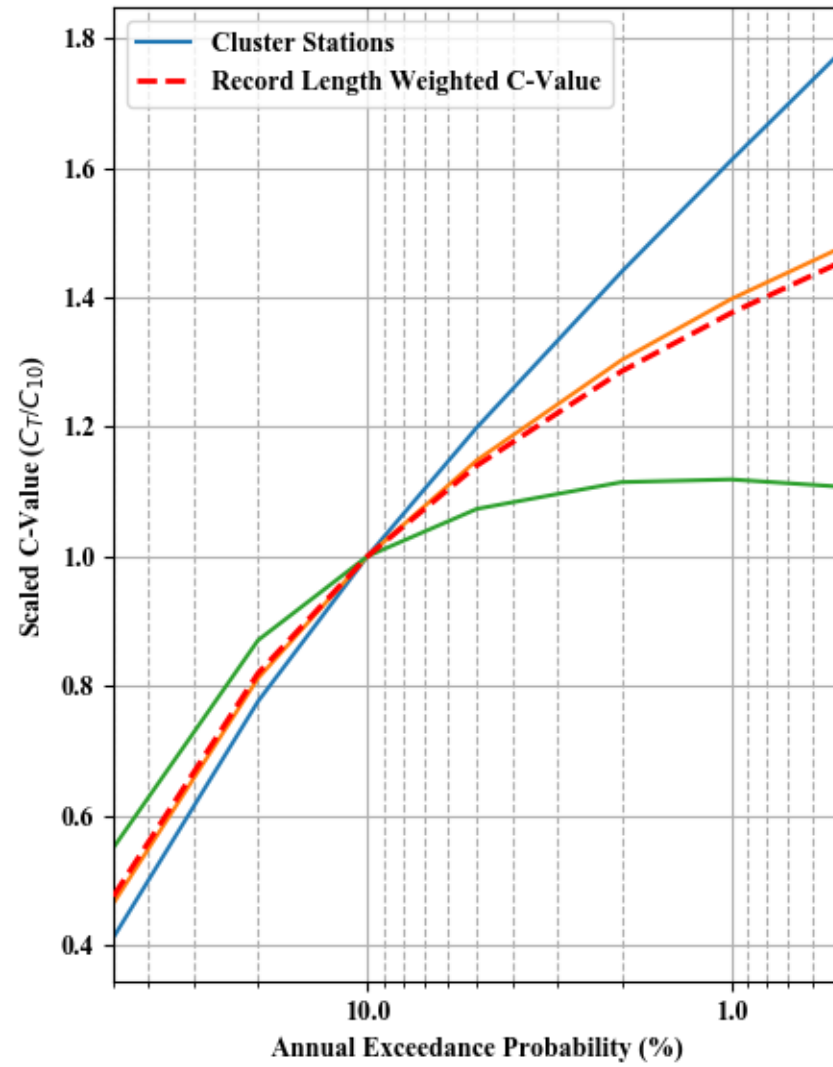
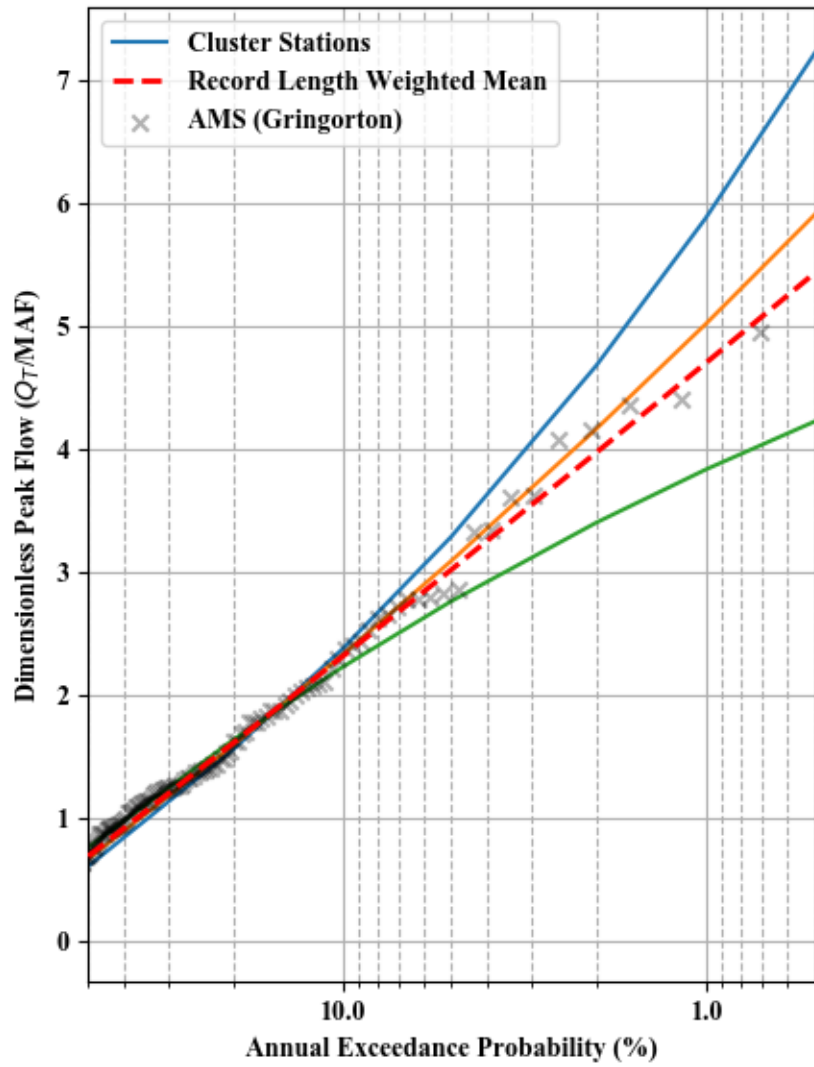
Dimensionless Peak Flow and Scaled C-value - Cluster 17



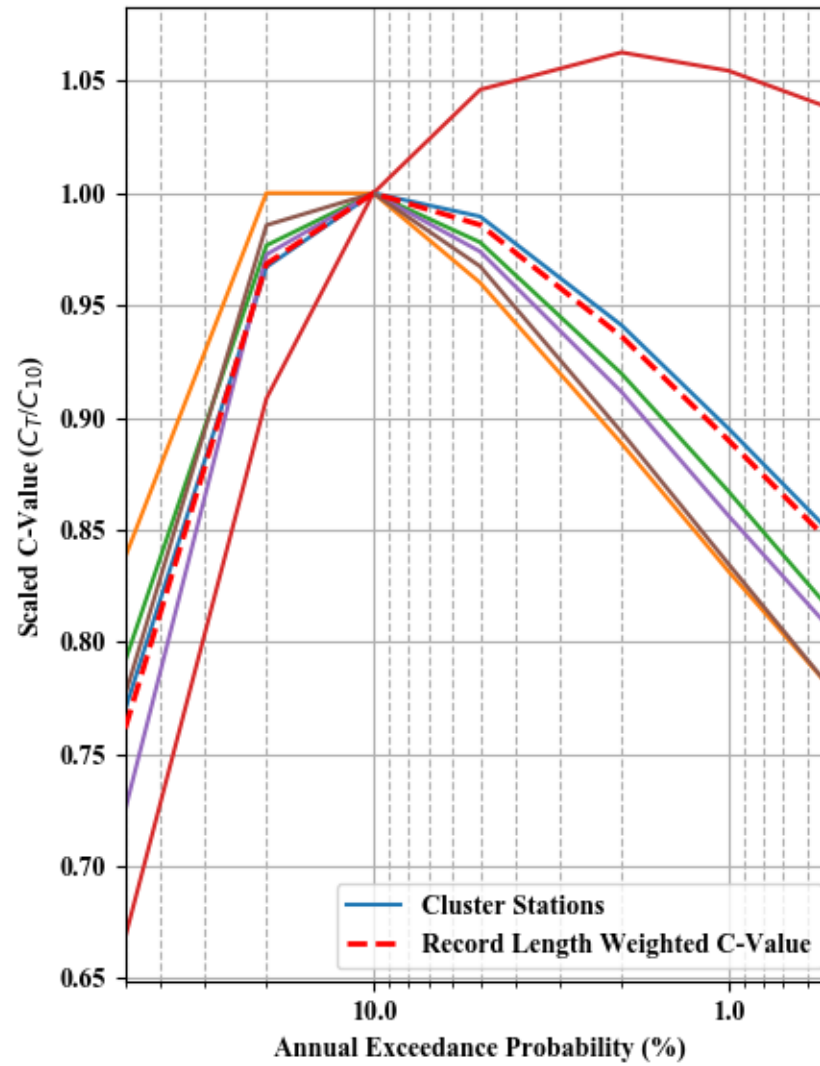
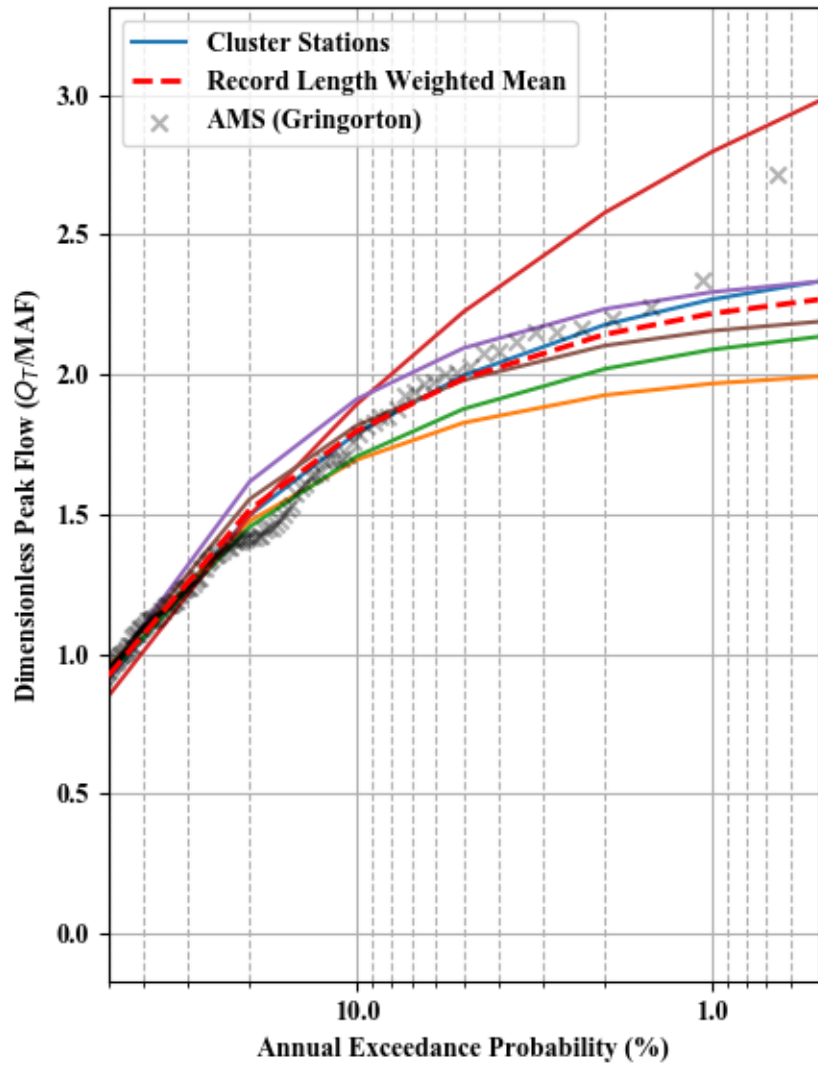
Dimensionless Peak Flow and Scaled C-value - Cluster 18



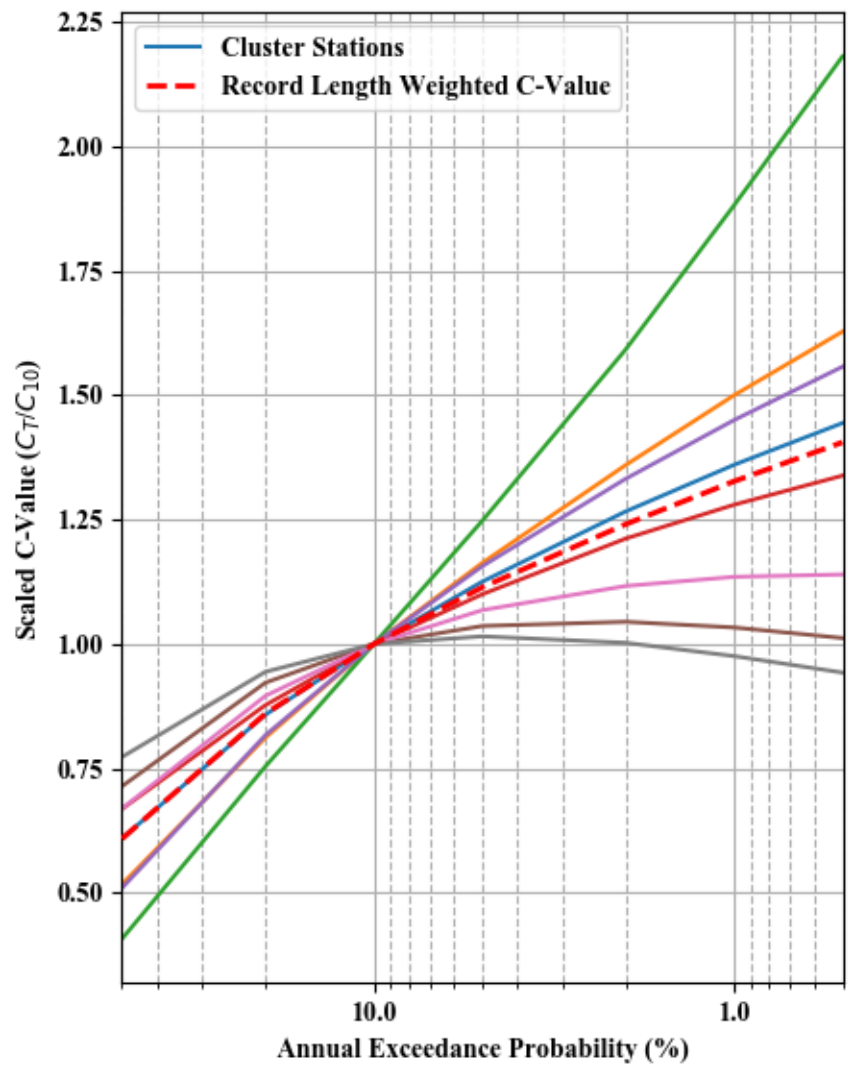
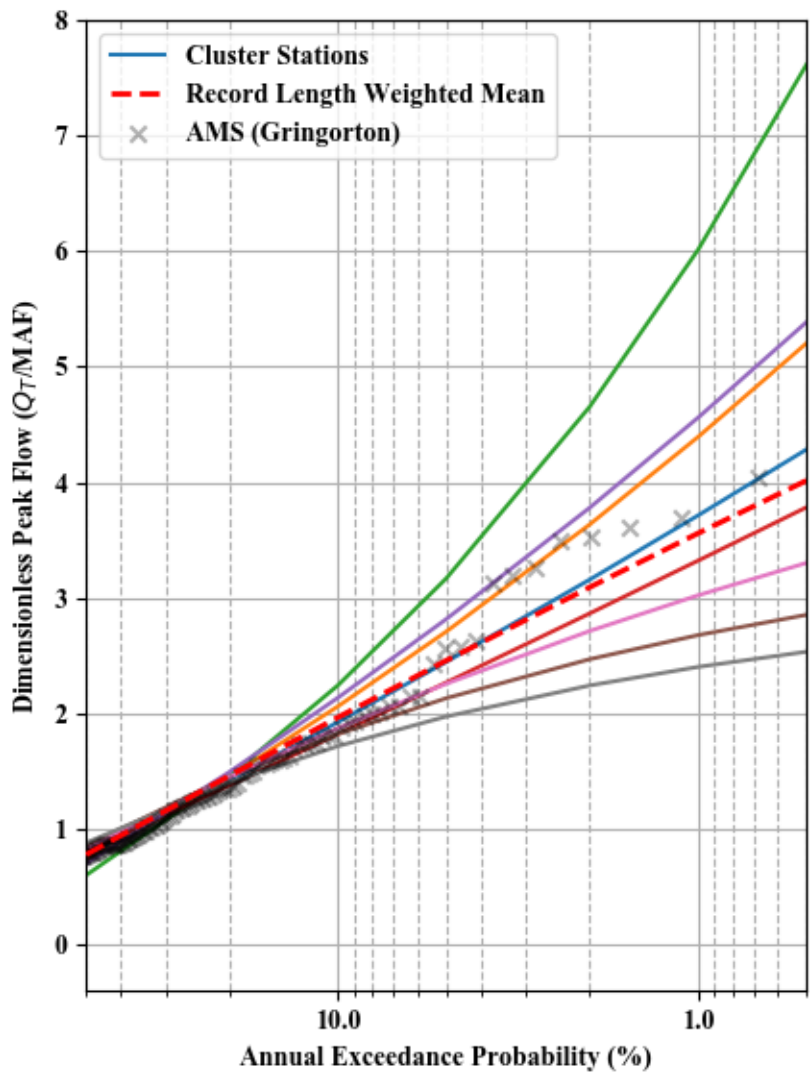
Dimensionless Peak Flow and Scaled C-value - Cluster 19



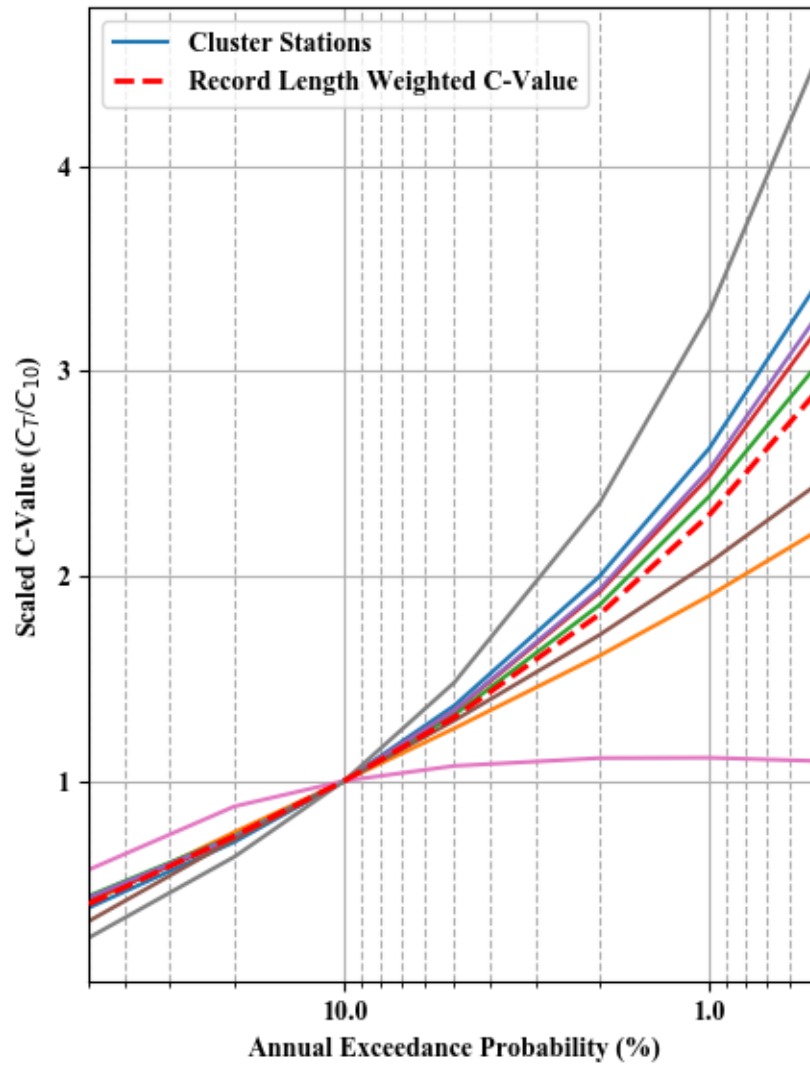
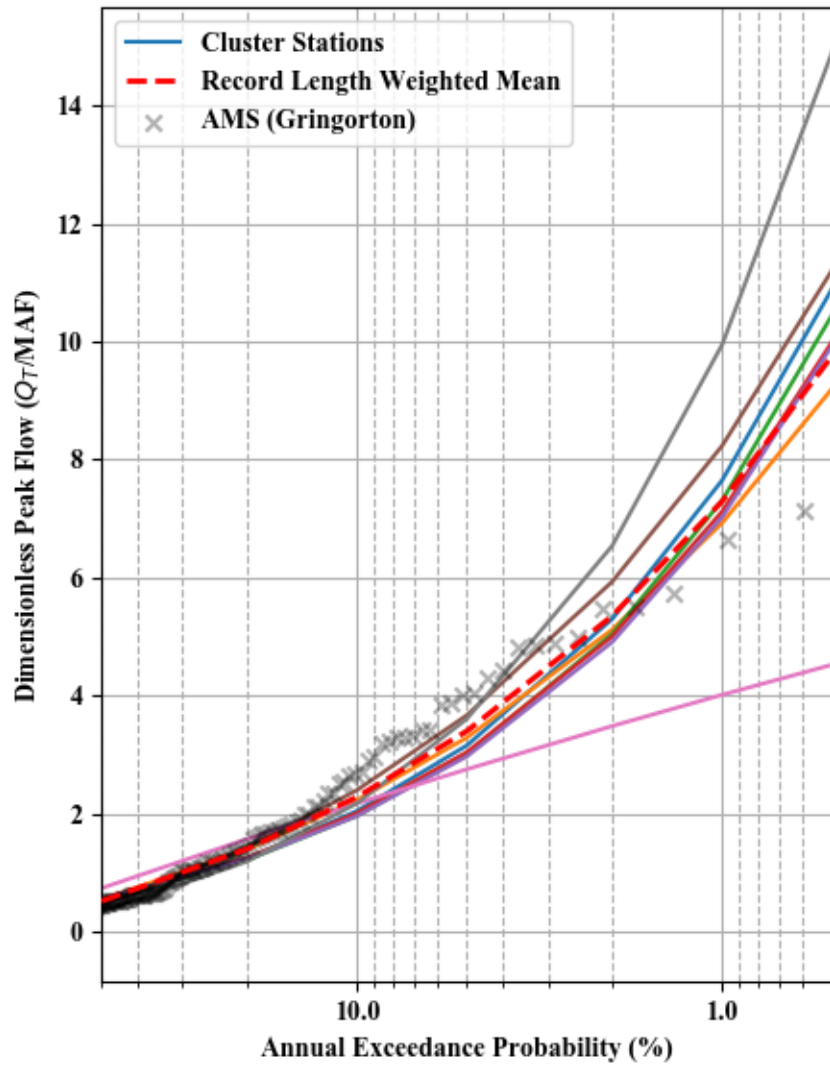
Dimensionless Peak Flow and Scaled C-value - Cluster 20



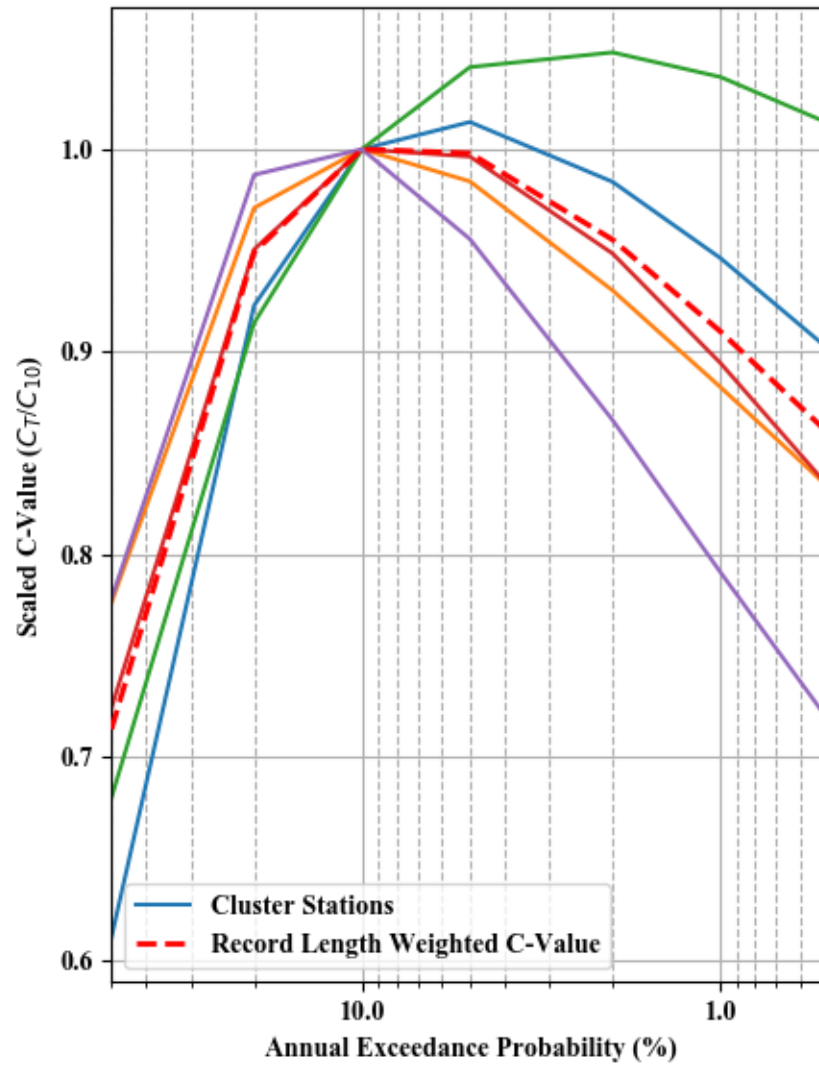
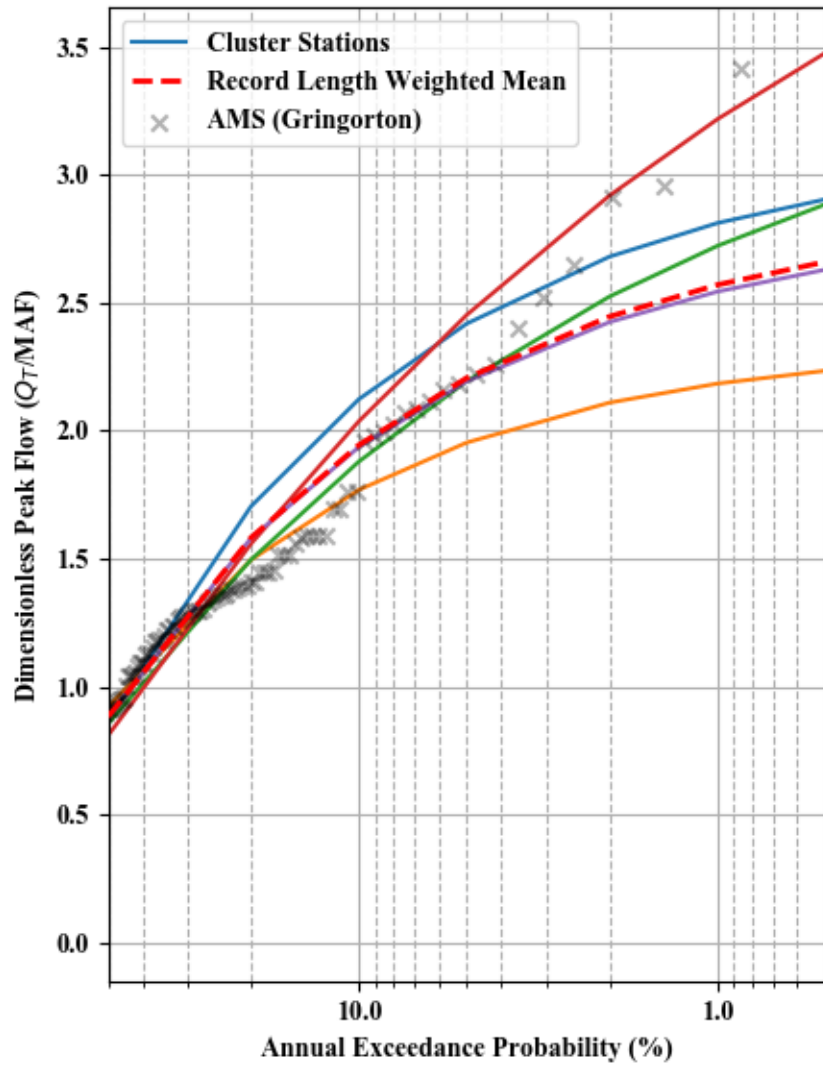
Dimensionless Peak Flow and Scaled C-value - Cluster 21



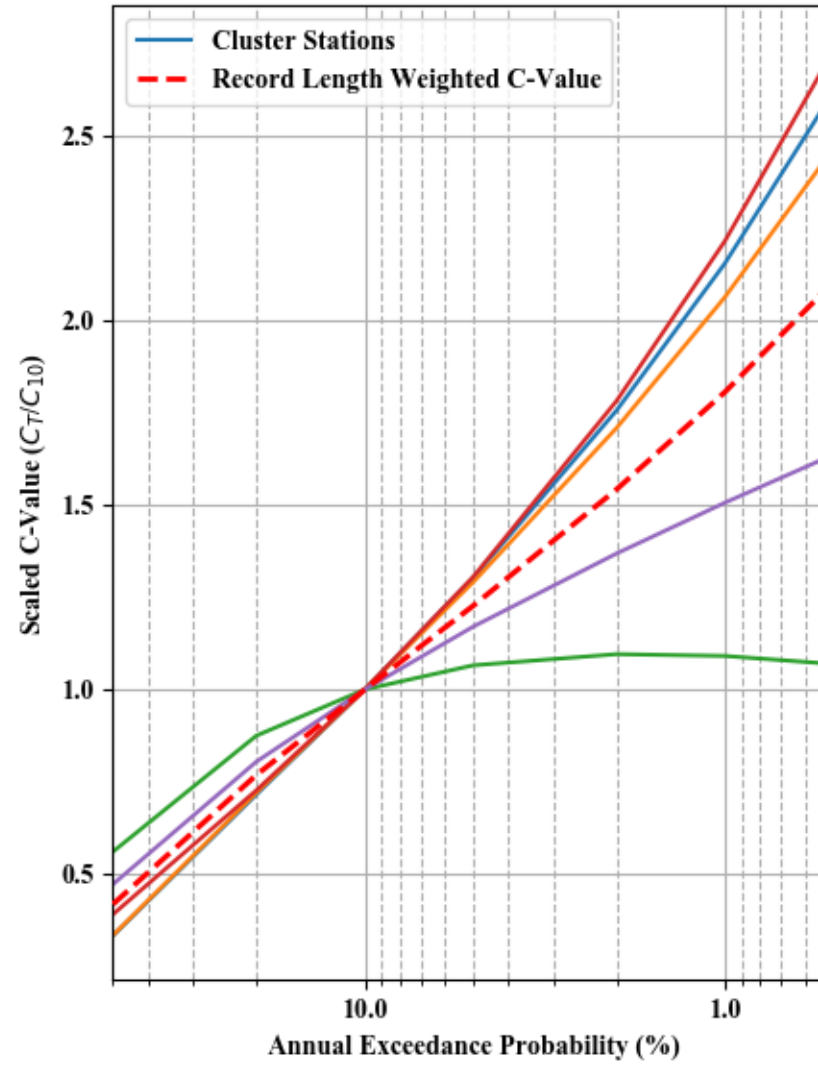
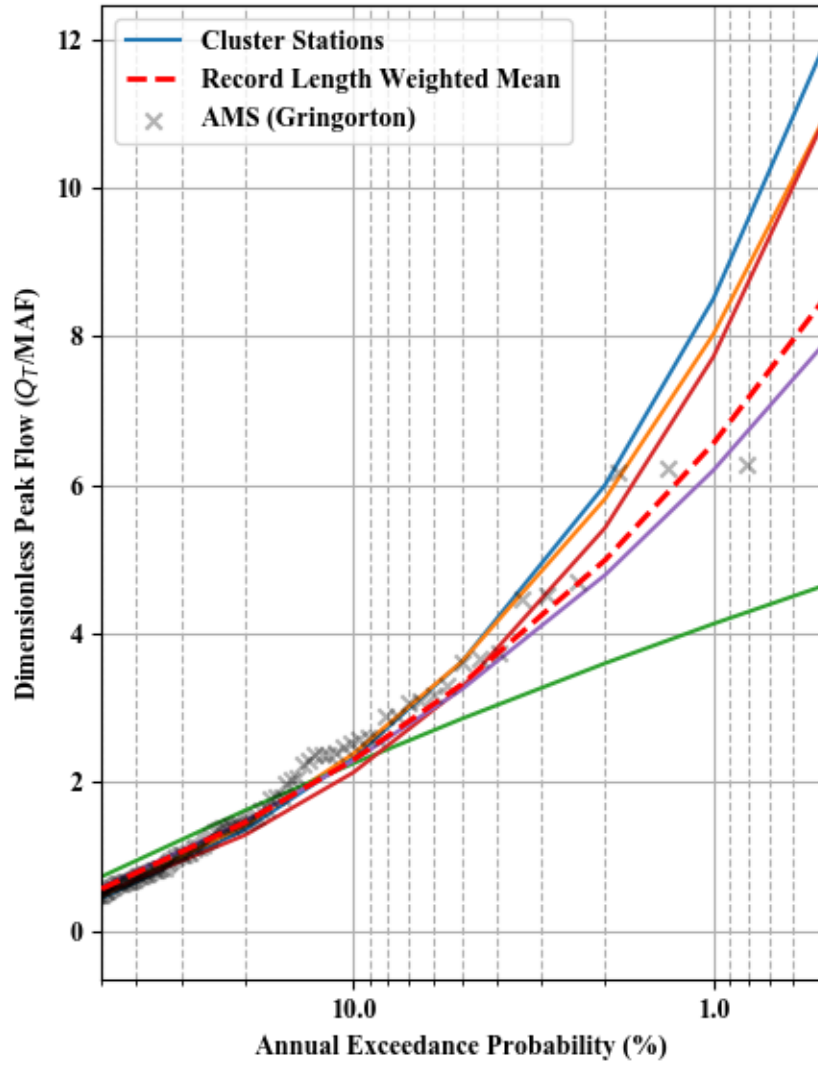
Dimensionless Peak Flow and Scaled C-value - Cluster 22



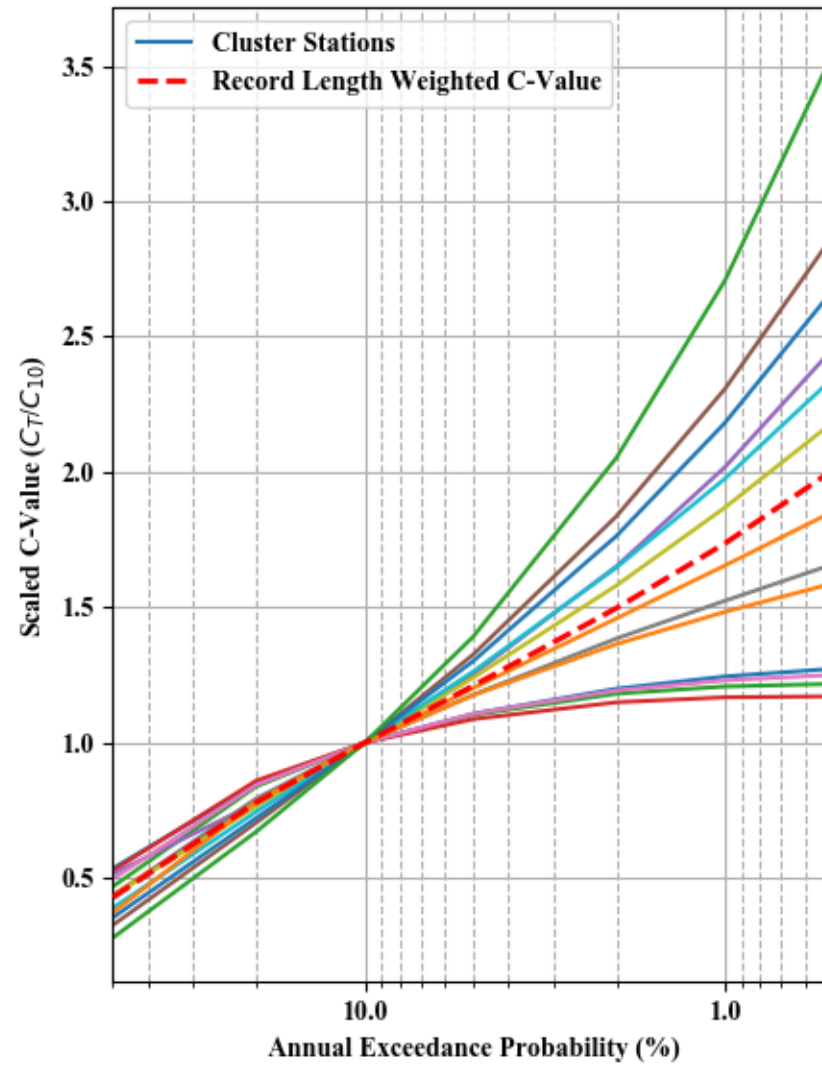
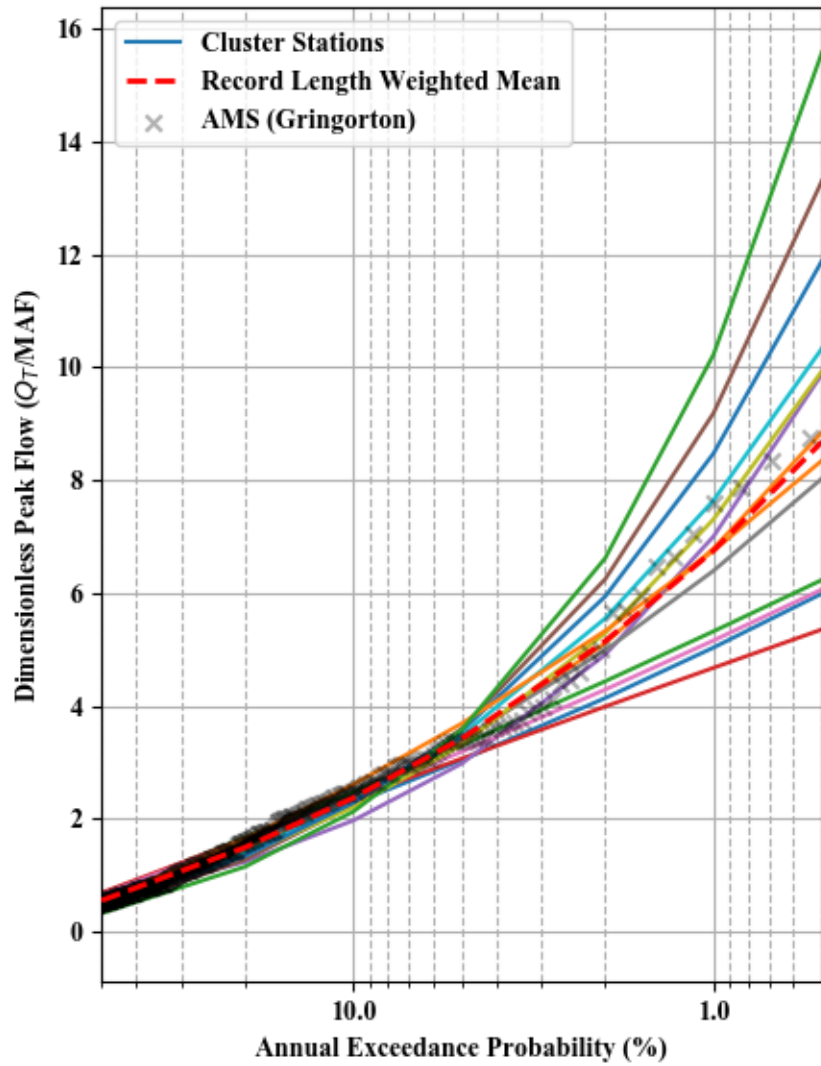
Dimensionless Peak Flow and Scaled C-value - Cluster 23



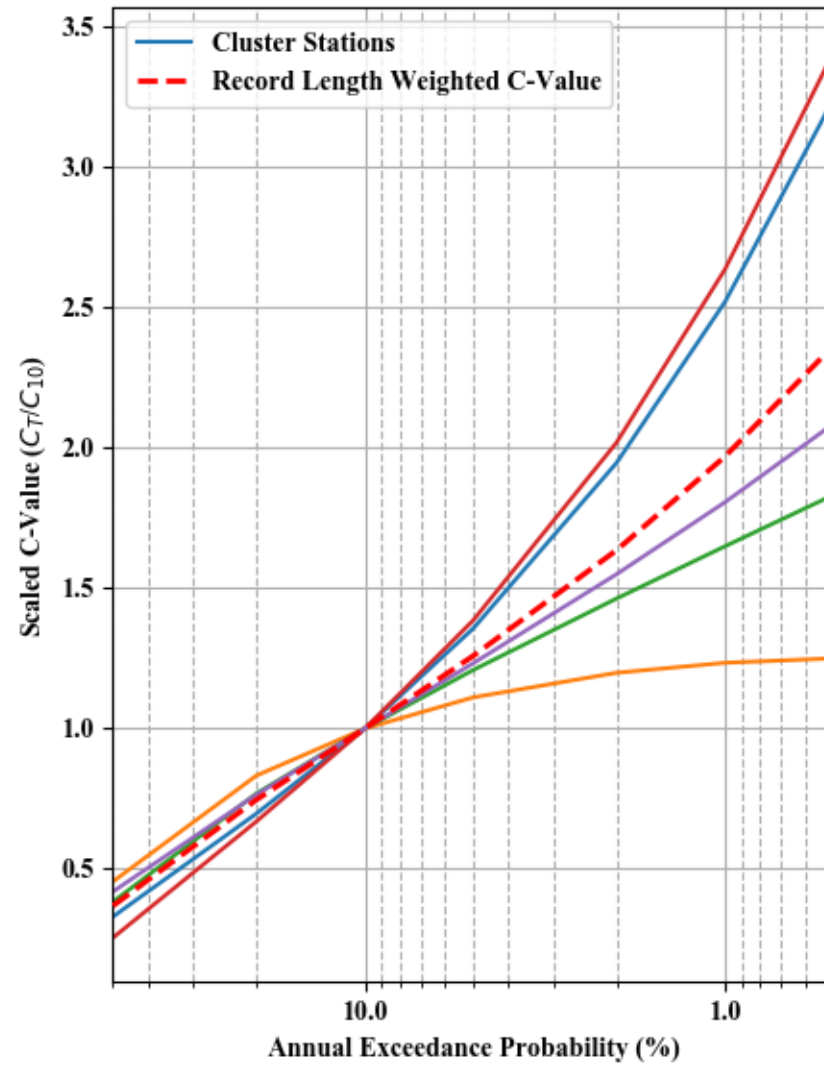
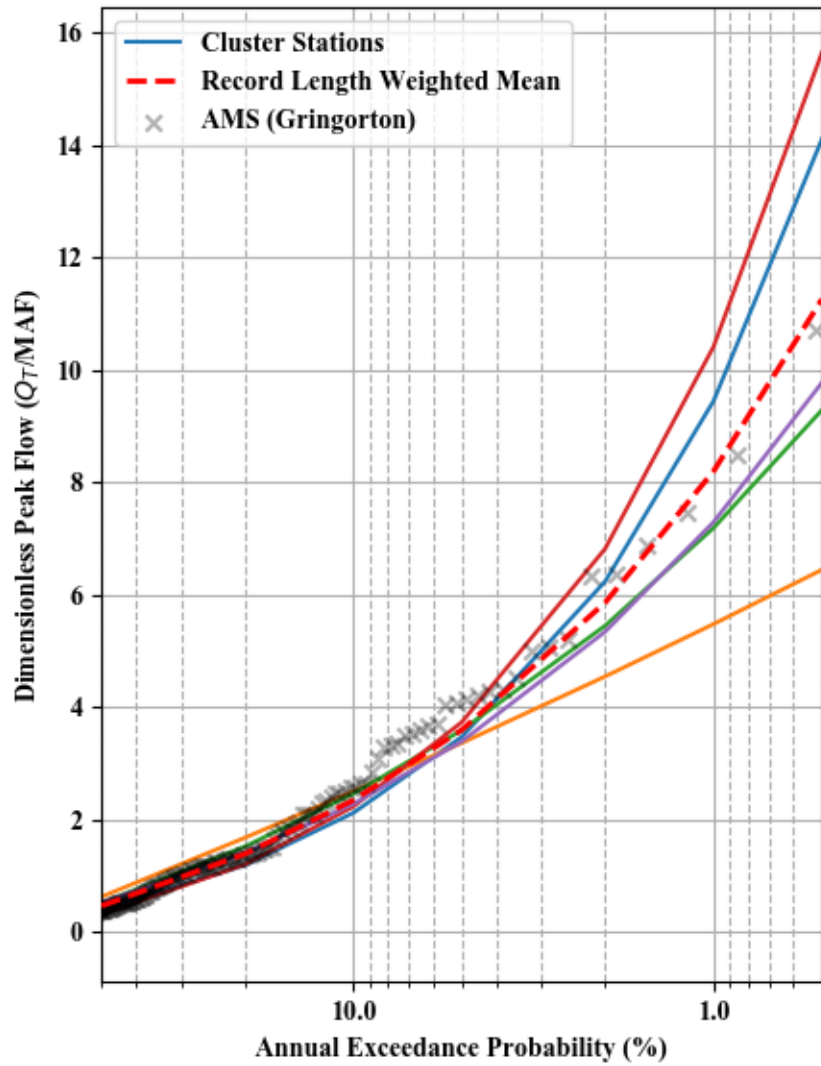
Dimensionless Peak Flow and Scaled C-value - Cluster 24



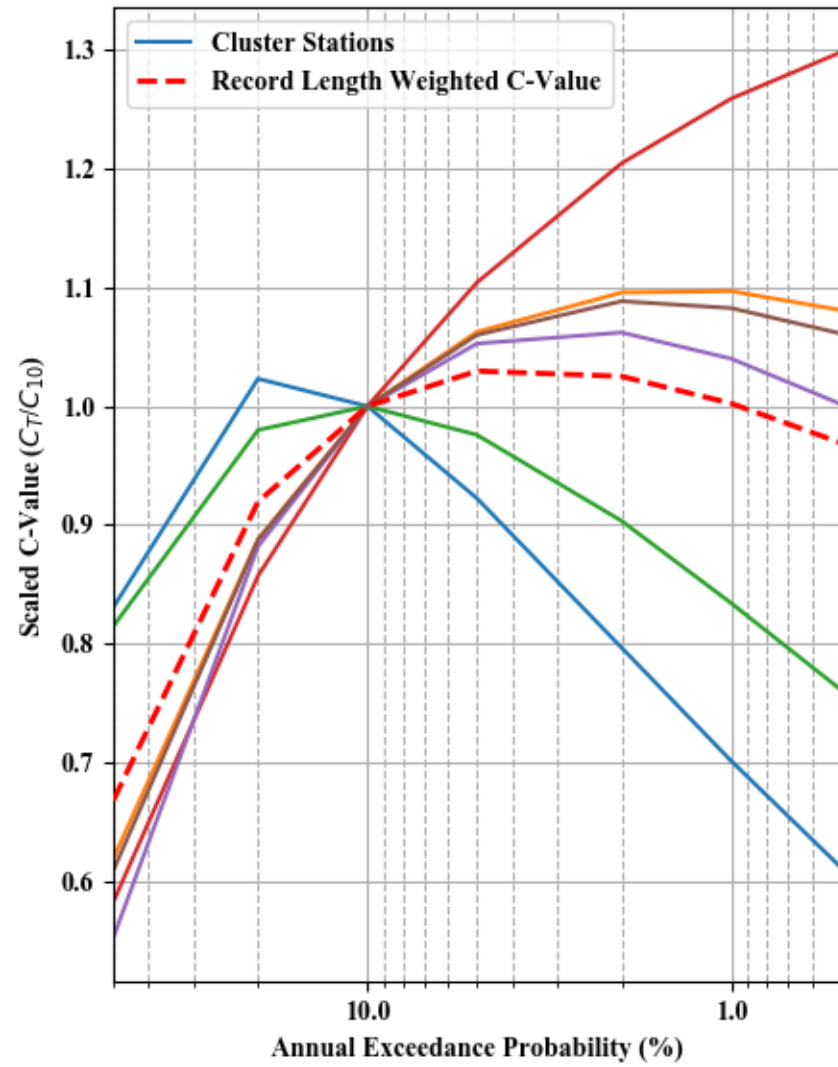
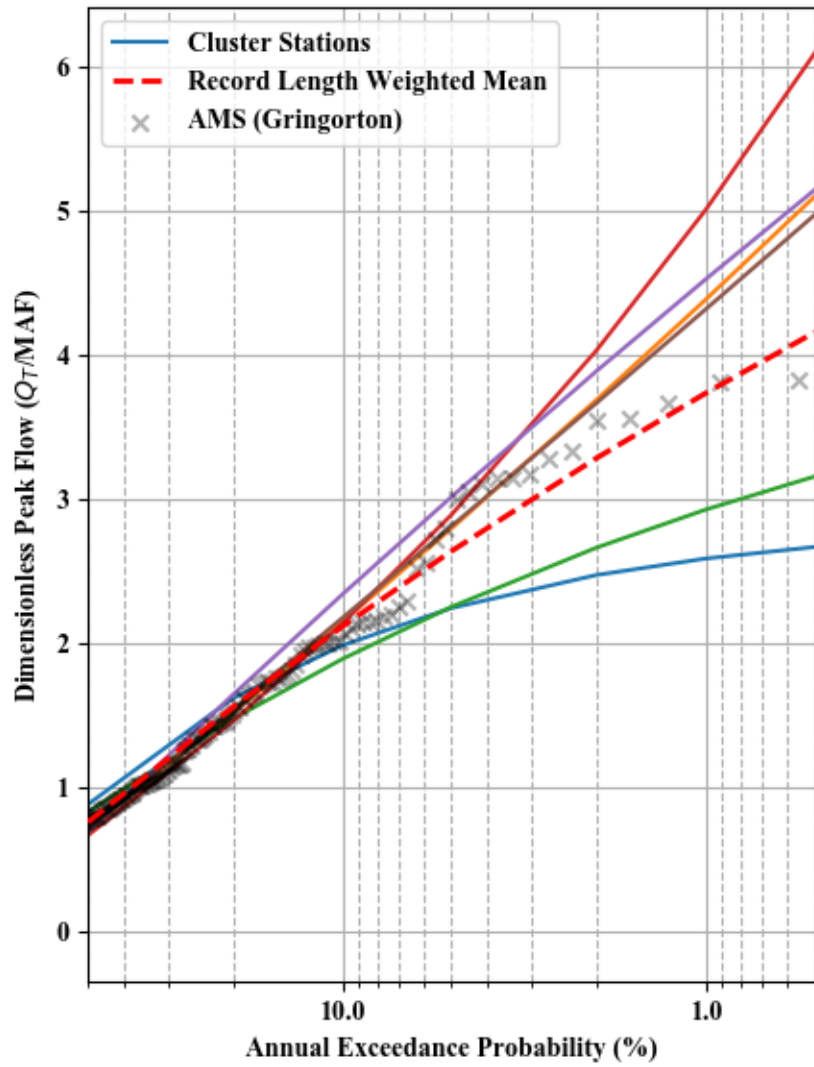
Dimensionless Peak Flow and Scaled C-value - Cluster 25



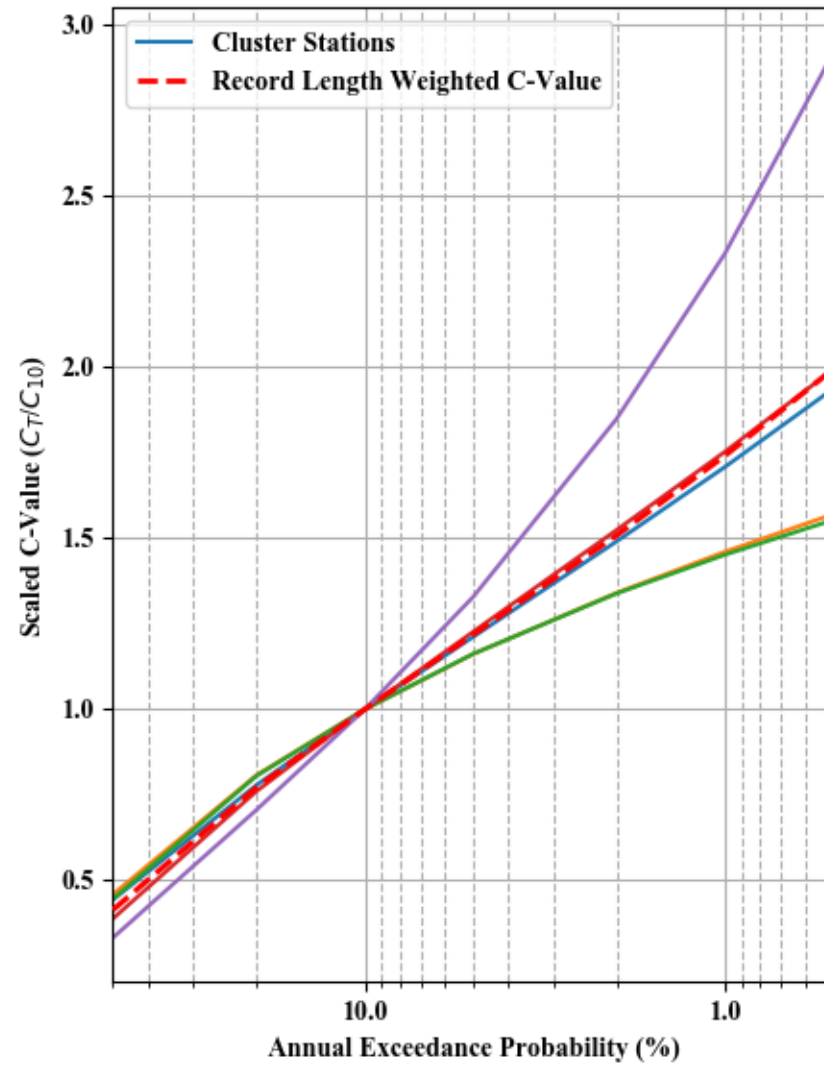
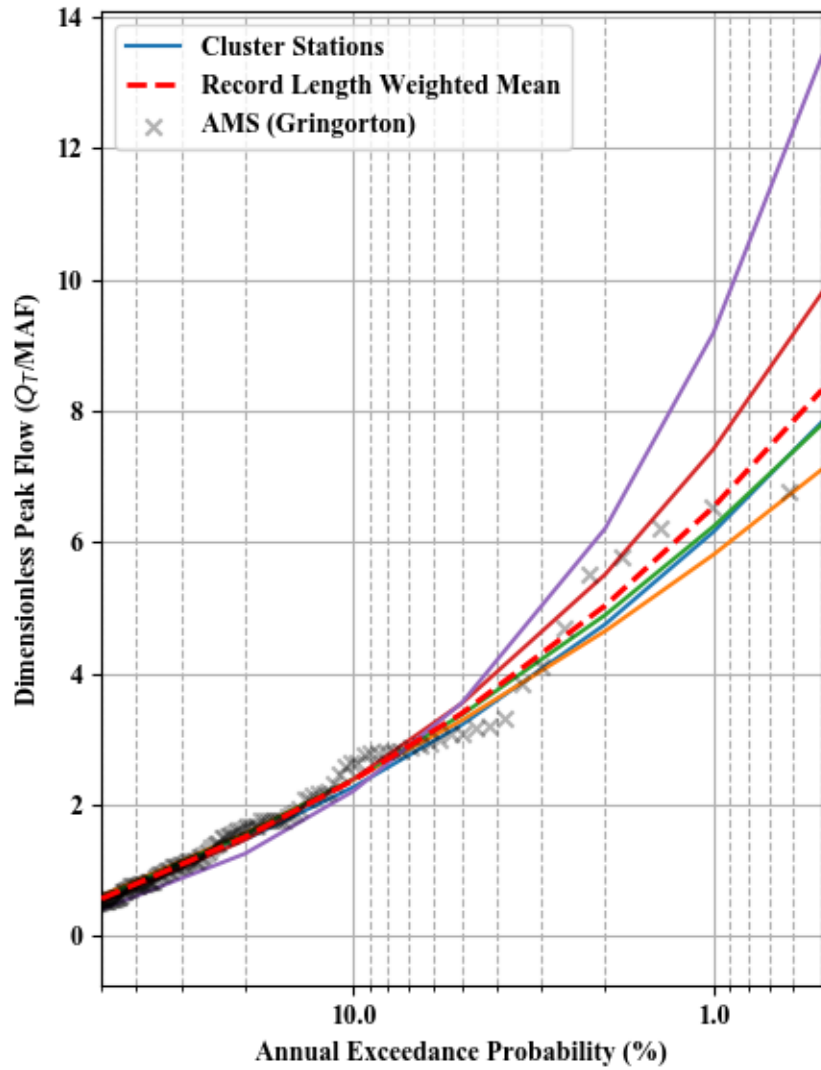
Dimensionless Peak Flow and Scaled C-value - Cluster 26



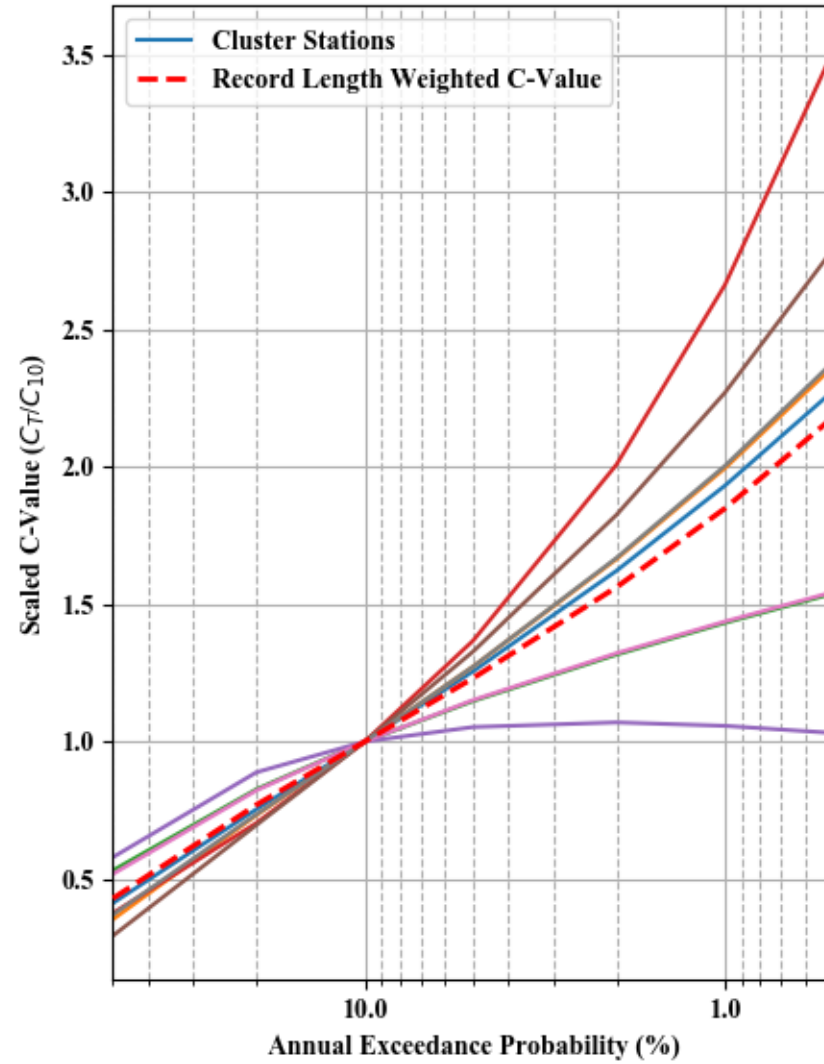
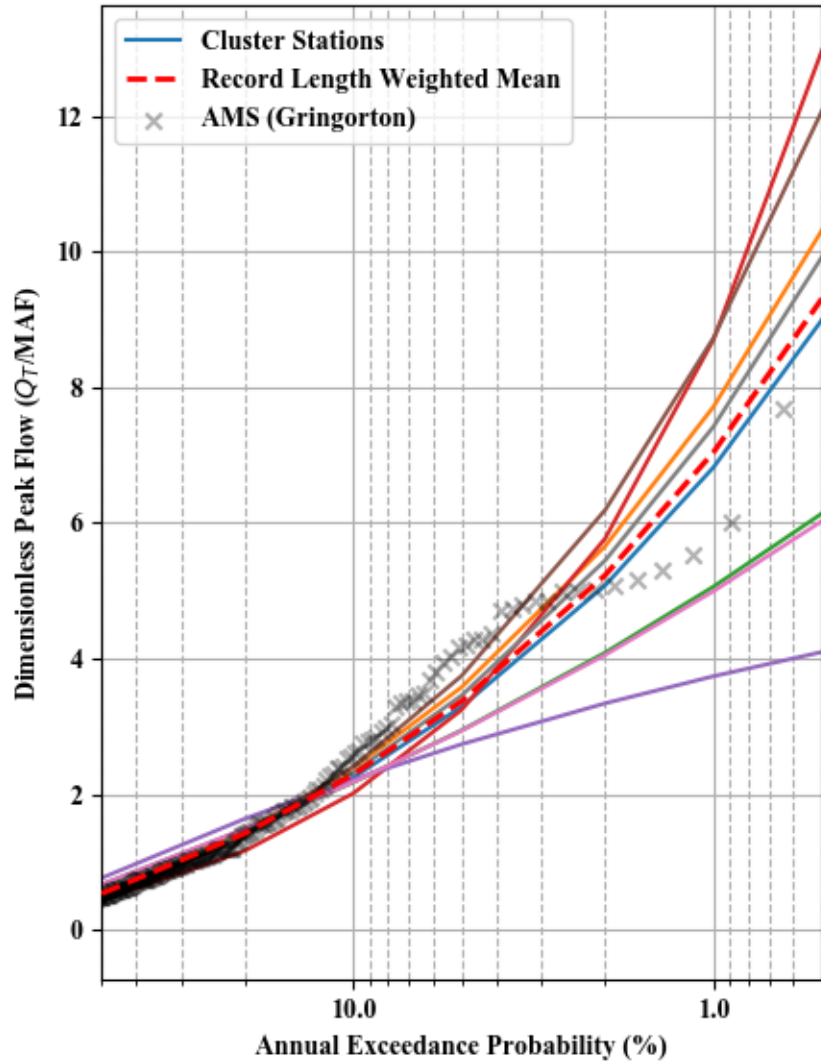
Dimensionless Peak Flow and Scaled C-value - Cluster 27



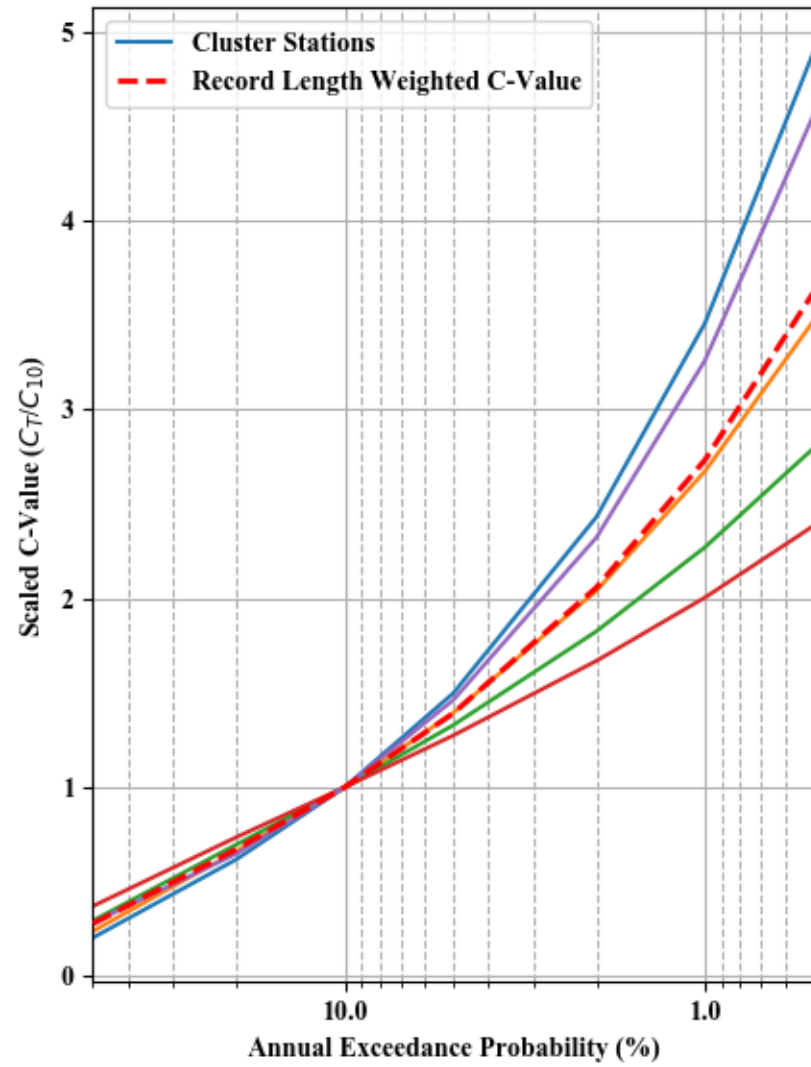
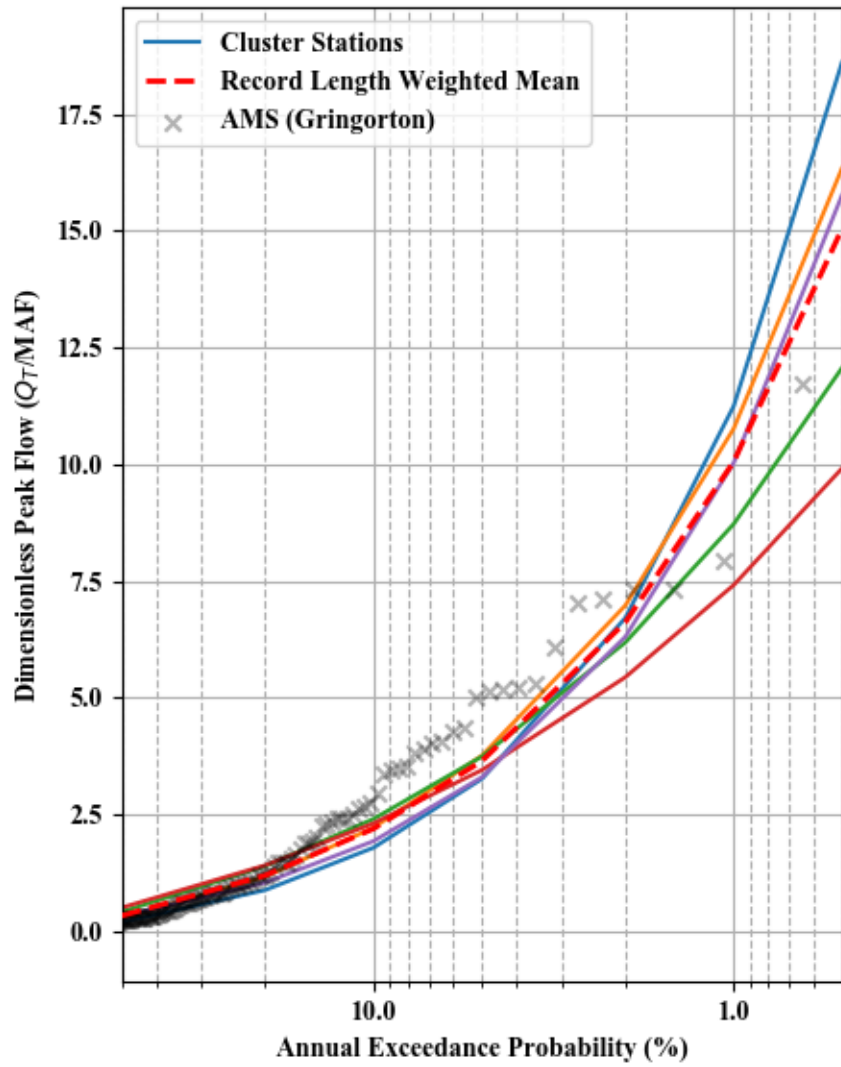
Dimensionless Peak Flow and Scaled C-value - Cluster 28



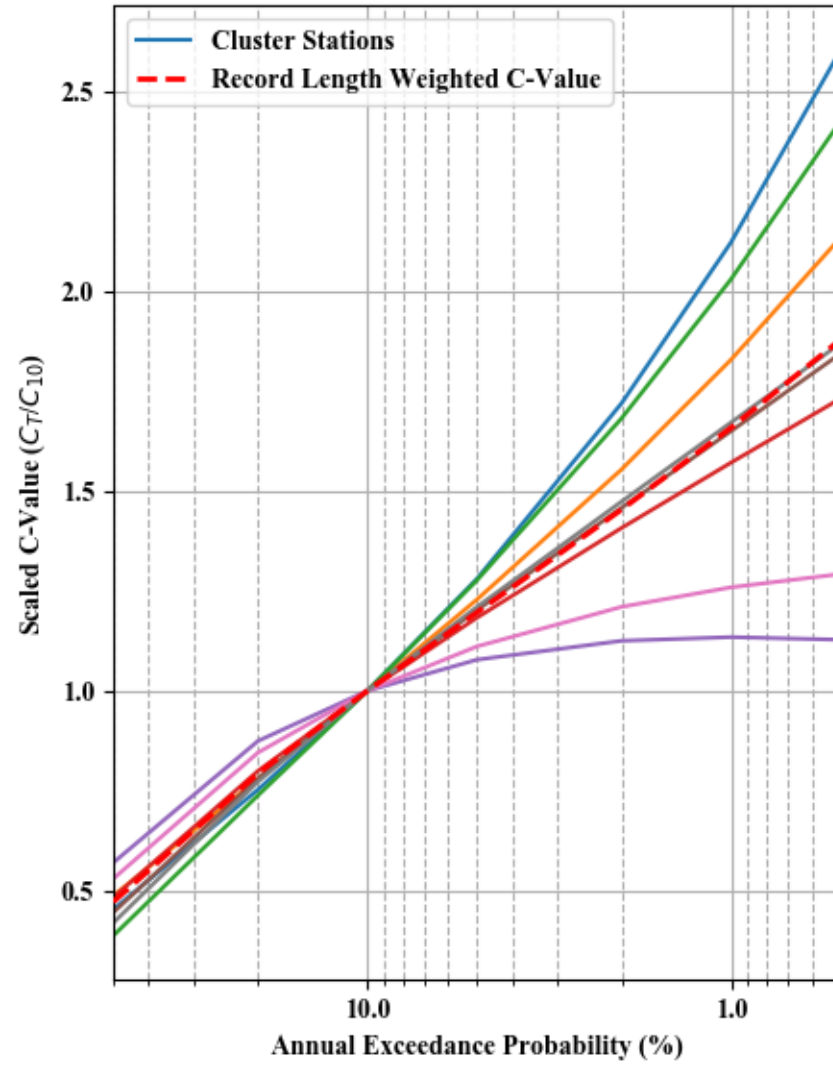
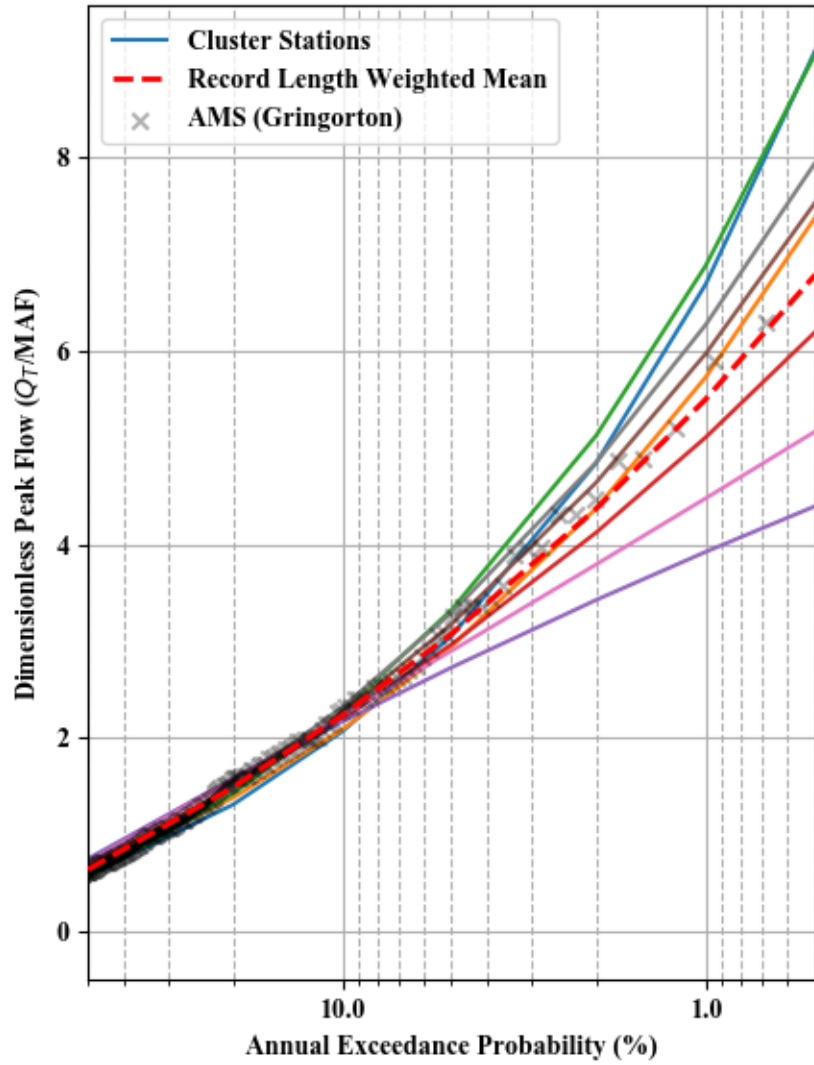
Dimensionless Peak Flow and Scaled C-value - Cluster 29



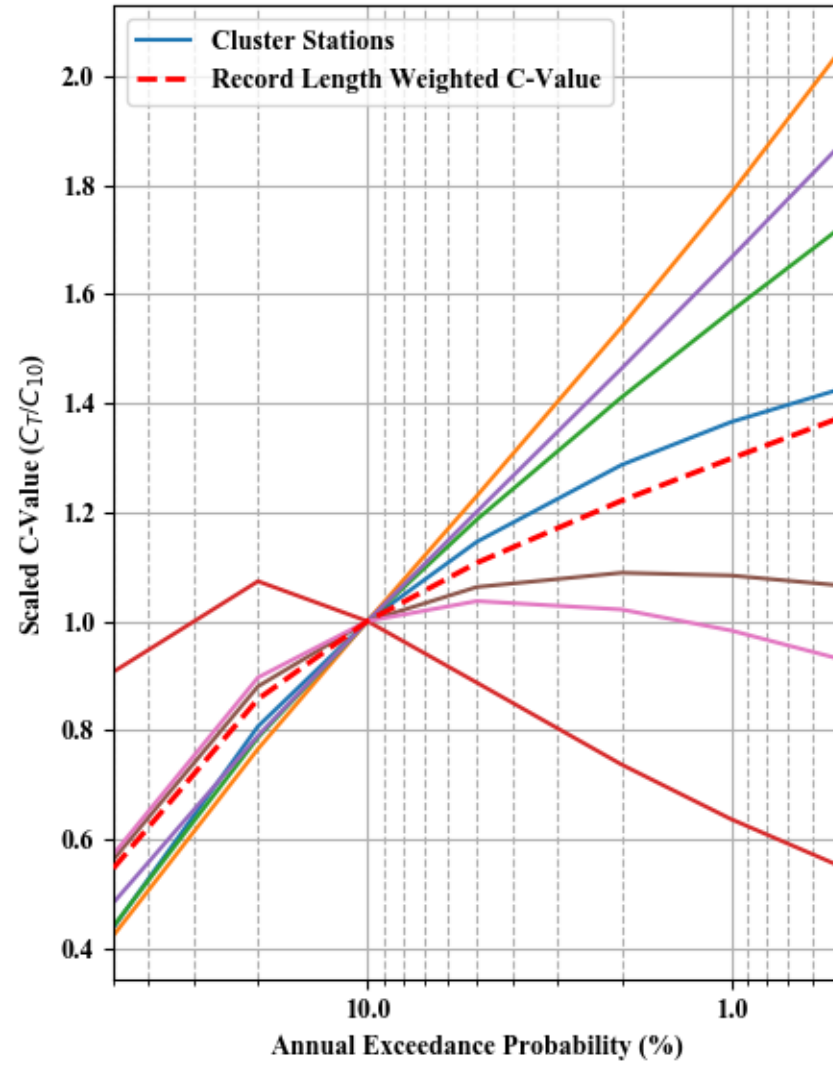
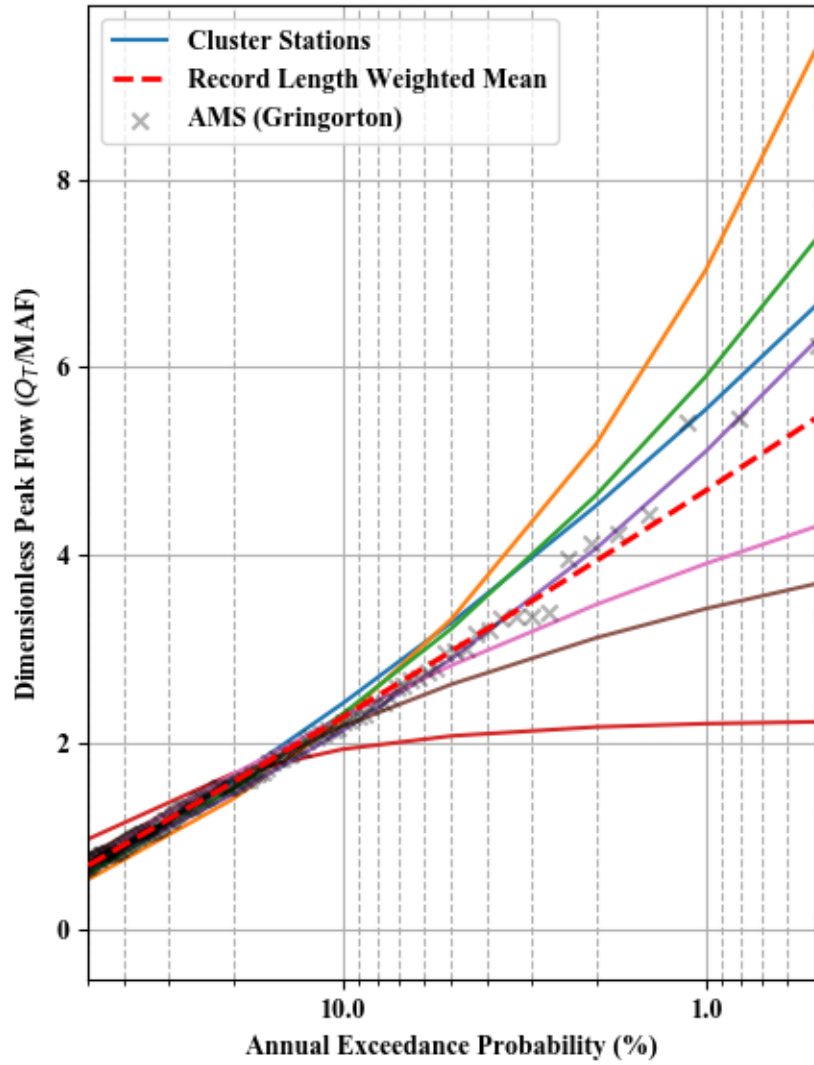
Dimensionless Peak Flow and Scaled C-value - Cluster 30



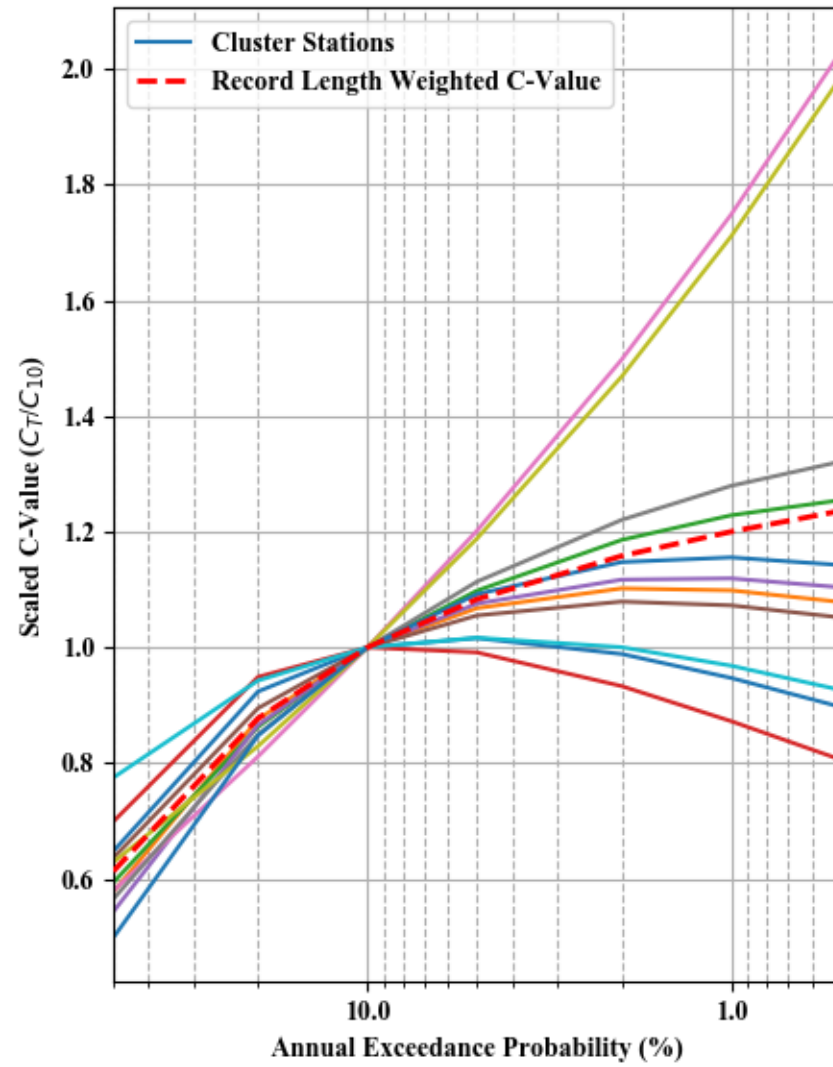
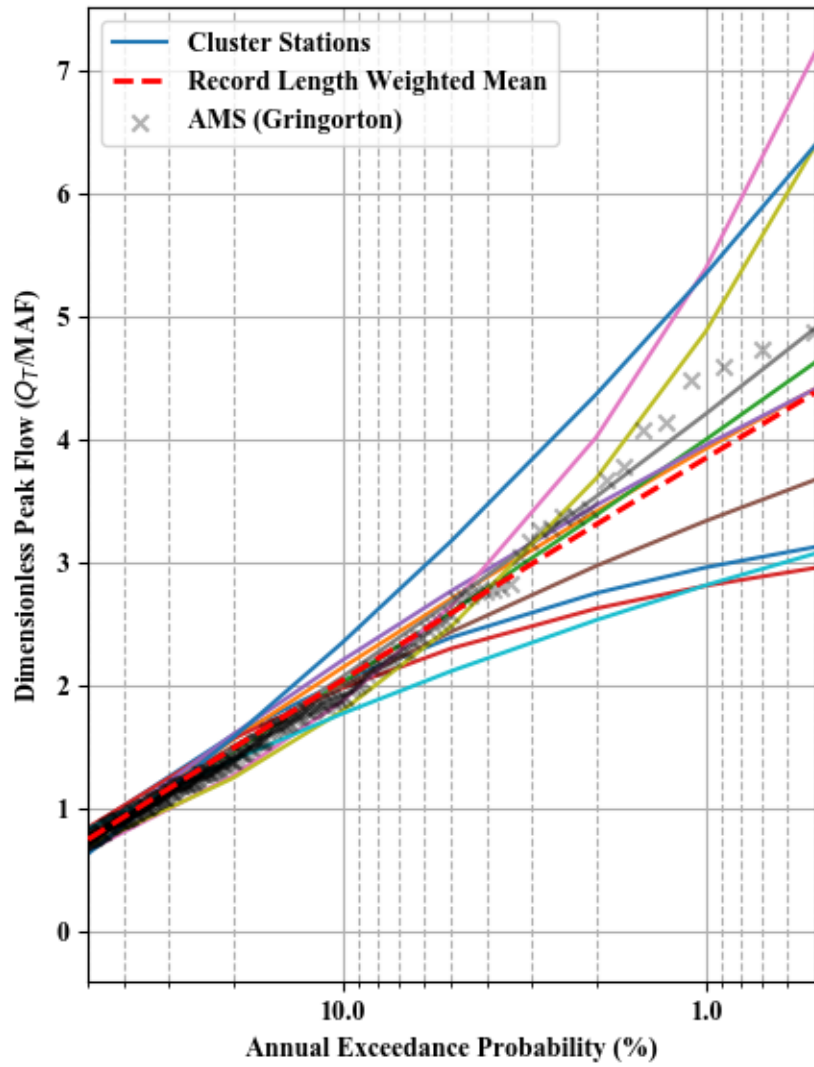
Dimensionless Peak Flow and Scaled C-value - Cluster 31



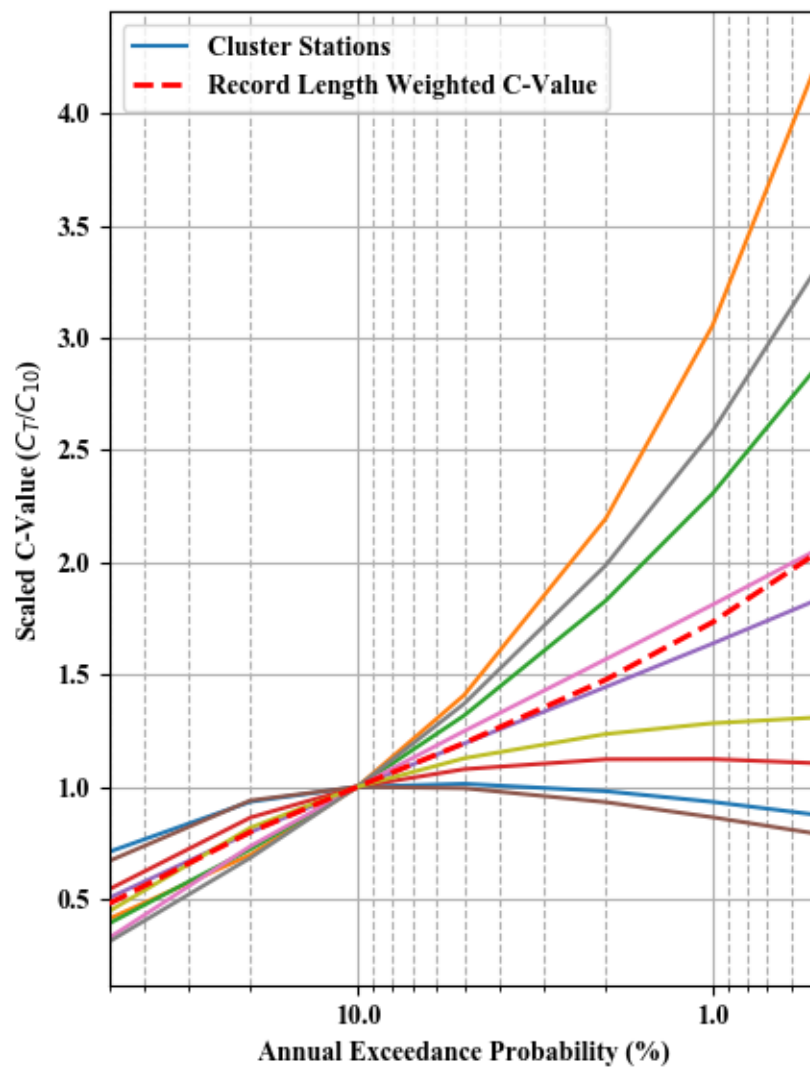
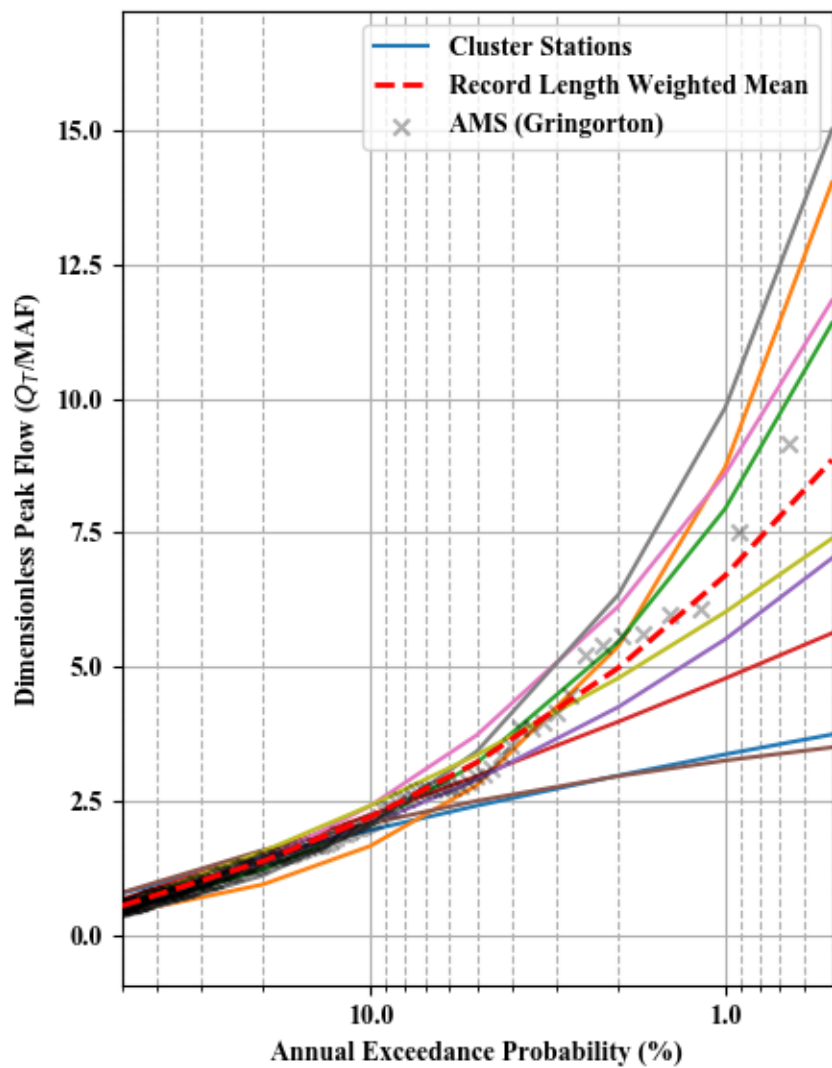
Dimensionless Peak Flow and Scaled C-value - Cluster 32



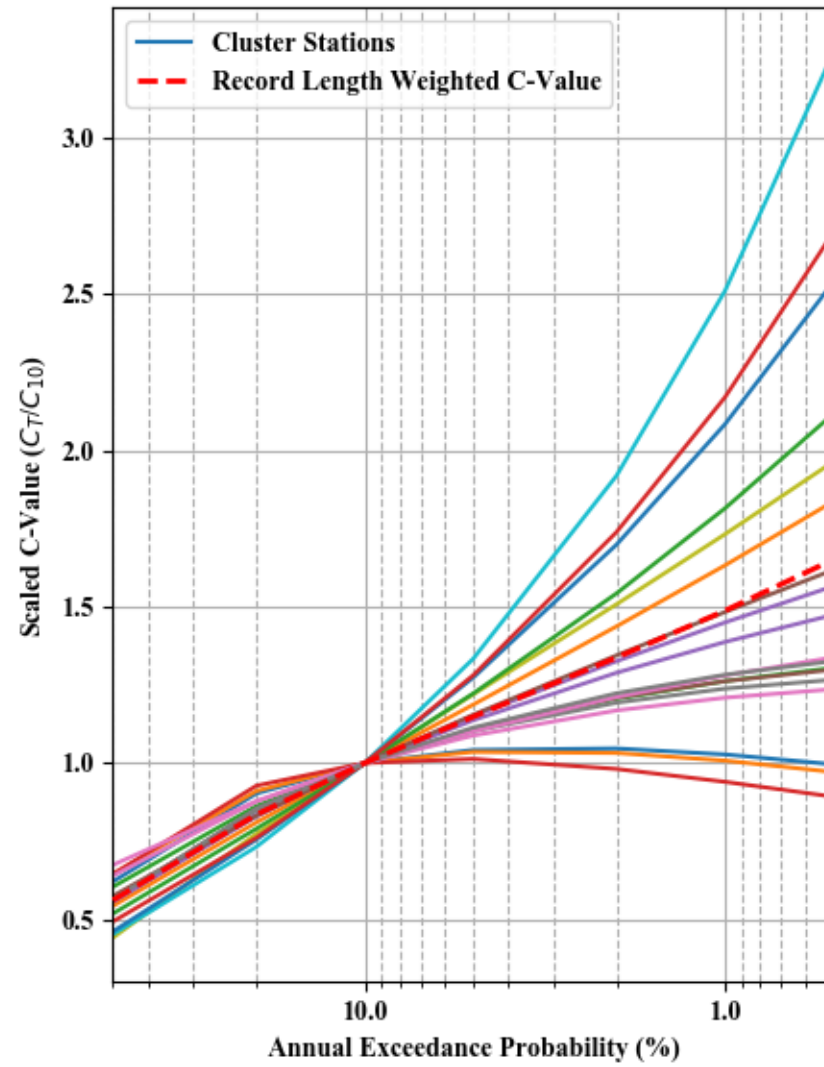
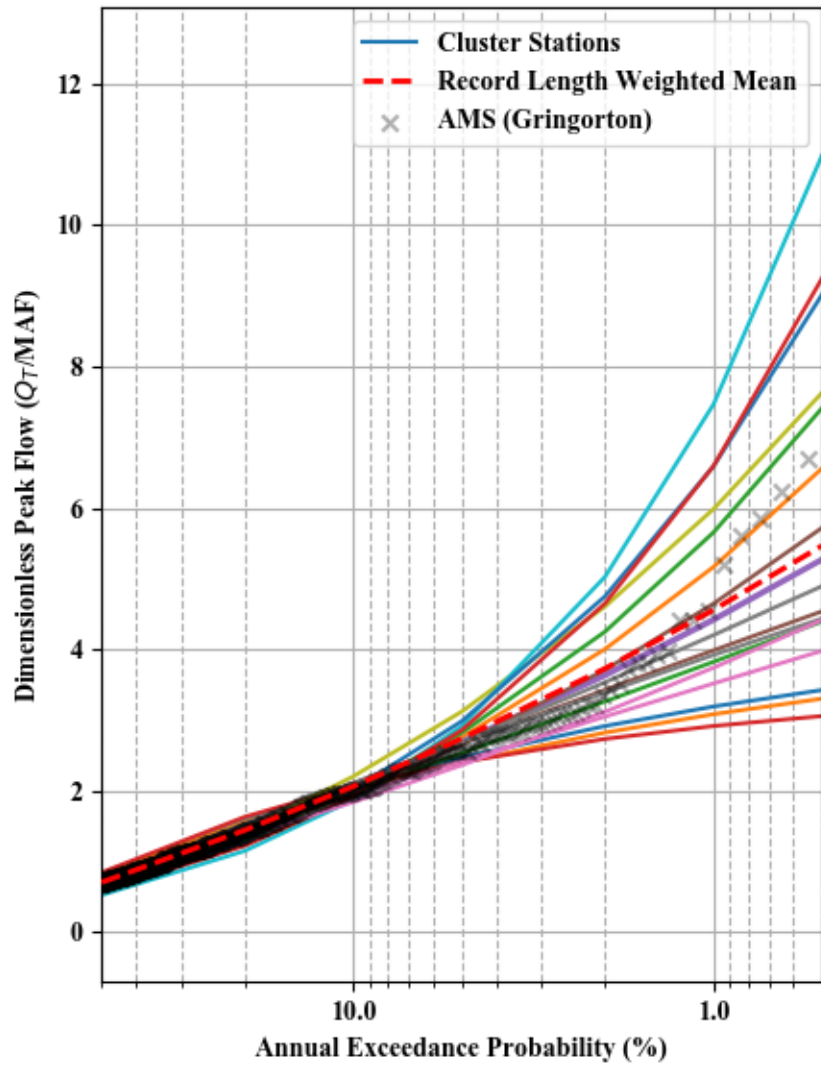
Dimensionless Peak Flow and Scaled C-value - Cluster 33



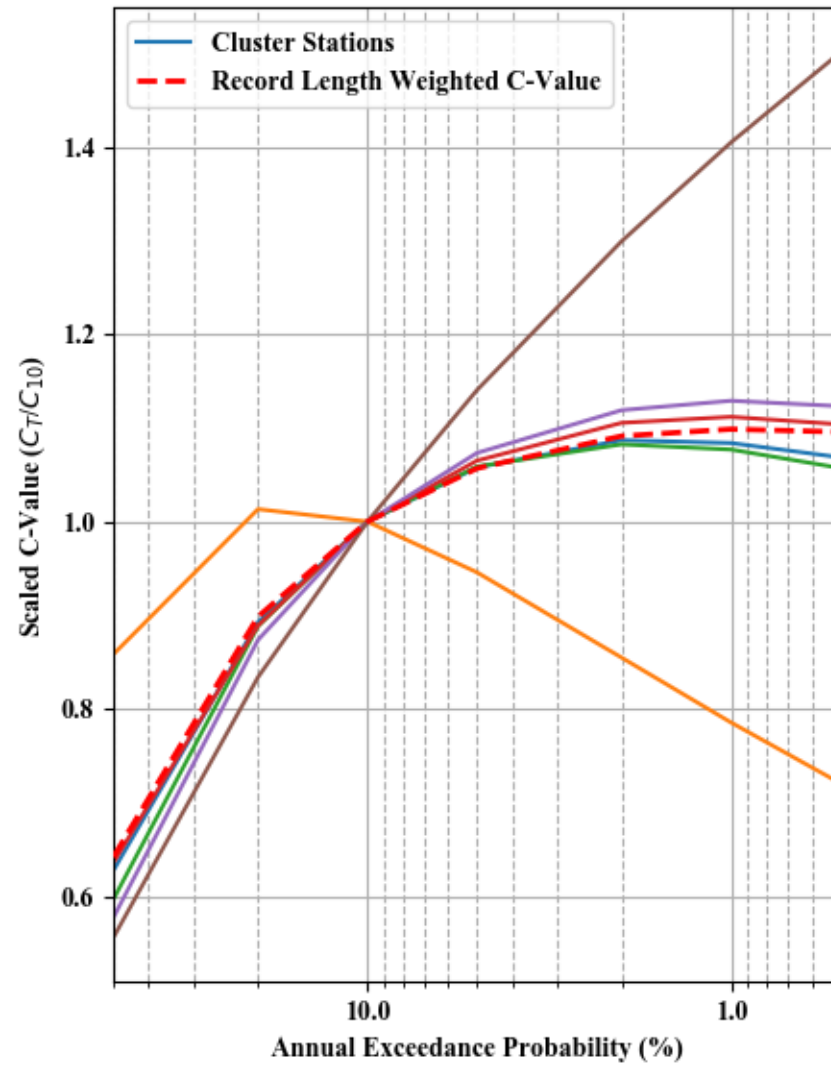
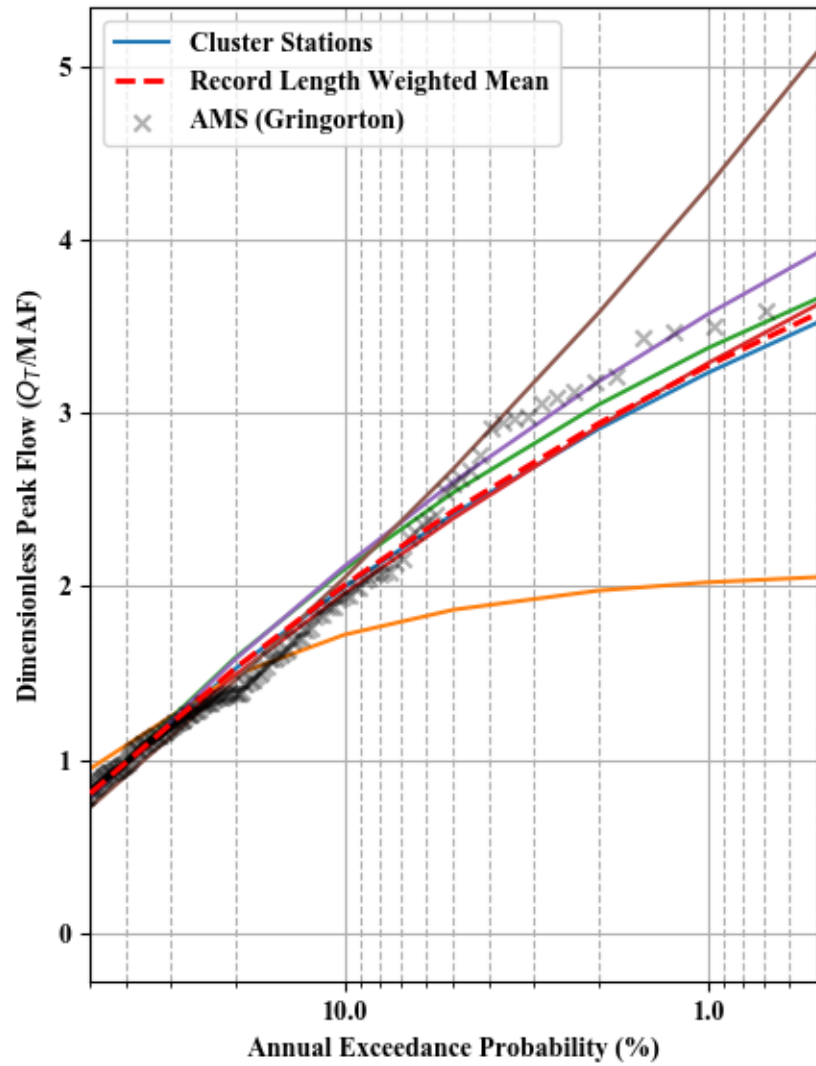
Dimensionless Peak Flow and Scaled C-value - Cluster 34



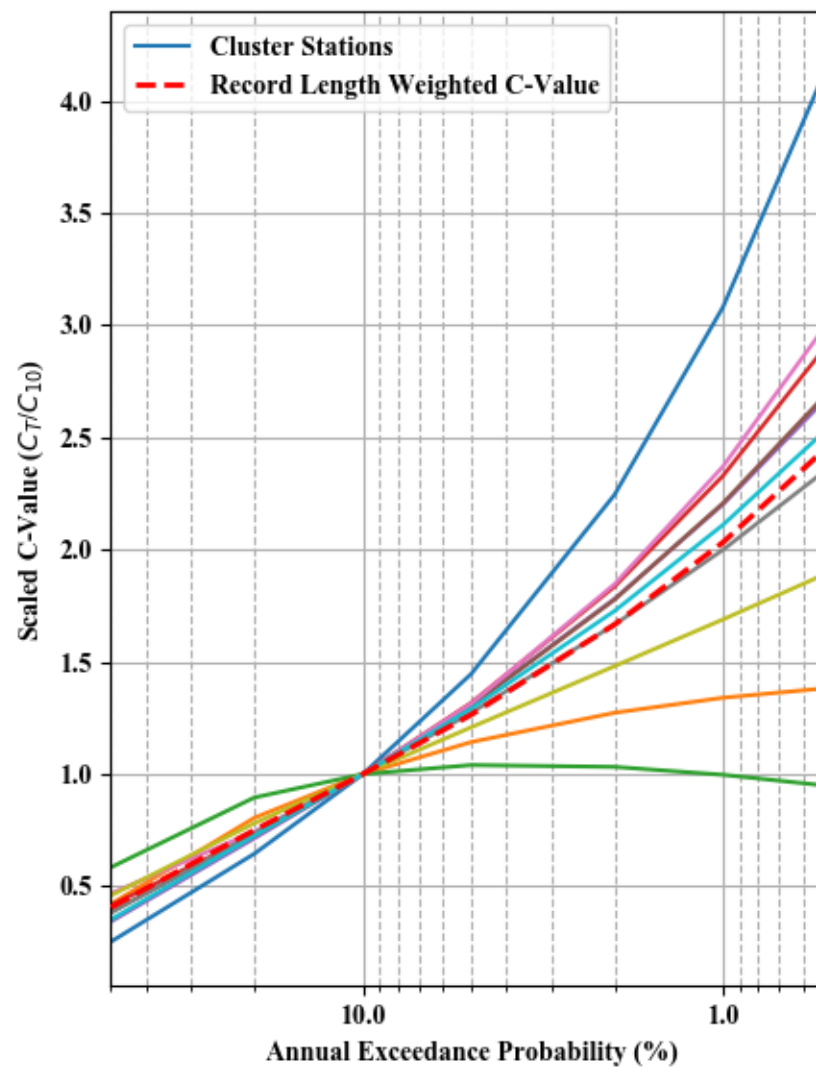
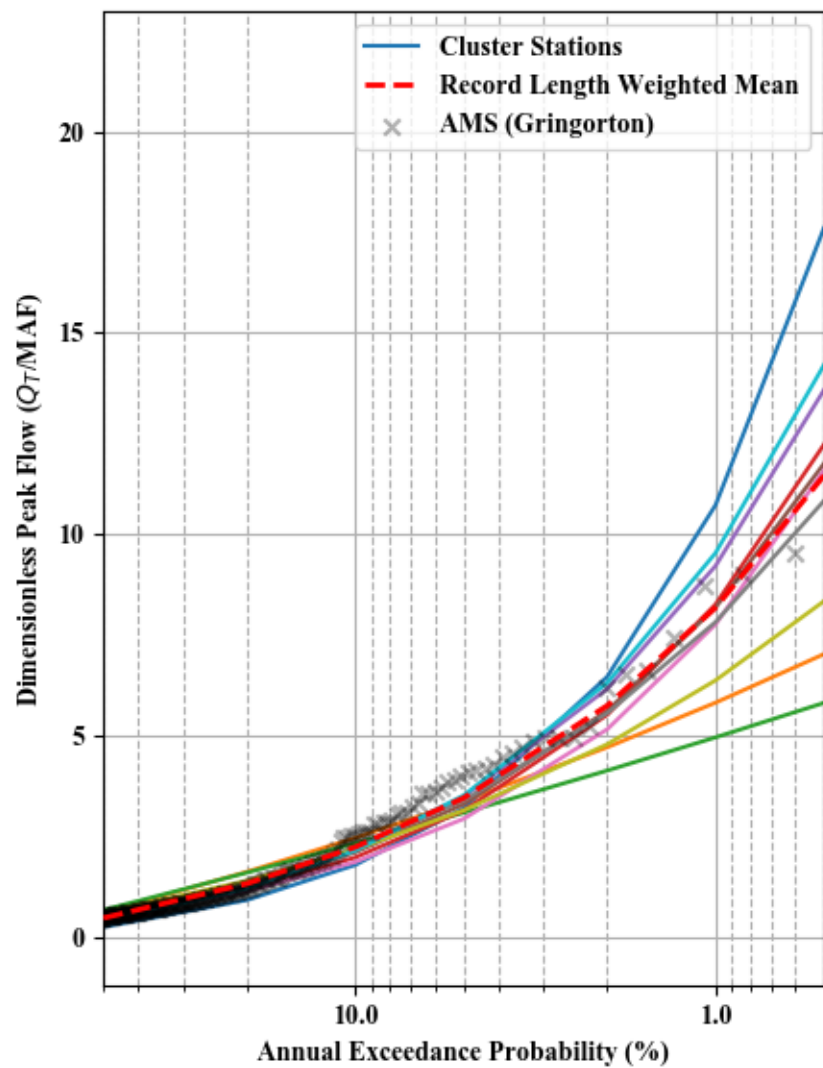
Dimensionless Peak Flow and Scaled C-value - Cluster 35



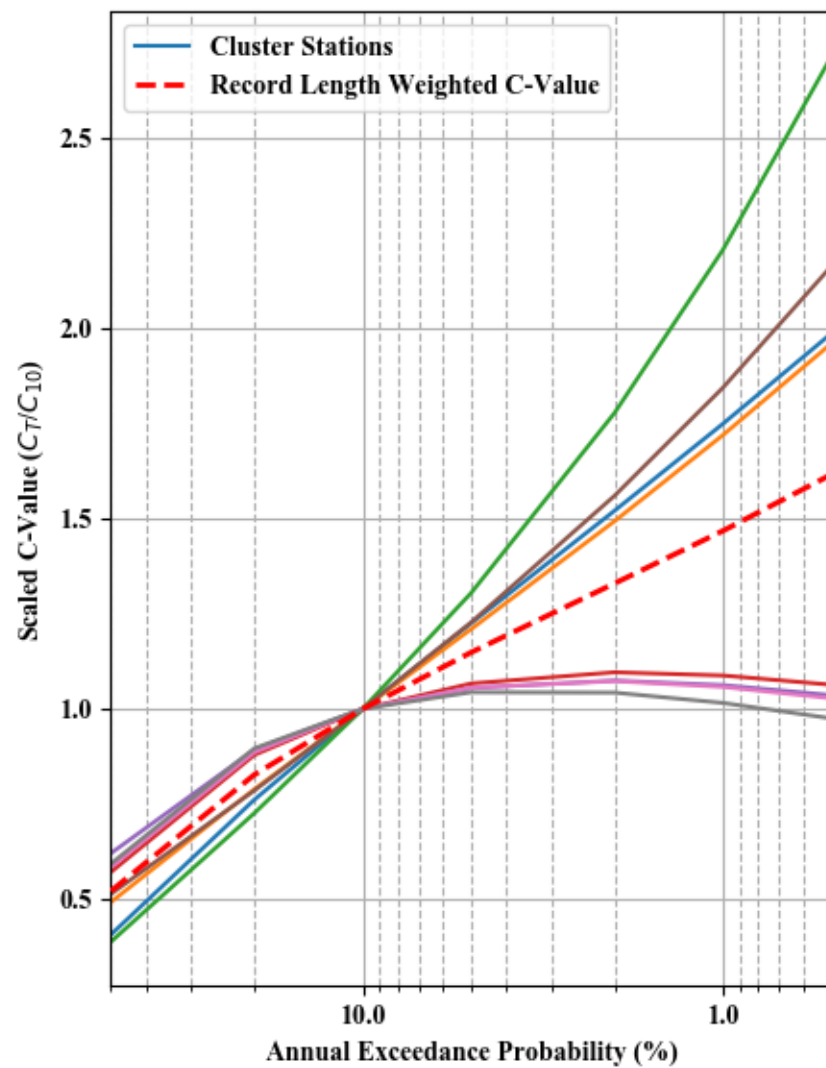
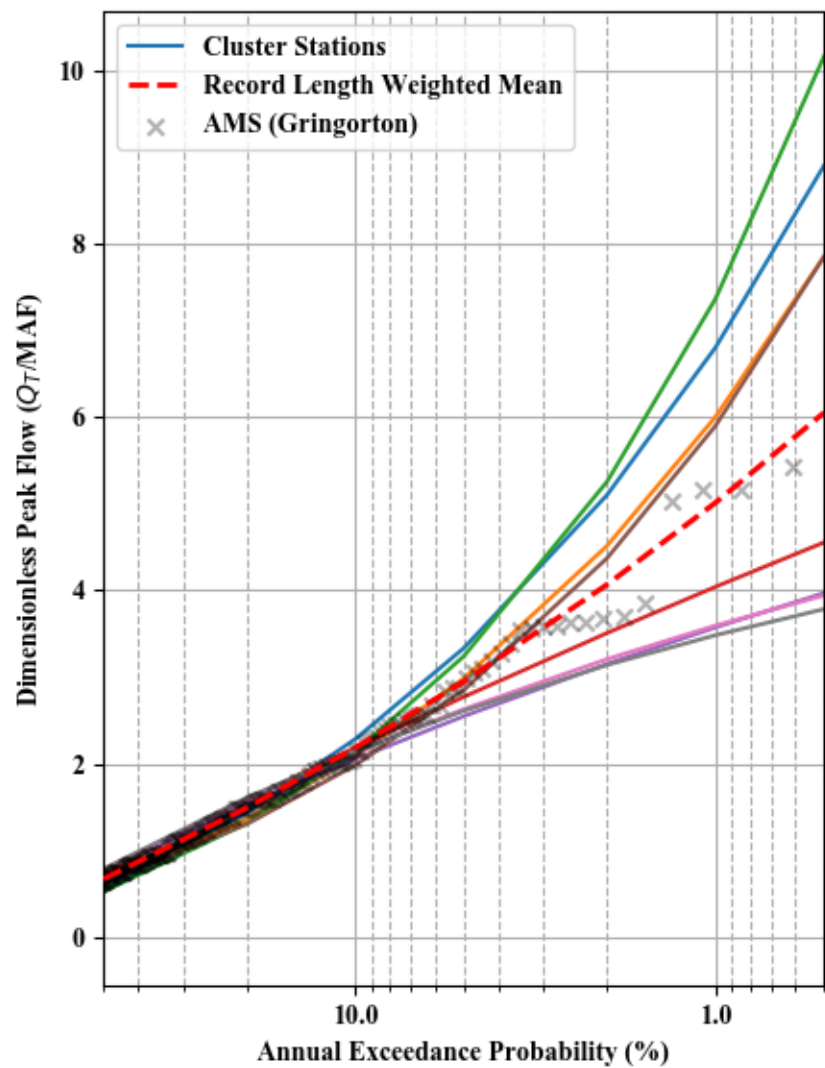
Dimensionless Peak Flow and Scaled C-value - Cluster 36



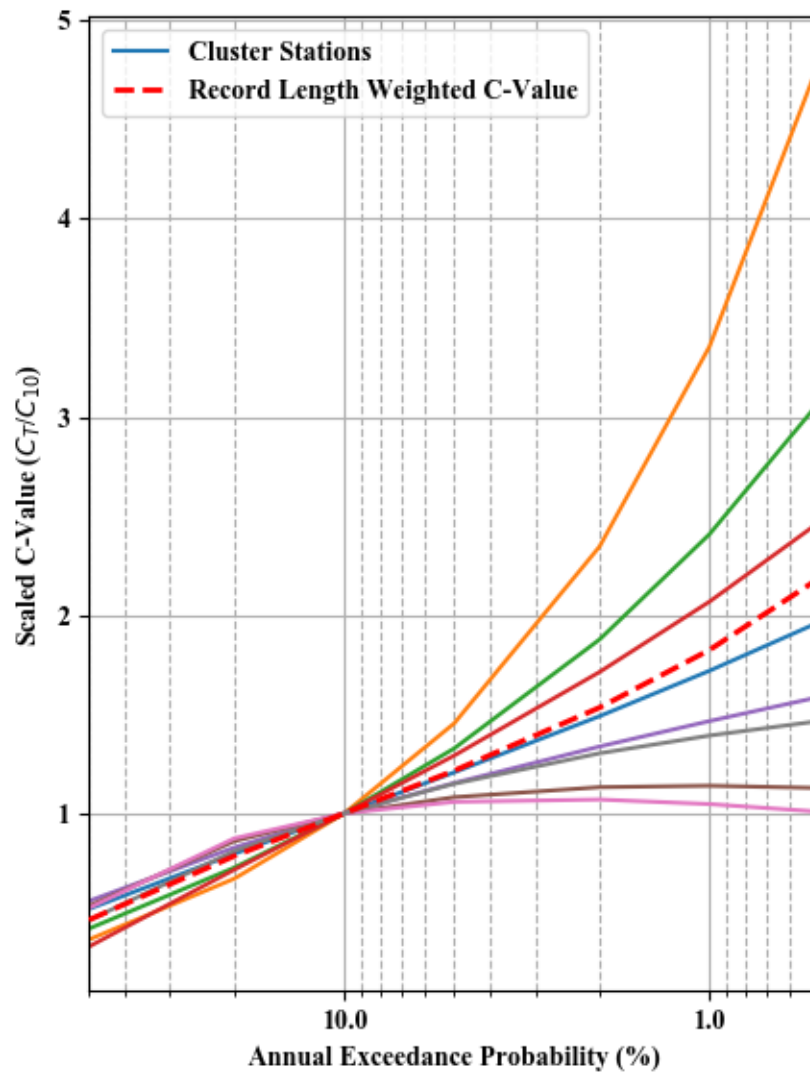
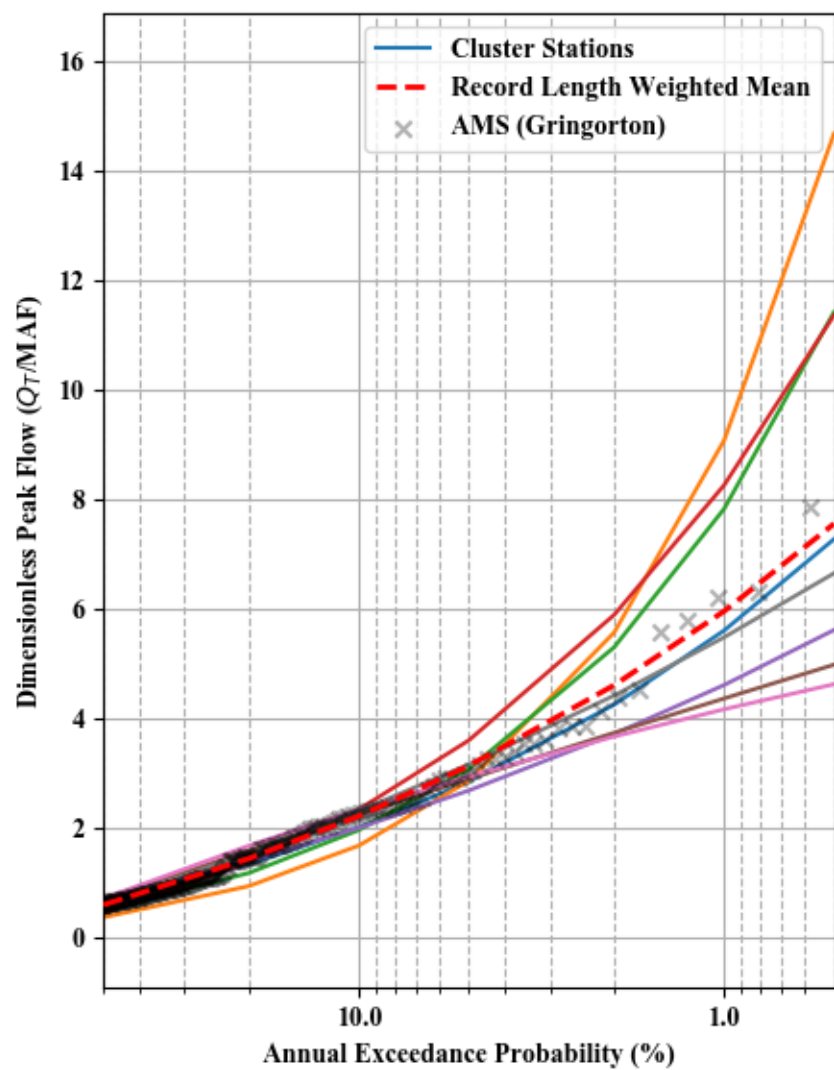
Dimensionless Peak Flow and Scaled C-value - Cluster 37



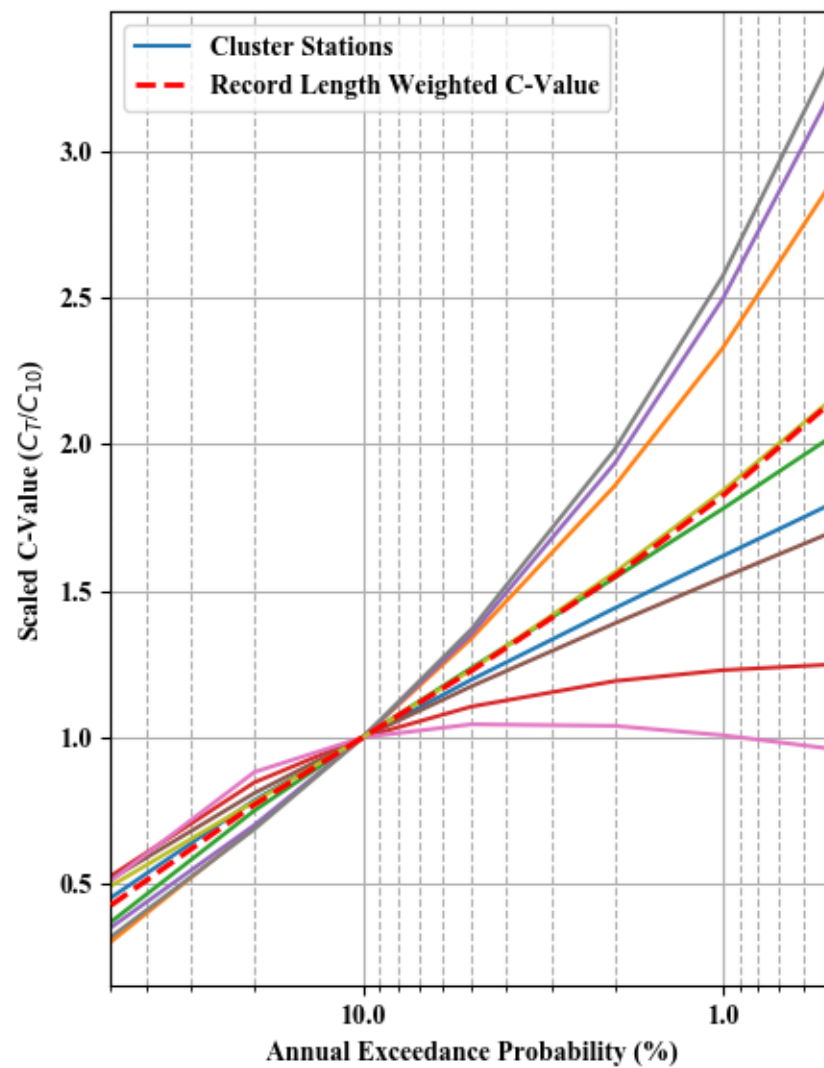
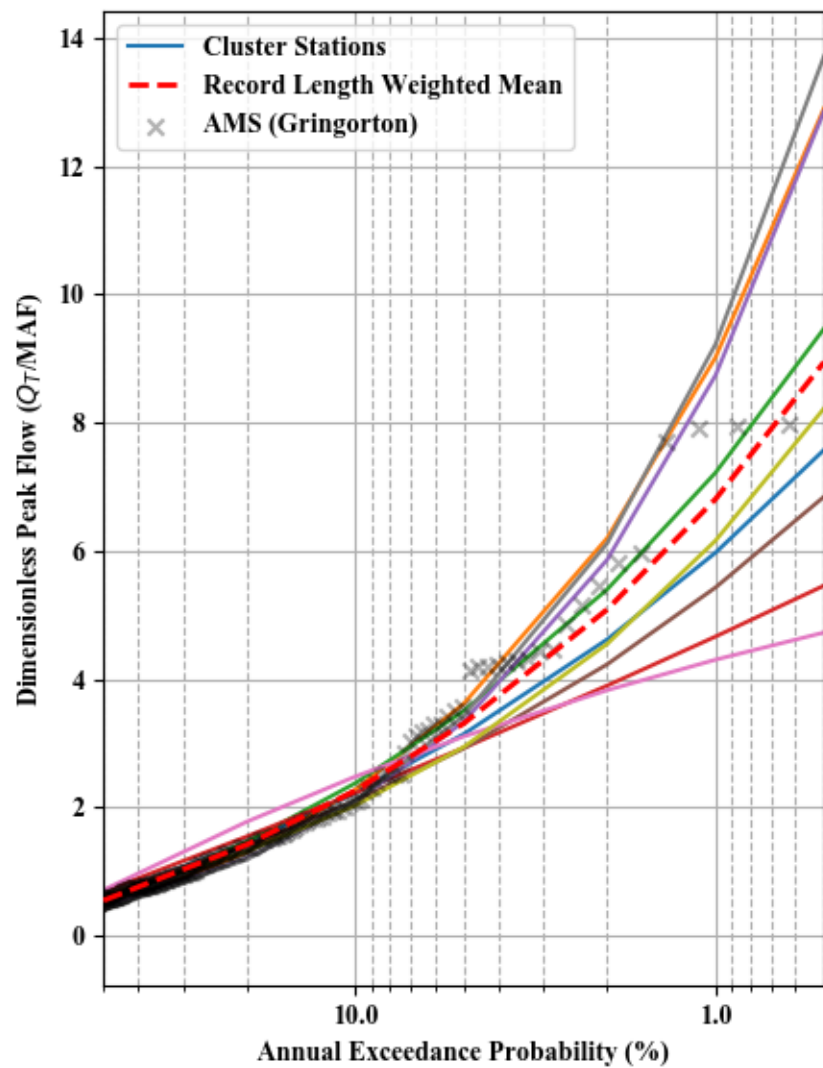
Dimensionless Peak Flow and Scaled C-value - Cluster 38



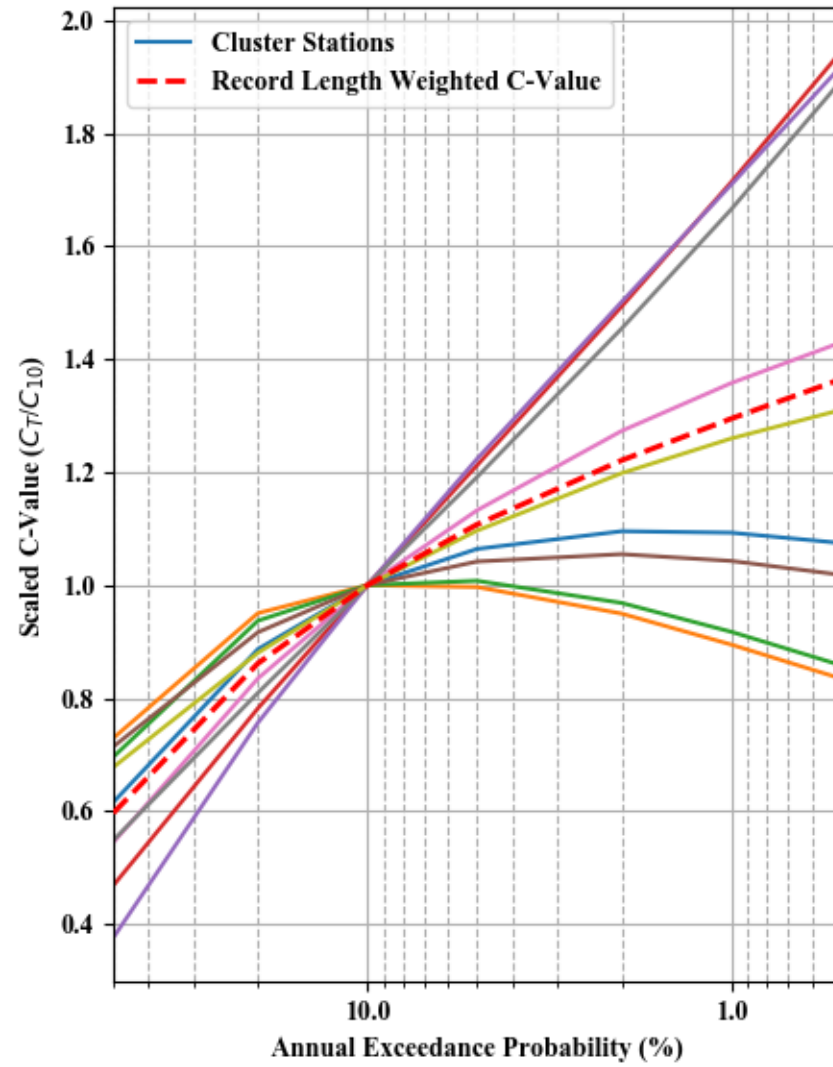
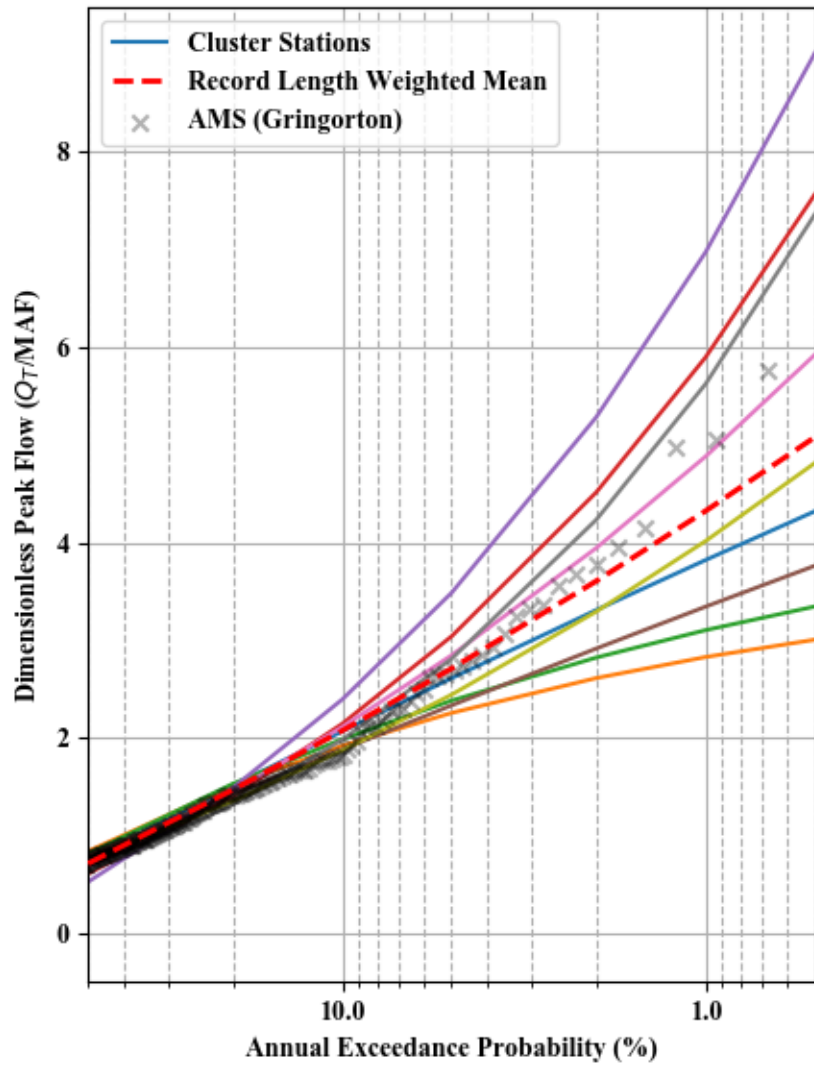
Dimensionless Peak Flow and Scaled C-value - Cluster 39



Dimensionless Peak Flow and Scaled C-value - Cluster 40



Dimensionless Peak Flow and Scaled C-value - Cluster 41



Dimensionless Peak Flow and Scaled C-value - Cluster 42

